Elemental Analysis by Alpha-Induced Prompt Gamma-Ray Spectrometry

by

IAN STEWART GILES

A thesis submitted to the University of Cape Town in fulfilment of the requirements for the degree of Doctor of Philosophy

March 1978

To Elizabeth Jane

Acknowledgements

The author wishes to express his indebtedness to

Dr. Max Peisach for his able guidance, help and stimulating enthusiasm throughout this investigation,

Professor I.J. van Heerden, Head of the Southern Universities Nuclear Institute, for the use of the Institute's facilities,

Dr. J.J. Kritzinger and the technical personnel of the Institute for their assistance and efficient operation of the accelerator and equipment.

the staff of the School of Chemical Sciences, University of Cape Town, for their co-operation,

Professor J.P.F. Sellschop, Head of the Nuclear Physics Research Unit, University of the Witwatersrand, for the use of the Unit's facilities,

his colleagues, who, although too numerous to mention individually, all contributed by their discussion,

the Cape Portland Cement Co. Ltd. and Mr. A.M. Swartz of Blue Circle Cement Ltd., Johannesburg, for kindly supplying cement samples,

Mr. T.W. Steele, Head of the Analytical Chemistry Division of the National Institute for Metallurgy, Johannesburg, for the analysis of the cement samples and the

supply of the fluorspar standards,

the Department of Gemology, University of Stellenbosch, for polishing the steel specimens,

Mr. P. Groenewald for his patient and expert execution of the drawings and Mr. A.R.A. Giles for his assistance therewith,

Mr. S. Hendricks for producing the photographs,

Mr. and Mrs. J.A. Lewis for their constant encouragement during this work and particularly for checking the figures,

Miss M.L. Niven for undertaking the arduous task of proof-reading the manuscript and his wife for typing it,

the Council for Scientific and Industrial Research and the South African Atomic Energy Board for financial assistance.

Finally, a word of thanks to family and friends for their forbearance and moral support.

Abstract

Alpha-induced prompt gamma-rays generated by excitation, or in nuclear reactions, were studied for 57 elements, to select those elements having gamma-rays of sufficient intensity for analytical application. Several light, medium and heavy elements show promise. Of these nitrogen, fluorine, manganese and vanadium were selected for more detailed study. The applicability of this technique was tested by studying the determination of fluorine in cements and of nitrogen, vanadium and manganese in steels.

Contents

A Summary of this work and reprints of publications therefrom are to be found inside the back cover.

CHAPTER I

INTRODUCTION

INTRODUCTION

The demand for rapid, accurate analyses which has grown quickly in recent years, has led to the development of many new analytical techniques. The field of nuclear analytical chemistry has been in the forefront of this search and many techniques previously restricted to the highly specialised nuclear laboratory are now increasingly applied to practical problems.

Activation analysis, since its early beginnings in 1936 [He 36], has become the best established of nuclear analytical techniques. The bulk of applications have made use of neutron activation but some years ago the use of charged-particle activation became more widespread. More recently the spectrometry of prompt products from nuclear reactions for analytical purposes has resulted in the development of a parallel field, where applicability of the technique is no longer related to the radioactive properties of the product nucleus. As a result, reactions which produce stable nuclides, without long-lived metastable states, and which were therefore entirely useless for activation analysis can now be applied with advantage. In addition, there is no need for using rapid transfer equipment if the product is very short lived and data may be accumulated at a constant rate throughout the period of measurement.

The main general disadvantage of charged-particle activation is that the particle energy is degraded rapidly along the path through the target. Therefore only the outer surface

layers are analysed and the results are only valid if the sample is homogeneous. In addition, since the emission counted is from a particular excited state, the cross-section for the reaction only constitutes a fraction of the total cross-section for activation, which measures the total yield of radioactive product, irrespective of the excited states in which it was produced.

CHARGED-PARTICLE REACTIONS

The main applications of charged-particle reactions for analysis have been the determination of the light elements. The height of the Coulomb barrier precludes the determination of the heavier elements except by the use of very high-energy bombarding beams.

The course of a nuclear reaction can be represented diagrammatically as in Figure 1.

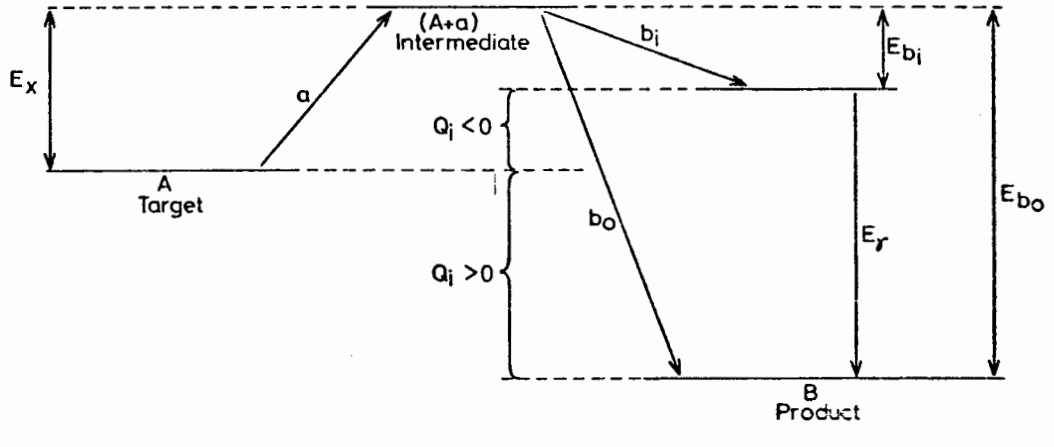

Figure 1. Schematic representation of the nuclear reaction A(a,bγ)B by compound nucleus formation showing the kinetic energies involved and the energies of the gamma-rays produced. E_x is the excitation energy of the compound nucleus, which is the sum of the binding energy and a term proportional to the kinetic energy, E_a, of the bombarding particle.

The target nucleus A is bombarded with particle a of energy E_a. At the time the reaction occurs it may be considered that an intermediate nucleus is produced from which prompt particles are emitted to produce the product nucleus B, either in its ground state or an excited state. The energy of the prompt particle b decreases as the excitation energy of the product B, increases. If the reaction yields excited nuclei the emission of prompt particles b_i will be followed by the decay of the excited levels to the ground state or some long-lived metastable state through the emission of prompt gamma-rays E_γ as shown in the figure. The Q_i-value for the reaction $A(a,b_i)B$ is given by the energy difference between the ground state of the target nucleus and the particular excited state i of the product B.

The spectrometry of the prompt gamma-rays resulting from charged-particle reactions has been used increasingly for elemental analysis. Much of this work has used the resonances which occur in the excitation functions of some reactions. The high cross-sections at the resonance energies have been utilised to increase the sensitivities of analysis, a technique which has been applied particularly to the analysis of fluorine, using the resonances in the reaction $^{19}F(p,\alpha\gamma)^{16}O$ [eg. Mo 67, Be 69, Ga 72 and Ma 73]. In this case the gamma-rays have such high energies (6-7 MeV) that very little background is observed and thus the analytical sensitivity is high. The use of beams having energies higher than the resonance energy permits the determination of the desired nuclide at that predetermined depth within the sample where the energy of the beam is reduced to the

resonance energy. Hence by changing the bombarding energy the concentration of the nuclide as a function of depth, that is, the concentration profile, can be determined.

Many of the lighter elements, and even as far as nickel, copper and zinc [De 73, Bo 77], have been analysed by the use of (p,γ) and other proton-induced reactions [eg. De 72a, Go 72]. However, little use has been made of alpha-particle bombardment. The Coulomb barrier for alpha particles is much higher than for protons or deuterons, hence at energies of a few MeV, alpha particles cause reactions with far fewer nuclei. Generally the cross-section for 5-MeV alpha particles falls to a negligible level if the atomic number exceeds 16, although reactions with vanadium (Z = 23) are reported here (Chapter III). When therefore alpha-particle induced reactions are used for analysis, interference from the heavier nuclides is much reduced.

COULOMB EXCITATION

The excitation of atomic nuclei to discrete (bound) low-lying energy levels (of the order of 1 MeV or less) by the Coulomb field of moving, heavy, charged particles is known as Coulomb excitation [He 56]. The occurrence of this type of process was claimed as early as 1921 [Sl 21] but it was not until 1953 that unquestionable evidence for the excitation of nuclei by the purely electromagnetic interaction between passing charged particles and the nuclear protons, was reported [Hu 53, Mc 53]. Since then, use of Coulomb excitation has revealed a number of new properties of

low-lying nuclear excited states and the method has become one of the most powerful tools for the study of many properties of stable nuclei.

There are essentially two methods for the detection of this inelastic scatter process :

(a) detection of the inelastic group or groups of particles, or

(b) detection of the radiation emitted from the excited nuclear state or states resulting from the nuclear encounter. This radiation consists of de-excitation gamma-rays and internal conversion electrons.

By far the most extensive research using Coulomb excitation has been carried out with protons and alpha-particle beams from Van der Graaff accelerators. The effect has only been observed in a few isolated instances under cyclotron bombardment, mainly because of the unfavourable background conditions. Generally the bombarding energy is limited to values well below the Coulomb barrier. In this way reaction and consequent formation of a compound nucleus is avoided, thus facilitating the interpretation of results.

An outstanding feature of the nuclear spectra revealed by Coulomb-excitation studies is the systematic occurrence throughout the periodic system of low-energy electronic quadrupole transitions of a strength greatly exceeding that which would be associated with excitation of a single nucleon [A1 56]. Most elements exhibit E2 transitions of a strength more than 10 times that for a single nucleon and in certain regions, transitions occur with a probability

exceeding this amount by a factor of more than 100. These enhanced transitions are due to the co-operative effects of a large number of nucleons and most of the observed levels can be interpreted in terms of simple collective excitations of a rotational or vibrational nature [A1 56].

The cross-sections for magnetic excitation are very much smaller than for electric excitation therefore, even in cases where the radiative de-excitation process takes place by a mixed M1 and E2 transition, the excitation will almost always be of E2 type [A1 56].

Although the *a priori* E1 excitation probability is typically some 300 times larger than that of E2 excitation with similar factors applying for successively higher multipolarities, there are two main reasons against the observation of these transitions [He 56]. These are :

(a) the scarcity of states of opposite polarity within a few hundred kilovolts of the ground state, and

(b) because even those relatively few E1 transitions which have been observed in the low-energy nuclear spectra have in most cases transition probabilities many orders of magnitude smaller than typical E2-type values.

By contrast E2 transitions are often strongly enhanced as mentioned earlier, thus it is that E2 transitions are of special importance in Coulomb excitation and the overwhelming majority of observed excitations have been of this type [A1 56]. The transitions therefore connect the ground state with excited states of the same parity and spins (respectively I_o and I*) which obey the selection rule $\rho \leq |I_o - I^*| \leq 2$ where

ρ = 2,1 or 0 according to whether I_o = 0, $\frac{1}{2}$ or $>\frac{1}{2}$ [He 56].

The only notable transition which is not of E2 in character is the weak E1 excitation of the 109-keV first excited state of ^{19}F [Sh 54, Mi 55]. The intensity of the 109-keV gamma-rays in the spectra shown in this work results from the cascading of other higher excited states decaying to the ground state by means of the 109-keV state.

The total cross-section for E2 excitation is given by [St 63]

$$\sigma_{E2} = \left(\frac{Z_1 e}{\hbar v_i}\right)^2 a^{-2} B(E2, J_i \rightarrow J_f) f_{E2}(\xi)$$

where a is half the distance of closest approach in a head-on collision, $B(E2, J_i \rightarrow J_f)$ is the reduced E2 transition probability (numerical values for many nuclides are tabulated in Ref. Al 56), $f_{E2}(\xi)$ is an integral taken over the classical orbits and $\xi = \frac{a\Delta E}{\hbar v_i}$ where ΔE is the energy of the excited state. The projectile has charge $Z_1 e$ and v_i is the initial relative velocity of projectile and target nuclei. Quantum-mechanical treatment only results in the replacement of $f_{E2}(\xi)$ with $f_{E2}(\eta_i \xi)$ where η_i is the Sommerfeld number. Numerical values for both $f_{E2}(\xi)$ and $f_{E2}(\eta_i \xi)$ may be found in Ref. Al 56 (and references contained therein).

In the case of thick-target Coulomb-excitation experiments the yield using protons is always larger than that obtained using heavier particles of the same energy, due to the longer range of the protons [Al 56]. However, there is a

good reason for the selection of alpha particles as the means of excitation. The background radiations produced by alpha-particle bombardment are, in general, considerably smaller than those produced by protons. This background arises from nuclear reactions leading to the same gamma-ray transition or to other gamma-rays causing undesirable background in the detector. In addition, bremsstrahlung from the bombarding particle gives rise to a continuum of gamma radiation and characteristic X-rays are emitted from the target. All these effects are minimised by the use of the heavier particles [He 56].

An appreciable fraction of the X-radiation emitted under bombardment is projectile-independent. It results from the filling of an electron site vacated by the internal conversion of a Coulomb-excited gamma transition. For example, in the case of ^{181}Ta excited by alpha particles, nearly all of the Ta K X-rays are accounted for by this process [He 56].

NOMENCLATURE OF GAMMA-RAYS

Prompt gamma-rays are emitted from the product nucleus of a reaction but the analyst is really concerned with that component of the sample on which the nuclear reaction was carried out. Accordingly, for analytical purposes, it is more meaningful to label spectral peaks with the target nucleus. In defining the conditions of the analysis the nature of the bombarding beam is known, and need not be stressed, thus the reaction is uniquely identified if the

light product particle is given. Accordingly the following convention is used for peak assignment [Pe 74].

In the nuclear reaction A(a,bγ)B, peak assignment is written Ab(r,s) where b is the prompt light particle of the reaction and the gamma-ray quantum is emitted by the de-excitation of the heavy product from level r to level s. If the target nucleus can be inferred unambiguously it may be omitted.

An example of the use of this convention is illustrated in Figure 2.

When the gamma-ray peak under consideration arises from a reaction not directly induced by the incident beam then both incident and product particles are specified.

All prompt gamma-ray peaks in spectra reported here are labelled according to this convention.

CORRECTING FOR RANGE EFFECTS

When charged particles are used to analyse thick, homogeneous samples, the yield of the measured nuclear product depends on the number of nuclei of the required element encountered along the path of the bombarding beam. This number is itself determined by the concentration of the element and the range of the bombarding particles in the target material. Since analysts are usually interested in the concentration, a knowledge of the range is required. Because this parameter is difficult to determine one usually resorts to one of the

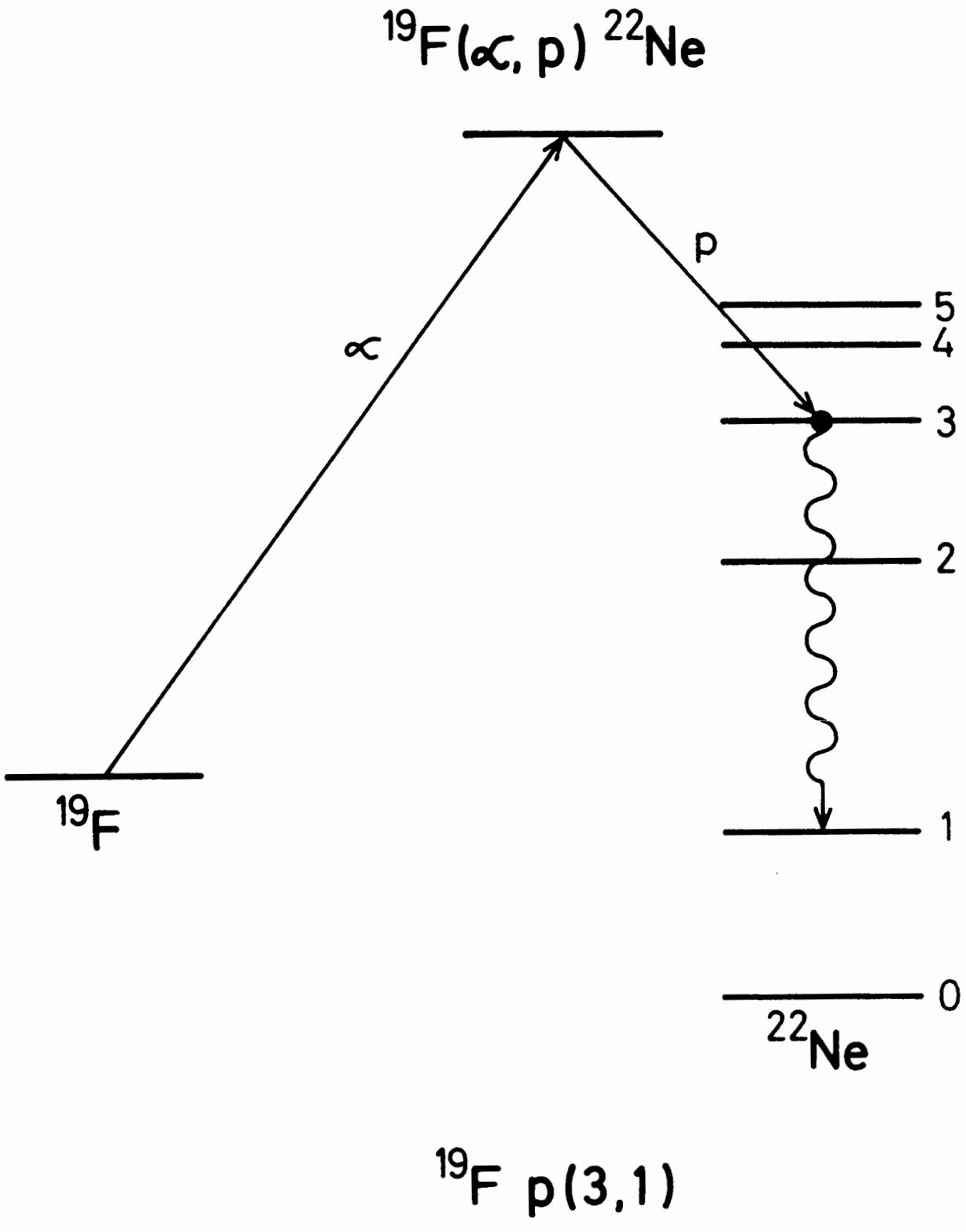

Figure 2 An example of the convention for labelling prompt gamma-rays, when the bombarding particle is implicitly known.

following three approaches :

(a) the experimental procedure of the "equivalent thickness" method [En 65];

(b) the semi-empirical calculation of the "average cross-section" method [Ri 65, Ri 67];

(c) comparison with standards [Si 60], where it is assumed that the stopping power of the standard is approximately equal to that of the unknown sample.

None of these procedures can be used alone when the composition of samples in a batch is unknown and varies markedly, but the number of samples of any one type is too small to warrant the manufacture of a suitable comparison standard.

If it is assumed that only the major components of a complex matrix contribute appreciably to its stopping power, and that the error introduced by ignoring minor and trace components is negligible compared to the accuracy of the analysis being undertaken, it then becomes possible to carry out a range correction. Use of the method of the "average cross-section" relates the range in the matrix, to the weight fractions of, and ranges in, each of its component elements. The latter ranges may be obtained from tables calculated for the elements [Wi 66, No 70]. The empirical composition may be deduced from a Rutherford backscattering spectrum of the thick target, by consideration of backscatter events in the surface and near-surface layers of the target where penetration is minimal and energy losses within the sample can be neglected. A disadvantage of using Rutherford backscattering is the fact that the backscatter cross-

sections for light elements are relatively very small. However, the ease with which the heavier elements can be determined and an empirical composition deduced are such important advantages that they outweigh the above disadvantage. In addition, it is seldom that the nature of the sample is entirely unknown. In many metal samples, for example, the analyst knows that he can safely ignore the presence of light elements in range calculations because their concentrations are too low to affect the accuracy of his result. On the other hand, geological material is likely to contain oxides, the presence of which can safely be taken into account from a knowledge of the metal composition, even though the observed spectrum gives only slight indication of the presence of oxygen because of its low backscatter cross-section.

Principle of the method

The use of the prompt products of charged-particle irradiation for the analysis of a given element is based on the fact that the number of such product particles is directly proportional to the number of atoms of that target element present in the sample. Generally applications of prompt-product spectrometry rely on bombardment of standards of known composition under the same conditions as the sample, thus relating induced activities to concentrations by a comparator technique. However, whilst neutrons and photons penetrate matter easily, enabling sample sizes to be chosen such that flux variations and energy distribution changes are negligible, charged particles are easily

stopped. Ranges of 5-MeV alpha particles in common materials are typically of the order of 44 μm (calcuim) and hence the nuclear reaction cross-section varies with depth as the charged-particle energy is degraded in the sample.

The stopping power $-dE/dx$ of a given medium [Ri 72] is given by $-\frac{dE}{dx} = \frac{\nu K Z^2 M}{E} \ln\left(\frac{4mE}{Mi}\right)$ where $\underline{E}$, $\underline{M}$ and $\underline{Z}$ are the kinetic energy, mass and atomic number of the incident charged particle, $\underline{\nu}$ and $\underline{i}$ are the number of electrons per unit volume and the effective ionization potential of the sample and $\underline{K}$ is a constant,

$$K = \frac{2\pi e^4}{m}$$

where $\underline{e}$ and $\underline{m}$ are the electron charge and mass respectively. The stopping power therefore depends on the nature of the matrix (ν,i) as well as the nature (Z,M) and kinetic energy (E) of the bombarding particle.

The method of the "average cross-section" is one of the current techniques used for the mathematical treatment of charged-particle activation analysis [Ri 72]. This makes use of the "theorem of the averages" to define an average cross-section $\bar{\sigma}$,

$$\bar{\sigma} = \frac{\int_0^R \sigma_x dx}{\int_0^R dx}$$

which reduces to

$$\bar{\sigma} \simeq \frac{\int_0^{E_o} \sigma_E E dE}{\int_0^{E_o} E dE}$$

Consequently the average cross-section $\bar{\sigma}$ is approximately independent of the nature of the target material and constant for a given nuclear reaction (σ_E) and particle energy (E_o) over the total range $\underline{R}$. It has been shown [Ri 72] that the total variation of $\bar{\sigma}$ for $\underline{Z}$ from 4 to 95 is no larger than 8%.

For the irradiation of a thick target, the activity induced, dA[disintegrations per second], for a given element at saturation within the differential layer dx at a depth x[gcm^{-2}] of the sample is given by

$$dA = nI\sigma_x dx$$

where the reaction cross-section, $\underline{\sigma}$, at depth $\underline{x}$, is expressed in cm^2, $\underline{n}$ is the number of sought nuclei per gram of target material and the beam intensity, $\underline{I}$, is expressed in particles per second as deduced from the measured beam currents [Ha 69].

If it is assumed that the sought element is uniformly distributed throughout the sample the total absolute activity induced at saturation

$$A = nI\int_0^R \sigma_x dx \qquad (1)$$

Since the range

$$R = \int_0^R dx$$

and

$$\int_0^R \sigma_x dx = \bar{\sigma}\int_0^R dx = \bar{\sigma}R$$

then from (1) it follows that

$$A = nI\bar{\sigma}R$$

Therefore since $\bar{\sigma}$ is approximately independent of the nature of the irradiated matrix the activities induced in sample (A) and standard (A_s) may be compared by writing

$$\frac{A}{A_s} = \frac{nIR}{n_s I_s R_s}$$

which leads directly to the more practical expression

$$\frac{a}{a_s} = \frac{cIR}{c_s I_s R_s} \qquad (2)$$

where $\underline{a}$ and a_s are the measured count rates and, $\underline{c}$ and c_s the concentrations of the nuclide under consideration in sample and standard respectively.

The values of the range $\underline{R}$ can be obtained from tables, interpolating where necessary, and using the expression [Fr 64]

$$\frac{1}{R} = \frac{w_1}{R_1} + \frac{w_2}{R_2} + \frac{w_3}{R_3} + \cdots\cdots\cdots \qquad (3)$$

which relates, approximately, the range R_i of an element and its weight fraction w_i in a compound or mixture, to

the range $\underline{R}$ in the complex matrix.

It follows therefore that provided the weight fraction of each component is known, the method of the "average cross-section" provides a means of correcting for range effects in charged-particle analysis of thick targets.

It has been shown [Gi 77] that Rutherford backscattering can provide sufficient data for characterisation of the major components of a thick target. These components largely determine the stopping power of the matrix and hence the range of the bombarding particles. The contribution provided by minor and trace components is small and the error introduced by ignoring it is negligible compared to the accuracy of the analysis.

When a monoenergetic beam of charged particles with energy $\underline{E}$ is scattered from the surface atoms of a target the energy $\underline{E}'$ of the backscattered particle is given by

$$E' = E\left(\frac{M_1\cos\theta + M_2\cos\alpha}{M_1 + M_2}\right)^2$$

where M_1 and M_2 are the masses of the bombarding and target nuclei respectively, $\underline{\theta}$ is the angle between the direction of incidence of the bombarding beam and the direction in which the scattered particle is observed. The difference between the centre-of-mass and laboratory scatter angles, $\underline{\alpha}$, is given by

$$\sin\alpha = \frac{M_1}{M_2}\sin\theta$$

The Rutherford cross-section for elastic scattering (σ)

is given by the expression

$$\sigma = \left(\frac{Z_1 Z_2 e^2}{4E}\right)^2 \cdot \frac{1}{\sin^4\left(\phi/2\right)} \cdot \left(\frac{M_1 + M_2}{M_2}\right)^2 f(M,\theta) \qquad (4)$$

where $f(M,\theta) = \left(\frac{M_1 \cos\theta + M_2 \cos\alpha}{M_2^2 \cos\alpha}\right)^2$

and $\phi = \alpha + \theta$, $\underline{Z}$ is the atomic number, $\underline{e}$ the charge on the electron and, 1 and 2 refer to the incident and target nuclei respectively.

When thick targets are bombarded the incident beam loses energy along its path through the material to the scatter site, after which the scattered particle again loses energy until it escapes from the target. The energy of the detected particle thus ranges from $\underline{E}'$ to almost zero, depending on the depth of the scatter site below the surface. The energy spectrum of the scattered particles therefore appears as a series of plateaux separated from each other by steps. The energy corresponding to the inflexion point of a step is used to determine the mass number of the component, whilst the height of the step is proportional to the atomic concentration at the surface of the matrix. If it is assumed that the target is homogeneous then the elemental composition of the surface is representative of the bulk of the sample.

In equation 4 the quantity $\left(\frac{e^2}{4E}\right)^2$ is a constant for a given bombarding beam, thus a value for the scatter cross-section may be calculated using that equation for each

element revealed by the scatter analysis, in terms of this constant. Then, using the measured heights (h) of each step, the relative atomic concentrations, n_i/n_j of any two elements i and j in the sample can be calculated from the relation

$$\frac{n_i}{n_j} = \frac{h_i}{h_j} \cdot \frac{\sigma_j}{\sigma_i}$$

and therefore the elemental fraction w_i of element i,

$$w_i = \frac{n_i}{\sum n}$$

By this means approximate analysis of samples is possible without the use of standards since all the elements in a particular target are determined from a single bombardment. A computer programme SCATER has been written which computes the w_i values when given the quantities h_i, M_i and Z_i. From these data and with the use of equation 3 the range of the bombarding particle in the complex matrix can be calculated. Once the ranges in both standard and sample are known the concentration c of the sought element may be obtained from equation 2.

In practice, the scatter spectrum is differentiated [Pe 73], the differential then consists of a series of peaks the maxima of which correspond to the energies of the inflexion points at the steps of the original spectrum, whilst the areas under the peaks correspond to the step heights. Such spectra can be handled easily by available computer programmes and areas under peaks readily integrated.

Because of the difficulty of determining the exact energy

corresponding to any given inflexion point in the spectrum, an error of a few units of atomic number is possible. However it is assumed that the stopping powers of elements of approximately equal atomic number would be sufficiently alike and acceptable within the error of determination. It is irrelevant therefore, for the purpose of range correction, whether the elements are correctly identified or not. It is only important that the bombarding beam behaves as if these elements are present in the observed proportions at the bombarded spot on the target.

Applications of this method of range correction are to be found in Chapter IV.

SCOPE OF THIS INVESTIGATION

To date the use for analysis of prompt gamma-ray spectrometry, has been limited largely to utilisation of the few suitable resonance reactions [eg. Be 69, De 72b]. Coulomb excitation by means of proton bombardment has only recently been applied to analytical problems [eg. Ch 72, De 72b, De 72c, Co 72, Ru 74]. However the advantages of using alpha particles have been recognised [Gi 75] and, indeed, prompted this investigation.

A study of those prompt gamma-rays emitted under alpha-particle bombardment was undertaken. Beams with energies of 5 MeV and 11 MeV were supplied by the Van der Graaff accelerator of the Southern Universities Nuclear Institute (SUNI) whilst those of 16 MeV were obtained using the Tandem Van der Graaff of the Nuclear Physics Research Unit,

University of the Witwatersrand, Johannesburg.

A survey of 56 elements was carried out using 5-MeV alpha-particle bombardment and most of these elements were also irradiated using the higher energy beams. A catalogue of observed gamma-rays was drawn up which lists their calculated interference-free sensitivities for analysis.

Several gamma-rays offered sufficiently high sensitivities to permit their use for the determination of their parent elements. Analysis of fluorine in cements and of nitrogen, manganese and vanadium in steels was carried out using prompt gamma-ray spectrometry.

In addition, a compilation in numerical order of all observed gamma-rays was produced in order to facilitate their identification and indicate possible interferences.

CHAPTER II

EXPERIMENTAL

INTRODUCTION

For any analytical procedure to have ready applicability to everyday problems, minimal sample handling is desirable since clearly the fewer the steps involved in the preparation of the specimen for analysis, the less the chance of introducing error. In addition, there are occasions requiring the analysis of samples that may not be degraded in any way whatsoever. For the above reasons, the sample preparation methods used in these analyses involved only such treatment as was required for convenience. The use of pills was a convenient means of handling the materials under investigation, but since all the targets used were of infinite thickness with regard to the bombarding particles, the targets could, and on occasion did, take other forms.

PREPARATION OF SAMPLES

The preparation of the samples largely depended upon their original form. A large number of the materials used for the survey were plates of the pure metal, typically 25 mm square and with a mass of about 1.5 g. These were simply cleaned by boiling with absolute alcohol and mounted directly onto the target holder.

Most other samples were in granular form. These materials were crushed and approximately 1.5 g portions were pressed into pills with a diameter of 13 mm, using a Beckman 13 mm KBr die and 25-ton hydraulic press. The system used is

shown in Figure 3. Paper rings were used to give the pills some additional mechanical strength and in addition the use of paper discs was found to eliminate virtually any possibility of cross-contamination without necessitating lengthy cleaning procedures between samples. Their use also served to protect the die from damage by small crystals of some of the harder materials.

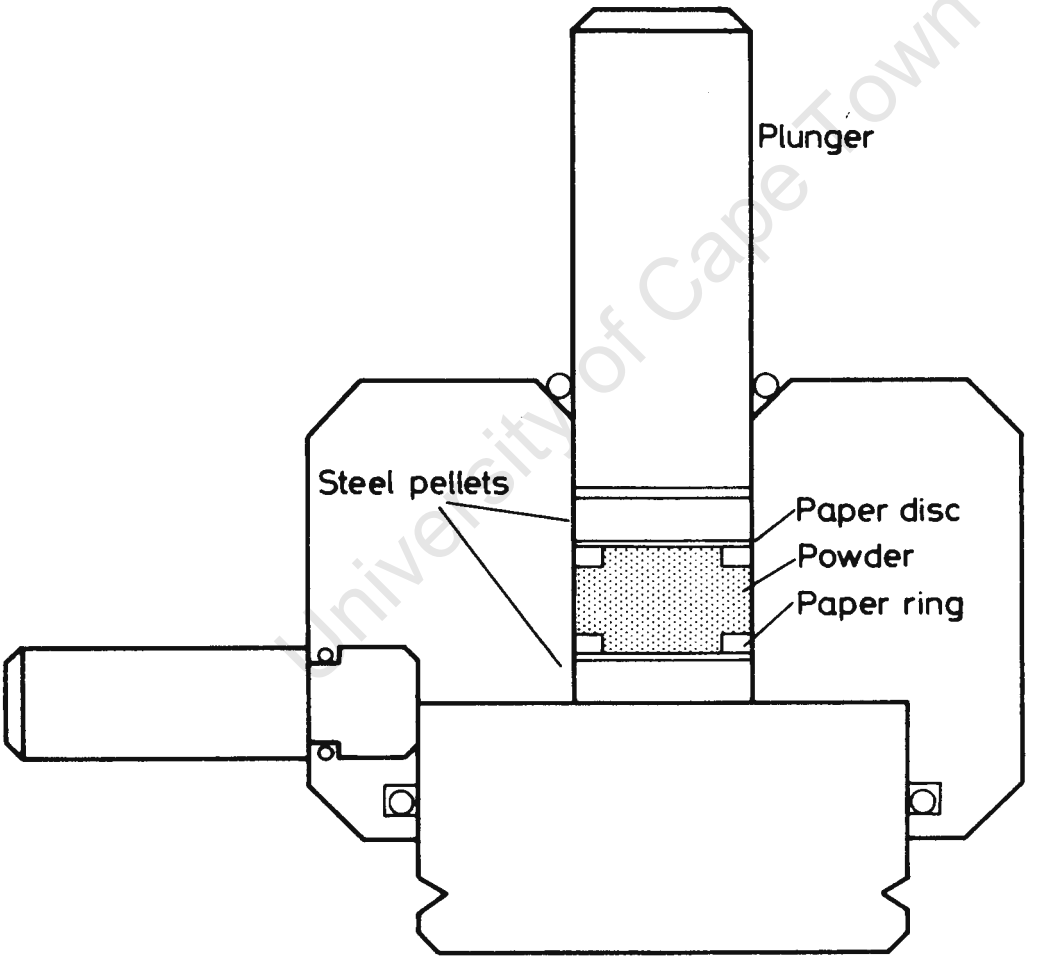

Figure 3. Schematic representation of the die used for making target pills

Compression of the material was carried out under vacuum to remove trapped air. The maximum pressure employed was 10 tons since this was the maximum permissable for the die used. The length of time for which the powder was compressed was found to have little apparent effect, thus, once the limiting pressure was reached, it was only held for about a minute.

Some of the powdered samples would not press into pills. A number of these materials were mixed with KBr or borax prior to pressing, allowance subsequently being made for the known amount of binding material.

Some of the samples were expensive pure materials which for that reason could not be mixed with binder and an alternative preparation procedure had to be used. Cells of aluminium were constructed as shown in Figure 4. The window material was KAPTON, $(C_{22}H_{10}N_2O_4)_n$, obtainable from the du Pont Corporation, U.S.A., and a cell was prepared with new windows for each sample. At 5-MeV bombarding energy the energy loss due to the window was of the order of 800 keV. Each cell when filled contained about 0.5 g of powder, the amount was not important as long as it occupied an area greater than that of the beam spot. To prevent ejection of the powder when pumping vacuum or under bombardment, a fine mesh gauze was cemented over the top of the filled cell.

The steel samples used were obtained from the U.S. Bureau of Standards. They were machined into discs 2 mm thick and up to 13 mm in diameter, depending on their original size. The smaller discs were pressed into aluminium rings to make

them up to 13 mm diameter. Their faces were mechanically polished and then carefully cleaned with absolute alcohol before mounting into the target holder.

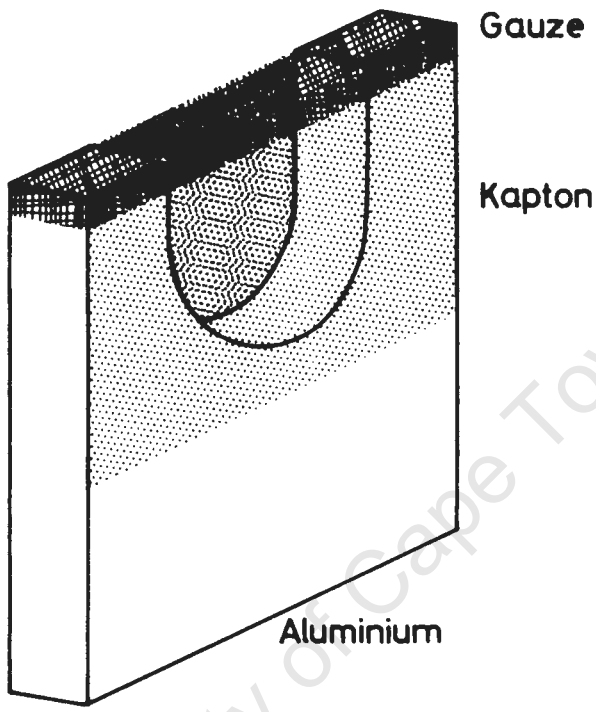

Figure 4. Irradiation cell for bombardment of powders

MIXING OF POWDERS

The preparation of homogeneous samples of known fluorine content over a wide concentration range was investigated. There are three main ways of obtaining such standards; by using gases, solutions or solid mixtures.

An attempt was made to use gaseous fluorides at various known pressures. These irradiations had to be carried out in a special gas cell thus necessitating a completely different geometrical arrangement of the apparatus, including

the detector. Because of this the results obtained from the gases were not directly comparable with those obtained from the solid samples and so the method was rejected.

Standard solutions would appear to be the most obvious and accurate way to prepare homogeneous standards. Liquid-vacuum coupled systems however present many experimental problems solving which would not have added to this investigation.

It was therefore decided to prepare the standards in the solid state by mixing together a fluoride and a relatively inert material, in this case, calcium hydroxide. Since errors could possibly be introduced on mixing small amounts of material with much larger amounts it was decided to work with components each having a total mass of about 20 g. Three initial mixtures were prepared having calcium fluoride:calcium hydroxide ratios of 1:1, 1:3, 3:1. The other mixtures were then prepared by diluting these with pure calcium hydroxide and so on.

Another series of solid state mixtures was made by mixing together weighed amounts of sodium fluoride and calcium hydroxide in n-hexane. The suspension was kept under agitation with an ultrasonic generator for half an hour. The hexane was then removed by evaporation over a steam bath. It was assumed that since the particles of sodium fluoride and calcium hydroxide were of similar size and density, there was no reason to expect any preferential deposition.

The two series of samples produced in this way were pressed into pills prior to analysis.

THE ELECTRONIC MEASURING SYSTEM

A block diagram of the electronic system is shown in Figure 5. Essentially there were three separate measuring systems counting gamma-rays, charged particles and neutrons. The gamma-ray spectra for the analysis were acquired using a 50 cm^3 Ge(Li) detector. The charged-particle data were used to obtain information on the major elements in the sample matrix, whilst the neutron counter provided continuous neutron monitoring. Spectra were accumulated in a multi-channel analyser and subsequently written onto magnetic tape, for off-line processing.

THE SCATTERING CHAMBERS

The irradiations at 5 and 11 MeV were carried out in a scattering chamber specially designed for analytical purposes. Although constructed for simultaneous use with five detectors (see Figure 6) in this investigation only the surface barrier and Ge(Li) detectors were used. The wall of the chamber immediately in front of the Ge(Li) detector was thinned to reduce the absorption of gamma-rays. The target holder, which could take four samples was positioned in the centre of the chamber at right angles to the beam. The time required to break vacuum and insert four new targets was of the order of twenty minutes.

Since it was essential that the total bombarding current be accurately integrated the chamber was constructed as a self-contained Faraday cup, electrically insulated from the beam tube and from all the detectors. Collimation of the

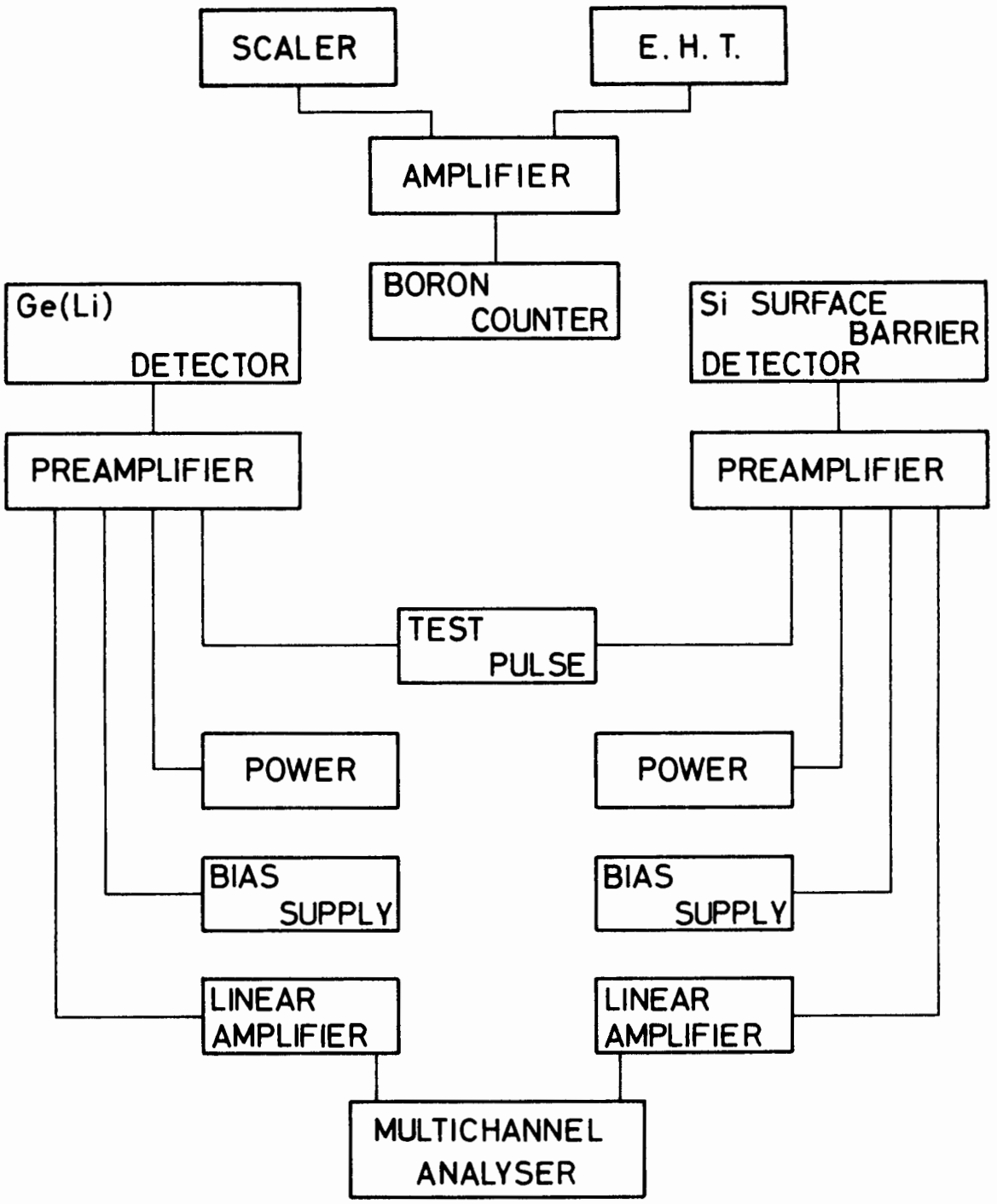

Figure 5 Block diagram of electronic equipment used for gamma, particle and neutron measurements.

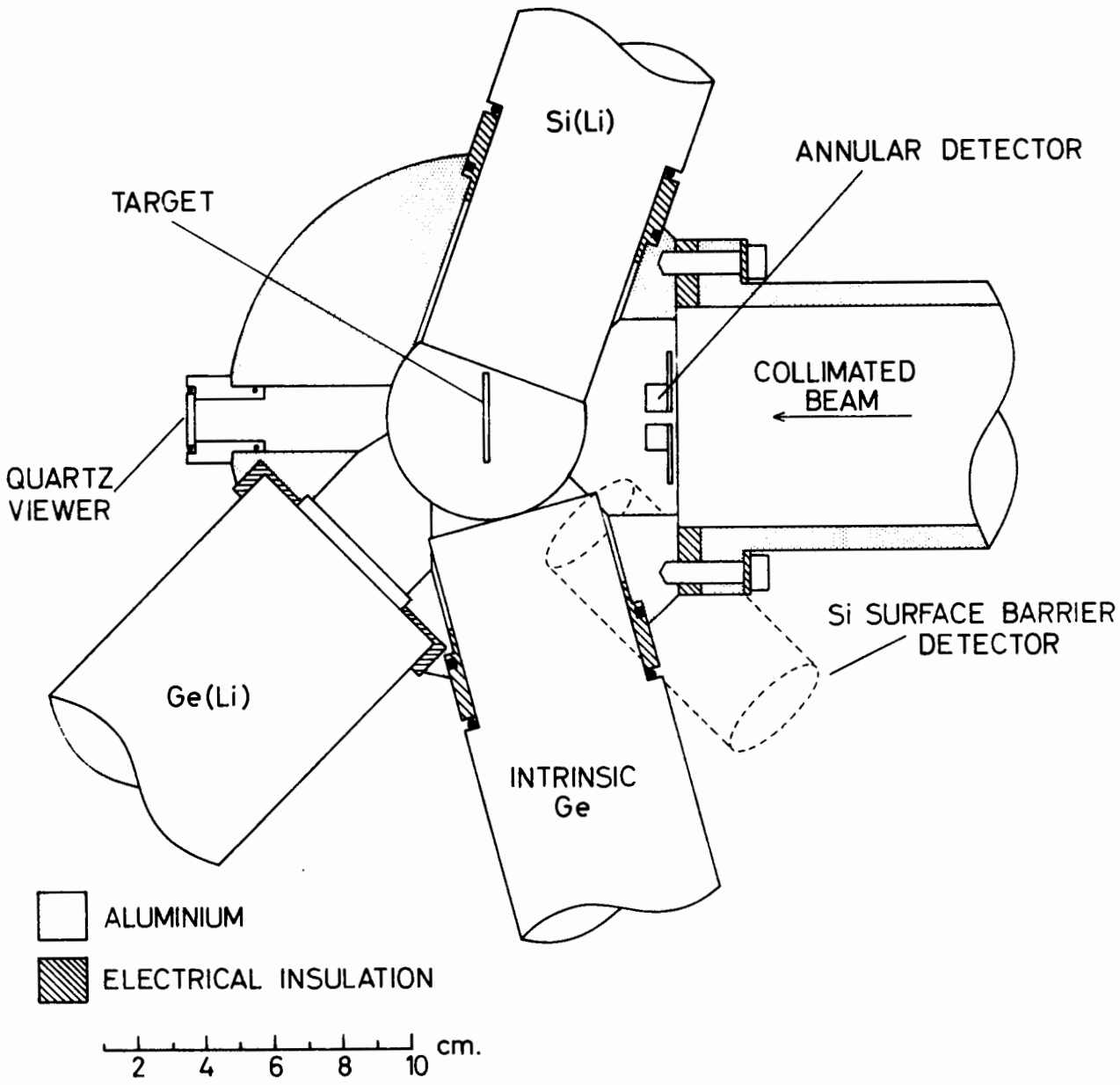

Figure 6 Insulated scattering chamber specially constructed for analytical use with up to five different detectors.

bombarding beam was achieved initially, 49 cm from the target, with tantalum collimators, and the beam-spot size was defined by another collimator positioned in the beam tube just outside the chamber. The beam entered the chamber through an aperture about 5 mm in diameter in front of which was placed an anti-scatter collimator electrically insulated and charged to -300 V, to prevent secondary electrons from entering the chamber. Secondary electron loss from the target could take place at two points, through the beam-entrance aperture and through the collimator in front of the surface-barrier detector, but their combined solid angle subtended at the target was negligibly small. For all the survey and quantitative studies at the two lower energies, *viz.* 5 MeV and 11 MeV, the beam-spot defining collimator was made of copper.

The scattering chamber used for the survey carried out at 16 MeV was essentially similar. Only two targets could be mounted at one time, the target holder being rotated through 180^{o} to bring the second target into the beam. Measurement of the gamma-rays was carried out at 90^{o} to the incident beam direction. Current was measured directly from the target holder. Since the copper collimator was found to give a high gamma-ray background with beams of this energy, a lead-backed tantalum collimator was used.

IRRADIATION

The samples were irradiated at 5 MeV and 11 MeV by beams of $^{4}He^{+}$ and $^{4}He^{2+}$ ions respectively, obtained from the 6 MV Van der Graaff accelerator at SUNI. The irradiating

COMPUTER PROCEDURES

With the ready availability of fast on-line and off-line computers a large proportion of data handling has been taken over by computer programmes, so much in fact that these programmes may be regarded as part of the experimental procedure.

Little use was made of on-line processing except that a PDP-15 computer was used to supply information such as peak positions, energy calibrations and peak integrals to assist in the actual running of the experiments. All the spectra were recorded onto magnetic tape for off-line processing which was carried out on the UNIVAC 1106 at the University of Cape Town.

During this study several new computer programmes were written, and some older ones re-written, in FORTRAN V for the UNIVAC. This was done so that a "modular" system of programmes could be produced. Such a system facilitates the writing of programmes since the main programme which controls the entire processing of the data, merely calls the required sub-routines. New sub-routines, each performing one specific task, are easily written. By simply adding and removing sub-routines, the main programme remains essentially unaltered, but can be made to perform different tasks. Sub-routines written or re-written into this form are shown in Table 1 together with the function of each.

Table 1. Computer routines written for this investigation

Name of Routine	Task Performed by Routine
ADITON	Adds any number of spectra together channel for channel.
CALRTO	Calculates the fractional elemental composition from scatter data.
CRSECT	Calculates the Rutherford backscatter cross-section for given elements.
DERIVE	Takes the derivative of a spectrum according to the method of SAVITZKY and GOLAY [Sa 64].
DERSIG	Calculates the value of the differential divided by the standard deviation of the smoothed data.
INTGRT	Carries out peak integration and background subtraction for given peaks.
READTP	Controls the reading of data off magnetic tape, spectrum by spectrum.
SMOOTH	Smoothes spectra channel for channel by the method of SAVITZKY and GOLAY [Sa 64].
SPCLSD	Prints a spectrum in floating format.
SPRINT	Prints a spectrum in integer format.
Non-Modular Programmes	
QSORT	Sorts Q-values into ascending order.
SMOSPC	Smoothes data and subtracts neutron and natural backgrounds on the basis of the monitored neutron count and live-time respectively.

DETERMINATION OF GAMMA-RAY YIELDS

Covell's method [Co 59] was normally used for the determination of the total areas under gamma-ray peaks. The method of trapezoidal subtraction, illustrated by Figure 8, was used for subtraction of the background from the peak integral. Both functions were performed by the computer routine INTGRT.

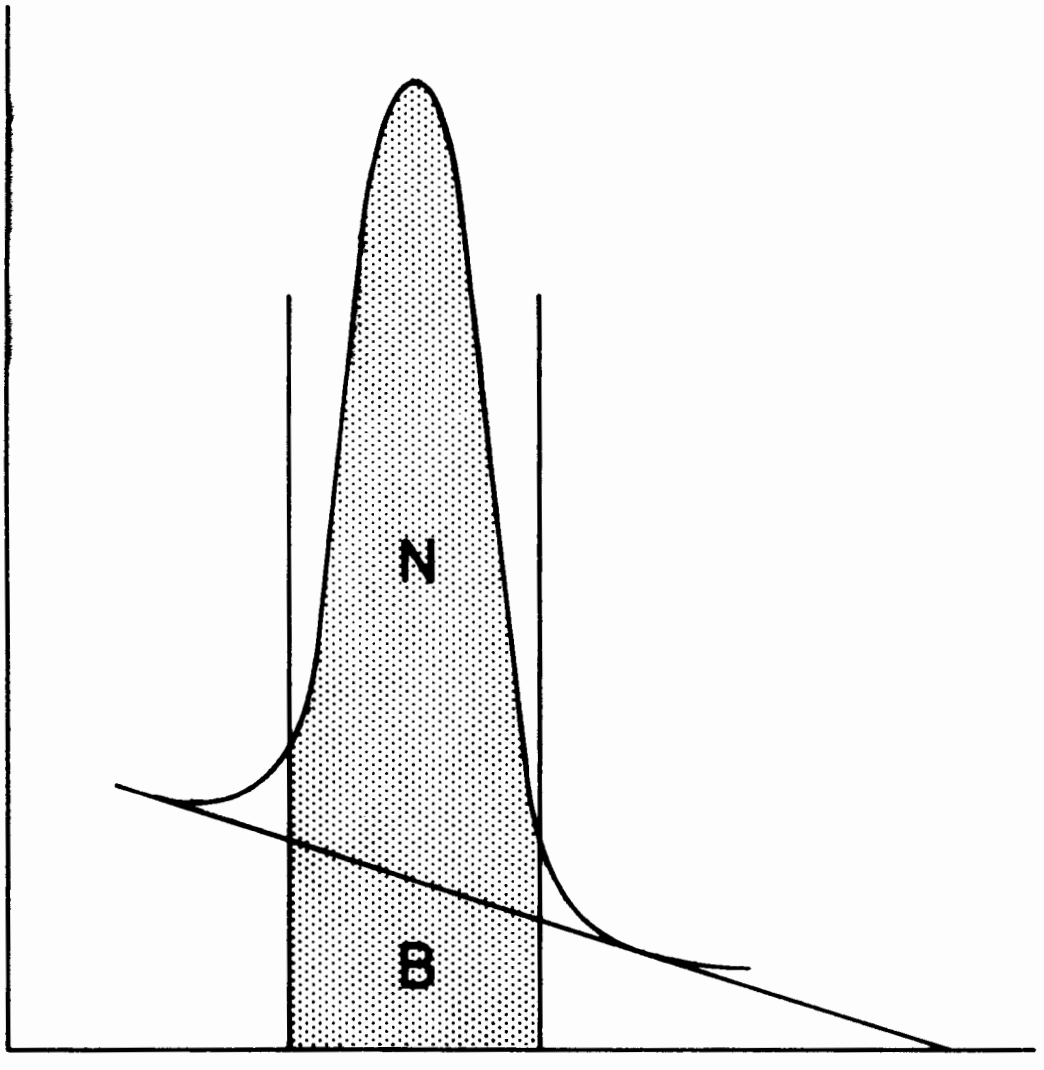

Figure 8 Covell's method for peak integration. The shaded area gives the total integral between the energy limits of integration. The nett count, N, is obtained by trapezoidal subtraction of the peak background, B, from the total. The slope of the presumed background is given by the mean spectrum height on either side of the peak. The unshaded areas above the background line are presumed, in this approach, to be a constant fraction of the nett area.

Chapter III

Survey of the Elements

INTRODUCTION

In order to ascertain the applicability of alpha-induced prompt gamma-ray spectrometry to elemental analysis, an empirical survey of gamma-ray spectra was found to be essential, since no similar work existed in the literature. What information was available was widely scattered over many investigations, each carried out at energies of interest to the particular nuclei studied. The most important part of the study here was carried out using 5-MeV $^{4}He^{+}$ ions, with supplementary data from irradiations using 11-MeV and 16-MeV $^{4}He^{2+}$ ions.

Before the peaks observed in the spectra could be identified, a thorough knowledge of the gamma-ray background, both radioactive and prompt, was necessary. Without prior information on the background gamma-rays, calculations of sensitivities would be open to error and peak assignments could be invalid.

GAMMA-RAY BACKGROUND

Radioactive Background

In general a radioactivity background would be expected to consist of radiations from natural, cosmogenic and artificially produced radionuclides. The gamma-ray background recorded at SUNI shows radiation from radionuclides representing each of these types. Examples of this background, measured *in situ* are given on pages 75 and 76. These spectra

were accumulated for about 12 hours each, at widely separated times. Background A was recorded during the initial experiments, whilst B is representative of the background present during the major portion of this work. Table 2 lists the energies of all those gamma-rays observed, together with the source of the radiation and the origin of the radionuclide. Where the radionuclide is a member of one of a naturally-occurring decay series, the series name is given [Fr 64]. The exact gamma-ray energies were obtained from Ref. Er 75. Escape peaks are shown as gamma-rays with assignments : - (photopeak energy - m_e) and (photopeak energy - $2m_e$) for the first and second escape peaks respectively.

Natural Radionuclides

Gamma-rays were observed from radionuclides belonging to two of the natural decay chains, namely the 4n and (4n + 2) series, together with the 1461-keV gamma-ray from ^{40}K. These natural radionuclides are present as trace amounts in the materials used in the construction of the laboratory building. The ^{232}Th and ^{238}U parents of the decay series together with their daughters are also present in the unrefined lead which is used for shielding in large quantities. The (4n + 3) series has, as parent, ^{235}U which constitutes only 0.72% of natural uranium. It is not surprising therefore that no gamma-rays were observed from this series. The (4n + 1) series is short-lived with artificially produced parents.

Table 2 Assignment and origin of peaks in the radioactivity background spectra

E_γ (keV)	Assignment	Origin or Natural Decay Chain
61		
74	^{208}Bi ; ^{212}Pb	^{209}Bi(n,2n)^{208}Bi ; 4n unresolved Kα X-rays
86	^{208}Bi ; ^{212}Pb	^{209}Bi(n,2n)^{208}Bi ; 4n unresolved Kβ X-rays
91		
129	^{228}Ac	4n
186	^{226}Ra	(4n + 2)
239	^{212}Pb ; ^{214}Pb	4n ; (4n + 2)
277	^{208}Tl ; ^{228}Ac	4n ; 4n
285	^{214}Bi	(4n + 2)
296	^{210}Tl ; ^{214}Pb	(4n + 2) ; (4n + 2)
328	^{228}Ac	4n
339	^{228}Ac	4n
352	^{214}Pb	(4n + 2)
463	^{228}Ac	4n
478	^{7}Be	cosmic-ray produced
511	β^+ ; ^{208}Tl	various ; 4n
583	^{208}Tl	4n
604		
609	^{214}Bi	(4n + 2)
666	^{214}Bi	(4n + 2)
727	^{212}Bi	4n
769	^{214}Bi	(4n + 2)
795	^{210}Tl ; ^{228}Ac	(4n + 2) ; 4n
835	^{54}Mn	^{54}Fe(n,p)^{54}Mn by fast neutrons
844	^{27}Mg	^{27}Al(n,p)^{27}Mg by fast neutrons
861	^{208}Tl	4n
911	^{228}Ac	4n

Table 2 (continued)

E_γ (keV)	Assignment	Origin or Natural Decay Chain
935	^{214}Bi	(4n + 2)
969	^{228}Ac	4n
1120	^{214}Bi	(4n + 2)
1155	^{214}Bi	(4n + 2)
1223		
1238	^{214}Bi	(4n + 2)
1275		
1369	^{24}Na	^{27}Al(n,α)^{24}Na by fast neutrons
1378	^{214}Bi	(4n + 2)
1408	^{214}Bi	(4n + 2)
1461	^{40}K	0.012 atom % of natural K
1509	^{214}Bi	(4n + 2)
1588	^{228}Ac	4n
1592	(2614-2m_e)	^{208}Bi ; ^{208}Tl
1693	(2204-m_e)	^{214}Bi
1732	(2754-2m_e) ; ^{214}Bi	^{24}Na ; (4n + 2)
1756		
1764	^{214}Bi	(4n + 2)
1850	^{214}Bi	(4n + 2)
2103	(2614-m_e)	^{208}Bi ; ^{208}Tl
2204	^{214}Bi	(4n + 2)
2243	(2754-m_e)	^{24}Na
2614	^{208}Bi ; ^{208}Tl	^{209}Bi(n,2n)^{208}Bi by fast neutrons ; 4n
2754	^{24}Na	^{27}Al(n,α)^{24}Na by fast neutrons

Cosmogenic Radionuclides

Some naturally-occurring radionuclides have half-lives too short for them to have survived since nucleosynthesis as have the radionuclides mentioned in the previous section. They occur as a result of a balance between continuous production by cosmic-rays and removal by radioactive decay and geophysical processes. Of all the cosmogenic radionuclides, ^{7}Be has the highest average specific activity in the atmosphere [La 62], with the exception of ^{3}H and ^{14}C which are not gamma-active. The ^{7}Be is formed by cosmic-ray spallation reactions with oxygen and nitrogen [Du 72], and emits a 478-keV gamma-ray with a 53-day half-life.

Artificial Radionuclides

Radionuclides produced as a result of neutron and charged-particle bombardment also contribute to the general background. No gamma-rays were observed that could be ascribed to the products of charged-particle activation, however gamma-rays were observed from ^{24}Na, ^{27}Mg, ^{54}Mn and ^{208}Bi. These nuclides were produced by fast-neutron activation of materials present in the laboratory environment. The first pair of nuclides was generated by irradiation with neutrons from (α,n) reactions in the target, whilst the second pair of nuclides with longer half-lives accumulated as a result of periodic high fluxes of fast neutrons produced for other experiments in the laboratory.

The radionuclides ^{24}Na and ^{27}Mg were produced as a result of fast-neutron activation of the aluminium target chamber.

The former nuclide has a half-life of 15 hours whilst the latter decays with a 9.5-minute half-life. Both therefore would be expected to be formed, and to decay away, cyclicly, depending on the availability of a reasonable flux of fast neutrons on the aluminium. The absence of ^{24}Na in Background A may be ascribed to the spectrum having been recorded early in the experiment, before the nuclide had had sufficient time to accumulate. In the case of ^{27}Mg which has a fairly short half-life, even a limited exposure to a fast-neutron flux will be sufficient for the concentration of ^{27}Mg to reach saturation. The intensity of the gamma radiation then ensures that the corresponding peak accumulated during the rapid decay still stands out clearly in the spectrum, even if the measurement continues long after the radionuclide has decayed away.

^{54}Mn is produced as a result of fast-neutron activation of ^{54}Fe which constitutes 5.9% of all iron present. Its half-life is 312.5 days, which means that the radionuclide is continuously present in the laboratory. The cross-section for its production by the reaction $^{54}Fe(n,p)^{54}Mn$ is 210 mb for a neutron energy of 3.6 MeV [Va 61], compared to 0.02 mb for the corresponding reaction [Te 58] with ^{56}Fe. Because the half-life of ^{56}Mn is 2.58 hours all that may have been produced during periods of neutron irradiation would have decayed away again, resulting in the absence of its gamma radiation in the background spectra.

Bismuth has a high cross-section (2.3 barns [Ro 57]) for the reaction $^{209}Bi(n,2n)^{208}Bi$, the product of which is radioactive. Lead contains bismuth as one of its main

impurities and at the time Background A was recorded, large quantities of lead were used as shielding for the detector and the beam transport tube. The bismuth in the shielding, once activated, would remain because of the very long half-life of ^{208}Bi (3.68×10^5 years), each successive period of neutron irradiation contributing to the accumulation of the radionuclide. Removal of all lead shielding from the immediate vicinity resulted in the disappearance of the high-intensity lead Kα and Kβ X-rays which are the only identifying features of ^{208}Bi in the presence of ^{208}Tl. Although the lead was still present in the laboratory the intensity of the X-rays was reduced to the level of the general background because of the much reduced solid angle subtended by the lead at the detector as well as by absorption in various materials interposed between source and detector.

The occurrence of a peak corresponding to a gamma-ray of 1275 keV is ascribed to the presence, in the vicinity, of a ^{22}Na source. The other unlabelled gamma-rays derive from unknown sources.

Prompt Background

In addition to the background resulting from radioactivity, gamma-rays were observed during irradiation, which did not emanate from the target nuclei. These gamma-rays also posed a threat to the correct assignment of peaks and to the accuracy of the calculated sensitivities. It was not possible however, simply to obtain a "blank" spectrum, since, although most of these gamma-rays did not come from

the target, the presence of a target was necessary to generate them.

A list of all the prompt background gamma-rays is given in Table 3 together with their assignments and origins. They come from two main sources, the detector itself and the target chamber.

Fast neutrons resulting from (α,n) reactions in the targets were the main source of prompt background. Excitation of levels of ^{72}Ge, ^{74}Ge, ^{76}Ge and ^{19}F by inelastic neutron scattering and of ^{70}Zn by the reaction $^{73}Ge(n,\alpha)^{70}Zn$ contributed the neutron-induced gamma-rays observed in the spectrum. This response of the Ge(Li) detector to fast neutrons was studied systematically by Chasman *et al.* [Ch 65].

The germanium peaks corresponding to 596 + 608 (unresolved) and 691 keV are skew because the recoil energy is added to the transition energy [Ch 65]. These germanium gamma-rays are clearly seen in the spectrum of boron on page 78 in the next section. They are inevitably part of the background for any neutron-producing target and cannot be eliminated.

The presence of fluorine has already been discussed in Chapter II.

Alpha reactions with ^{14}N, ^{18}O, ^{23}Na and ^{27}Al gave rise to gamma-rays which were observed in the backgrounds of many spectra. Traces of nitrogen and oxygen were expected from adsorbed gases on the surfaces of some targets and

Table 3. Assignment and origin of peaks in the background spectra of prompt radiation

E_γ keV	Assignment	Origin
57	Ta Kα X-rays	chamber lining
66	Ta Kβ X-rays	chamber lining
110	^{19}F n,n'(1,0)	neutron bombardment of detector
136	^{181}Ta α,α'(1,0)	collimators and chamber lining
197	^{19}F n,n'(2,0)	neutron bombardment of detector
301	^{181}Ta α,α'(2,0)	collimators and chamber lining
322		
351	^{18}O α,n(1,0)	oxygen on target surface
417	^{23}Na α,n(2,0)	sodium contamination of target
440	^{23}Na α α'(1,0)	sodium contamination of target
511	β^+	various
563	^{76}Ge n,n'(1,0)	neutron bombardment of detector
596	^{74}Ge n,n'(1,0)	neutron bombardment of detector
608	^{74}Ge n,n'(2,1)	neutron bombardment of detector
691	^{72}Ge n,n'(1,0)	neutron bombardment of detector
718		
806		
834	^{72}Ge n,n'(2,0)	neutron bombardment of detector
844	^{27}Al α,α'(1,0)	scattered-alpha excitation of chamber
871	^{14}N α,p(1,0)	nitrogen on target surface
885	^{73}Ge n,α(1,0)	neutron bombardment of detector
894	^{72}Ge n,n'(4,2)	neutron bombardment of detector
1015	^{27}Al α,α'(2,0)	scattered-alpha excitation of chamber
1214	(2236-2m_e)	^{27}Al
1406		
1464	^{72}Ge n,n'(3,0)	neutron bombardment of detector
1725	(2236-m_e)	^{27}Al
1809	^{23}Na α,p(1,0)	sodium contamination of targets
2236	^{27}Al α,p(1,0)	scattered-alpha excitation of chamber

the gamma-ray yields of the reactions $^{14}N(\alpha,p\gamma)^{17}O$ and $^{18}O(\alpha,n\gamma)^{21}Ne$ were sufficient for their presence to be observed. Sodium, observed as a result of gamma emission following $(\alpha,n),(\alpha,p)$ reactions and inelastic alpha scattering on ^{23}Na, was present in small quantities in some of the powdered compounds used as targets, notably potassium bromide.

The scattering chamber used in the analysis was manufactured from aluminium, thus the formation of gamma-rays from Coulomb excitation and (α,p) reactions was predictable. These reactions occur after scattering from the target and may be eliminated from the spectra by means of a cobalt or nickel chamber lining. It is possible that a proportion of the yield for the 844- and 1015-keV gamma-rays was the result of inelastic neutron scattering as well as inelastic alpha scattering. This contribution would, of course, not be removed by a chamber lining.

In the early part of this work a scattering chamber was used which had a tantalum lining. Spectra taken at that time showed prominent peaks corresponding to the Kα and Kβ X-rays of tantalum : - see for example the spectrum of aluminium on page 84. The lining was subsequently removed but spectra still showed the 136-keV and, to a lesser extent, the 301-keV gamma-rays from inelastic alpha scattering on the tantalum collimators used for initial beam collimation. These gamma-rays could be eliminated by the use of nickel or cobalt collimators which, under the conditions of the experiment, emit little

or no gamma radiation. Whilst these metals do not have as high a melting point as tantalum, they should be well able to withstand the beam currents used in this work.

SURVEY RESULTS

The following section constitutes an element-by-element commentary on the results of the survey as reflected in the Atlas of Spectra and the Catalogue of Gamma-Rays. It was felt that the data given in these sections are largely self-explanatory and remarks were kept to a minimum in order to avoid excessive repetition. The object of this work was to provide extensive information showing the analytical applications of the method of prompt gamma-ray spectrometry and as many of the likely interferences as possible. All the data provided were empirical and no special or separate experiments were conducted with the object of investigating the presence or absence of particular gamma-rays in the spectra. Explanations offered therefore, in respect of some arbitrary assignments of gamma-rays, have not been experimentally substantiated nor was it the purpose of this work to do so.

A list of all gamma-rays observed in the spectra obtained with 5-MeV alpha particles, as well as those from carbon and oxygen using the higher energy beams, is given in order of ascending energy as an appendix. This list provides a rapid means of identification of gamma-rays as well as providing an indication of those gamma-rays which could interfere in an analysis.

The elements bombarded, for each incident beam energy, are shown in Figure 9(a), (b) and (c).

Lithium (Z=3) : - The target used was lithium fluoride powder compressed into a pill. Only one gamma-ray assignable to lithium was observed. This gave a very intense peak corresponding to 478 keV resulting from Coulomb excitation of the first level of ^{7}Li. The sensitivity obtained was high thus offering good analytical potential, especially in such materials as geological ores.

Boron (Z=5) : - Irradiation of a target of pure boron resulted in many gamma-rays, some fairly intense. The majority of the peaks in the spectrum were due to the reaction $^{10}B(\alpha,p\gamma)^{13}C$ which has a Q-value of 4.063 MeV. One intense peak, corresponding to 2313 keV, together with its first and second escape peaks, was due to the reaction $^{11}B(\alpha,n\gamma)^{14}N$ with a Q-value of 0.157 MeV. The energy of the first excited state of ^{11}B is high (2125 keV) so only the fairly low-lying first level of ^{10}B was excited directly. Gamma-rays with energies of 573, 900, 984, 1040, 1066, 1701, 1720, 2212 and 3987 keV remained unassigned. There was no evidence relating these gamma-rays to the high neutron flux either by neutron reactions or by thermal-neutron capture.

Carbon (Z=6) : - Bombardment of a plug of pure graphite with 5-MeV $^{4}He^{+}$ ions yielded no gamma-rays assignable to carbon. The use of 11- or 16-MeV alpha particles however, caused excitation of the first excited state of ^{12}C which

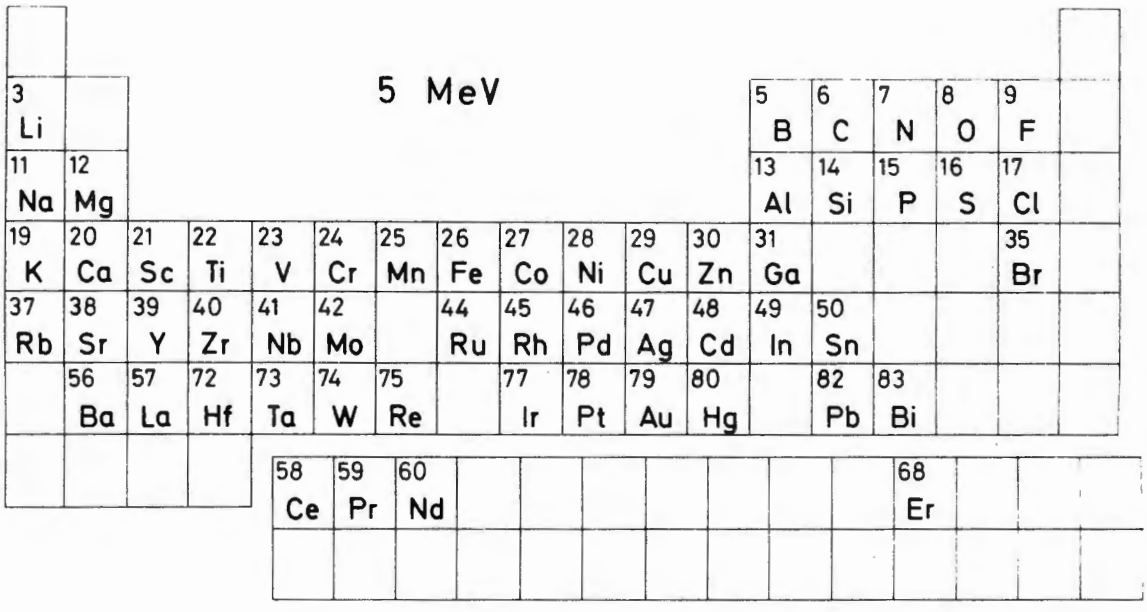

Figure 9(a)

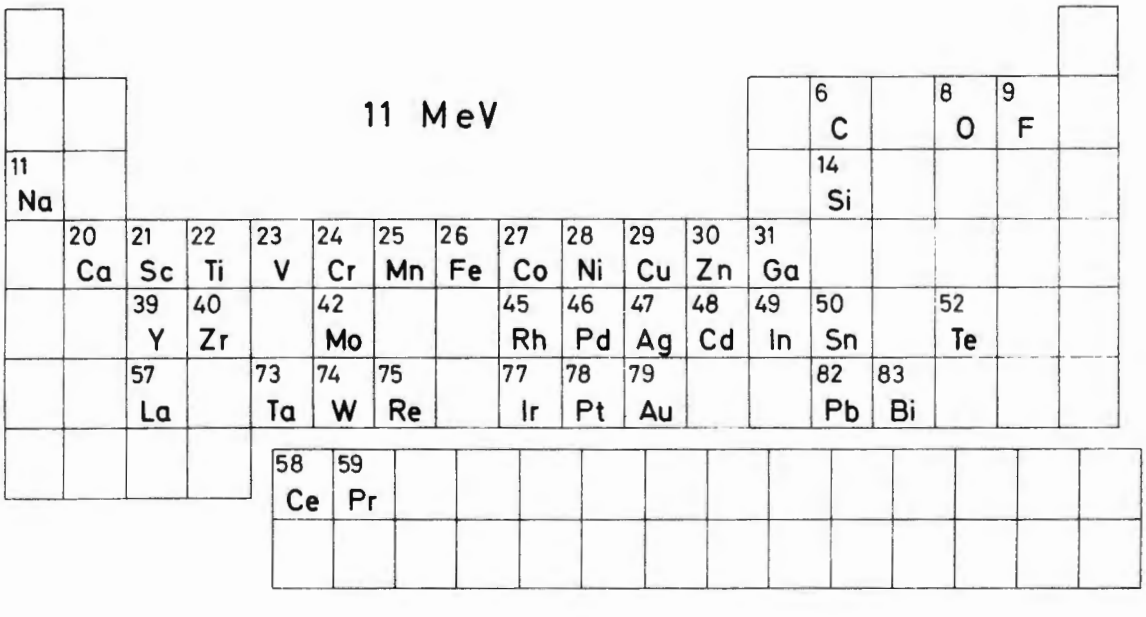

Figure 9(b)

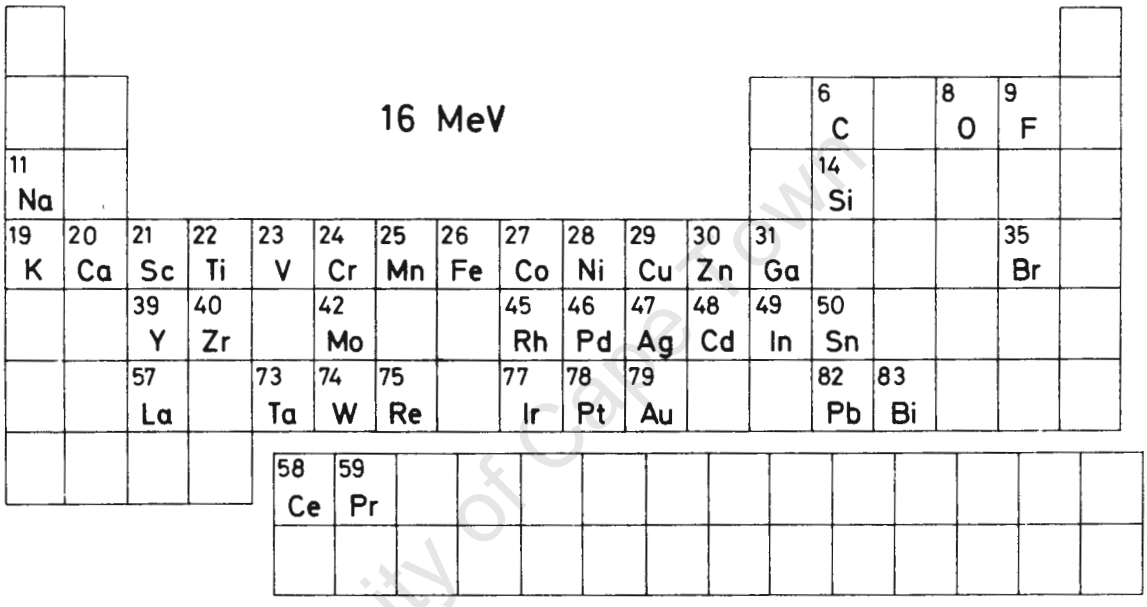

Figure 9(c)

Figure 9(a), (b) and (c) Outlines of the Periodic Table in which the elements named were those bombarded and studied with 5-MeV (Fig 9(a)), 11-MeV (Fig 9(b)) and 16-MeV (Fig 9(c)) alpha particles.

decayed promptly by emission of a 4439-keV gamma-ray. In addition to this, the two escape peaks were observed. The spectrum of carbon under irradiation with 16-MeV $^{4}He^{2+}$ ions shows however, that there are not just three peaks in the spectrum, but six. The existence of the higher energy satellites has not been reported in the literature and there is no firm indication as to their identity or origin. It seems certain that these peaks were connected with carbon since they appeared *in all spectra of targets containing carbon* bombarded at the higher energies. The energy difference between the gamma-rays and the satellites was about 70 keV and was independent of the incident alpha energy. The peaks were sufficiently resolved to be stripped successfully and promised fairly high sensitivity for carbon determination. Since these pairs of peaks were observed at different irradiation sites using different detectors, it is highly unlikely that they are spurious effects related to the detection system. This doubling was not found for any of the peaks arising from other elements *in the same target* or in any other target not containing carbon.

Nitrogen (Z=7) : - The spectrum of barium nitrate is given as an example of the yield of gamma-rays emitted from a nitrogen target. No gamma-rays other than those from the reaction $^{14}N(\alpha,p\gamma)^{17}O$ were observed, due mainly to the much greater energies needed to excite levels in ^{14}N. Excitation of this 871-keV gamma-ray offered a high sensitivity for the analysis of nitrogen and is dealt with more fully in Chapter V.

Oxygen (Z=8) : - The gamma-ray yield of an oxygen-containing target under irradiation with a 5-MeV alpha beam showed five peaks. Gamma-rays were observed as a result of the reactions $^{17}O(\alpha,n\gamma)^{20}Ne$ and $^{18}O(\alpha,n\gamma)^{21}Ne$. The reaction $^{16}O(\alpha,n\gamma)^{19}Ne$ has a Q-value of -12.136 MeV and the (α,p) reactions on each of the three stable isotopes of oxygen were also energetically impossible at this bombarding energy. With alpha particles having energies of 11 and 16 MeV Coulomb excitation of the levels of ^{16}O took place. The first level of ^{16}O decays by internal pair production and was therefore not directly observed in the gamma spectra. Some slight indication of gamma-rays from the third excited state of ^{16}O was found but the yield was of insufficient intensity to be included in the tabulated data. The 6131-keV gamma-ray together with its escape peaks were the main features of the spectrum of every oxygen-containing material bombarded with 11- and 16-MeV alpha particles. The example shown is for the target lanthanum oxide. The three peaks were each capable of yielding sensitive oxygen analyses and had the advantage of being in a region of very low background with little possibility of interference from reactions on other elements.

Fluorine (Z=9) : - Many targets containing fluorine were irradiated and the spectrum of calcium fluoride is given as an example. The observed fluorine peaks resulted from Coulomb excitation, and from the reactions $^{19}F(\alpha,n\gamma)^{22}Na$ and $^{19}F(\alpha,p\gamma)^{22}Ne$. The important peaks from an analytical point of view were those corresponding to

gamma-rays of 110, 197, 583, 1275 and 2081 keV. The sensitivity calculated from the 110-keV and 197-keV gamma-rays excited with alpha beams of all three energies studied, was good enough for low-level fluorine analysis. The use of these gamma-rays is discussed in Chapter IV.

The gamma-rays ^{19}F n(5,2) have an energy of 1280 keV and would therefore be masked by the prominent 1275-keV, ^{19}F p(1,0) gamma-rays. An unassigned gamma-ray of 806 keV was observed in some spectra but it is doubtful whether this gamma-ray is due to fluorine, because other materials, not containing fluorine, yielded a peak corresponding to the same energy.

Sodium (Z=11) : - Under irradiation with alpha-particle beams targets of sodium compounds emit gamma-rays as a result of Coulomb excitation, as well as from the reactions $^{23}Na(\alpha,p\gamma)^{26}Mg$ and $^{23}Na(\alpha,n\gamma)^{26}Al$. The first excited state of ^{26}Al, decays by positron emission and the gamma-ray, ^{23}Na n(1,0), was therefore not observed. The 1809-keV gamma-ray, ^{23}Na p(1,0), was very prominent in all spectra and was well suited for the analysis of elemental sodium. The peaks at 417 and 440 keV though intense, are in a region which has a number of possible interferences so that their use for analysis is not recommended.

Magnesium (Z=12) : - Analysis of the spectrum of magnesium fluoride bombarded with 5-MeV alpha particles, showed that gamma-rays were emitted as a result of Coulomb excitation of ^{25}Mg in addition to those from the reactions

$^{24}Mg(\alpha,p\gamma)^{27}Al$, $^{25}Mg(\alpha,n\gamma)^{28}Si$ and $^{26}Mg(\alpha,n\gamma)^{29}Si$. The reactions $^{24}Mg(\alpha,n\gamma)^{27}Si$, $^{25}Mg(\alpha,p\gamma)^{28}Al$ and $^{26}Mg(\alpha,p\gamma)^{29}Al$ all have fairly high reaction thresholds and no gamma-ray was observed from them. It is unfortunate that some of the gamma-rays from magnesium fall in the same energy regions as those from fluorine, aluminium and silicon. The magnesium gamma-rays subject to possible interference by fluorine are ^{26}Mg $\alpha(1,0)$ of 585 keV and ^{26}Mg n(1,0) of 1273 keV which fall in the same regions as the fluorine gamma-rays, ^{19}F n(1,0) of 583 keV and ^{19}F p(1,0) of 1275 keV. The aluminium gamma-rays ^{27}Al $\alpha(1,0)$ of 844 keV and ^{27}Al $\alpha(2,0)$ of 1015 keV have exactly the same energies as ^{24}Mg p(1,0) and ^{24}Mg p(2,0). In fact, the product nuclide of (α,p) reactions on ^{24}Mg is, of course, ^{27}Al. Similarly ^{28}Si is the product nucleus of the (α,n) reaction on ^{25}Mg so that the gamma-rays, ^{25}Mg n(1,0) of 1779 keV have the same energy as those from Coulomb excitation of the former nuclide.

Great care is required therefore in the determination by gamma-ray spectrometry of aluminium, silicon or magnesium in geological materials where one or more of these other elements is likely to be present. Analysis of fluorine using the 1275-keV gamma-ray would be unreliable in the presence of magnesium. The analysis of mixtures of magnesium with fluorine, aluminium or silicon could be attempted by means of peak-ratio methods.

Only the 1794-, 2028- and 2426-keV gamma-rays from $^{26}Mg(\alpha,n\gamma)^{29}Si$ offer any unique possibility for magnesium analysis since they are not subject to interference.

Aluminium (Z=13) : - Bombardment of an aluminium target with 5-MeV alpha particles produced gamma-rays from Coulomb excitation and $(\alpha,p\gamma)$ and $(\alpha,n\gamma)$ reactions. In addition, an unassigned gamma-ray, with an energy of 3062 keV, was observed. The most sensitive peaks for analysis of aluminium were also associated with silicon or magnesium and were therefore subject to interference from those elements. The gamma-rays generated by the reaction $^{27}Al(\alpha,n\gamma)^{30}P$ were interference-free but even the most intense of them, that of 709 keV, did not offer a very high sensitivity for analysis.

An attempt was made to use the 2236-keV gamma-ray for the analysis of aluminium in medical samples. Brain tissue samples, in which the presence of excess aluminium was to be determined, were supplied by Groote Schuur Hospital. These samples were ashed and compressed into pills with a KBr backing to provide mechanical strength. It was found however, that despite the concentration brought about by ashing, the use of alpha-induced prompt gamma-ray spectrometry did not provide sufficiently sensitive data for adequate differentiation between samples at the levels of aluminium concentrations involved (~50 ppm).

Silicon (Z=14) : - The sensitivities calculated for the possible determination of silicon using the gamma-rays resulting from Coulomb excitation and $(\alpha,p\gamma)$ reactions under 5-MeV $^{4}He^{+}$ bombardment were poor. The highest sensitivity was obtainable from the unresolved 2234- and 2236-keV gamma-rays assigned to ^{28}Si p(2,0) and ^{30}Si α(1,0)

respectively. The latter gamma-rays have exactly the same energy as those from ^{27}Al p(1,0), since they are both from the same gamma transition. These gamma-rays therefore constitute a serious source of interference.

The increased sensitivities attained with higher energy alpha particles were still subject to interference from elements commonly found together with silicon.

Phosphorus (Z=15) : - The target irradiated to give data on the gamma-rays from phosphorus was mercurous phosphate. Gamma-rays were observed from Coulomb excitation and from the reaction $^{31}P(\alpha,p\gamma)^{34}S$ as well as a broad peak, possibly a doublet, at 481 and 493 keV, which was unassigned. The gamma-ray of 2127 keV, identified as ^{31}P p(1,0) was very intense and offered a high sensitivity for the analysis of phosphorus. Possible interference could come from ^{23}Na p(4,1) which is a fairly intense peak corresponding to 2132 keV.

Sulphur (Z=16) : - No gamma-rays that could be ascribed to sulphur were observed from the lead sulphide target.

Chlorine (Z=17) : - When the copper(II) chloride target was irradiated with 5-MeV alpha particles, in addition to gamma-rays from copper, it yielded gamma-rays from the reactions $^{35}Cl(\alpha,p\gamma)^{38}Ar$ and $^{37}Cl(\alpha,p\gamma)^{40}Ar$. The thresholds for the corresponding $(\alpha,n\gamma)$ reactions were above the bombarding energy and gamma-rays resulting from these reactions were thus not observed. The first few

excited states of the two chlorine isotopes were high and they were not directly excited. The 2168-keV gamma-ray from ^{35}Cl p(1,0) offered a fairly good sensitivity for the determination of the element.

Potassium (Z=19) : - A target of potassium bromide was used to obtain data for the gamma-ray spectrum of potassium. Gamma-rays from the reaction $^{39}K(\alpha,p\gamma)^{42}Ca$ were the only ones observed. The corresponding $(\alpha,n\gamma)$ reaction had too high a Q-value and no gamma-rays were thus detected from this reaction. The potassium isotopes ^{40}K and ^{41}K have a far lower abundance in nature (0.012 and 6.91 atom % respectively) than ^{39}K and gamma-rays from reactions with these isotopes were not observed. Spectra for potassium were only measured with 5- and 16-MeV alpha beams and the ^{39}K p(1,0) gamma-rays of 1524 keV in each case offered the highest sensitivity for the determination of the element.

Calcium (Z=20) : - No gamma-rays, that could be ascribed to calcium, were observed from several calcium compounds (*viz.* $CaCO_3$, $CaCl_2$, $Ca(OH)_2$, CaF_2 and $Ca(CH_3COO)_2$) used as targets.

Scandium (Z=21) : - The scandium fluoride target used yielded only one peak from scandium which corresponded to 364 keV and was assigned to ^{45}Sc $\alpha(2,1)$. This was a peak of very low sensitivity and therefore of little analytical use. The first excited state of ^{45}Sc is 12.4 keV which was below the detection limit of the gamma-ray spectrometer used.

Titanium (Z=22) : - Coulomb excitation was the main source of gamma-rays from alpha bombardment of titanium. Gamma-rays were also observed from the reaction $^{48}Ti(\alpha,n\gamma)^{51}Cr$ but none were found from excitation of the levels of ^{49}Ti and ^{50}Ti which have relatively high-lying first excited states. With 5-MeV alpha particles only the 159-keV gamma-ray had analytical potential but using the higher energy beams the $(\alpha,n\gamma)$ reaction, yielding a 749-keV gamma-ray offered a better sensitivity (see Catalogue of Gamma-Rays). An unidentified low-intensity gamma-ray of about 320 keV was observed in this spectrum but it also appeared in the spectra of some other materials, such as calcium hydroxide, potassium bromide and palladium.

Vanadium (Z=23) : - The major isotope of vanadium is ^{51}V (99.75 atom %) and all the gamma-rays observed in this spectrum resulted from excitation of this nuclide. Coulomb excitation of ^{51}V gave the most prominent and analytically useful gamma-ray, that of 320 keV. In addition three gamma-rays were observed from the reaction $^{51}V(\alpha,n\gamma)^{54}Mn$. With increasing incident alpha energy the latter peaks became more intense than those due to Coulomb excitation. The sensitivities of the ^{51}V n(2,0) and ^{51}V n(3,2) were particularly promising for vanadium analysis with 11-MeV alpha particles.

Chromium (Z=24) : - No spectrum of chromium is given. The chromium gamma-rays observed resulted from excitation of three of the four chromium isotopes (see Catalogue of Gamma-Rays). The sensitivity for analysis using these peaks was

very low. Gamma-rays were not observed from excitation of ^{52}Cr despite the high abundance of this isotope in natural chromium, probably because of the relatively high energy of the first level (1434 keV). Only the 783-keV peak from ^{50}Cr was observed at all three bombarding energies. Gamma-rays from ^{53}Cr and ^{54}Cr were probably obscured because of the greatly increased background generated at the higher bombarding energies.

Manganese (Z=25) : - Excitation of the first level of ^{54}Mn resulted in a very intense peak corresponding to a gamma-ray of 126 keV. This peak offered a high sensitivity for the analysis of manganese. Only one other peak from manganese, corresponding to 858 keV, was observed. The use of the 126-keV peak is considered further in Chapter V. It is interesting to note the fall-off in potential sensitivity for this peak with increasing incident beam energy.

Iron (Z=26) : - The peaks offering the highest sensitivity for analysis of iron came from excitation of ^{56}Fe and ^{57}Fe. Gamma-rays from levels of three of the four stable iron isotopes were recorded. The energy of the first level of ^{54}Fe was high (1408 keV) and gamma-rays from its decay were not observed. The first excited state of ^{57}Fe lies 14 keV above the ground state and its decay gamma-ray was below the detection limit of the detector. It seems probable that the gamma-ray of 353 keV, ^{57}Fe $\alpha(3,1)$, was indeed observed but since it was not resolvable from the

351 keV gamma-ray, ^{18}O n(1,0), no data are given for it. High resolution gamma-spectrometry such as is obtainable with an intrinsic Ge-detector should be able to separate these two peaks. The 122-keV gamma-ray was situated on a rather high background and in a crowded region which made it less suitable for iron determination than the 847-keV peak which stood out clearly in a region of low background.

Cobalt (Z=27) : - No gamma-rays were observed that could be ascribed to cobalt.

Nickel (Z=28) : - No gamma-ray was observed that could be ascribed, with certainty, to nickel. Two clearly defined, but low-intensity peaks, corresponding to 1099 keV and 1193 keV were observed in the spectrum. These gamma-rays could be ^{61}Ni $\alpha(6,0)$ and ^{61}Ni $\alpha(8,0)$ respectively, but in that case it is reasonable to expect the observation of some gamma-rays from de-excitation of the lower energy levels. In fact only the two gamma-rays mentioned previously were observed.

The data that are available for Coulomb excitation of nickel [An 74] resulted from bombardments with 6.8-MeV alpha particles and 26-MeV carbon ions. The level scheme of ^{61}Ni, contained in Ref. Au 75, shows several levels with energies below 1190 keV that should be accessible by means of E2 transitions. No explanation is offered therefore in respect of the absence of gamma-rays from these levels and the two observed gamma-rays have not been assigned as being due to transitions in nickel.

Copper (Z=29) : - Two peaks were observed from each of the two copper isotopes present in nature. None of them offered high sensitivity for analysis.

Zinc (Z=30) : - Gamma-rays were observed from each of the zinc isotopes except ^{70}Zn which has an abundance of only 0.62 atom % in nature. None of the peaks offered a useful sensitivity at any of the incident alpha energies studied.

Gallium (Z=31) : - No gamma-rays were observed that could be ascribed to gallium. The target used was gallium fluoride.

Bromine (Z=35) : - The target used with both 5-MeV and 16-MeV alpha particles was potassium bromide. Intense peaks were observed corresponding to 217 keV and 276 keV resulting from Coulomb excitation of levels of ^{79}Br and ^{81}Br. De-excitation from the first level of ^{79}Br and the second level of ^{81}Br was not observed because these levels have parity different from that of their ground states, thus the transitions are not E2 in character. Reasonably good sensitivity for bromine analysis was offered at both bombarding energies for the observed spectral peaks.

Rubidium (Z=37) : - A rubidium fluoride target was used to obtain the gamma-ray spectrum of rubidium. Only one peak assignable to rubidium was observed. This peak was of very low intensity and of little analytical use.

Strontium (Z:38) : - No gamma-ray that could be ascribed to strontium was observed from the target of strontium carbonate powder contained in a KAPTON cell.

Yttrium (Z=39) : - No gamma-rays were observed that could be ascribed to yttrium.

Zirconium (Z=40) : - Only one gamma-ray of very low intensity was observed in the spectrum of zirconium. This was not observed at the higher bombarding energies and was of very little analytical significance.

Niobium (Z=41) : - No gamma-ray that could be ascribed to niobium was observed from the target of niobium powder in a KAPTON cell.

Molybdenum (Z=42) : - The low-lying levels of all the molybdenum isotopes except ^{92}Mo were excited under bombardment. The first excited state of ^{92}Mo is high (1509 keV) and no gamma-rays from it were observed. The gamma-rays from ^{94}Mo $\alpha(1,0)$ have the same energy as those from ^{14}N p(1,0). Since the presence of nitrogen on the surface of molybdenum was likely, it was not possible to give any reliable data on the intensity of the molybdenum gamma-ray. Reasonably good sensitivity was obtainable by the use of the 536-keV gamma-ray with each incident alpha energy.

Ruthenium (Z=44) : - The target used consisted of ruthenium sponge in a KAPTON cell. Gamma-rays were observed as a

result of excitation of those isotopes of ruthenium with the highest abundances in nature, that is ^{99}Ru, ^{100}Ru, ^{101}Ru, ^{102}Ru and ^{104}Ru. The isotopes which were not observed, ^{96}Ru and ^{98}Ru, are much less abundant than the others and had fairly high-lying first excited states. None of the spectral peaks was very intense and only the peak corresponding to 358 keV, ^{104}Ru $\alpha(1,0)$, showed any analytical potential.

Rhodium (Z=45) : - Only two peaks were observed in the gamma-ray spectrum of rhodium. These were from excitation of the third and fourth levels of ^{103}Rh (100 atom % in nature). Neither the first nor second excited states was accessible through an E2 transition since their parities were different from that of the ground state. Both gamma-rays observed offered fairly good analytical potential at all three incident alpha energies studied.

Palladium (Z=46) : - Gamma-rays from excitation of all the stable isotopes of palladium except ^{106}Pd were observed. The first excited state of ^{106}Pd is 511.9 keV and gamma-rays from its decay would be unresolvable from annihilation gamma-rays. The presence of sodium on the surface was attributed to possible traces of grease retained on the metal. Only the 374- and 434-keV peaks were of possible analytical application. The sensitivities attainable with an 11-MeV incident beam were particularly good.

Silver (Z=47) : - Gamma-rays from both stable isotopes of silver were observed. The first excited state of ^{109}Ag is not excited through an E2 transition since its parity is different from that of the ground state, and it was not observed. Four of the observed gamma-rays, those of 312, 325, 415 and 423 keV, were of sufficient intensity to be potentially useful for analysis.

Cadmium (Z=48) : - Gamma-rays were observed from excited states of four of the seven naturally-occurring isotopes of cadmium. The remaining three nuclides all have relatively high-lying first excited states and have low abundances in nature. The first excited state of ^{111}Cd has the correct spin and parity values for an E2 transition but no gamma-rays were observed from this level. There was some sign of a peak corresponding to the energy of the level (245 keV) but since there was a radioactive gamma-ray of 239 keV present in the background it was difficult to decide whether this peak could be due to the transition in ^{111}Cd or not.

In the case of ^{113}Cd the first excited state is of incorrect parity for an E2 transition. Coulomb excitation of only the second, sixth and eighth levels has been reported [Mc 58]. The gamma-rays from these levels were recorded using a NaI detector and from 2.1- to 2.3-MeV incident protons. The gamma-rays from the eighth level were found to be a factor of 10 less intense than those from the other two levels. Since a Ge(Li) detector (which is far less efficient than a NaI detector) was used in this work,

it is not surprising that the gamma-rays corresponding to the eighth level were not observed. The spins of the third, fourth and fifth levels have not been firmly established [Ra 71] thus it is not known whether E2 transitions to these levels are possible.

Indium (Z=49) : - No gamma-ray was observed that could be ascribed to indium.

Tin (Z=50) : - No gamma-ray was observed that could be ascribed to tin.

Tellurium (Z=52) : - This element was only irradiated with 11-MeV alpha particles and no gamma-ray was observed that could be ascribed to tellurium.

Barium (Z=56) : - No gamma-ray that could be ascribed to barium was observed from a barium nitrate target.

Lanthanum (Z=57) : - No gamma-ray that could be ascribed to lanthanum was observed from a lanthanum oxide target.

Cerium (Z=58) : - No gamma-ray that could be ascribed to cerium was observed from a cerium fluoride target.

Praseodymium (Z=59) : - No gamma-ray that could be ascribed to praseodymium was observed from a praseodymium fluoride target.

Neodymium (Z=60) : - No gamma-ray that could be ascribed to neodymium was observed from a neodymium fluoride target.

Erbium (Z=68) : - The target of erbium oxide powder in a KAPTON cell was only irradiated with the 5-MeV alpha beam. Levels of four of the six naturally-occurring erbium isotopes were excited. The abundances in nature of the remaining nuclides are low. The low-energy threshold of the gamma-ray spectrometer used was too high for gamma-rays from the first excited states of the erbium nuclides to be observed. The sensitivities offered for erbium analysis were very poor.

Hafnium (Z=72) : - Gamma-rays were observed from four of the six naturally-occurring hafnium isotopes during the bombardment of hafnium lumps in a KAPTON cell. The abundances of the remaining two stable isotopes, ^{174}Hf and ^{176}Hf, were very low. The sensitivities calculated from observed gamma-rays were poor and offered little potential analytical use.

Tantalum (Z=73) : - The 136-keV gamma-rays observed from tantalum, during bombardment with beams of each alpha energy, offered good sensitivity for the analysis of this element in that concentration range corresponding to a minor, but not trace, component. Such analysis, of course, necessitated <u>all</u> collimators being manufactured from materials other than the normal tantalum ones used in these investigations.

Tungsten (Z=74) : With the exception of ^{180}W, which has a very low abundance in nature, all the stable tungsten isotopes contributed to the gamma spectrum of the element. The first excited state of ^{183}W had an energy well below the threshold of the spectrometer used and so was not observed. A peak at 293 keV remained unassigned. The 122-keV gamma ray offered a fairly good sensitivity for analysis using 5-MeV alpha particles (provided Fe is known to be absent) because the peak in the spectrum overlapped that corresponding to ^{57}Fe $\alpha(2,1)$ which has the same energy.

Rhenium (Z=75) : - Gamma-rays were observed from the excitation of levels of both stable rhenium isotopes. Because the second level of ^{187}Re was of different parity from the ground state, it was not excited by Coulomb excitation and its decay gamma-ray was therefore not observed. Only the 125- and 134-keV gamma-rays offered a reasonable sensitivity for the analysis of the element.

Iridium (Z=77) : - Levels of both stable iridium isotopes were excited. The energy of the first excited state of ^{193}Ir coincided exactly with that of the iridium Kβ X-rays, therefore the data given for peak intensity and sensitivity in the tables represent the combined value of both gamma- and X-rays. The parity of the third energy level of ^{191}Ir is different from that of the ground state; the transition is therefore not of E2 type and no gamma-rays were observed from decay of that state.

Platinum (Z=78) : - Gamma-rays were observed from excitation of levels of five of the six platinum isotopes present in nature. The natural abundance of ^{190}Pt is very low and it did not contribute to the spectrum. Although the fourth and fifth levels of ^{195}Pt contributed to the spectrum, no gamma-rays were observed from the third excited state, even though the state was of the same parity as the ground state and of the correct spin for excitation by an E2 transition. Gamma-rays from this level have been Coulomb excited by means of protons of 4.5 MeV [Mc 59], alpha particles of 10 and 15 MeV [Br 70] and also ^{16}O ion beams of 35 MeV [Ku 69]. The observed gamma-rays were, in each case, of very low intensity as compared to the 211-keV ^{195}Pt $\alpha(4,0)$ gamma-rays and in the present work some indication of a small peak in this region of the spectrum was observed.

Only the 329-keV gamma-ray, ^{194}Pt $\alpha(1,0)$, offered a reasonable sensitivity for analysis under 5-MeV alpha bombardment, but ^{195}Pt $\alpha(4,0)$ and ^{196}Pt $\alpha(1,0)$ became useful when 11- and 16-MeV alpha particles were used.

Gold (Z=79) : - Several levels of the stable gold isotope were excited. The energy of the first excited state of ^{197}Au coincided exactly with that of the gold Kβ X-rays, therefore the data given for peak intensity and sensitivity are the sum of both gamma- and X-rays. Two levels of ^{197}Au, the fourth and fifth were not excited. The fourth level has a parity different from that of the ground state, thus it was not excited by an E2 transition, and was not

observed. The existence of the fifth level is not well established [Le 72] and therefore the failure to observe a gamma-ray from this level is not surprising. Only the combined X-ray and gamma-ray peak and ^{197}Au $\alpha(3,0)$ offered potentially useful sensitivities for analysis using 5-MeV alpha particles whilst with increasing incident-alpha energy, ^{197}Au $\alpha(6,0)$ became comparable in sensitivity.

Mercury (Z=80) : - The target irradiated to give data on the gamma-rays from mercury was mercurous phosphate. Gamma-rays were observed from Coulomb excitation of levels of four of the seven stable mercury isotopes. No gamma-rays were observed from ^{196}Hg which has a very low natural abundance, or from ^{201}Hg and ^{204}Hg for which only inconclusive and fragmentary nuclear level schemes are available. It seems possible that the unassigned complex peak listed as the doublet 481/493 keV could be the result of excitation of these nuclides. None of the gamma-rays that was observed was of sufficient intensity to be of analytical use.

Lead (Z=82) : - No gamma-ray that could be ascribed to lead was observed from a target of pure lead.

Bismuth (Z=83) : - No gamma-ray that could be ascribed to bismuth was observed from a pure bismuth target.

CATALOGUE OF GAMMA-RAYS

Identification of the origins of peaks observed in the spectra involved the comparison of the spectra with a compilation of those gamma-rays that could be expected as a result of reactions on, or Coulomb excitation of, all the stable isotopes of each element studied. The latter information was contained in various volumes of Nuclear Data Sheets. Individual references for each nuclide are not given since the "Cumulative Index to A-Chains" contained in Ref. Nu 77 was used, thus avoiding unnecessary repetition.

The catalogue which follows contains a list, element by element, in order of atomic number, of all identified gamma-rays observed in the spectra of the 56 elements studied whilst under irradiation with 5-MeV $^{4}He^{+}$ ions. Additional data for these gamma-rays were provided by irradiations with 11- and 16-MeV $^{4}He^{2+}$ ions. For each gamma-ray, the energy, assignment, net count/mC, background count/mC and sensitivity in parts per mil ($^{o}/_{oo}$) are given to two significant figures. Those values for 11- and 16-MeV $^{4}He^{2+}$ ions have been normalised to 1 mC of singly charged particles.

The sensitivity for each gamma-ray was calculated as that concentration of the element which would give a nett count in the peak equal to three times the standard deviation of the peak background.

Although, generally, 5-MeV alpha irradiation produced mainly Coulomb-excited gamma-rays, once the energy was increased to 11 and 16 MeV many more peaks appeared in the spectra. For this reason the data obtained with the higher energy beams were only used to provide further information on those gamma-rays observed using 5-MeV alpha irradiation. Exception was made in the cases of carbon and oxygen where data were obtained for Coulomb-excited gamma-rays which had thresholds that were too high for 5-MeV alpha excitation. In addition, tellurium was only irradiated with 11-MeV alpha particles.

The values of "nett counts" and "background counts" were included in order that fair estimations could be made of the gamma-ray intensities as well as the magnitude of their backgrounds, since both parameters affected the calculated sensitivities. The actual numbers given were normalised from experimental data and are, of course, peculiar to the particular system used to measure them. In all cases the count rate, and therefore the sensitivity calculated, depended upon the solid angle subtended by the detector and its effeciency; the figures given should be regarded as comparative and order of magnitude values. However the inter-comparison among the data is relevant and of value for analytical application, both for possible determinations and prediction of any interferences that may occur.

CATALOGUE OF GAMMA-RAYS

Element	Assignment	E_γ (keV)	5 MeV			11 MeV			16 MeV		
			c/mC	bg/mC	$^o/_{oo}$	c/mC	bg/mC	$^o/_{oo}$	c/mC	bg/mC	$^o/_{oo}$
Lithium	^{7}Li α(1,0)	478	72000	6300	0.03						
Boron	^{10}B p(3,2)	170	4700	3600	1.2						
	^{10}B p(2,1)	593	not possible to integrate								
	^{10}B α(1,0)	718	3100	1800	1.3						
	^{10}B p(3,1)	768	38	710	66						
	^{11}B $-2m_e$	1291	170	830	16						
	^{11}B $-m_e$	1802	18	280	88						
	^{11}B n(1,0)	2313	1200	570	1.9						
	^{10}B $-2m_e$	2662	880	1100	3.7						
	^{10}B $-2m_e$	2832	390	570	5.9						
	^{10}B p(1,0)	3086	230	890	12						
	^{10}B $-m_e$	3173	580	1200	5.6						
	^{10}B $-m_e$	3343	210	470	9.9						
	^{10}B p(2,0)	3684	1300	210	1.1						
	^{10}B p(3,0)	3854	460	18	0.87						
Carbon	^{12}C $-2m_e$	3417	not observed			110000	180000	0.38	34000	50000	0.62
	^{12}C $-m_e$	3928	not observed			47000	150000	0.80	16000	50000	1.4
	^{12}C α(1,0)	4439	not observed			80000	21000	0.17	28000	11000	0.36
Nitrogen	^{14}N p(1,0)	871	1500	40	0.04						
Oxygen	^{18}O n(1,0)	351	120	12	1.2	2000	26000	3.4	not observed		
	^{18}O n(2,1)	1395	6.8	3.3	11	not observed			not observed		
	^{17}O n(1,0)	1634	2.2	1.6	24	not observed			not observed		
	^{18}O n(3,1)	2438	1.2	0.94	34	not observed			not observed		
	^{17}O n(2,1)	2614	0.15	0.4	170	not observed			not observed		
	^{16}O $-2m_e$	5109	not observed			5800	5200	0.18	28000	23000	0.08
	^{16}O $-m_e$	5620	not observed			2700	3500	0.30	18000	22000	0.11
	^{16}O α(2,0)	6131	not observed			2300	760	0.17	15000	22000	0.14
Fluorine	^{19}F n(2,1)	74	430	3500	7.9	290000	1800000	0.25	cut off electronically		
	^{19}F α(1,0)	110	9600	3700	0.37	1500000	1500000	0.04	3200000	1900000	0.02
	^{19}F α(2,0)	197	17000	2500	0.17	2000000	810000	0.02	930000	1100000	0.05
	^{19}F n(1,0)	583	3600	660	0.42	400000	260000	0.07	250000	270000	0.10
	^{19}F n(4,3)	637	32	500	40	23000	120000	0.82	10000	130000	1.6

Element	Assignment	E_γ (keV)	5 MeV			11 MeV			16 MeV		
			c/mC	bg/mC	$^o/_{oo}$	c/mC	bg/mC	$^o/_{oo}$	c/mC	bg/mC	$^o/_{oo}$
Fluorine (continued)	^{19}F n(3,0)	891	890	550	1.5	78000	120000	0.23	51000	160000	0.36
	^{19}F α(3,1)	1236	240	180	3.3	70000	100000	0.24	56000	130000	0.30
	^{19}F p(1,0)	1275	3200	280	0.30	160000	100000	0.10	130000	120000	0.12
	^{19}F n(5,2)	1280	not resolved			not resolved			not resolved		
	^{19}F α(4,1)	1349	220	170	3.4	49000	120000	0.39	49000	180000	0.39
	^{19}F α(5,2)	1357	50	82	11	not resolved			not resolved		
	^{19}F n(6,1)	1369	63	100	9.3	75000	88000	0.21	65000	110000	0.23
	^{19}F n(7,1)	1400	21	74	23	43000	77000	0.35	40000	92000	0.35
	^{19}F α(4,0)	1459	47	150	15	4200	54000	3.0	3000	50000	3.4
	^{19}F n(4,0)	1528	180	85	3.0	36000	55000	0.35	27000	66000	0.44
	^{19}F $-m_e$	1570	9.6	56	45	8300	38000	1.2	2900	54000	3.7
	^{19}F p(2,1)	2081	240	41	1.5	54000	65000	0.25	48000	73000	0.26
	^{19}F $-2m_e$	2160	16	35	21	10000	42000	1.1	9200	58000	1.2
	^{19}F $-m_e$	2671	6.7	18	37	2100	25000	4.0	4200	38000	2.2
	^{19}F p(3,1)	3182	34	7	4.5	3900	17000	1.8	3800	21000	1.8
Sodium	^{23}Na n(2,0)	417	860	320	0.54	140000	200000	0.09	96000	180000	0.12
	^{23}Na α(1,0)	440	1300	280	0.32	180000	210000	0.07	200000	170000	0.05
	^{23}Na $-2m_e$	787	100	440	5.4	4100	46000	1.4	2400	48000	2.4
	^{23}Na n(3,1)	830	26	150	12	33000	92000	0.24	25000	66000	0.27
	^{23}Na p(4,2)	1003	110	170	3.0	26000	51000	0.22	14000	51000	0.43
	^{23}Na p(2,1)	1130	670	240	0.59	30000	56000	0.20	24000	46000	0.23
	^{23}Na $-m_e$	1298	36	220	11	1700	30000	2.6	980	30000	4.6
	^{23}Na p(7,2)	1412	34	190	11	7800	50000	0.75	4500	32000	1.0
	^{23}Na p(3,1)	1780	37	74	6.1	2200	17000	1.6	3300	26000	1.3
	^{23}Na p(1,0)	1809	1300	94	0.19	53000	41000	0.10	38000	36000	0.13
	^{23}Na p(8,2)	1897	1.5	16	71	not observed			1700	16000	1.9
	^{23}Na $-2m_e$	1916	1.8	17	60	2200	14000	1.4	570	16000	5.7
	^{23}Na p(4,1)	2132	30	31	4.9	2500	14000	1.3	3300	19000	1.1
	^{23}Na $-m_e$	2427	4.9	12	19	not observed			not observed		
	^{23}Na p(5,1)	2511	30	15	3.3	10000	21000	0.38	4600	18000	0.76
	^{23}Na p(6,1)	2524	19	9.0	4.0	not resolved			not resolved		
	^{23}Na p(7,1)	2541	16	9.7	5.1	3900	16000	0.85	2100	17000	1.6
	^{23}Na p(2,0)	2938	27	5.5	2.3	1700	14000	1.8	680	9900	3.8
	^{23}Na p(9,1)	3092	2.3	1.5	14	2000	8500	1.2	2500	16000	1.3

Element	Assignment	E_γ (keV)	5 MeV			11 MeV			16 MeV		
			c/mC	bg/mC	$^o/_{oo}$	c/mc	bg/mC	$^o/_{oo}$	c/mc	bg/C	$^o/_{oo}$
Magnesium	^{25}Mg α(1,0)	585	170	660	5.6						
	^{26}Mg n(2,1)	755	26	520	32						
	^{24}Mg p(1,0)	844	270	950	4.3						
	^{24}Mg p(2,0)	1015	160	650	5.9						
	^{26}Mg n(1,0)	1273	290	280	2.1						
	^{25}Mg n(1,0)	1779	170	86	2.0						
	^{26}Mg n(4,1)	1794	16	56	18						
	^{26}Mg n(2,0)	2028	31	27	6.2						
	^{25}Mg $-m_e$	2328	4.2	14	32						
	^{26}Mg n(3,0)	2426	36	20	4.6						
	^{25}Mg n(2,1)	2839	24	16	6.2						
Aluminium	^{27}Al n(1,0)	677	56	220	25						
	^{27}Al n(2,0)	709	380	340	4.6						
	^{27}Al α(1,0)	844	91	270	17						
	^{27}Al α(2,0)	1015	77	280	21						
	^{27}Al $-2m_e$	1214	220	300	7.4						
	^{27}Al p(2,1)	1263	510	330	3.4						
	^{27}Al p(5,2)	1311	63	220	22						
	^{27}Al p(6,2)	1332	13	200	100						
	^{27}Al n(3,0)	1454	43	210	32						
	^{27}Al p(3,1)	1534	69	240	21						
	^{27}Al p(4,1)	1552	30	240	50						
	^{27}Al $-m_e$	1725	110	410	10						
	^{27}Al p(1,0)	2236	1400	170	0.87						
	^{27}Al $-2m_e$	2476	96	110	10						
	^{27}Al p(5,1)	2574	6.2	63	120						
	^{27}Al p(6,1)	2595	100	94	9.2						
	^{27}Al $-2m_e$	2748	14	98	68						
	^{27}Al $-m_e$	2987	59	94	16						
	^{27}Al $-m_e$	3259	obscured by Compton edge								
	^{27}Al p(2,0)	3498	160	39	3.8						
	^{27}Al p(3,0)	3770	40	26	12						
Silicon	^{29}Si p(1,0)	78	97	140	12	25000	350000	2.2	cut off electronically		
	(^{28}Si+^{30}Si) $-2m_e$	1213	5.4	8.1	50	7600	61000	3.1	9400	67000	2.6
	^{28}Si p(1,0)	1266	7.4	4.3	26	90000	130000	0.38	160000	90000	0.18
	^{29}Si α(1,0)	1273	3.1	3.9	60	380	5400	18	not resolved		

Element	Assignment	E_γ (keV)	5 MeV			11 MeV			16 MeV		
			c/mC	bg/mC	$^o/_{oo}$	c/mC	bg/mC	$^o/_{oo}$	c/mC	bg/mC	$^o/_{oo}$
Silicon (continued)	$(^{28}Si+^{30}Si)$ $-m_e$	1724	2.7	4.5	75	2500	2400	1.8	3000	28000	5.4
	^{28}Si α(1,0)	1779	4.2	6.1	56	170000	90000	0.17	130000	74000	0.20
	^{30}Si α(1,0)	2235	29	1.9	4.6	38000	20000	0.35	42000	22000	0.33
	^{28}Si p(2,0)		not resolved			not resolved			not resolved		
Phosphorus	^{31}P $-2m_e$	1105	5.7	9.6	2.3						
	^{31}P p(2,1)	1176	7.4	7.9	1.6						
	^{31}P α(1,0)	1266	1.6	5.1	6.1						
	^{31}P $-m_e$	1616	2	7	5.6						
	^{31}P p(1,0)	2127	47	2.6	0.15						
	^{31}P $-2m_e$	2282	0.52	0.77	7.1						
	^{31}P $-m_e$	2793	0.49	0.54	6.4						
	^{31}P p(2,0)	3304	1.0	1.4	4.8						
Sulphur		-									
Chlorine	^{35}Cl $-2m_e$	1146	3.7	5.0	30						
	^{35}Cl p(2,1)	1210	1.1	3.1	77						
	^{37}Cl p(1,0)	1461	0.56	3.6	170						
	^{35}Cl p(3,1)	1643	3.6	6.5	35						
	^{35}Cl $-m_e$	1657	2.2	4.5	49						
	^{35}Cl p(1,0)	2168	32	1.5	1.9						
Potassium	^{39}K p(2,1)	313	2.8	8.6	17				5200	140000	2.2
	^{39}K p(3,1)	899	1.6	3.9	19				14000	82000	0.63
	^{39}K p(1,0)	1524	14	2.4	1.7				120000	50000	0.06
Calcium		-									
Scandium	^{45}Sc α(2,1)	364	43	650	31	22000	320000	1.1	6700	240000	3.1
Titanium	^{47}Ti α(1,0)	159	390	91	2.3	2600	260000	19	not observed		
	^{48}Ti n(1,0)	749	16	9.9	19	90000	62000	0.26	92000	130000	0.37
	^{46}Ti α(1,0)	889	11	3.6	16	5000	62000	4.7	5900	66000	4.2
	^{48}Ti α(1,0)	983	40	3.4	4.4	10000	58000	2.3	23000	70000	1.1
Vanadium	^{51}V n(1,0)	54	5.1	110	190	110000	570000	0.68	cut off electronically		
	^{51}V n(2,0)	157	32	130	34	1000000	430000	0.06	610000	500000	0.11
	^{51}V n(3,2)	207	10	43	61	480000	220000	0.09	430000	320000	0.13
	^{51}V α(1,0)	320	620	36	0.91	13000	63000	1.8	4200	69000	6.0
	^{51}V α(2,1)	609	0.75	1.9	170	13000	100000	2.3	2800	66000	8.7
	^{51}V α(2,0)	929	2.5	1.3	43	not observed			not observed		

Element	Assignment	E_γ (keV)	5 MeV			11 MeV			16 MeV		
			c/mC	bg/mC	$^o/_{oo}$	c/mC	bg/mC	$^o/_{oo}$	c/mC	bg/mC	$^o/_{oo}$
Chromium	^{53}Cr α(1,0)	564	8.2	13	42	not observed			not observed		
	^{50}Cr α(1,0)	783	8.4	5.1	26	2600	32000	6.6	5400	31000	3.1
	^{54}Cr α(1,0)	835	3.5	4.0	54	not observed			not observed		
Manganese	^{55}Mn α(1,0)	126	3700	610	0.63	42000	580000	0.70	29000	390000	1.2
	^{55}Mn α(2,1)	858	3.6	1.6	34	14000	110000	0.96	14000	84000	1.2
Iron	^{57}Fe α(2,1)	122	70	44	9.0	not observed			not observed		
	^{57}Fe α(2,0)	137	8.6	34	64	not observed			not observed		
	^{57}Fe α(3,2)	230	1.6	18	250	not observed			not observed		
	^{57}Fe α(3,1)	353	obscured by ^{18}O			not observed			not observed		
	^{57}Fe α(3,0)	367	2.5	10	120	4600	65000	5.2	1800	60000	13
	^{58}Fe α(1,0)	811	0.54	1.1	180	not observed			1400	21000	9.9
	^{56}Fe α(1,0)	847	59	1.7	2.1	26000	46000	0.77	37000	120000	0.88
Cobalt		-									
Nickel		-									
Copper	^{63}Cu α(1,0)	670	9.6	2.4	15	1400	18000	8.7	2600	62000	9.0
	^{65}Cu α(1,0)	771	1.8	0.70	46	1400	21000	10	760	33000	23
	^{63}Cu α(2,0)	962	2.3	1.1	43	2700	10000	3.5	12000	71000	2.1
	^{65}Cu α(2,0)	1116	0.56	1.4	200	720	6500	11	1200	26000	13
Zinc	^{67}Zn α(1,0)	93	6.2	40	97	6300	140000	5.6	cut off electronically		
	^{67}Zn α(2,0)	185	36	7.1	11	not observed			not observed		
	^{64}Zn α(1,0)	992	6.2	0.85	14	7700	13000	1.4	10000	52000	2.1
	^{66}Zn α(1,0)	1039	2.0	0.71	41	8600	15000	1.4	8500	47000	2.4
	^{68}Zn α(1,0)	1077	0.90	0.63	84	1300	7500	6.5	890	25000	17
Gallium		-									
Bromine	^{79}Br α(2,0)	217	130	43	1.6				140000	680000	0.37
	^{79}Br α(3,0)	261	12	22	13				70000	410000	0.59
	^{81}Br α(1,0)	276	110	26	1.4				11000	230000	2.8
	^{79}Br α(4,0)	306	33	17	4.0				not observed		
	^{79}Br α(5,0)	397	2.5	7.0	33				not observed		
	^{79}Br α(6,0)	523	16	5.2	4.6				240000	170000	0.11
	^{81}Br α(3,0)	538	4.3	6.9	19				1000	53000	14
	^{79}Br α(7,0)	606	0.93	5.0	76				12000	75000	1.5

Element	Assignment	E_γ (keV)	5 MeV			11 MeV			16 MeV		
			c/mC	bg/mC	$^o/_{oo}$	c/mC	bg/mC	$^o/_{oo}$	c/mC	bg/mC	$^o/_{oo}$
Rubidium	^{85}Rb α(1,0)	151	82	2400	46						
Strontium		-									
Yttrium		-									
Zirconium	^{96}Zr α(1,0)	1594	0.26	0.54	270	not observed			not observed		
Niobium		-									
Molybdenum	^{95}Mo α(1,0)	204	57	30	9.0	2600	17000	4.7	11000	51000	1.9
	^{97}Mo α(1,0)	481	1.9	2.7	83	890	7000	8.9	3800	20000	3.5
	^{100}Mo α(1,0)	536	23	2.1	6.0	2300	3800	2.5	13000	25000	1.2
	^{96}Mo α(1,0)	778	1.5	0.50	44	940	2600	5.8	2200	11000	4.5
	^{95}Mo α(2,0)	786	1.5	0.60	50	1300	2500	3.8	1400	10000	6.9
	^{98}Mo α(2,0)	787	not resolved			not resolved			not resolved		
	^{94}Mo α(1,0)	871	obscured by ^{14}N								
Ruthenium	^{99}Ru α(1,0)	89	38	330	45						
	^{101}Ru α(1,0)	127	48	250	31						
	^{104}Ru α(1,0)	358	94	57	7.6						
	^{102}Ru α(1,0)	475	25	73	33						
	^{100}Ru α(1,0)	540	3.7	39	160						
Rhodium	^{103}Rh α(3,0)	295	1000	130	1.1	44000	36000	0.41	30000	60000	0.78
	^{103}Rh α(4,0)	358	690	31	0.77	37000	22000	0.39	30000	48000	0.69
Palladium	^{105}Pd α(1,0)	281	8.8	31	60	950	19000	14	1800	51000	12
	^{110}Pd α(1,0)	374	150	33	3.6	15000	28000	0.29	9200	65000	2.6
	^{108}Pd α(1,0)	434	130	40	4.5	21000	35000	0.23	1900	38000	9.8
	^{110}Pd α(2,1)	440	13	14	28	not resolved			not resolved		
	^{104}Pd α(1,0)	556	11	3.9	17	3200	13000	0.93	2700	25000	5.7
	^{102}Pd α(1,0)	557									
Silver	^{107}Ag α(2,1)	98	20	150	58	2900	73000	8.9	cut off electronically		
	^{109}Ag α(3,2)	103	18	180	70	1400	73000	19	5700	49000	3.7
	^{109}Ag α(2,0)	312	380	69	2.1	11000	45000	1.9	7400	37000	2.5
	^{107}Ag α(1,0)	325	310	41	2.0	12000	48000	1.7	6800	37000	2.7
	^{109}Ag α(3,0)	415	140	16	2.7	16000	17000	0.81	9900	23000	1.5
	^{107}Ag α(2,0)	423	120	11	2.6	14000	16000	0.89	11000	23000	1.2

Element	Assignment	E_γ (keV)	5 MeV			11 MeV			16 MeV		
			c/mC	bg/mC	$^o/_{oo}$	c/mC	bg/mC	$^o/_{oo}$	c/mC	bg/mC	$^o/_{oo}$
Cadmium	^{113}Cd α(2,0)	299	25	14	14	3900	33000	4.4	1100	17000	11
	^{111}Cd α(2,0)	342	17	9.5	17	1800	16000	6.7	430	8500	21
	^{114}Cd α(1,0)	558	20	2.9	8.1	5100	6500	1.5	7700	22000	1.8
	^{113}Cd α(6,0)	584	3.3	1.7	38	2000	4600	3.2	820	8400	11
	^{112}Cd α(1,0)	617	8.2	2.2	17	2300	6700	3.4	3300	12000	3.1
	^{110}Cd α(1,0)	658	2.2	1.0	43	1100	3700	5.5	2300	11000	4.4
Indium		-									
Tin		-									
Tellurium		-									
Barium		-									
Lanthanum		-									
Cerium		-									
Praseodymium		-									
Neodymium		-									
Erbium	^{167}Er α(2,0)	178	16	140	61						
	^{170}Er α(2,1)	182	3.6	100	230						
	^{166}Er α(2,1)	184	not resolved								
	^{168}Er α(2,1)	184	not resolved								
Hafnium	^{178}Hf α(1,0)	93	120	190	11						
	^{180}Hf α(1,0)	93	not resolved								
	^{177}Hf α(1,0)	113	41	120	25						
	^{179}Hf α(1,0)	123	28	110	35						
Tantalum	^{181}Ta α(1,0)	136	1200	200	1.1	29000	31000	0.58	53000	24000	0.28
	^{181}Ta α(2,1)	165	62	78	14	3700	16000	3.2	9700	15000	1.2
	^{181}Ta α(2,0)	301	39	16	9.7	3800	13000	2.9	4500	6200	1.7
Tungsten	^{183}W α(2,0)	99	not resolved			not resolved			not resolved		
	^{182}W α(1,0)	100	110	210	12	1600	55000	14	15000	14000	0.74
	^{184}W α(1,0)	111	260	150	4.5	1000	34000	17	20000	18000	0.64
	^{186}W α(1,0)	122	400	100	2.4	3100	38000	5.9	260	9600	35

Element	Assignment	E_γ (keV)	5 MeV			11 MeV			16 MeV		
			c/mC	bg/mC	$^o/_{oo}$	c/mC	bg/mC	$^o/_{oo}$	c/mC	bg/mC	$^o/_{oo}$
Rhenium	^{185}Re α(1,0)	125	650	420	3.0	18000	45000	1.1	8000	30000	2.1
	^{187}Re α(1,0)	134	1100	210	1.2	5400	35000	3.3	12000	22000	1.2
	^{185}Re α(2,1)	159	45	63	17	1900	31000	8.8	2200	22000	6.4
	^{187}Re α(3,1)	167	58	53	12	6900	38000	2.7	4000	15000	3.0
	^{185}Re α(2,0)	285	5.7	15	65	160	9700	59	350	5900	21
	^{187}Re α(3,0)	301	6.4	14	55	750	6800	10	840	5400	8.3
Iridium	^{193}Ir α(1,0)	73	510	260	3.0	13000	29000	1.2	cut off electronically		
	^{193}Ir α(3,1)	107	9.9	97	94	1100	30000	14	obscured by cut-off		
	^{191}Ir α(2,0)	129	290	150	3.9	6800	39000	2.7	5000	11000	1.9
	^{193}Ir α(2,0)	139	450	89	2.0	12000	25000	1.2	7800	9600	1.2
	^{191}Ir α(4,0)	179	6.4	32	84	7800	26000	1.9	260	6400	29
	^{193}Ir α(3,0)	180	not resolved			not resolved			not resolved		
	^{191}Ir α(5,2)	214	13	24	36	not resolved			not resolved		
	^{193}Ir α(4,2)	219	19	19	21	5700	18000	2.2	7800	9500	1.2
	^{191}Ir α(5,0)	343	14	5.7	16	2100	7400	3.9	1700	3400	3.2
	^{193}Ir α(4,0)	358	2.9	4.3	67	4300	8900	2.1	2600	3000	2.0
	^{193}Ir α(5,0)	362	16	4.6	13	not resolved			not resolved		
Platinum	^{195}Pt α(1,0)	99	4.1	72	200	350	17000	35	cut off electronically		
	^{195}Pt α(2,0)	130	3.2	59	230	180	15000	66	670	12000	15
	^{195}Pt α(5,1)	140	6.7	54	100	not observed			500	8500	18
	^{195}Pt α(4,0)	211	65	35	8.6	2700	25000	5.6	4000	6500	1.9
	^{195}Pt α(5,0)	239	23	18	17	1200	25000	13	1200	5800	5.9
	^{192}Pt α(1,0)	317	2.8	9.6	100	11000	11000	0.87	not resolved		
	^{194}Pt α(1,0)	329	70	10	4.3	13000	31000	1.3	8800	5800	0.82
	^{196}Pt α(1,0)	356	30	9.0	9.5	7100	17000	1.8	5200	4000	1.2
	^{198}Pt α(1,0)	407	3.0	2.6	52	1200	7900	7.1	870	2900	5.9
Gold	^{197}Au α(1,0)	77	190	140	5.7	24000	36000	0.76	cut off electronically		
	^{197}Au α(2,1)	192	15	36	39	680	17000	18	1800	7000	4.4
	^{197}Au α(2,0)	269	2.0	6.8	120	1800	8900	4.9	240	2600	20
	^{197}Au α(3,0)	279	70	15	5.0	4900	13000	2.2	5800	5100	1.2
	^{197}Au α(6,0)	548	1.2	1.5	97	2000	2400	2.3	2900	1900	1.4

Element	Assignment	E_γ (keV)	5 MeV			11 MeV			16 MeV		
			c/mC	bg/mC	$^o/_{oo}$	c/mC	bg/mC	$^o/_{oo}$	c/mC	bg/mC	$^o/_{oo}$
Mercury	^{199}Hg α(1,0)	158	16	65	42						
	^{199}Hg α(2,0)	208	2.7	28	160						
	^{200}Hg α(1,0)	368	3.5	16	94						
	^{198}Hg α(1,0)	412	1.5	15	220						
	^{202}Hg α(1,0)	439	1.9	7.7	120						
Lead		-									
Bismuth		-									

ATLAS OF SPECTRA

The spectra in this section are arranged in the order of atomic number. Where the spectrum is of a compound, it is placed in the order of the lightest element it illustrates. The elements represented in this compilation are given in the form of an outline of the periodic table which precedes the spectra (see Figure 10). Each spectrum is titled, thus no captions or figure numbers are necessary. Each identified peak is labelled with the energy and assignment of the corresponding gamma-ray. Peaks, the origins of which are unknown, are labelled with their corresponding energy. Escape peaks from high-energy gamma-rays are labelled as "-me" and "-2me" for the first and second escape respectively.

Spectra are presented in the form of blocks, each of one thousand channels. Commonly the first block contains all the features of interest, in which case the elements are given two to a page. When however, more than one block is required only that element is illustrated on a page. In order that gamma-rays of low intensity can be plotted together with those of high intensity all spectra are plotted on semi-log paper. Some spectra which have densely populated regions have insets in which the circled portion of the spectrum is illustrated below it, using the same vertical scale, but an enlarged energy axis for the sake of clarity.

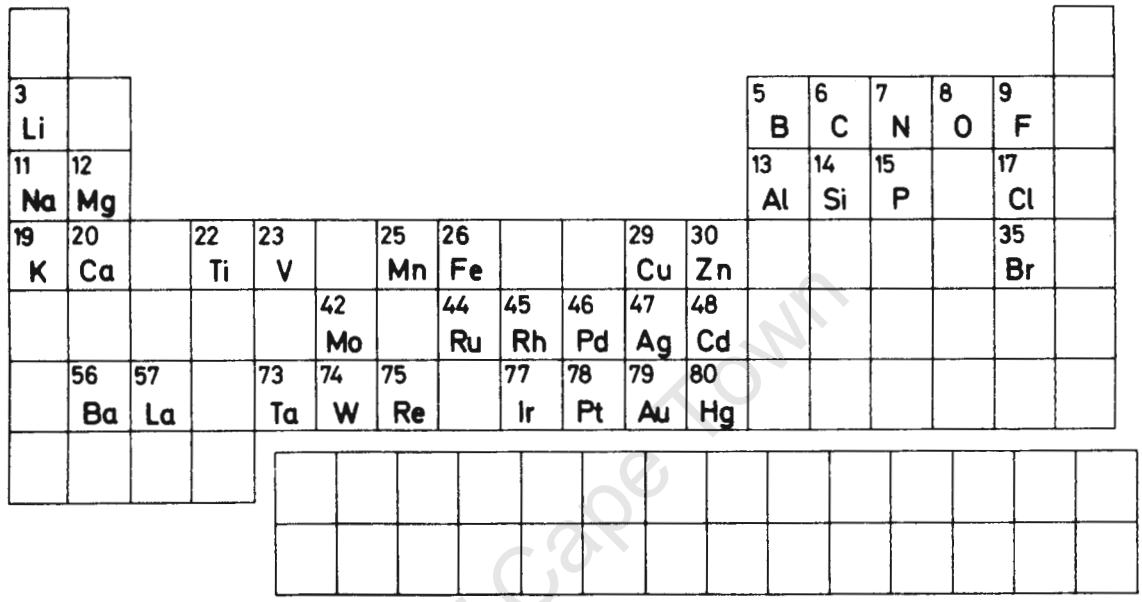

Figure 10 Outline of the Periodic Table in which the named elements are those for which spectra are reproduced in the Atlas of Spectra.

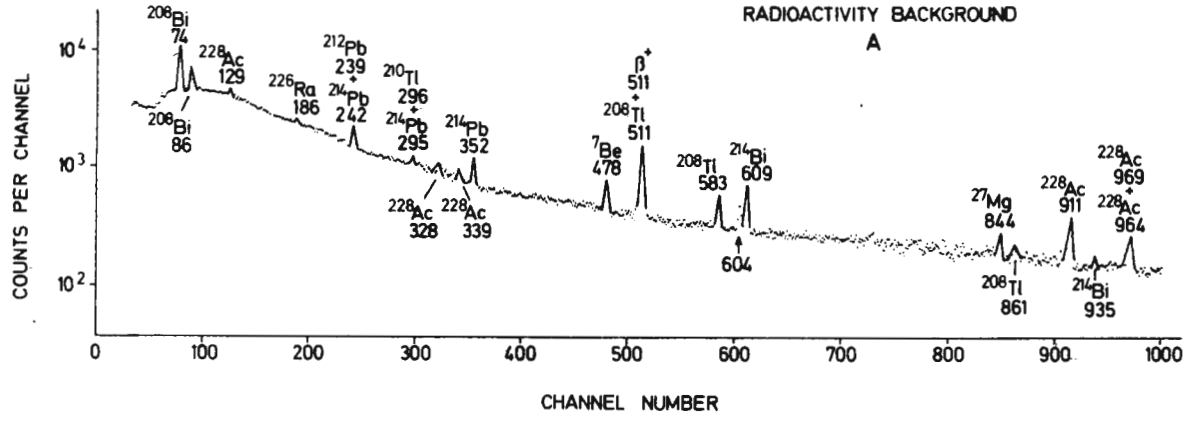

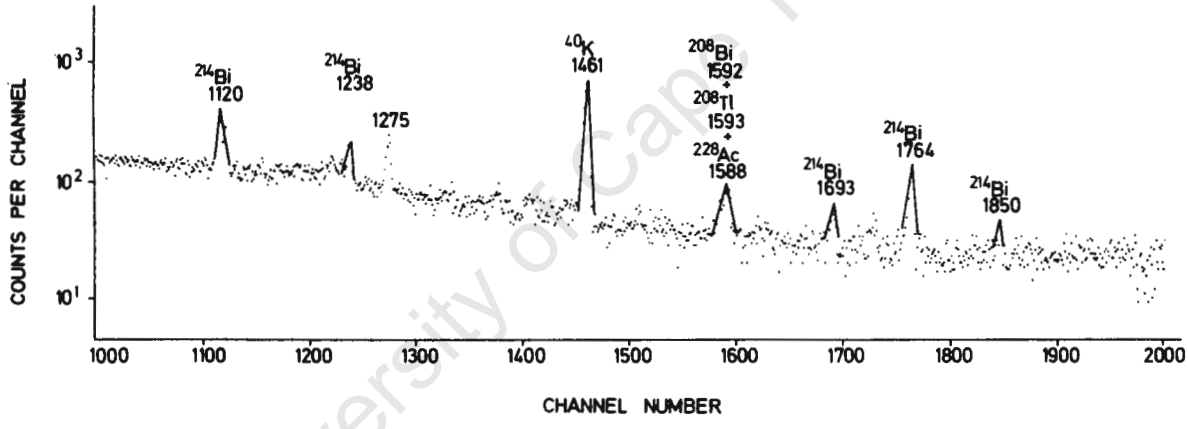

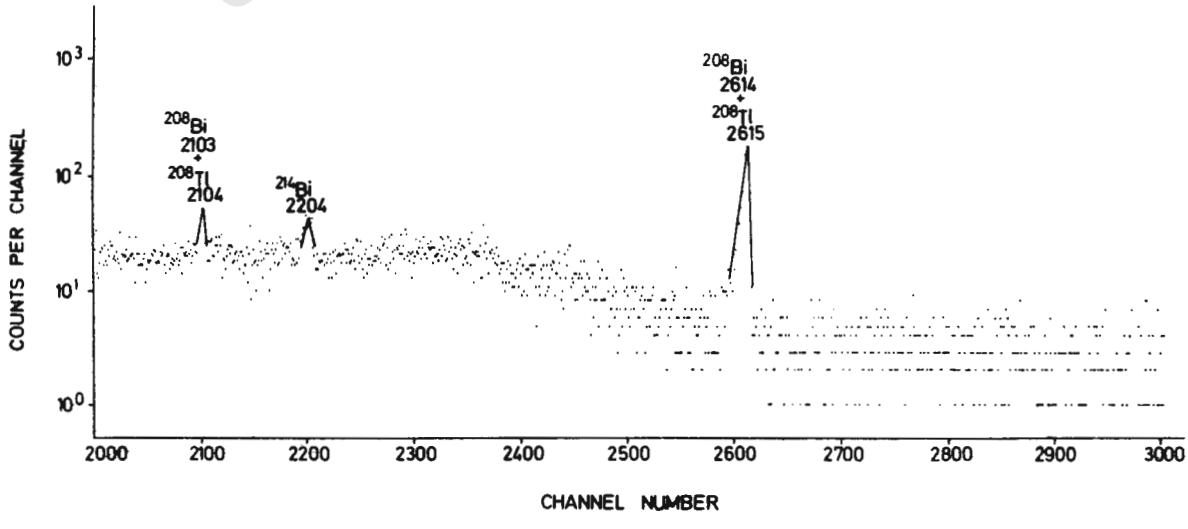

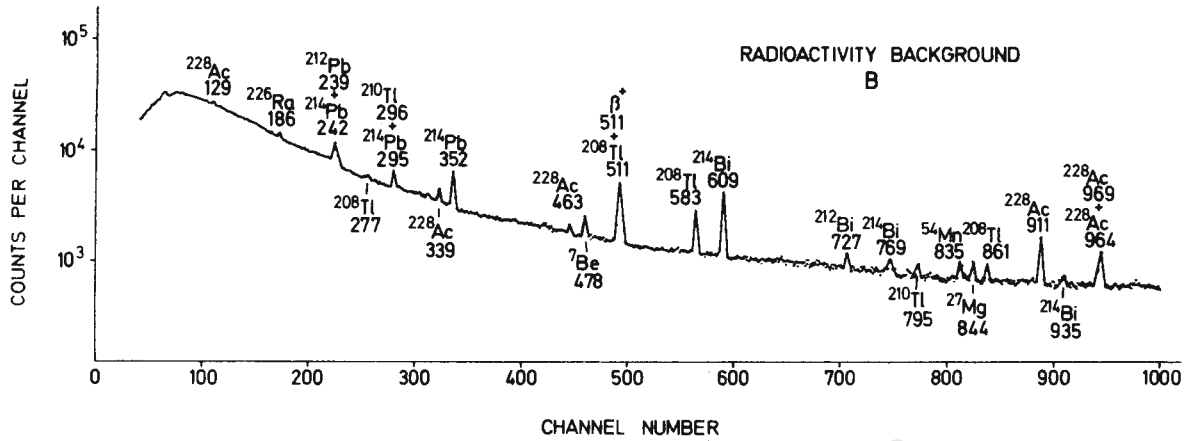

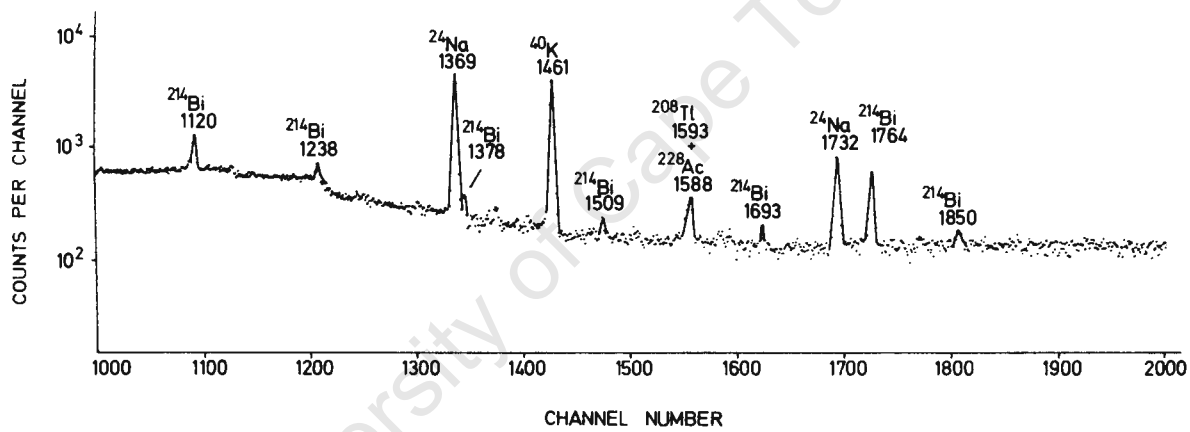

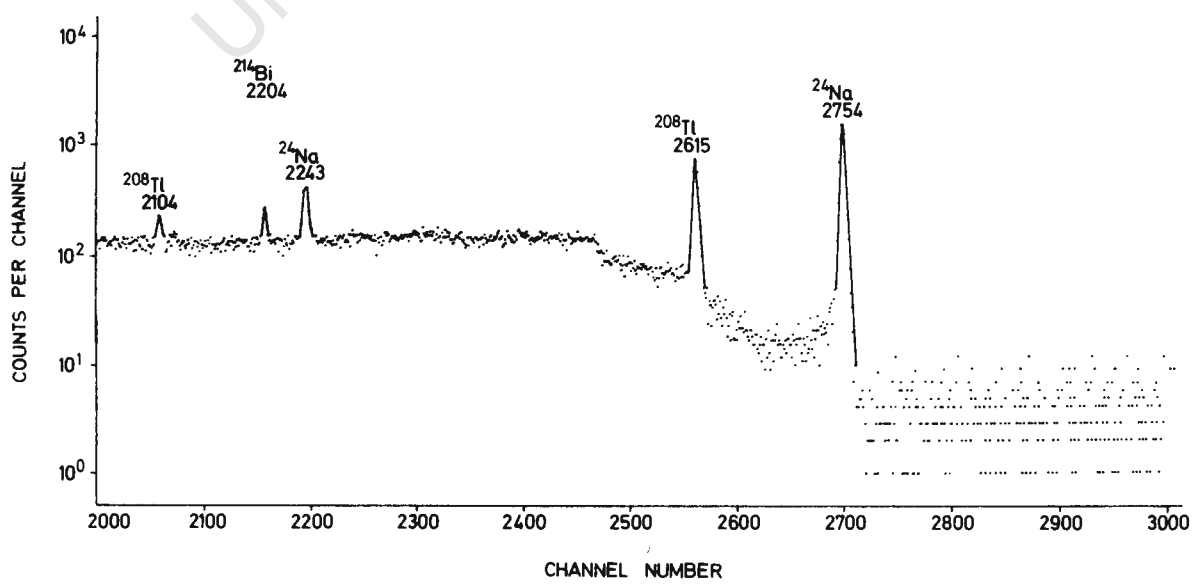

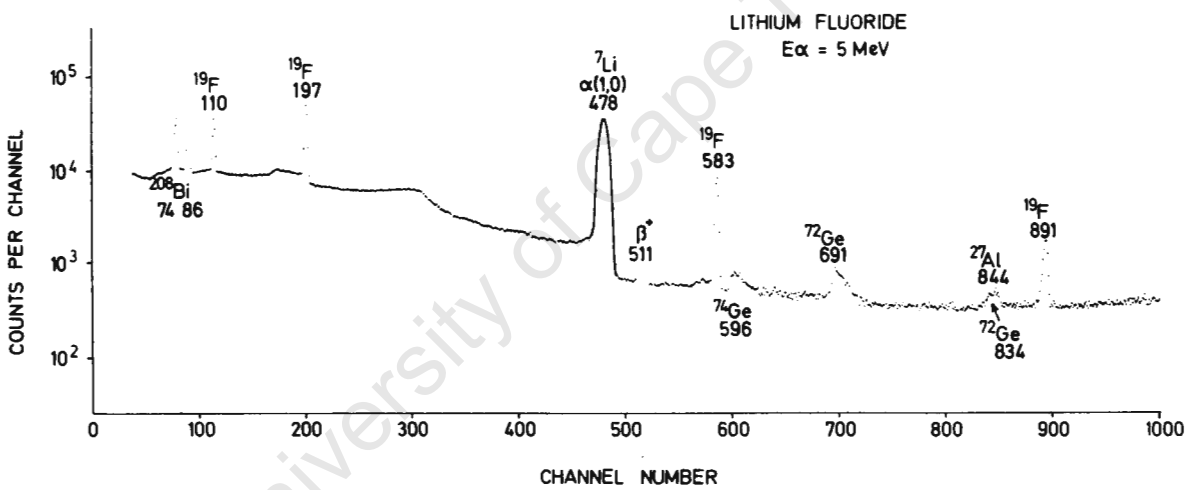

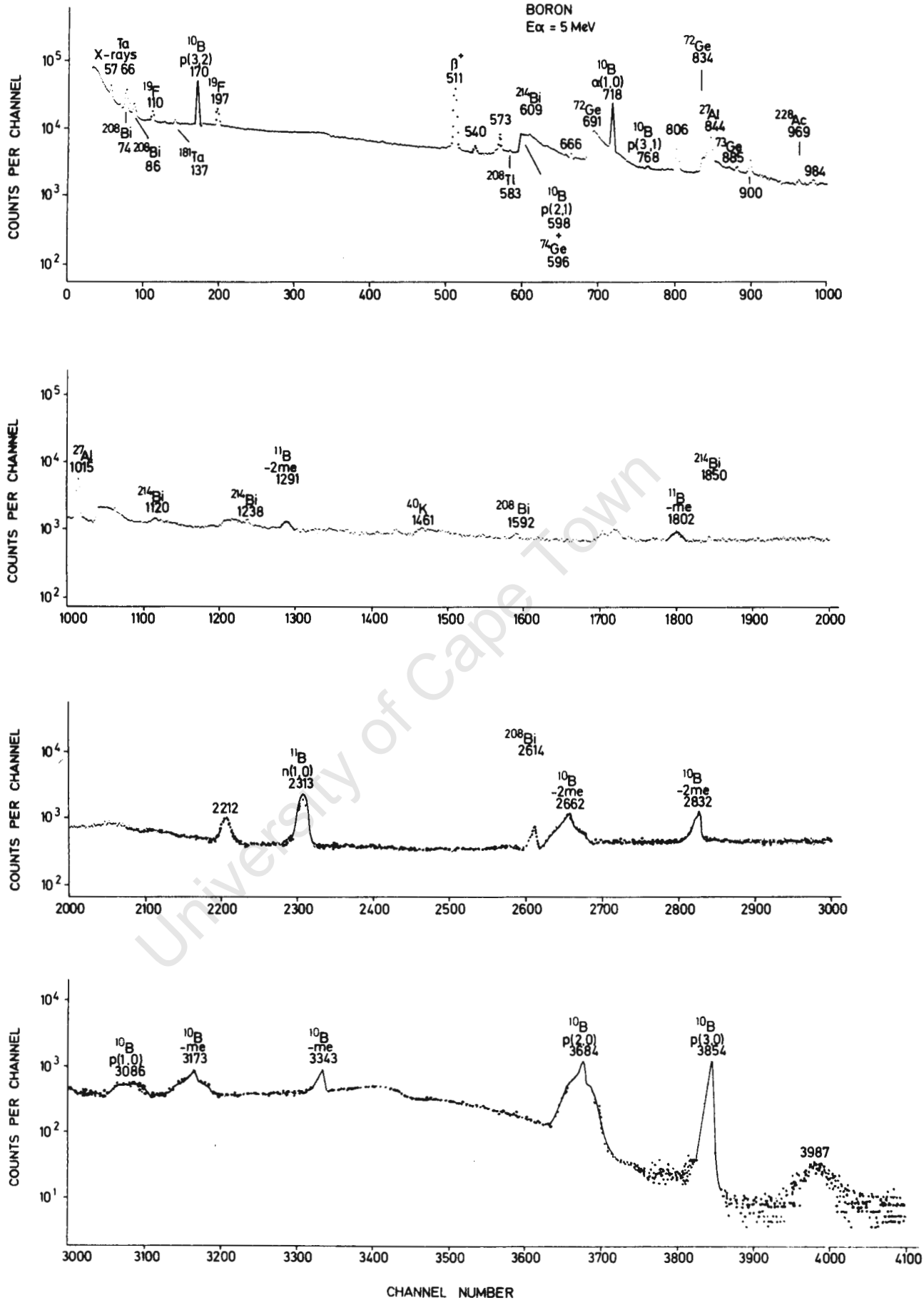

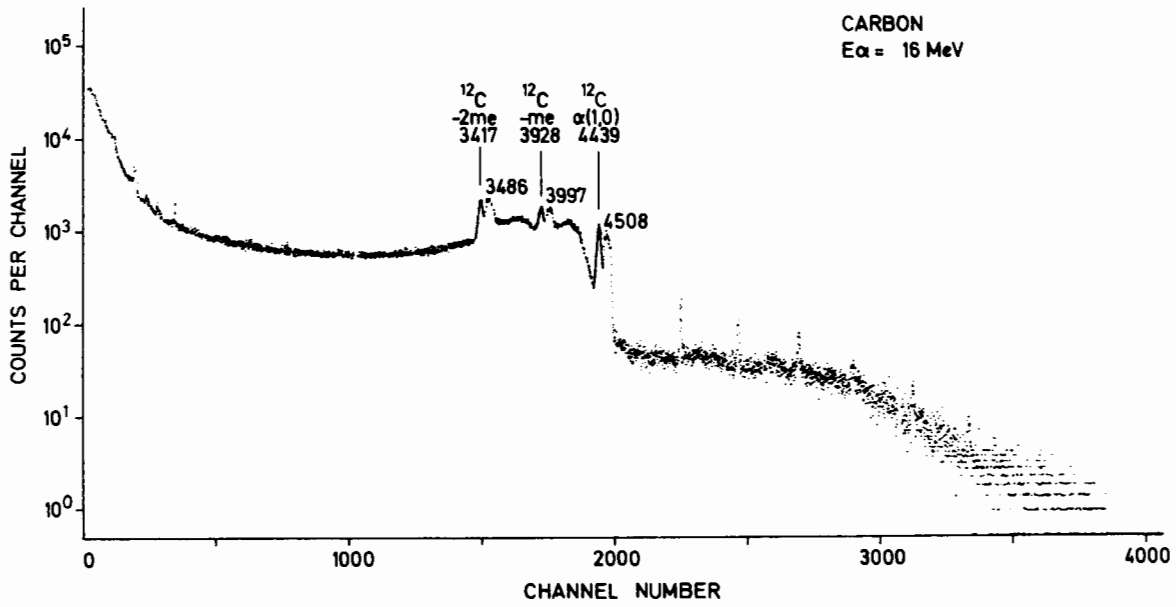
CARBON
Eα = 16 MeV
^{12}C -2me 3417
^{12}C -me 3928
^{12}C α(1,0) 4439
3486
3997
4508
COUNTS PER CHANNEL
CHANNEL NUMBER

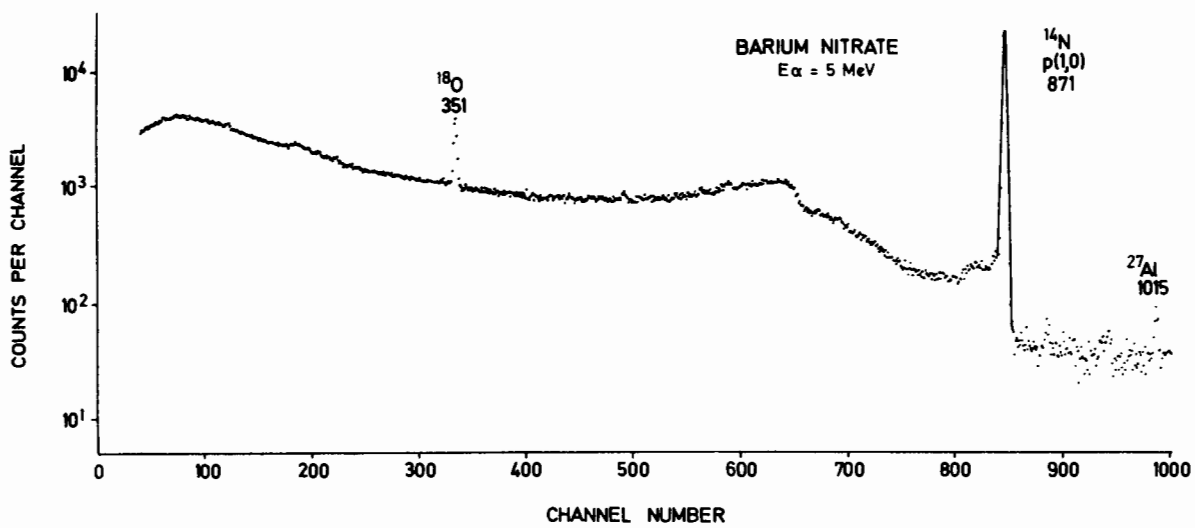
BARIUM NITRATE
Eα = 5 MeV
^{18}O 351
^{14}N p(1,0) 871
^{27}Al 1015
COUNTS PER CHANNEL
CHANNEL NUMBER

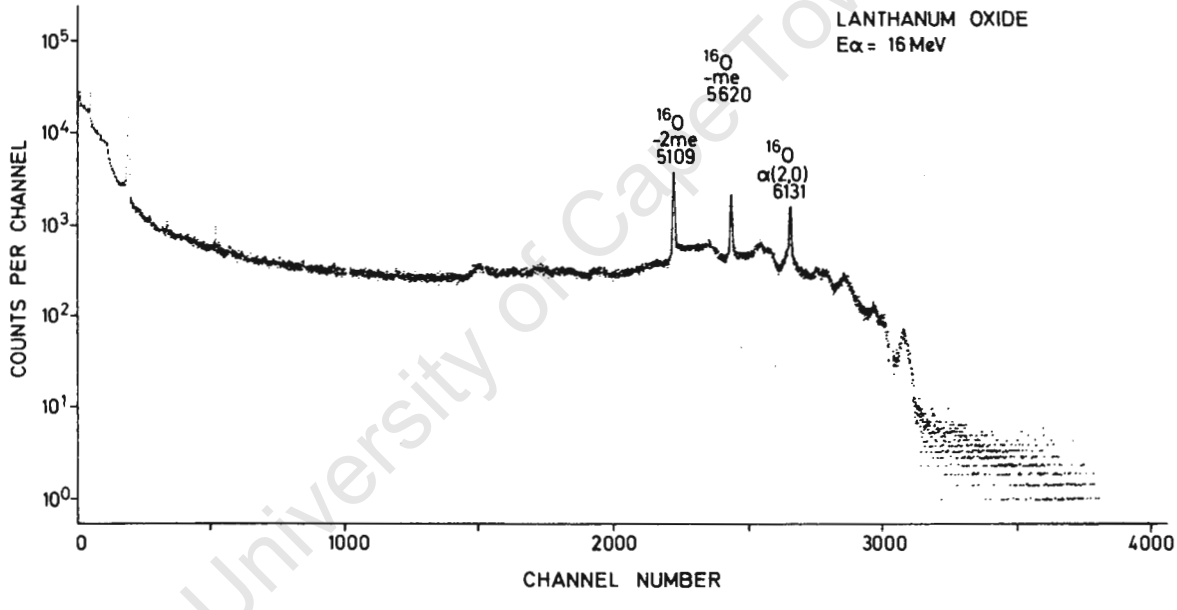

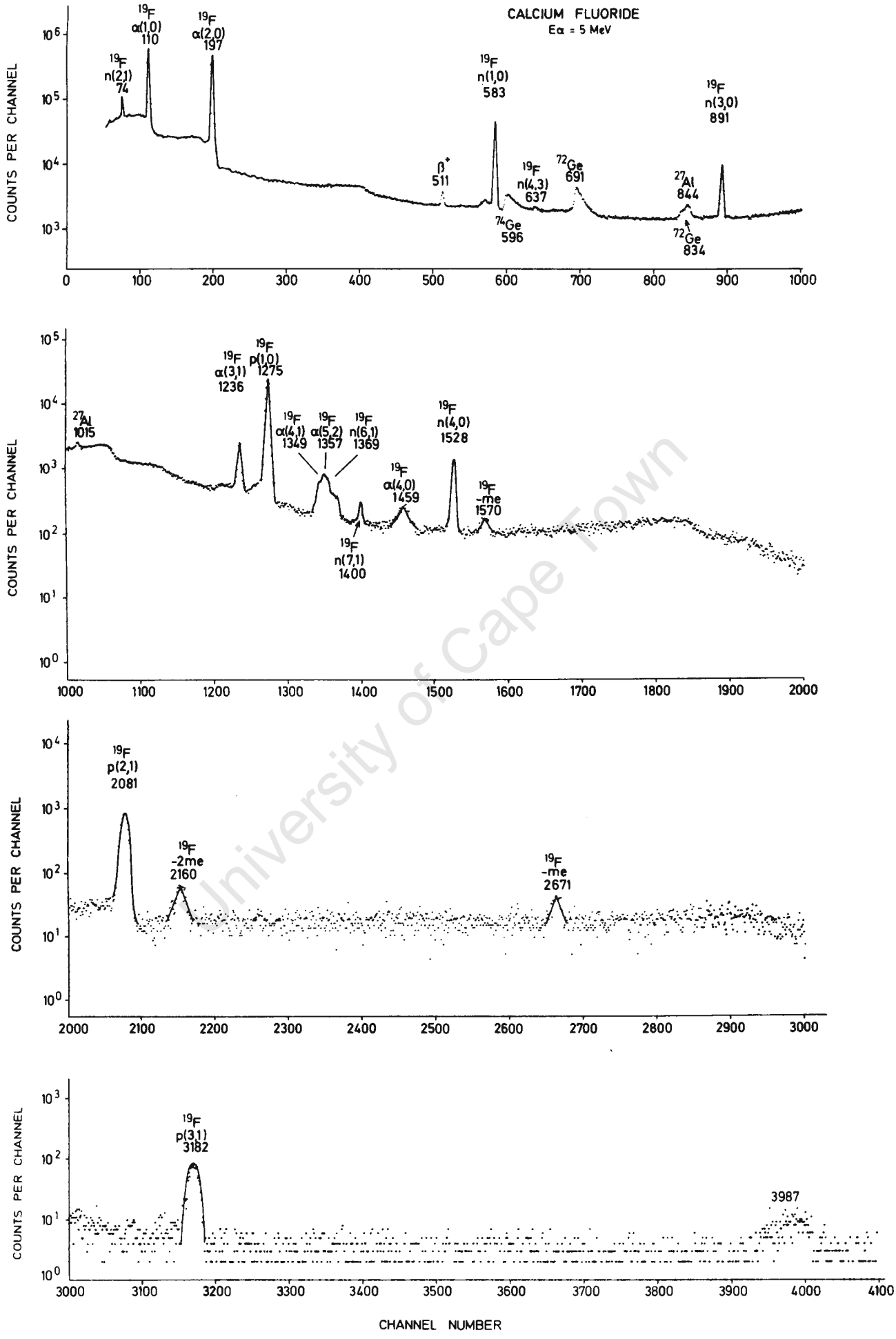

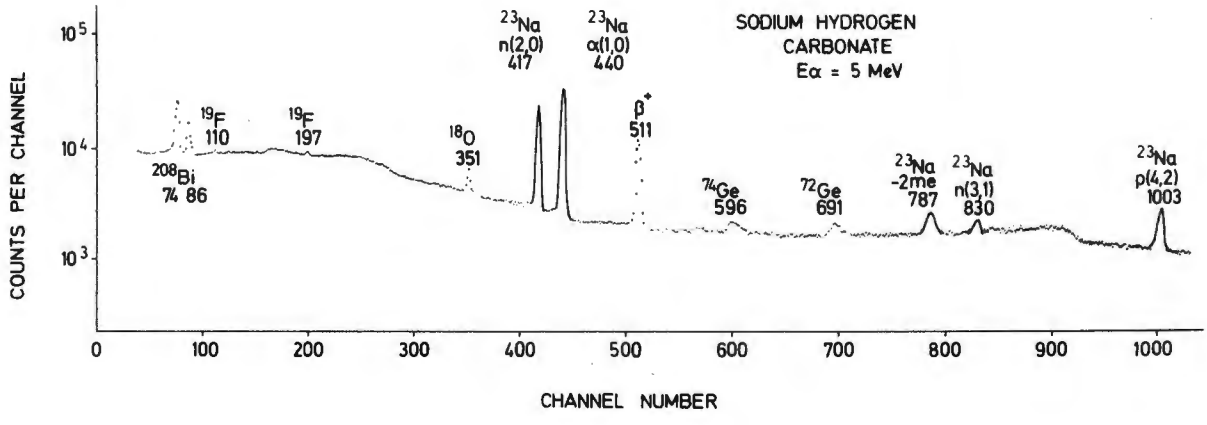
SODIUM HYDROGEN
CARBONATE
Eα = 5 MeV
COUNTS PER CHANNEL
CHANNEL NUMBER
208Bi 74 86
19F 110
19F 197
18O 351
23Na n(2,0) 417
23Na α(1,0) 440
β+ 511
74Ge 596
72Ge 691
23Na -2me 787
23Na n(3,1) 830
23Na p(4,2) 1003

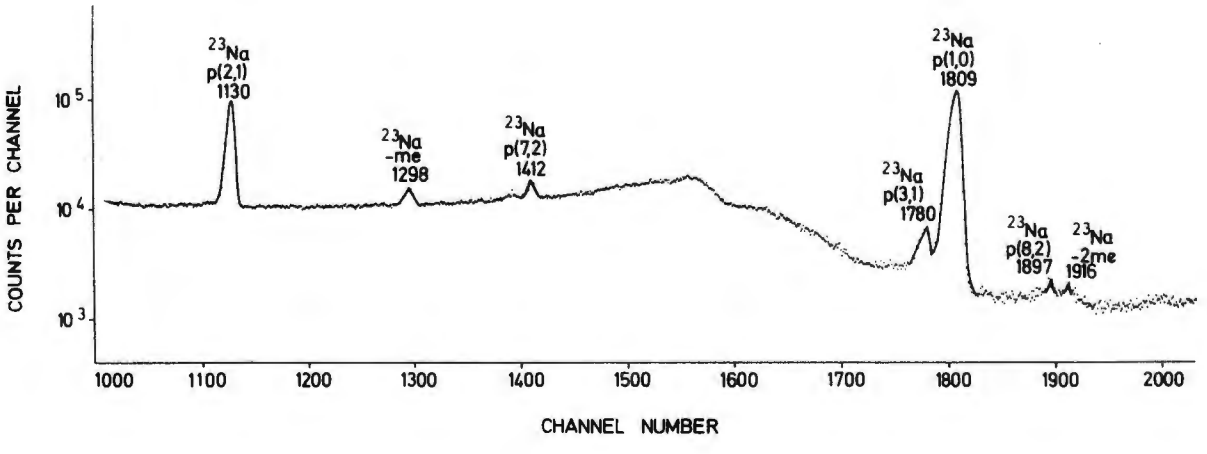
COUNTS PER CHANNEL
CHANNEL NUMBER
23Na p(2,1) 1130
23Na -me 1298
23Na p(7,2) 1412
23Na p(3,1) 1780
23Na p(1,0) 1809
23Na p(8,2) 1897
23Na -2me 1916

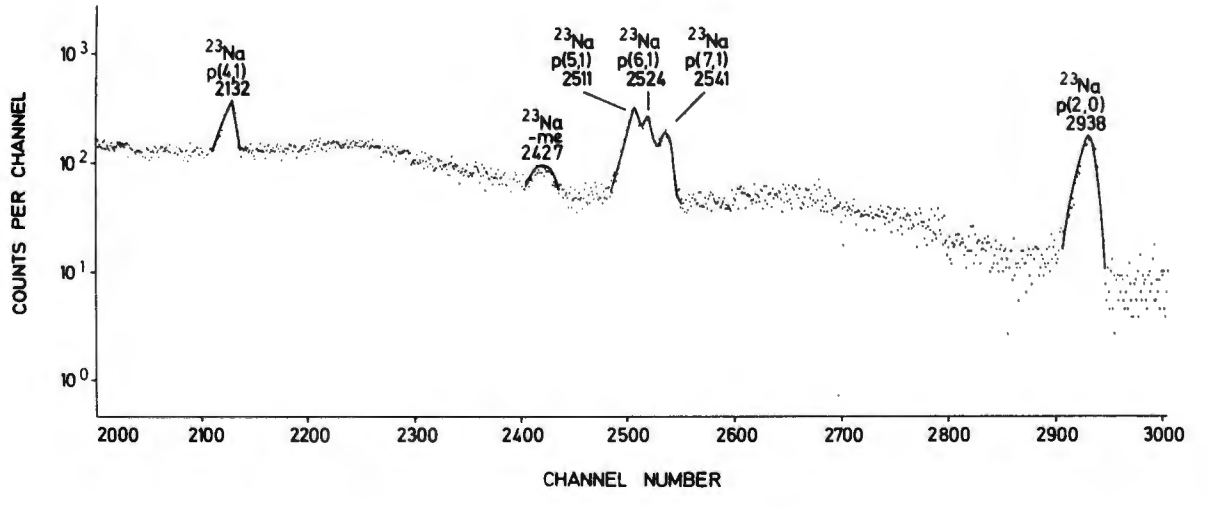
COUNTS PER CHANNEL
CHANNEL NUMBER
23Na p(4,1) 2132
23Na -me 2427
23Na p(5,1) 2511
23Na p(6,1) 2524
23Na p(7,1) 2541
23Na p(2,0) 2938

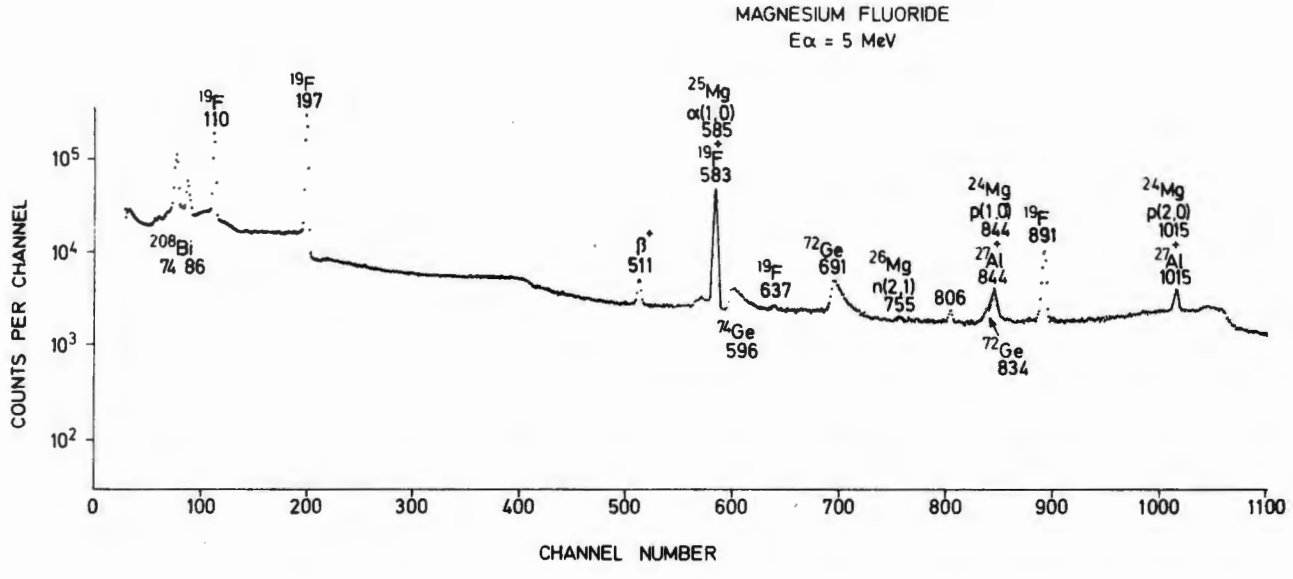
MAGNESIUM FLUORIDE
Eα = 5 MeV
COUNTS PER CHANNEL
CHANNEL NUMBER
19F 110
19F 197
25Mg α(1,0) 585
19F* 583
208Bi 74 86
β+ 511
72Ge 691
19F 637
74Ge 596
26Mg n(2,1) 755
806
24Mg p(1,0) 844
27Al* 844
72Ge 834
19F 891
24Mg p(2,0) 1015
27Al* 1015

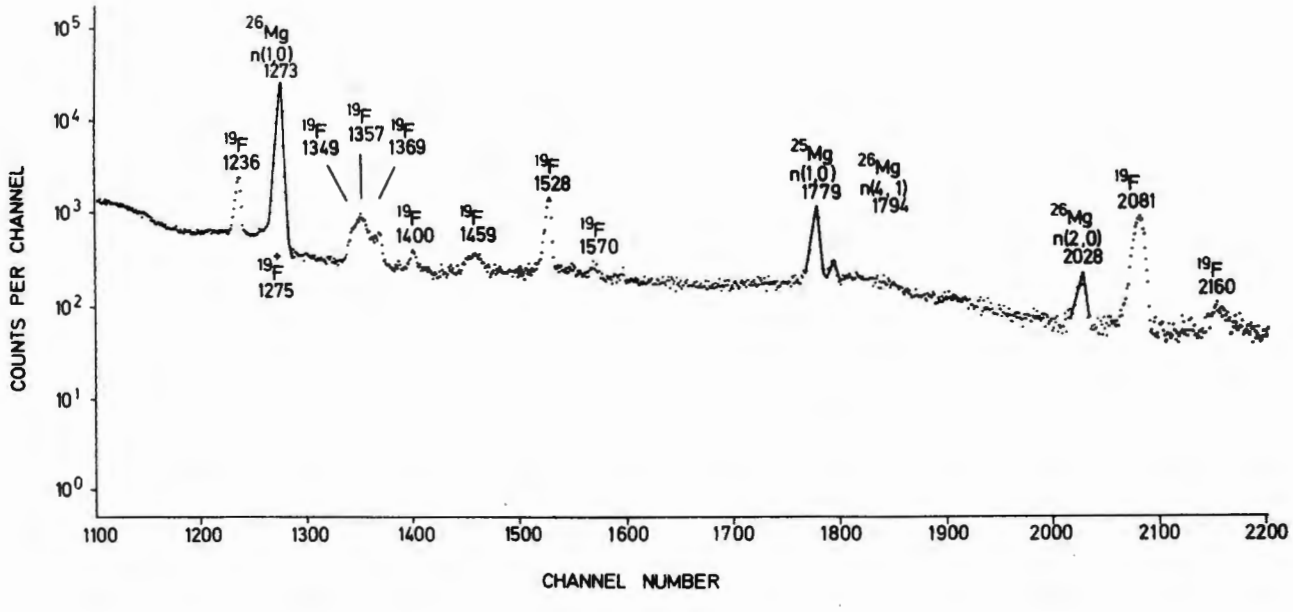
COUNTS PER CHANNEL
CHANNEL NUMBER
26Mg n(1,0) 1273
19F 1236
19F* 1275
19F 1349
19F 1357
19F 1369
19F 1400
19F 1459
19F 1528
19F 1570
25Mg n(1,0) 1779
26Mg n(4,1) 1794
26Mg n(2,0) 2028
19F 2081
19F 2160

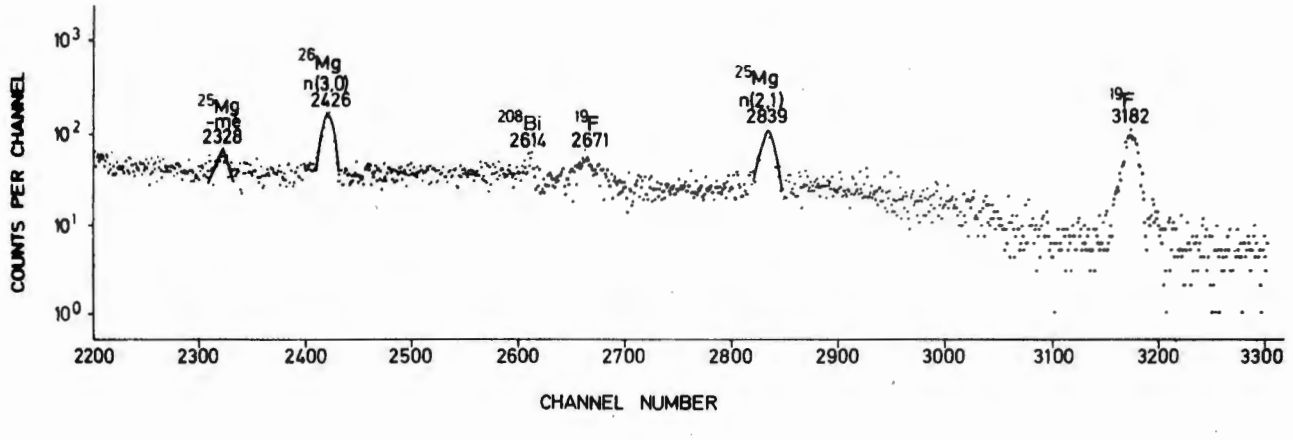
COUNTS PER CHANNEL
CHANNEL NUMBER
25Mg -me 2328
26Mg n(3,0) 2426
208Bi 2614
19F 2671
25Mg n(2,1) 2839
19F 3182

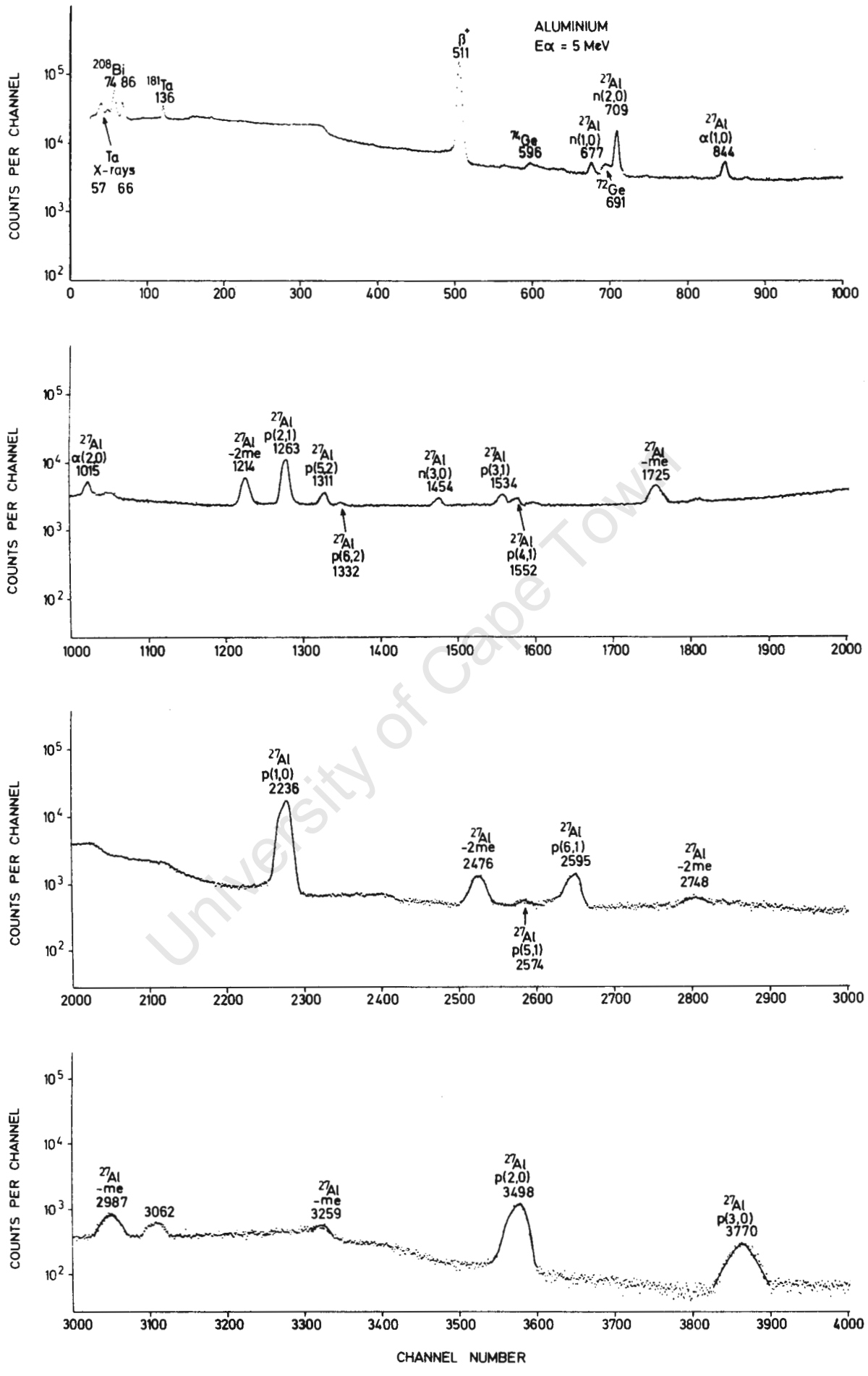

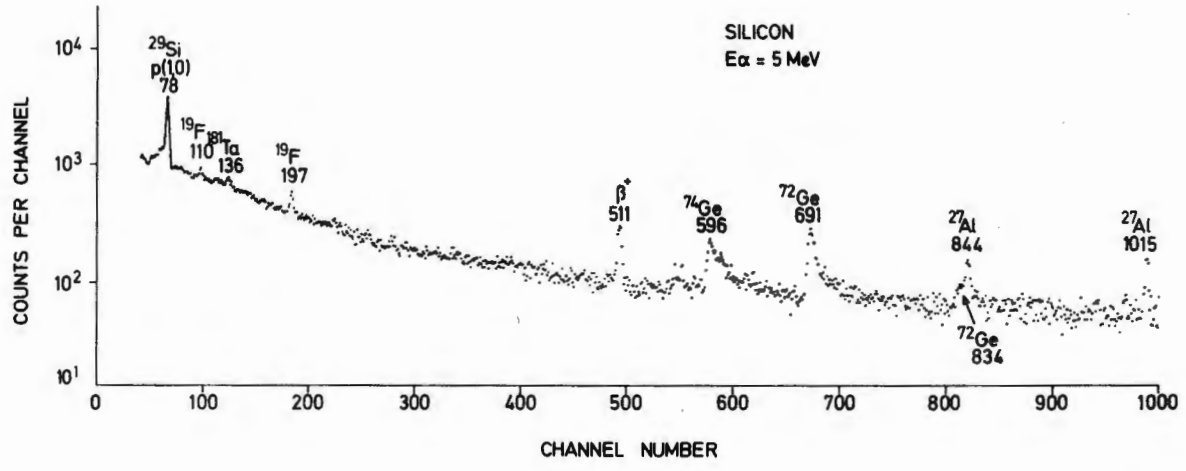
SILICON
Eα = 5 MeV
29Si p(1,0) 78
19F 110
181Ta 136
19F 197
β+ 511
74Ge 596
72Ge 691
27Al 844
72Ge 834
27Al 1015
COUNTS PER CHANNEL
CHANNEL NUMBER

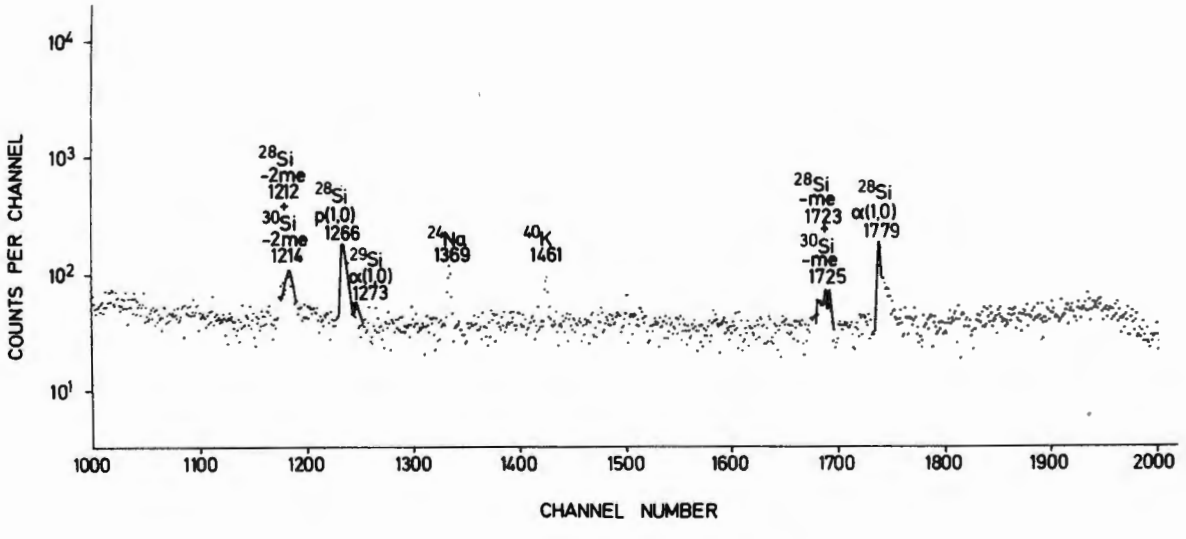
28Si -2me 1212
30Si -2me 1214
28Si p(1,0) 1266
29Si p(1,0) 1273
24Na 1369
40K 1461
28Si -me 1723
30Si -me 1725
28Si α(1,0) 1779
COUNTS PER CHANNEL
CHANNEL NUMBER

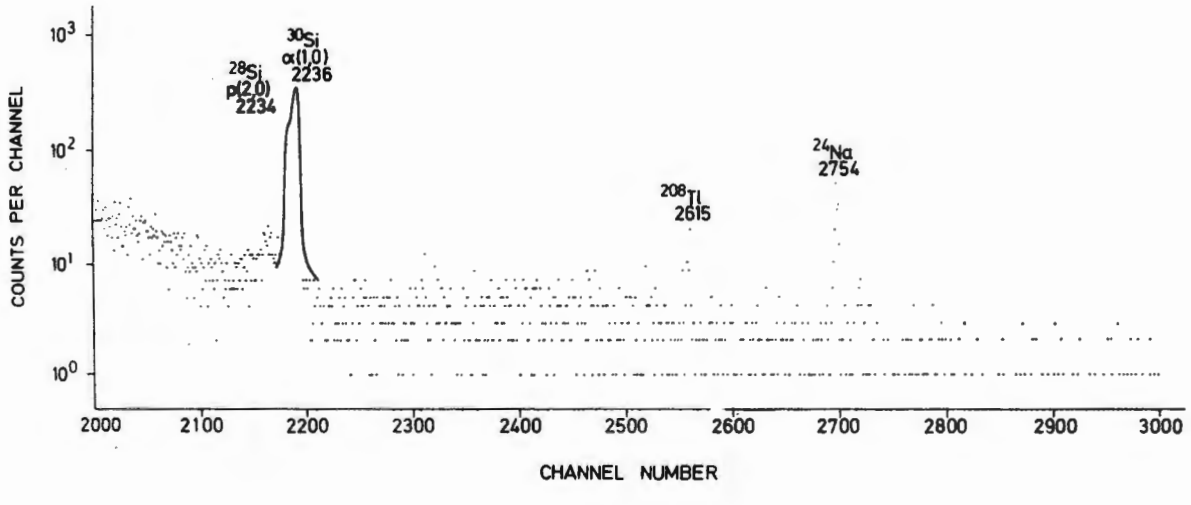
30Si α(1,0) 2236
28Si p(2,0) 2234
208Tl 2615
24Na 2754
COUNTS PER CHANNEL
CHANNEL NUMBER

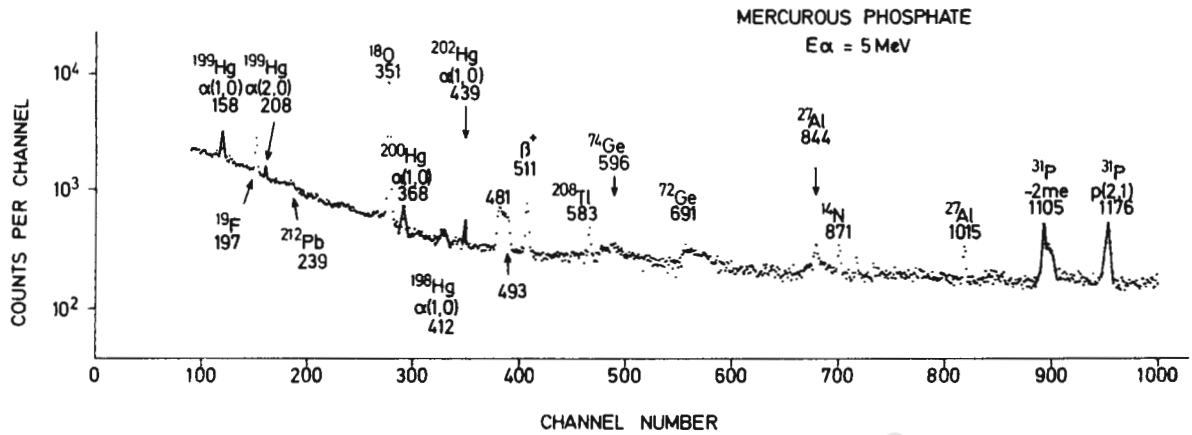

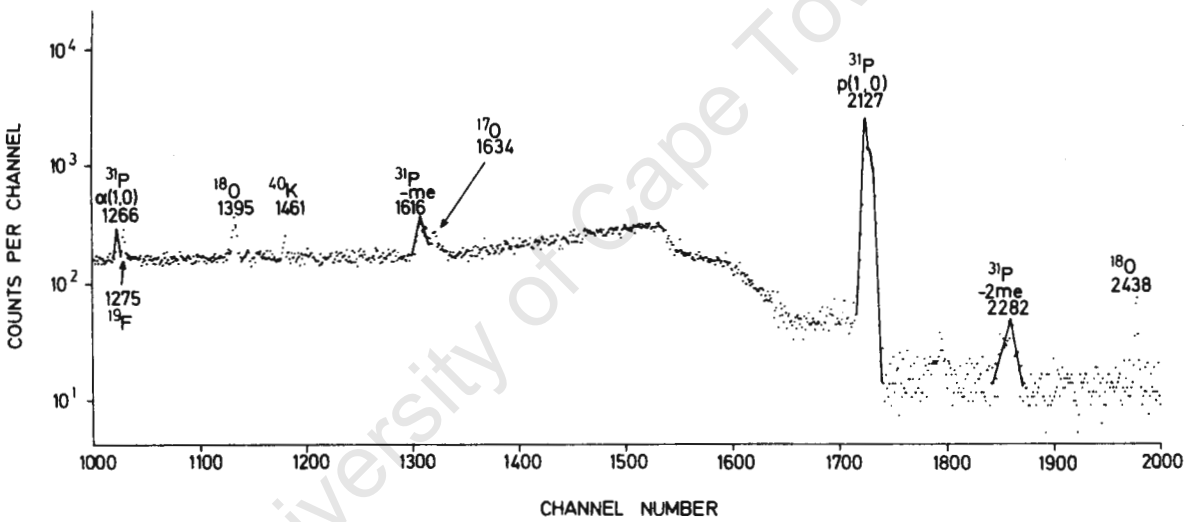

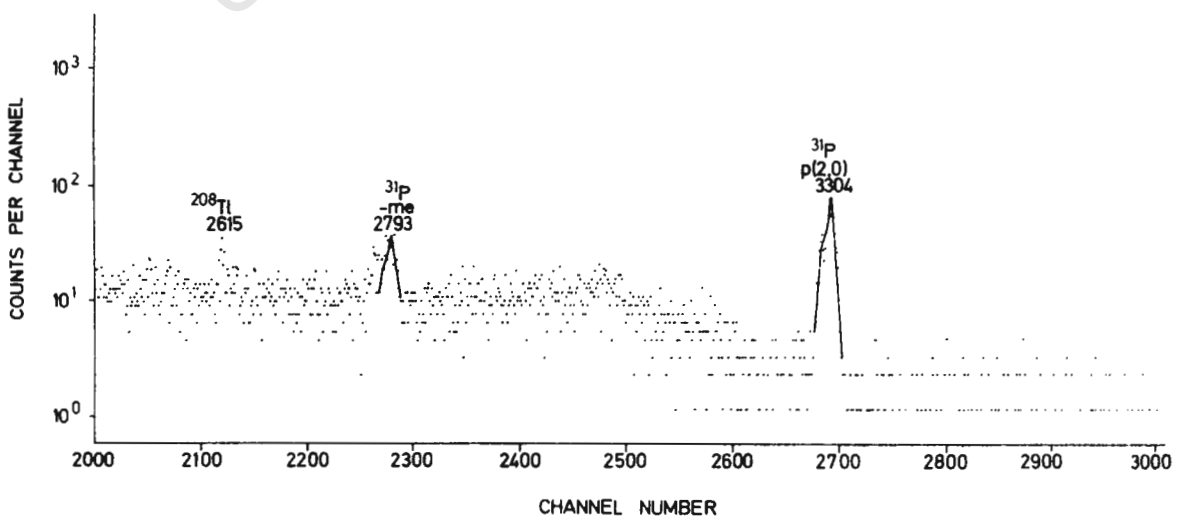

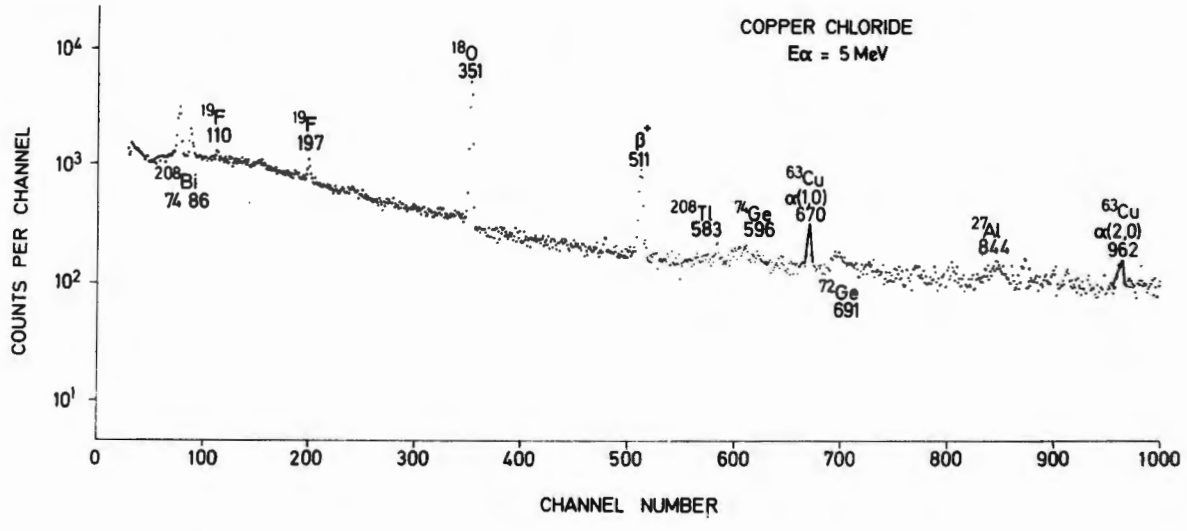
COPPER CHLORIDE
Eα = 5 MeV
COUNTS PER CHANNEL
CHANNEL NUMBER
18O 351
19F 110
19F 197
β+ 511
208Bi 74 86
208Tl 583
74Ge 596
63Cu α(1,0) 670
72Ge 691
27Al 844
63Cu α(2,0) 962

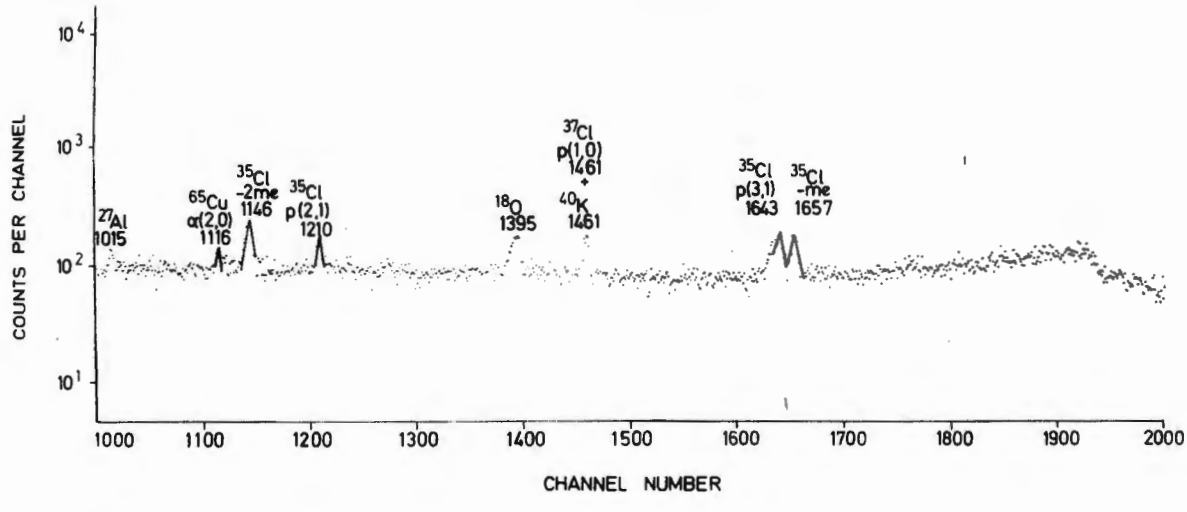
COUNTS PER CHANNEL
CHANNEL NUMBER
27Al 1015
65Cu α(2,0) 1116
35Cl -2me 1146
35Cl p(2,1) 1210
18O 1395
37Cl p(1,0) 1461
40K 1461
35Cl p(3,1) 1643
35Cl -me 1657

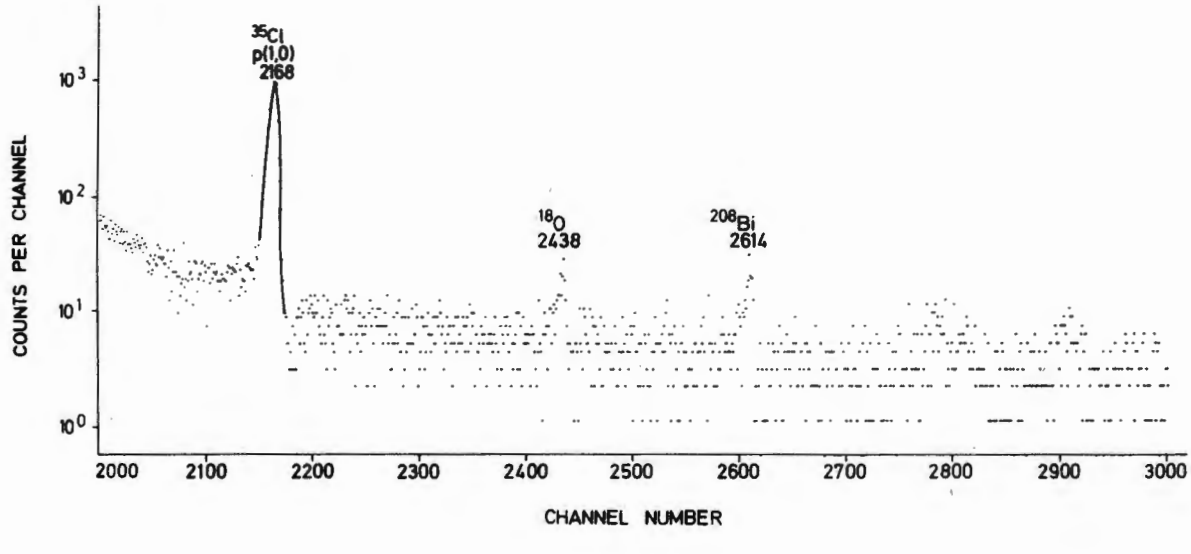
COUNTS PER CHANNEL
CHANNEL NUMBER
35Cl p(1,0) 2168
18O 2438
208Bi 2614

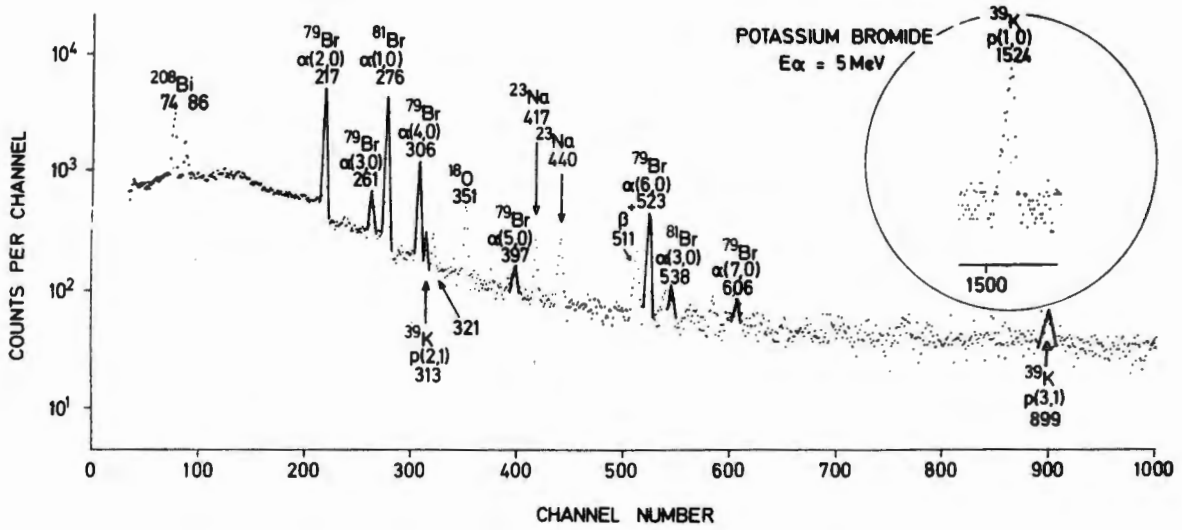
POTASSIUM BROMIDE
Eα = 5 MeV
COUNTS PER CHANNEL
CHANNEL NUMBER
208Bi 74 86
79Br α(2,0) 217
81Br α(1,0) 276
79Br α(3,0) 261
79Br α(4,0) 306
18O 351
23Na 417
23Na 440
79Br α(5,0) 397
β+ 511
79Br α(6,0) 523
81Br α(3,0) 538
79Br α(7,0) 606
39K p(2,1) 313
321
39K p(1,0) 1524
1500
39K p(3,1) 899

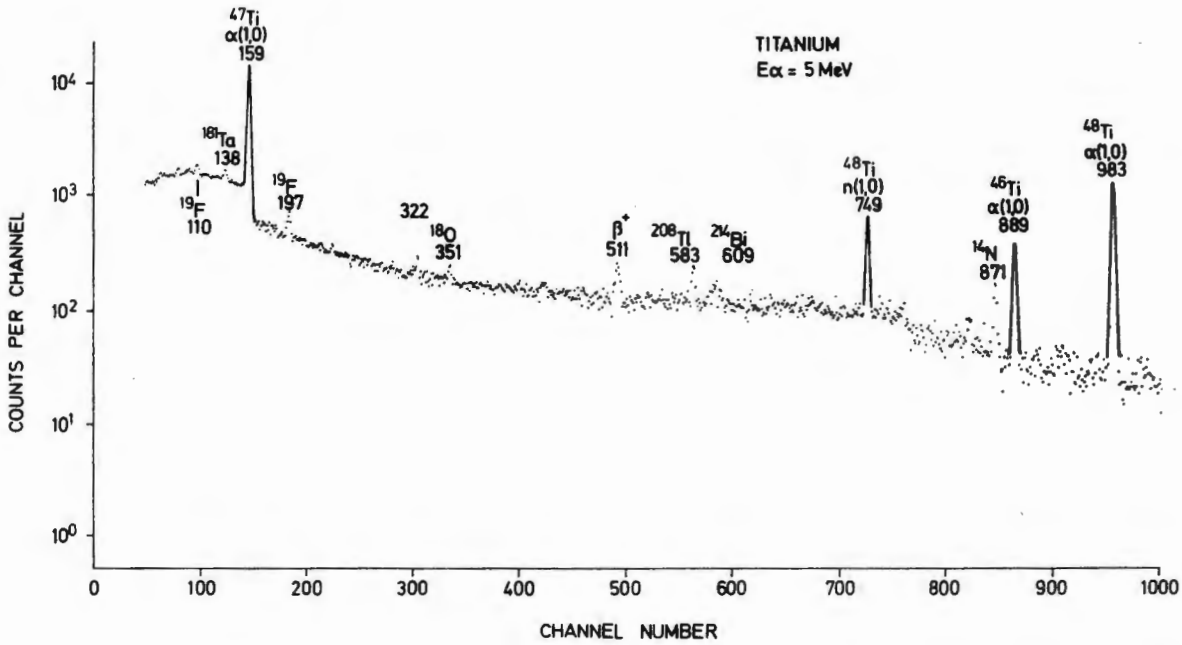
TITANIUM
Eα = 5 MeV
COUNTS PER CHANNEL
CHANNEL NUMBER
47Ti α(1,0) 159
181Ta 138
19F 110
19F 197
322
18O 351
β+ 511
208Tl 583
214Bi 609
48Ti n(1,0) 749
46Ti α(1,0) 889
14N 871
48Ti α(1,0) 983

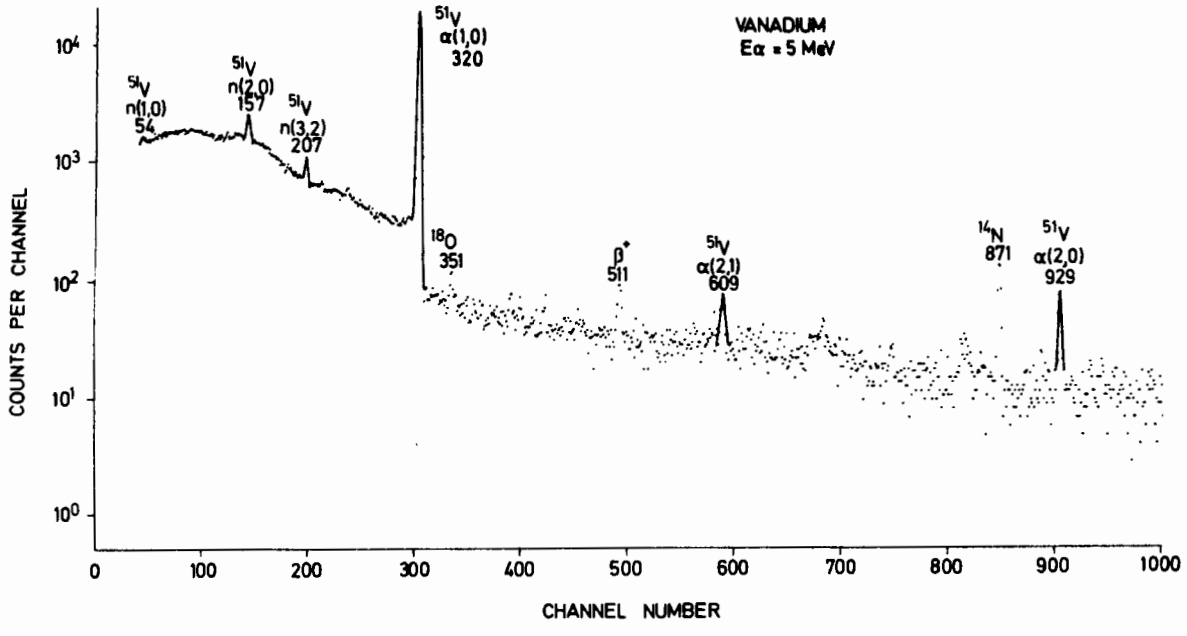
VANADIUM
Eα = 5 MeV
51V n(1,0) 54
51V n(2,0) 157
51V n(3,2) 207
51V α(1,0) 320
18O 351
β+ 511
51V α(2,1) 609
14N 871
51V α(2,0) 929
COUNTS PER CHANNEL
CHANNEL NUMBER

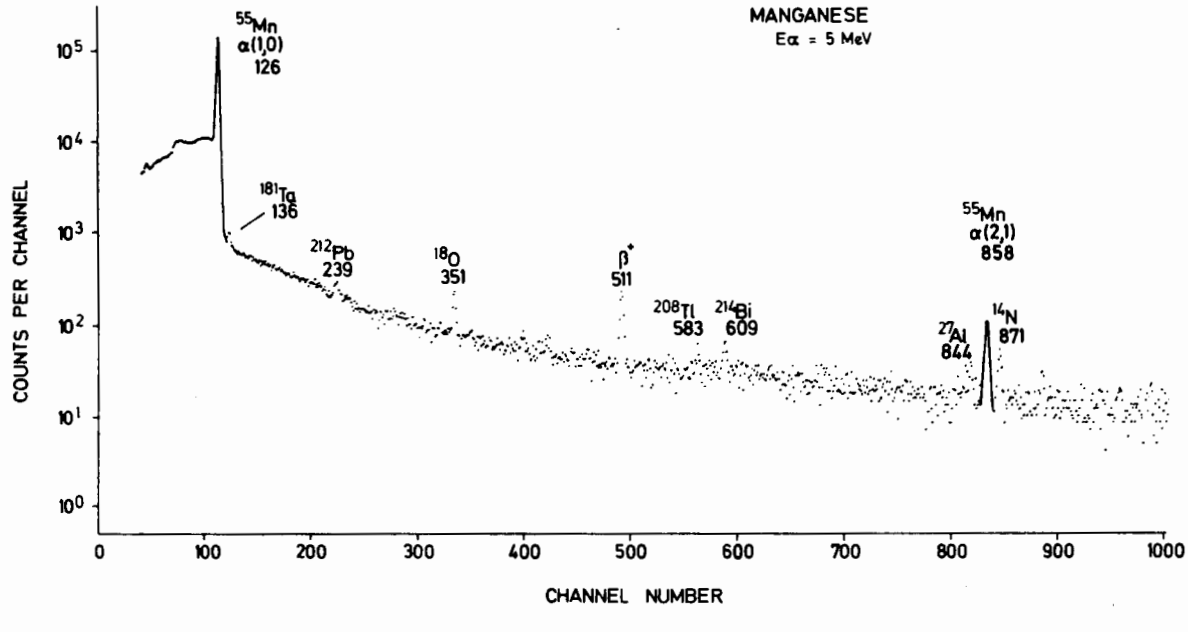
MANGANESE
Eα = 5 MeV
55Mn α(1,0) 126
181Ta 136
212Pb 239
18O 351
β+ 511
208Tl 583
214Bi 609
27Al 844
14N 871
55Mn α(2,1) 858
COUNTS PER CHANNEL
CHANNEL NUMBER

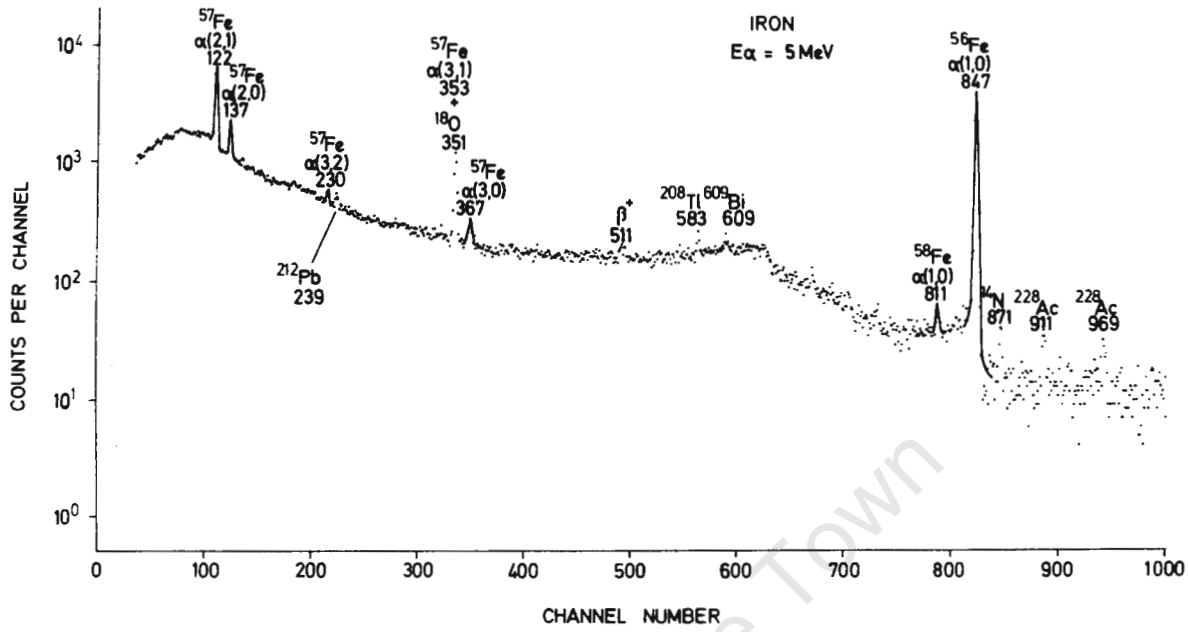

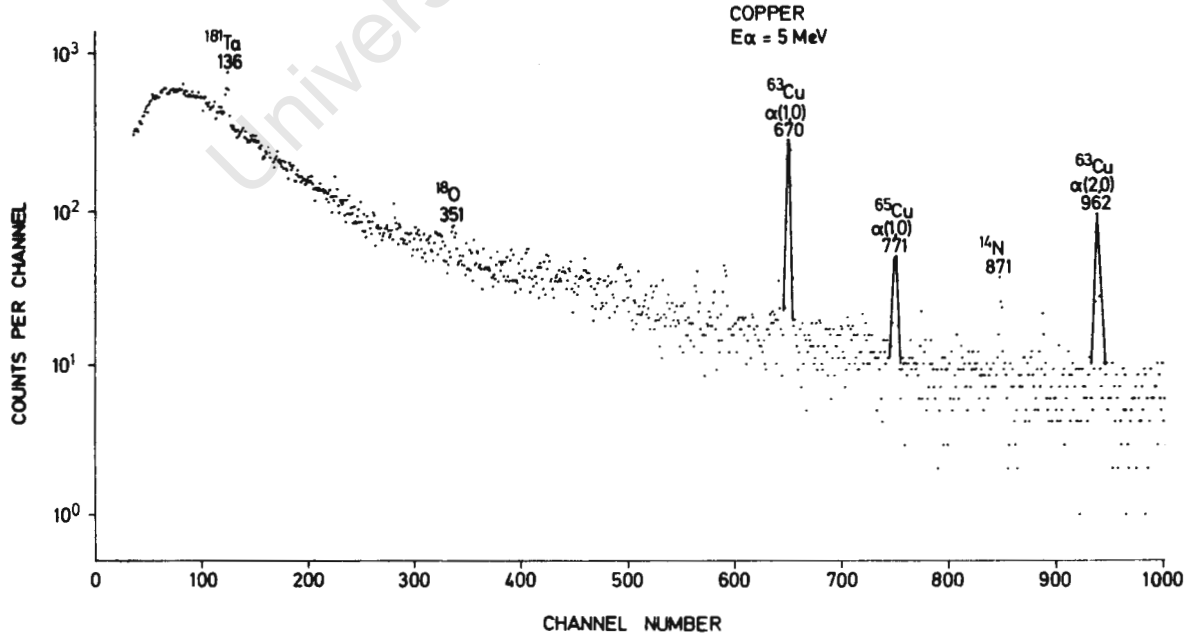

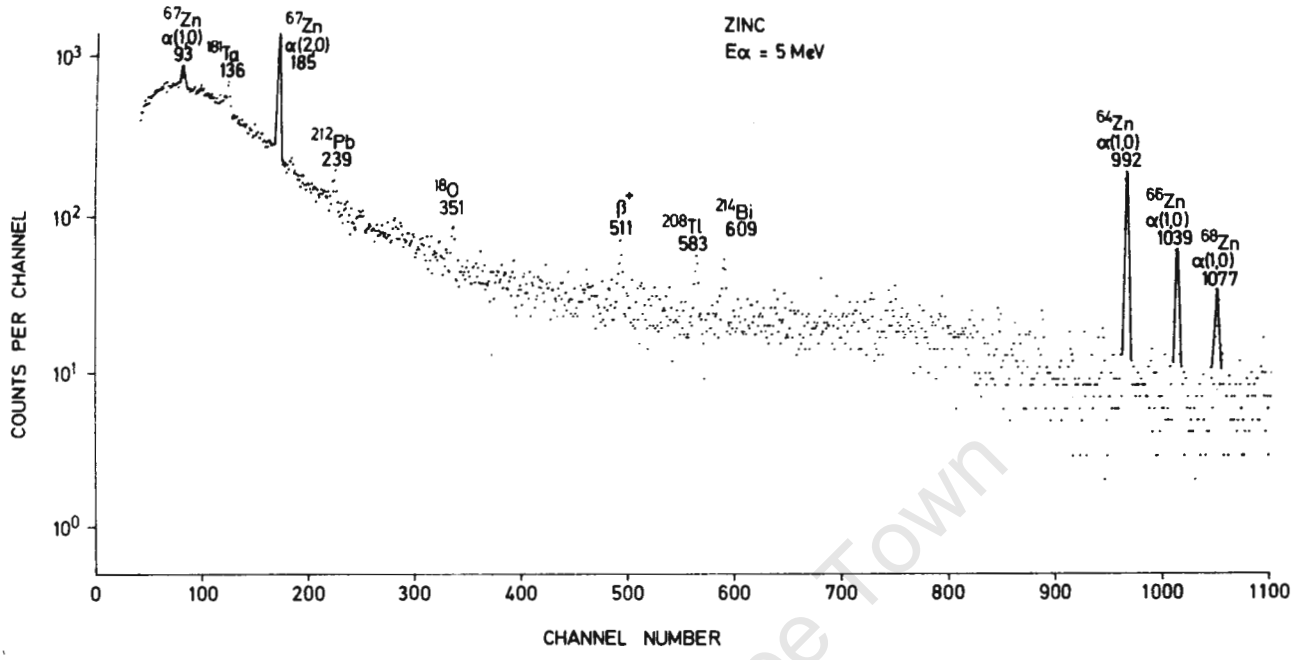

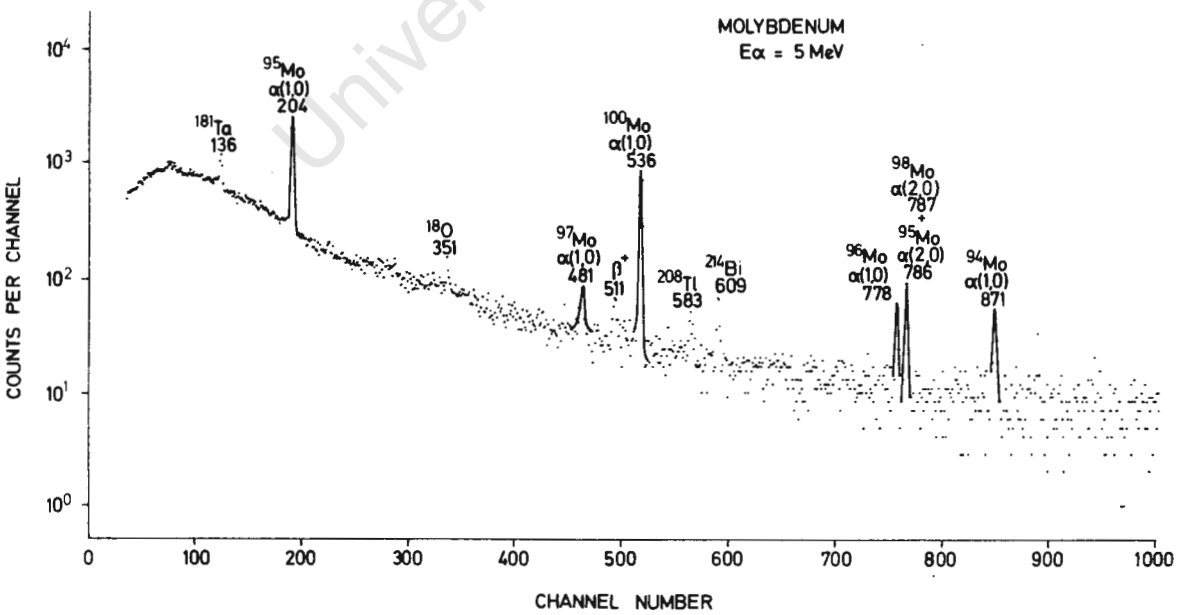

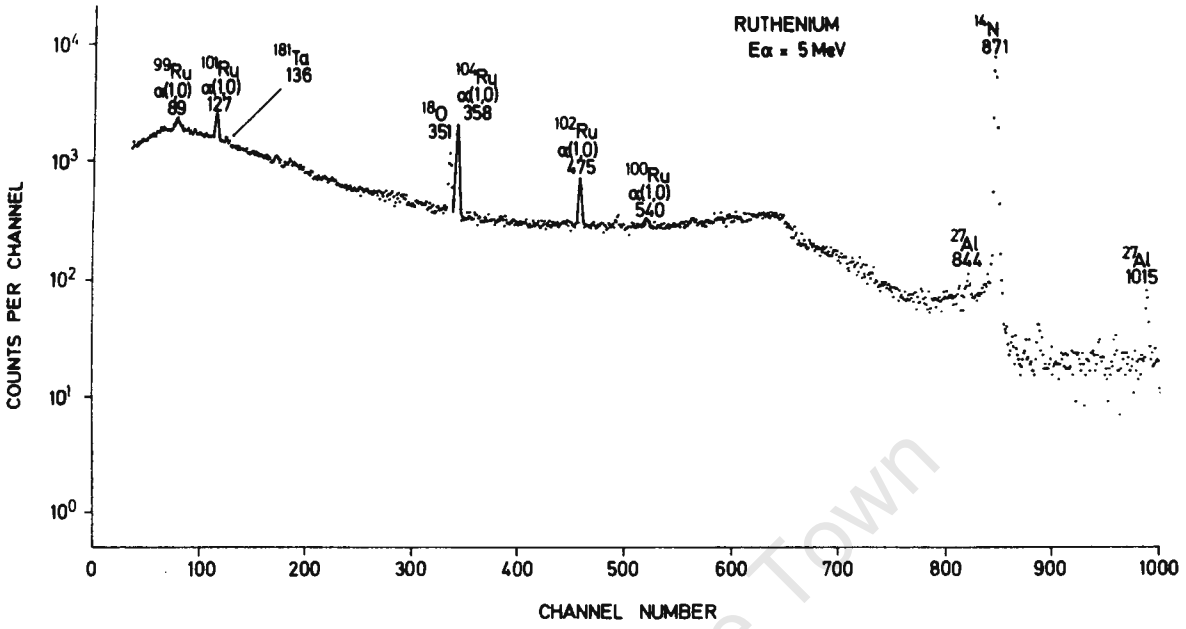

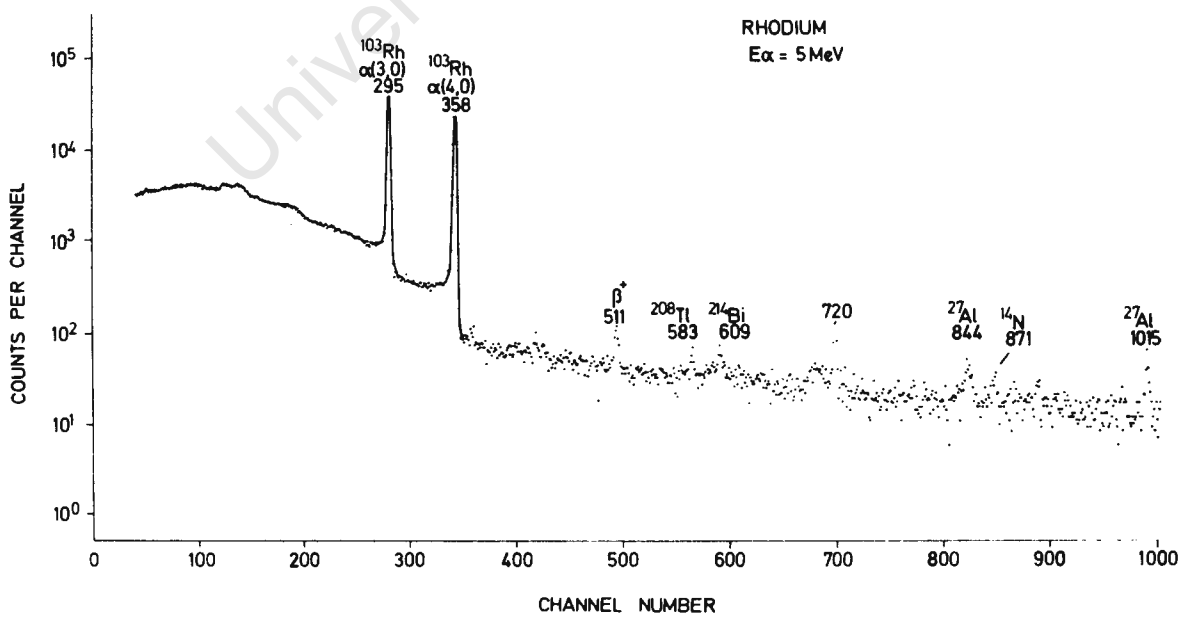

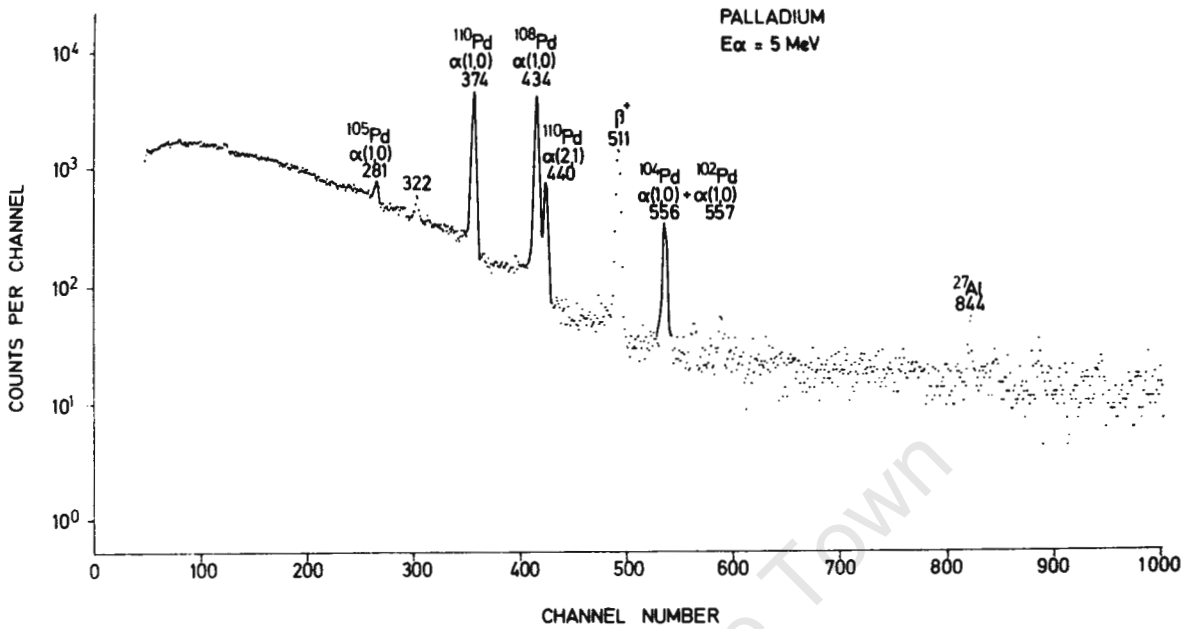

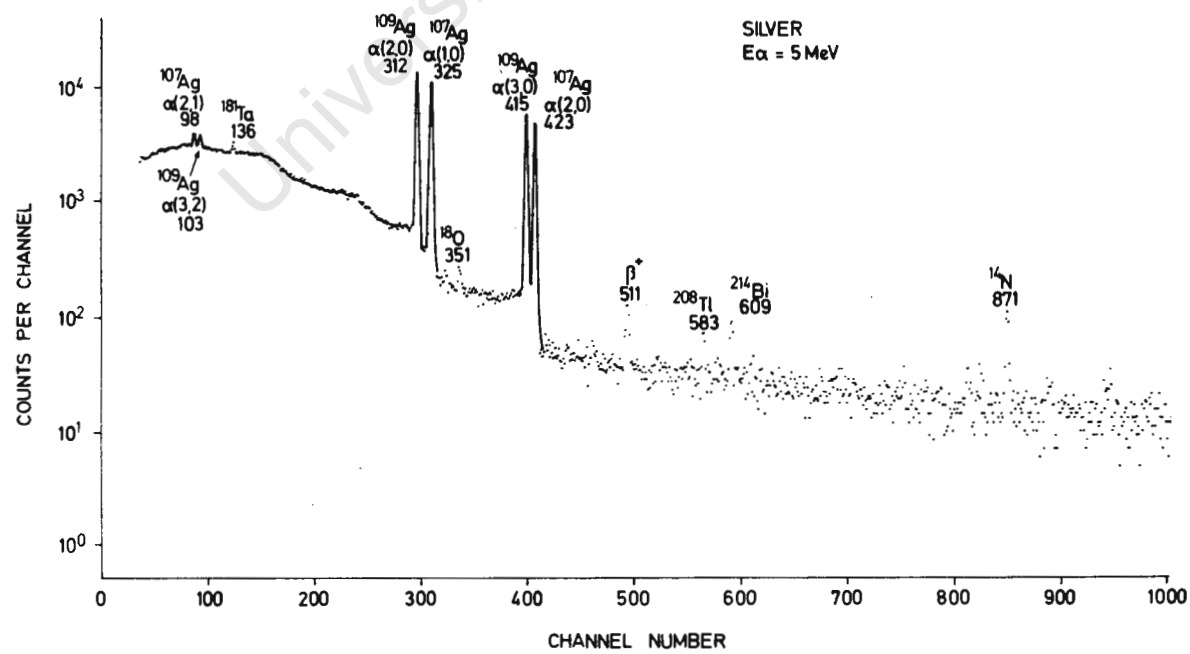

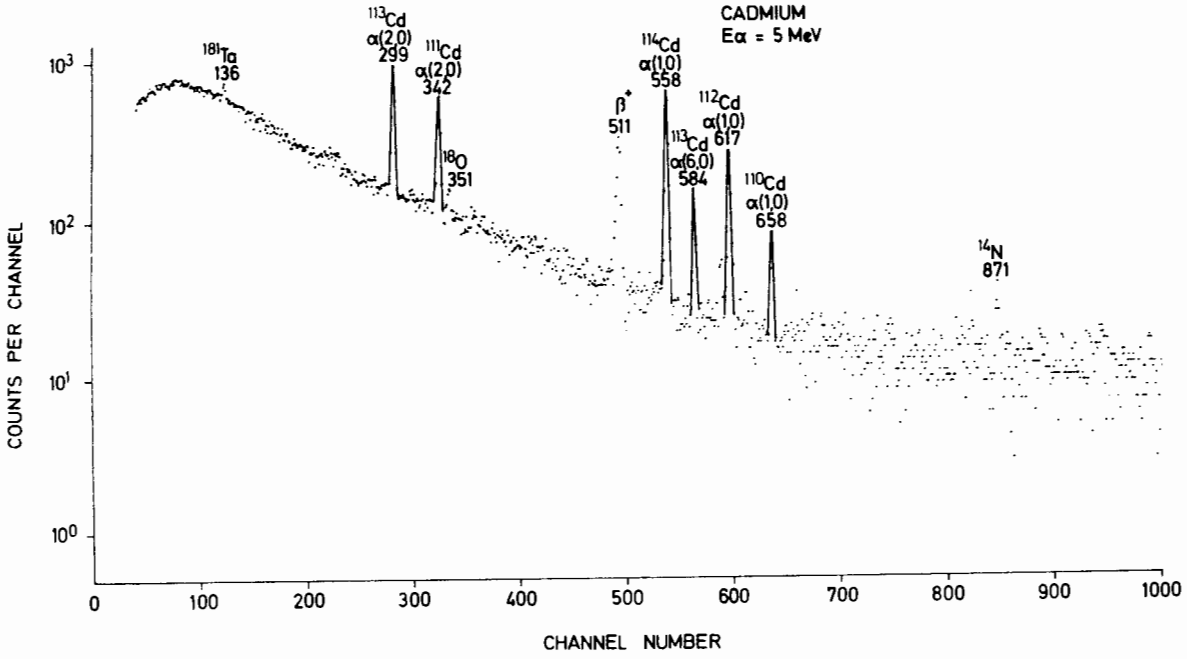
CADMIUM
Eα = 5 MeV
181Ta 136
113Cd α(2,0) 299
111Cd α(2,0) 342
18O 351
β+ 511
114Cd α(1,0) 558
113Cd α(6,0) 584
112Cd α(1,0) 617
110Cd α(1,0) 658
14N 871
COUNTS PER CHANNEL
CHANNEL NUMBER

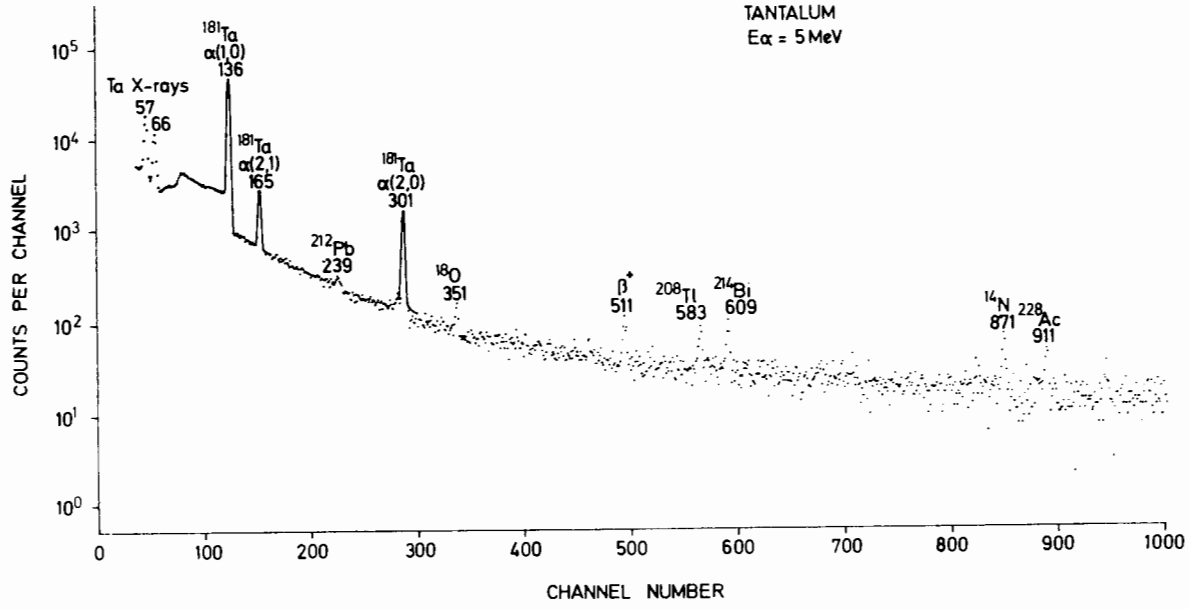
TANTALUM
Eα = 5 MeV
Ta X-rays 57 66
181Ta α(1,0) 136
181Ta α(2,1) 165
212Pb 239
18Ta α(2,0) 301
18O 351
β+ 511
208Tl 583
214Bi 609
14N 871
228Ac 911
COUNTS PER CHANNEL
CHANNEL NUMBER

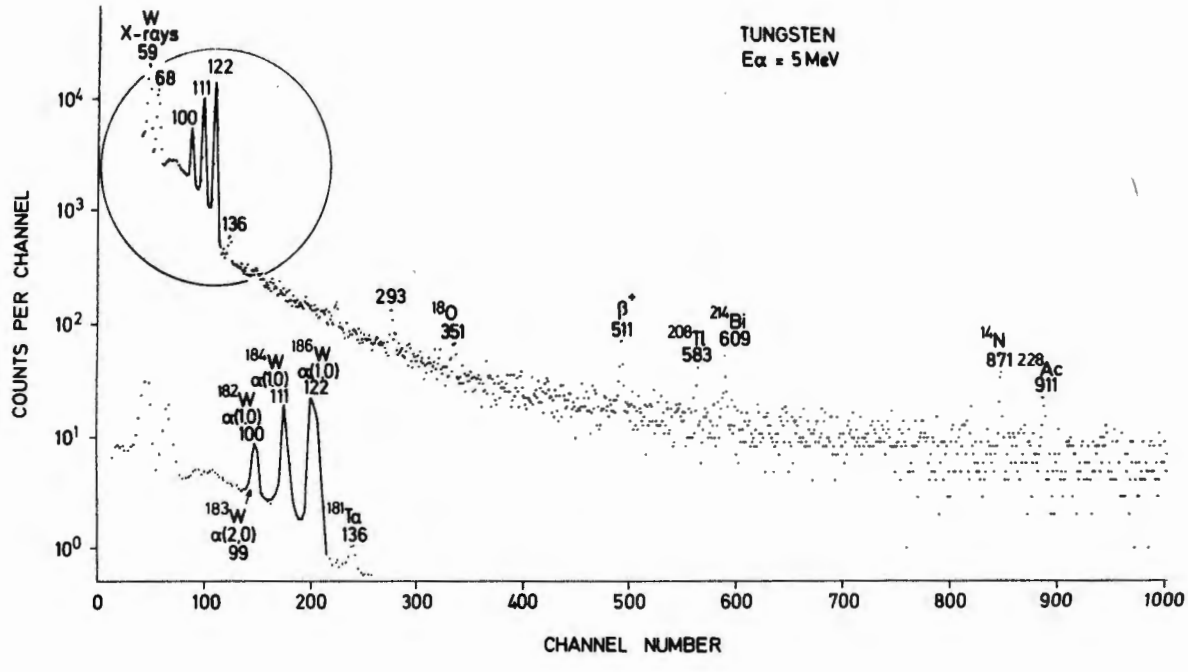
TUNGSTEN
Eα = 5 MeV
W X-rays 59
68
122
111
100
136
293
18O 351
β+ 511
208Tl 583
214Bi 609
14N 871
228Ac 911
184W α(1,0) 111
186W α(1,0) 122
182W α(1,0) 100
183W α(2,0) 99
181Ta 136
COUNTS PER CHANNEL
CHANNEL NUMBER

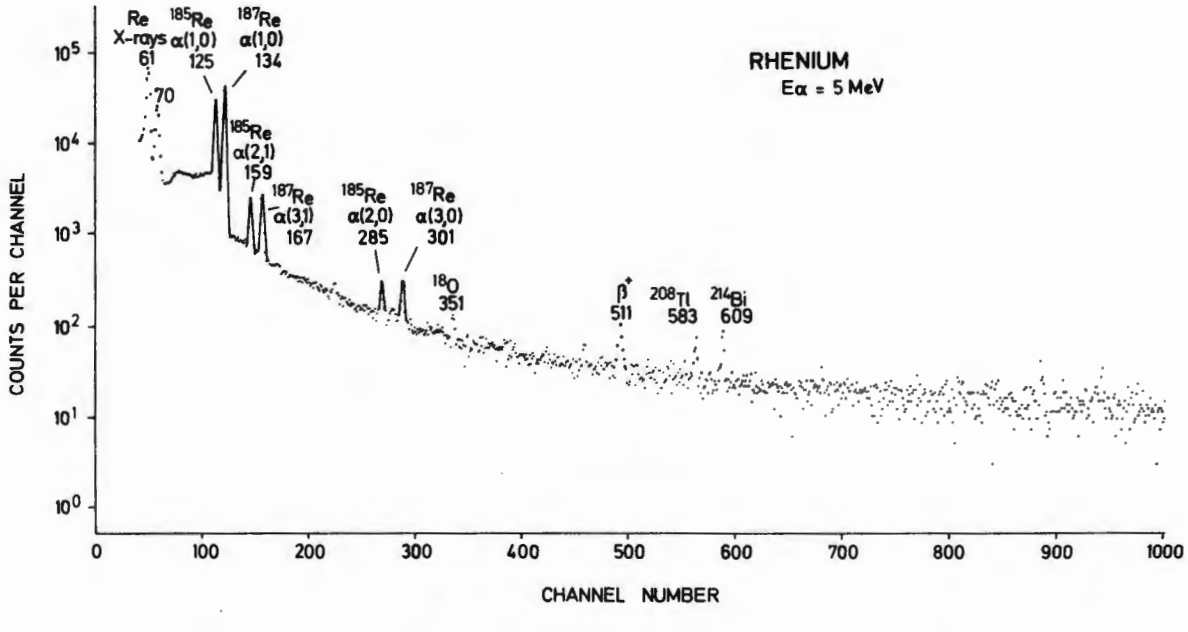
RHENIUM
Eα = 5 MeV
Re X-rays 61
70
185Re α(1,0) 125
187Re α(1,0) 134
185Re α(2,1) 159
187Re α(3,1) 167
185Re α(2,0) 285
187Re α(3,0) 301
18O 351
β+ 511
208Tl 583
214Bi 609
COUNTS PER CHANNEL
CHANNEL NUMBER

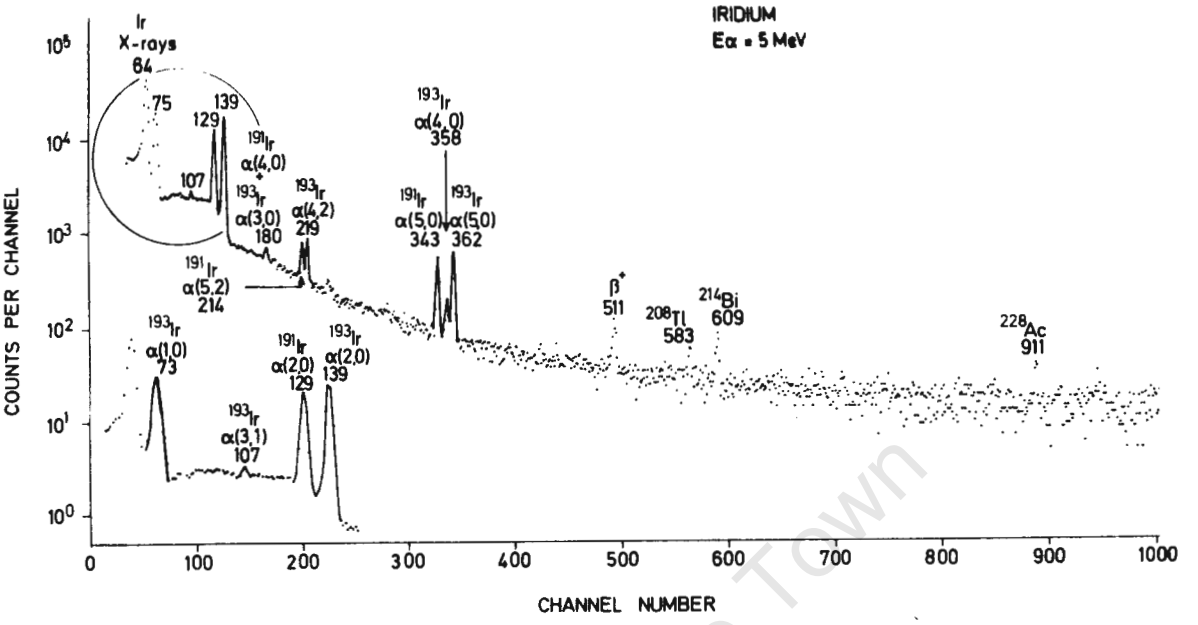

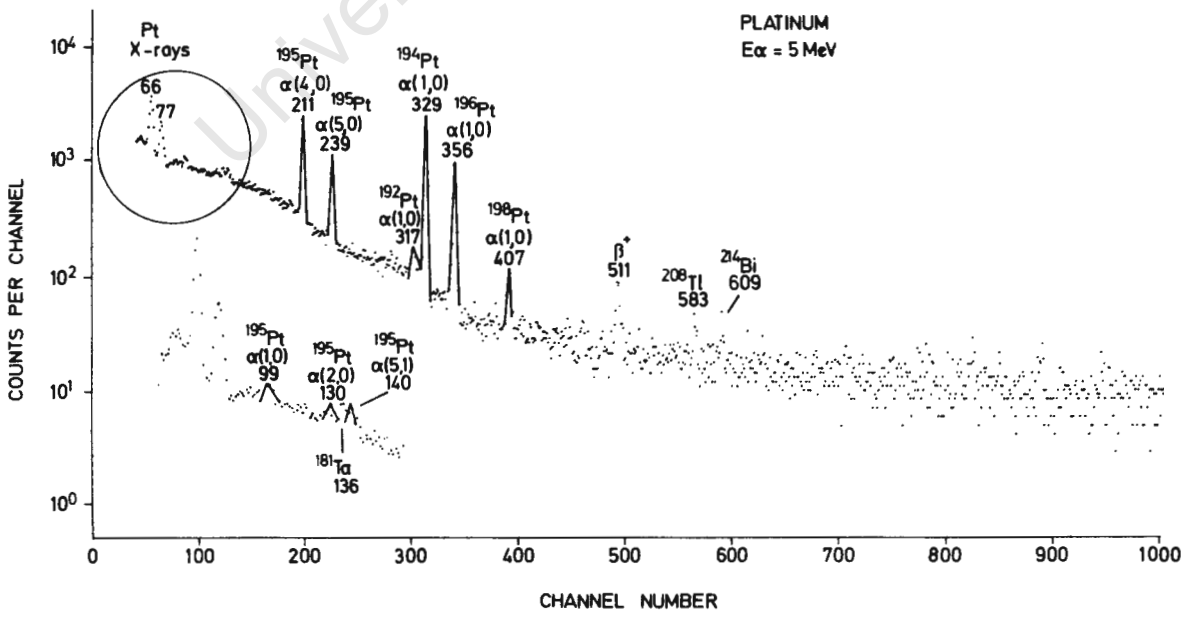

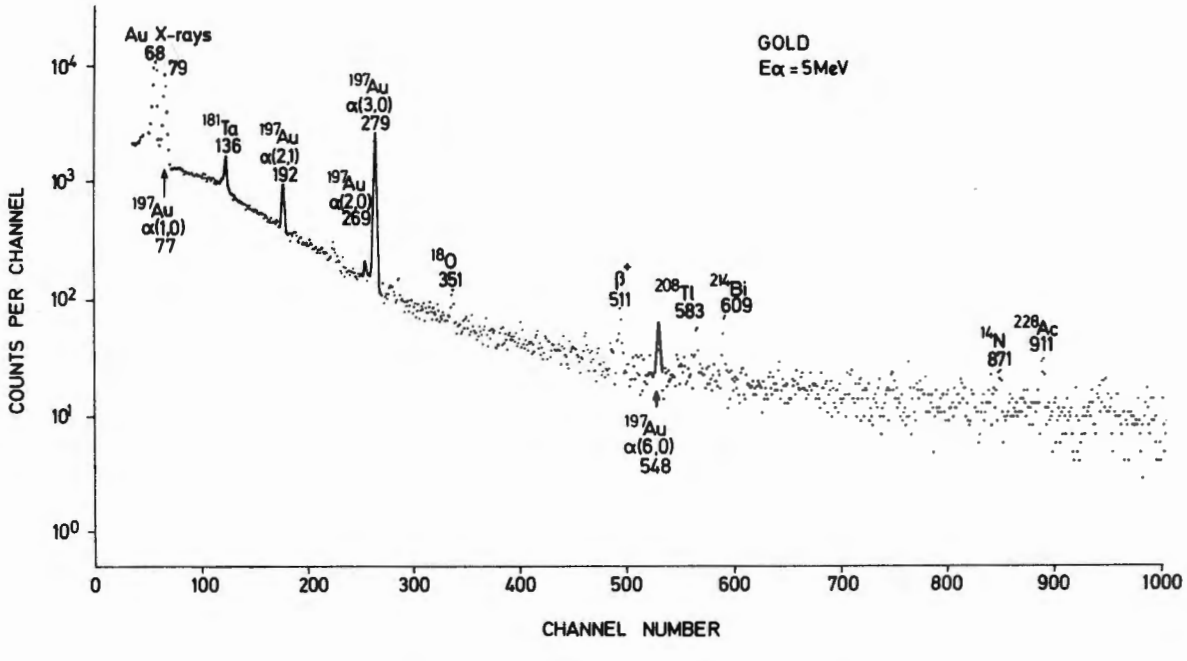
Au X-rays
68
79
GOLD
Eα = 5MeV
197Au α(3,0) 279
181Ta 136
197Au α(2,1) 192
197Au α(2,0) 269
197Au α(1,0) 77
18O 351
N
β+ 511
208Tl 583
214Bi 609
14N 871
228Ac 911
197Au α(6,0) 548
COUNTS PER CHANNEL
CHANNEL NUMBER
10⁰
10¹
10²
10³
10⁴
0
100
200
300
400
500
600
700
800
900
1000

CONCLUSION

Generally speaking increased alpha energy brought increased potential analytical sensitivity. This was not necessarily true for those gamma-rays which resulted from nuclear reactions, for which the 11-MeV alpha particles seemed to provide the highest sensitivity, even better than that with 16-MeV particles. However, with this increased sensitivity came an increased general background which was often several orders of magnitude greater than the background in spectra measured during 5-MeV alpha bombardment.

With regard to the data obtained for 5-MeV alpha irradiation, it was found that the sensitivities calculated were order-of-magnitude values, the actual sensitivities being rather better than those given in the catalogue, for all elements that were subsequently investigated individually.

It is felt that the results of the survey permitted intelligent selection of those elements which had analytical potential using prompt gamma-ray spectrometry. The sensitivity, dependent, as it was, on the background, had to be determined for the particular matrix under consideration. Possible interference from both radioactive and prompt backgrounds, as well as from other matrix components, had to be investigated thoroughly. It was intended that the spectra and tabulated data should provide a reference allowing such interference to be predicted.

The broad conclusions that may be drawn from this survey are summarised in Table 4 below.

Table 4. Summary of sensitivities calculated for the elements at the different alpha bombarding energies

Sensitivity	E_γ		
	5 MeV	11 MeV	16 MeV
Greater Than 10 $^{o}/_{oo}$	Sc Cr Cu Zn Rb Zr Er Hf Hg		
Between 1 and 10 $^{o}/_{oo}$	O Mg Si Cl K Ti Fe Br Mo Ru Pd Ag Cd Ta W Re Ir Pt Au	Sc Cr Cu Zn Mo Cd W Re Ir	Sc Cr Mn Cu Zn Mo Pd Ag Cd Re Ir Au
Better Than 1 $^{o}/_{oo}$	Li B N F Na Al P V Mn Rh	C O F Na Si Ti V Mn Fe Rh Pd Ag Ta Pt Au	C O F Na Si K Ti V Fe Br Rh Ta W Pt

Bombarding particles of 5 MeV were easier to obtain in relatively intense beams than were 11-MeV particles at

the 6 MV Van der Graaff at SUNI. This energy was therefore used to investigate analysis in more detail of some elements which showed the best potential sensitivities.

Chapter IV

Determination of Fluorine

INTRODUCTION

Consideration of the nuclear methods available for the determination of fluorine shows a division of the techniques into activation analysis and prompt spectrometry. Activation with thermal neutrons results in the formation of 11.1-sec ^{20}F, whilst fast neutrons form 109.8-min ^{18}F, both of which are produced in relatively low yields and hence analyses are not sensitive. Charged-particle activation is usually subject to interference from oxygen. By contrast, prompt methods make use of specific properties of the ^{19}F nucleus so that analyses are less subject to interference, yield results relatively quickly and where high precision is needed, it may be achieved by extending the duration of the bombardment.

The prompt nuclear method previously used [Mo 67, Be 69] depended on the measurement of prompt gamma-rays that are emitted from the high resonances that occur in the reaction $^{19}F(p,\alpha\gamma)^{16}O$ at proton energies of 1348 and 1375 keV. The gamma-rays emitted from the excited levels of ^{16}O have energies of 6.131 MeV, 6.919 MeV and 7.119 MeV. This technique is sensitive and well-suited for the measurement of the spatial distribution of fluorine concentration because the resonance is sharp, thus limiting the region of analysis to that where the proton energy is at the resonance energy [Ga 72].

In order to determine <u>average</u> fluorine concentrations, the

value most often required, the use of gamma-rays produced as a result of inelastic scattering is preferred. The excitation functions for two of the different gamma-rays resulting from inelastic scattering of alpha particles on a calcium fluoride target are shown in Figure 11; that for the proton resonance reaction is shown as an inset. The cross-sections for the alpha-induced gamma-rays increase smoothly and slowly with alpha-particle energy. Hence the gamma-ray yields are far less sensitive to bombarding-particle energy and thus to the depth distribution of the fluorine in the portion of the sample analysed [Gi 76].

RESULTS AND DISCUSSION

Chemically pure fluorides of the twenty-one metals illustrated in Figure 12 were bombarded with 5-MeV $^{4}He^{+}$ ions in order to assist in establishing the identity of the large number of gamma-rays recorded in the spectrum. In this way a thorough knowledge of the fluorine spectrum was built up. The gamma-rays observed, together with their assignments are listed under *fluorine* in the Catalogue of Gamma-Rays. Typical spectra may be seen in the Atlas of Spectra on pages 81 (CaF_2) and 83 (MgF_2).

The origin of these prompt gamma-rays is illustrated diagramatically in Figure 13. The nuclear levels of the product nuclei and the observed spontaneous radiative transitions between them are given for each of the observed reactions.

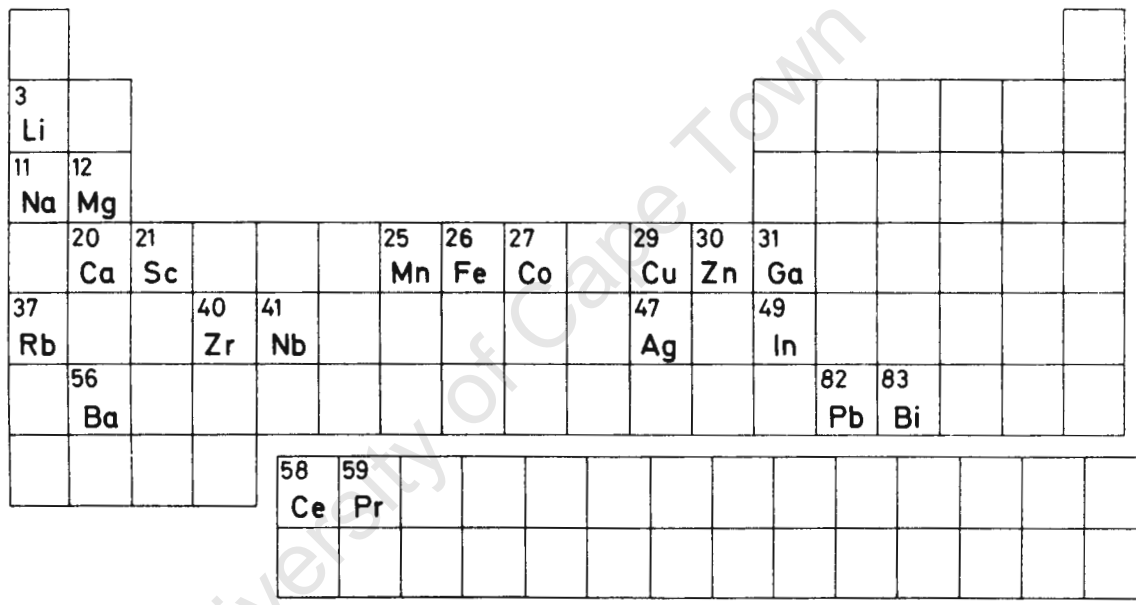

Figure 12 Outline of the Periodic Table in which the named elements refer to pure fluorides irradiated in this investigation.

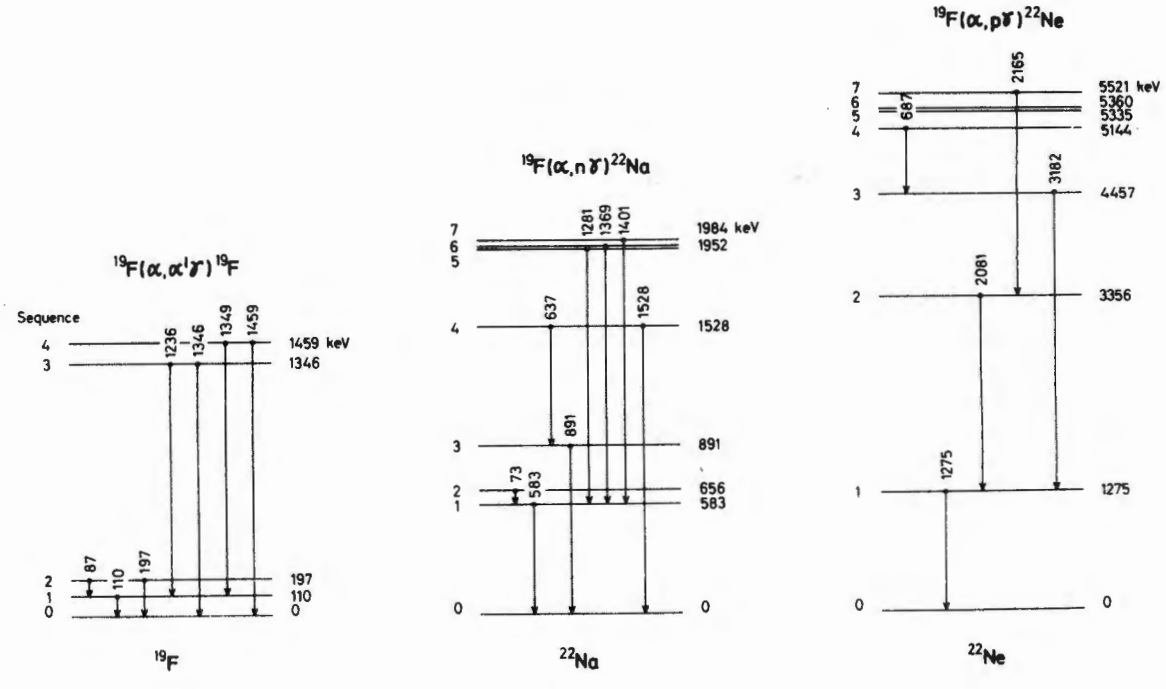

Figure 13. Decay transitions resulting in observed gamma-rays from the reactions $^{19}F(\alpha,\alpha'\gamma)^{19}F$, $^{19}F(\alpha,n\gamma)^{22}Na$ and $^{19}F(\alpha,p\gamma)^{22}Ne$.

Despite the apparent complexity of the gamma-ray spectrum the gamma-rays of 110, 197 and 1275 keV were so intense even for short bombarding durations, that they were highly suited for analytical purposes. The gamma-rays of 583 keV appear to be intense but the signal-to-background ratio in this region of the spectrum is detrimental to attaining good precision at low concentration. The tremendous intensity of the two low-energy fluorine peaks as compared to the background is clear from Figure 14.

The use of the peaks corresponding to 110 and 197 keV in addition to those of 1275 keV was investigated for the

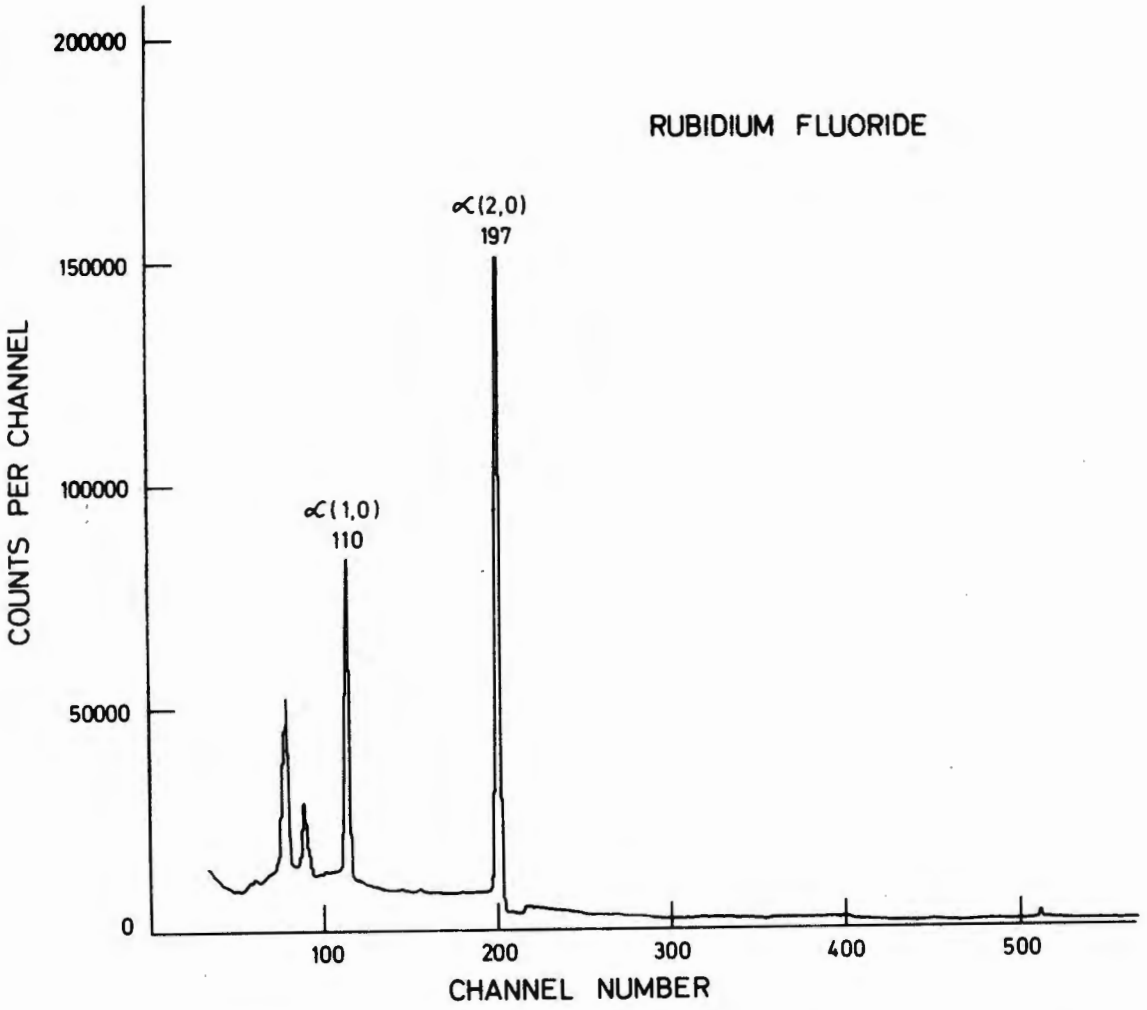

Figure 14. Typical spectrum of a pure fluoride showing the remarkable intensities of the 110- and 197-keV gamma-rays.

quantitative determination of fluorine. The procedures described in Chapter II for the integration of peaks and background subtraction were used.

The determination of absolute fluorine concentrations required a calibration using standards of known fluorine content. Initially this calibration was attempted by means of a series of calcium fluoride - calcium hydroxide mixtures with fluoride content ranging from 0.8% to 33%,

the preparation of which has been described in Chapter II. Three pills were made from each mixture thus enabling triplicate analyses using a beam of 5-MeV $^{4}He^{+}$ ions. A summary of these data is presented in Table 5 which lists, for each sample, the mean value of the "counts per μC" together with its error and percentage error obtained from integration of the peaks corresponding to the 110-keV, 197-keV and 1275-keV gamma-rays. Plots of all the data for the 110-keV and 197-keV gamma-rays are shown in Figures 15 and 16, in which the lines were calculated by the method of least squares.

By computing the value "counts per μC per 1% F" for each sample it was possible to compare all the results with one another. From Table 6 it is seen that the values of the overall standard deviation of the results for each peak were 9.2%, 6.1% and 5.2% respectively. Since the expected error due to statistical fluctuations was of the order of 1% these fluctuations are too large. However, as has been been explained in Chapter I the change in the range of the alpha particles has to be taken into account. In this case, the correction was simplified since the exact composition of the mixtures was known. Values were obtained for each analysis for the quantity "counts per μC per 1% F per unit range", and the mean values and errors are also contained in Table 6. An obvious improvement in precision was observed but a large error, greater than that ascribable to statistical errors on raw data, still remained.

Table 5 Results of analyses of mixtures of calcium fluoride with calcium hydroxide

Known fluorine content %	110 keV Counts per μC			197 keV Counts per μC			1275 keV Counts per μC		
	Mean	Error	Error %	Mean	Error	Error %	Mean	Error	Error %
0.8081	90.8	12.1	13.4	115.9	11.9	10.3	22.6	1.7	7.3
1.1203	121.3	5.4	4.4	159.2	3.2	2.0	29.9	2.0	6.6
1.6171	192.4	19.9	10.3	251.0	15.9	6.3	45.8	3.0	6.6
2.2789	262.0	6.5	2.5	336.0	5.7	1.7	63.1	0.8	1.3
3.2156	355.0	45.2	12.7	461.4	35.7	7.7	87.1	4.1	4.8
4.9313	536.3	19.1	3.6	685.3	14.2	2.1	129.5	1.9	1.4
6.3948	669.8	60.8	9.1	893.0	45.9	5.1	172.9	7.9	4.6
9.1642	1122.5	30.8	2.7	1420.7	22.1	1.6	258.8	1.7	0.6
12.3093	1342.0	89.4	6.7	1759.3	72.1	4.1	338.2	10.4	3.1
18.0123	2244.4	103.4	4.6	2809.5	90.3	3.2	516.7	9.6	1.8
24.3244	2657.6	23.1	0.9	3560.0	10.3	0.3	680.1	13.1	1.9
32.8107	4053.9	179.6	4.4	5226.7	201.7	3.9	1004.5	32.0	3.2

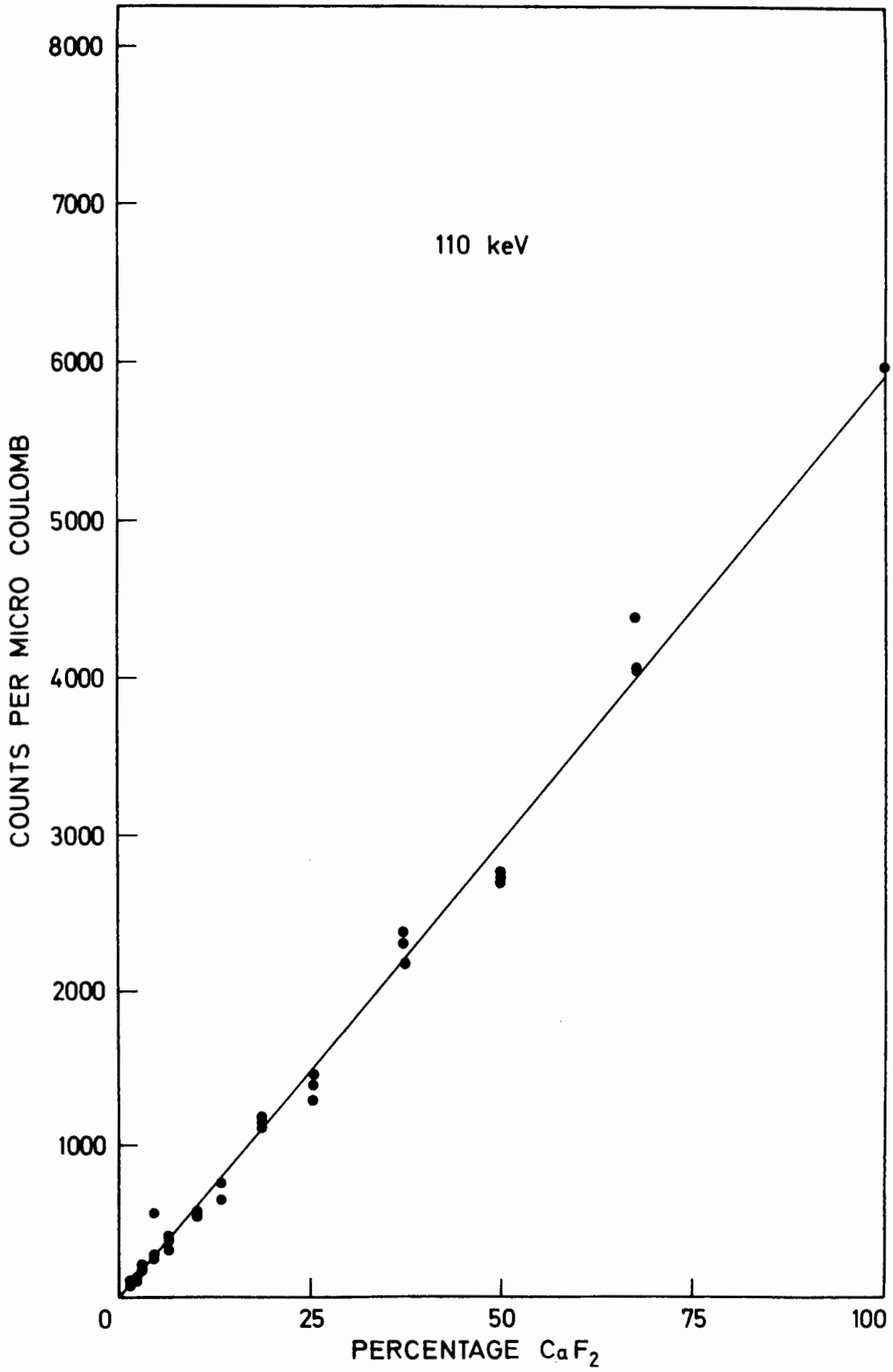

Figure 15 Variation of count rate of the alpha-induced 110-keV gamma-rays with calcium fluoride content.

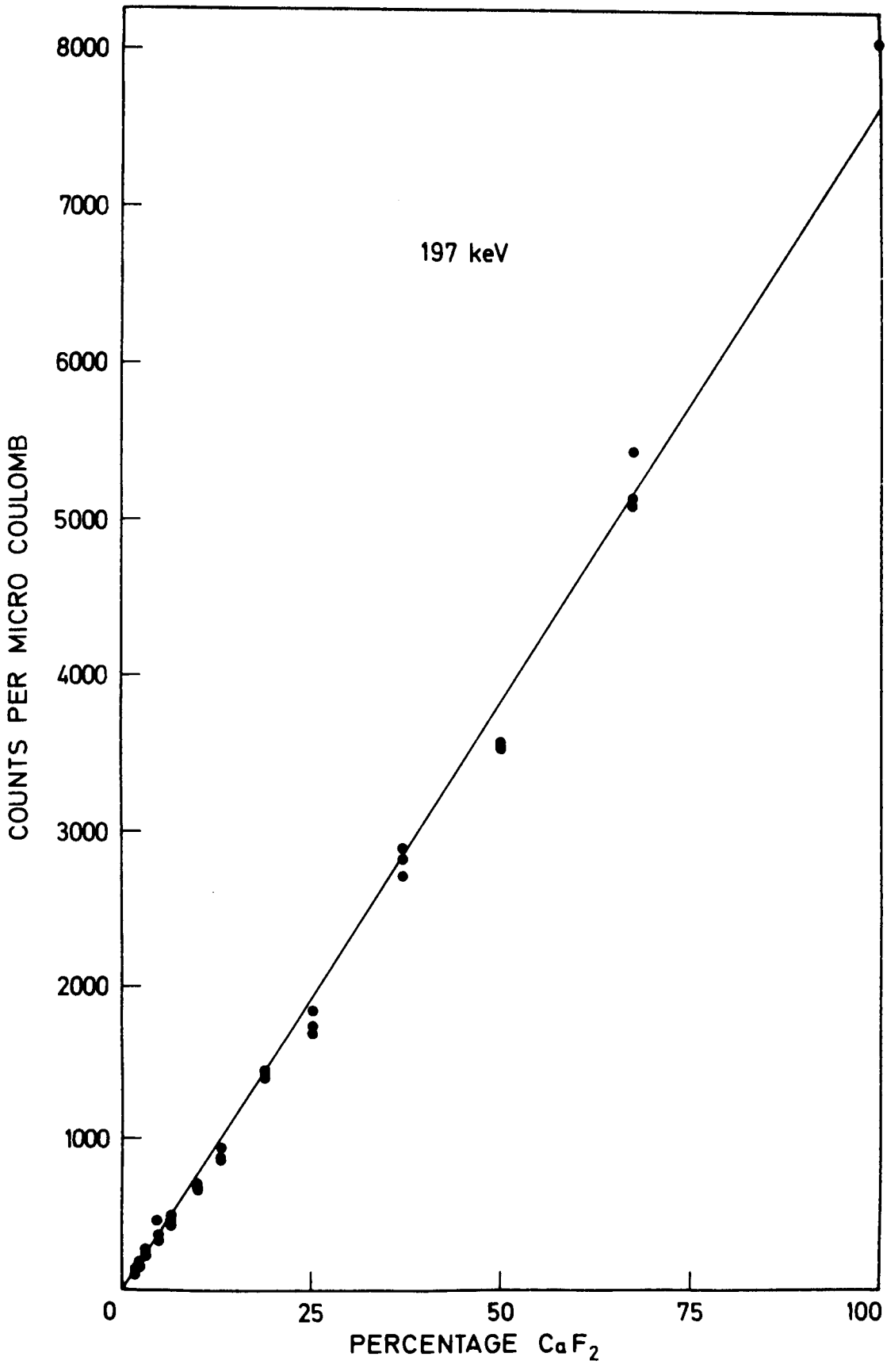

Figure 16 Variation of count rate of the alpha-induced 197-keV gamma-rays with calcium fluoride content.

Table 6. Summary of analyses with and without range corrections

	110 keV			197 keV			1275 keV		
	Mean	Error	Error %	Mean	Error	Error %	Mean	Error	Error %
Count/μC/ 1% F	113.41	10.4	9.2	146.49	8.9	6.1	27.83	1.5	5.2
Values per unit range	21.68	1.9	9.0	28.00	1.5	5.3	5.32	0.24	4.4

Using sodium fluoride another series of mixtures was made in the concentration range of 1 - 10%. Analysis of these mixtures by prompt gamma-ray spectrometry showed extremely poor correlation, not only between pills pressed from the same mixture but also from different mixtures. It was concluded that the cause for the scatter in the results from both series of mixtures lay in their inhomogeneity. It is clear from the small diameter of the bombarding beam (3 mm) and the short penetration of alpha particles into the materials under investigation (~20 μm) that the amount of the sample analysed is small. *The validity of the analysis then depends on the extent to which this small portion represents the bulk of the sample.*

In order to ascertain whether the excessive errors were due to inhomogeneous mixing, the analysis was repeated using standard fluorspar samples [St 74], obtained from the National Institute for Metallurgy, that had been carefully prepared so as to ensure homogeneity. Pills

were prepared from the five fluorspars numbered 63/70, 9/69, 42/70, 27/72 and 36/72 and between 4 and 9 replicate analyses were carried out on each mixture. An immediate improvement in the precision of the results from individual samples was observed. This is illustrated by Table 7 which contains the number of analyses together with the mean value of "counts per μC per 1% F", standard deviation and percent standard deviation for each sample. The standard deviation of the results was now of the order of that due to statistical fluctuations which typically was ~0.5%.

Table 7. Summary of analyses of standard fluorspars (the means given are the mean values of "counts per μC per 1% F")

Sample No.	No. of Analyses	110 keV			197 keV			1275 keV		
		Mean	Error	Error %	Mean	Error	Error %	Mean	Error	Error %
63/70	9	67.92	2.25	3.32	96.20	2.00	2.08	13.08	0.14	1.09
9/69	7	68.83	0.49	0.71	96.03	1.60	1.67	12.78	0.14	1.09
42/70	4	64.20	0.99	1.54	91.10	0.58	0.63	12.19	0.16	1.30
27/72	4	74.82	1.19	1.59	104.56	0.67	0.65	14.05	0.12	0.88
36/72	6	58.32	0.65	1.11	85.07	0.62	0.72	12.11	0.14	1.12

When these data were plotted in an attempt to obtain a calibration line of "counts per μC" against % F it was found that by no means could a straight line be drawn through all the points, (see Figure 17). This is due to the wide difference in the composition of the fluorspars and hence in the ranges of alpha particles in them. In order to obtain one straight line linking all the points it was necessary to

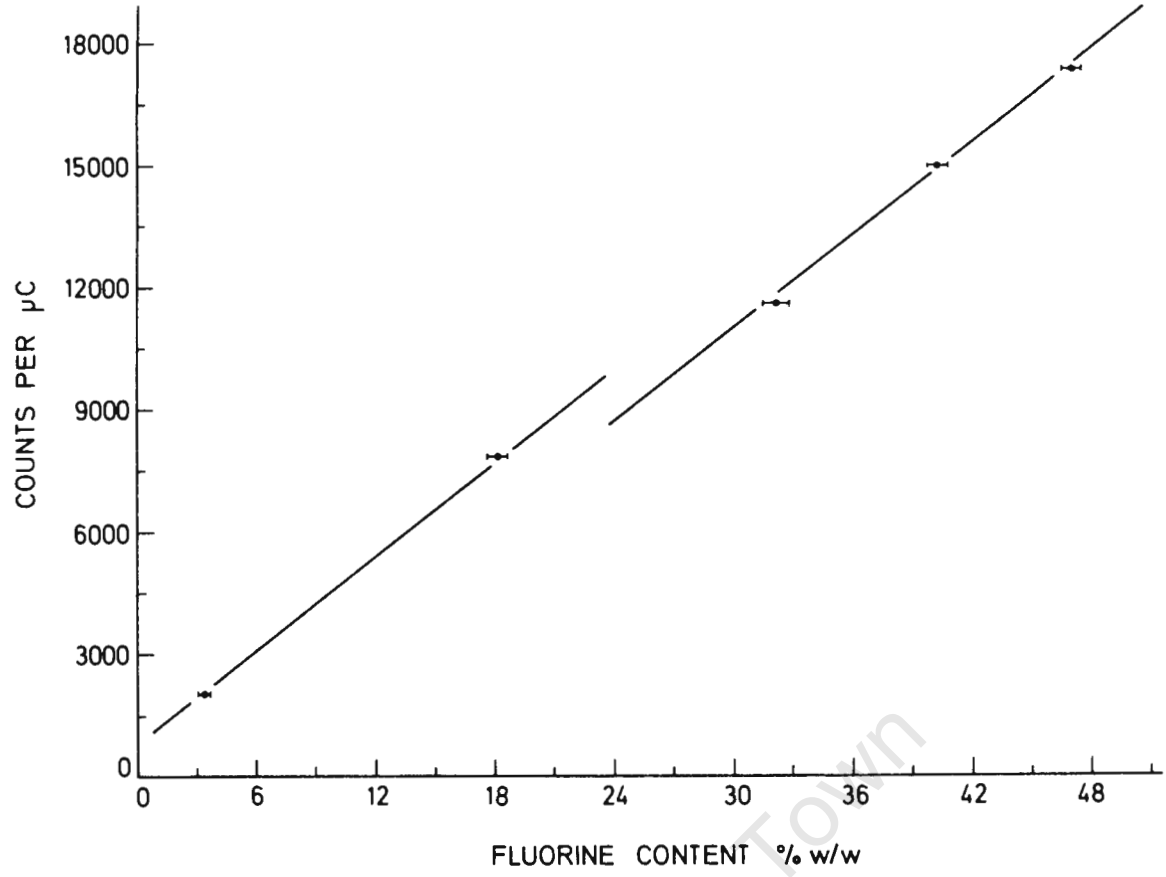

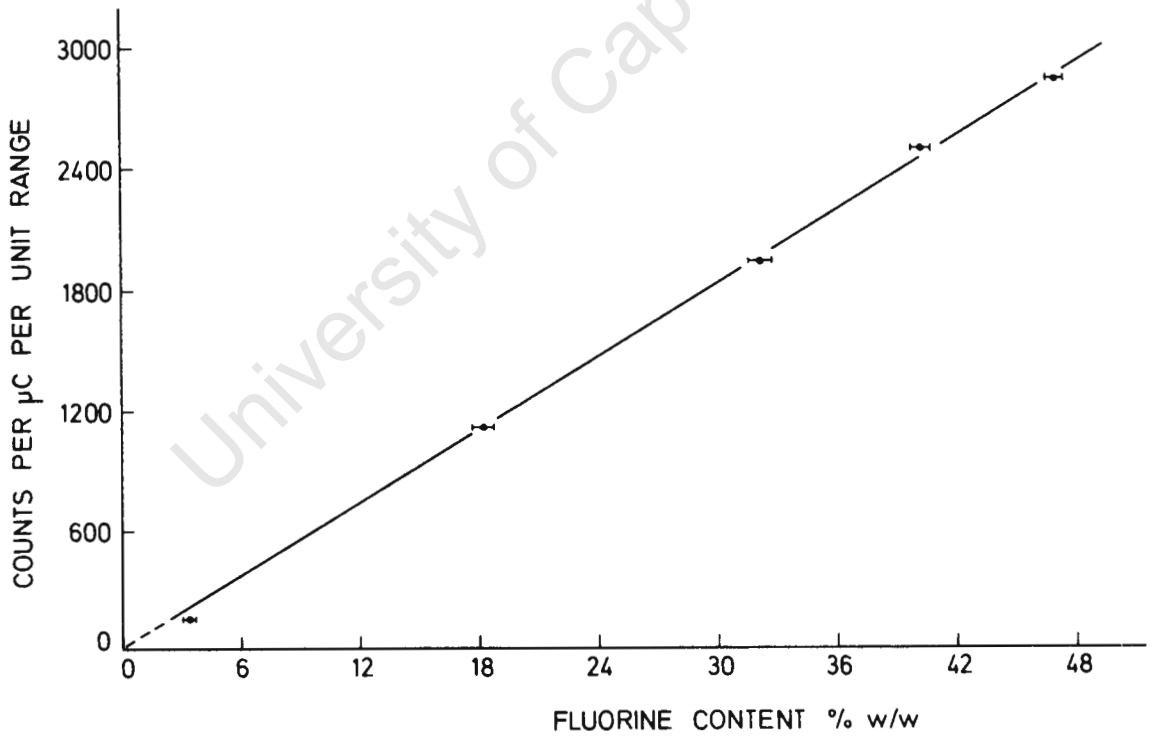

Figure 17 The variation of alpha-induced prompt gamma-ray yield with fluorine content. The upper curve, uncorrected for range effects, shows two lines corresponding to two essentially different ore types. The lower curve shows the same data corrected for range effects. Error bars correspond to 95% confidence limits of National Institute for Metallurgy Standards [St 74].

carry out a correction for range. However the exact composition of all the fluorspars was not known [St 74]. The composition of the fluorspars 27/72 and 36/72, apart from their calcium fluoride content, was unknown, except that they both contained a large proportion of iron oxide. Since the necessity for a range correction had been forseen, scatter data were acquired at the same time as the gamma-ray spectra. The analysis of the scatter spectra was accomplished as follows [Gi 77]. The raw scatter data (an example of which is shown in Figure 18) consisting of several ill-defined steps were smoothed and differentiated. The differentiated spectrum consisted of a series of negative peaks, one at each of the steps in the original data. The position of the peaks was easily determined and the area under the peak calculated by familiar procedures. In this way the major elements of the samples were determined (see Table 8). However all of the spectra had been acquired with the heights of the peaks in the gamma-spectrum as the criteria upon which the duration of bombardment depended, with the result that scatter spectra were acquired for a less than optimum time.

Table 8. Example of empirical composition derived from backscatter data

Element	Fe	Ti	Sc	Ca	F	O
Atomic fraction	0.308	0.036	0.023	0.238	0.226	0.169

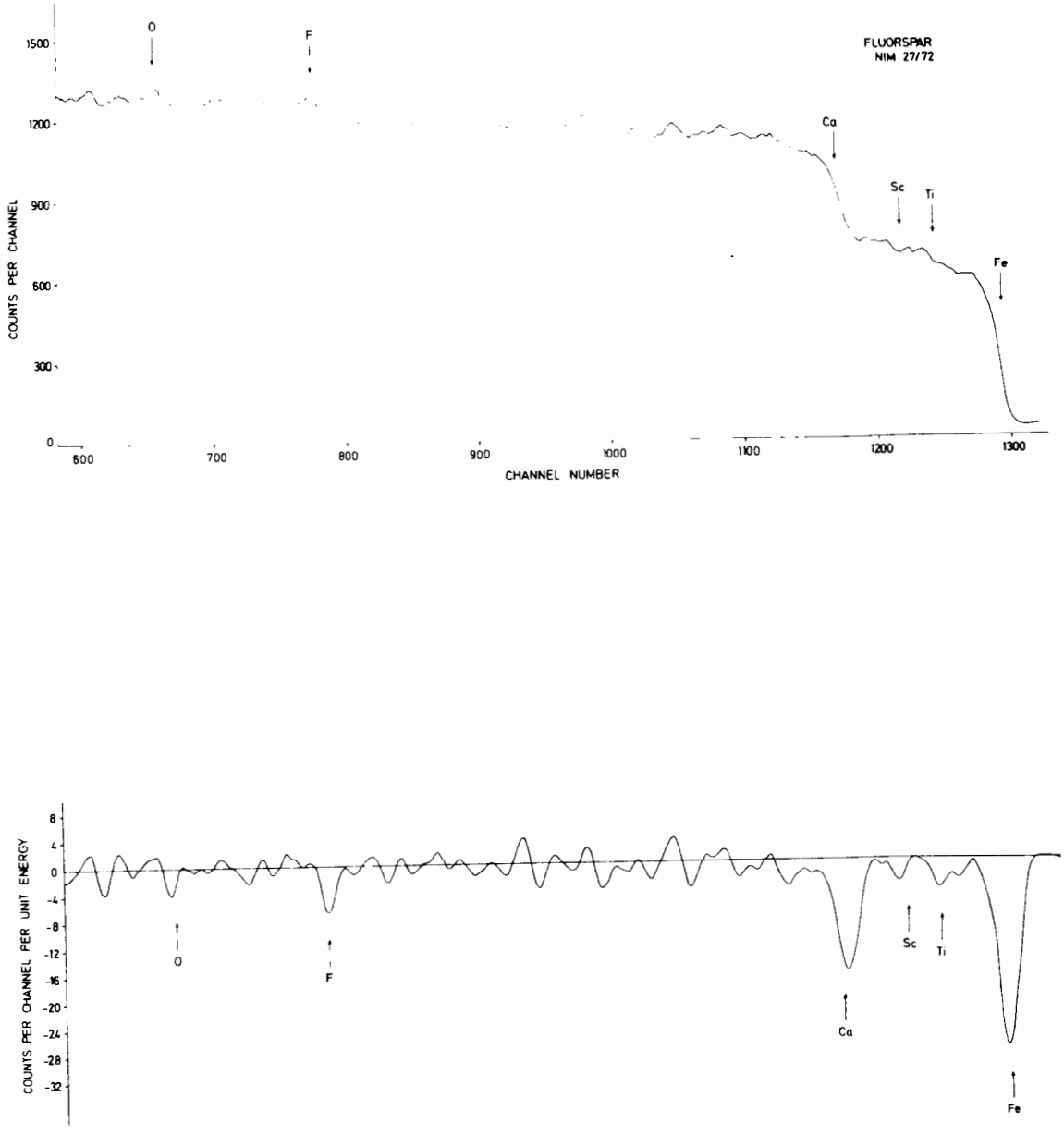

Figure 18 Alpha-particle backscatter spectrum from a thick target of National Institute for Metallurgy standard material fluorspar 27/72 measured at 135° (upper spectrum). Unmarked peaks and steps are due to nuclear reaction products. E_α = 5 MeV. The lower spectrum shows a plot of the same data smoothed and differentiated. Arrows mark the calculated positions of the maximum energies for the elements shown.

Hence the lower energy (and therefore lower atomic number), peaks of the scatter spectra were not as well defined as they could have been with a longer bombardment. In order to overcome any errors that may have been introduced because of this, all cations shown in the spectra were assumed to be present as the oxides, with the exception of calcium which was assumed to be present only as CaF_2. Heights of peaks from oxygen and fluorine were thus calculated on the basis of the concentrations of the other elements present. The peak heights were then used, together with the mass numbers of the found elements, as data for the computer programme described in Chapter II. The output of the programme consisted of the fractional composition of the samples. This composition was used to calculate a value for the range of 5-MeV $^4He^+$ ions in each fluorspar, and "counts per μC per unit range" against % F was plotted as illustrated in Figure 17. Whilst the points still did not fall exactly on a straight line a valid best straight line could be drawn and it is clear that if better scatter data had been available a more accurate composition could have been found for each sample, thus improving the calculated range. The validity of the technique of utilizing scatter data to calculate a value for the range is clearly shown despite the poor counting statistics of the original scatter spectra.

An examination of Table 9 further illustrates the improvement in the results once a range correction is applied. A "least squares" straight line was fitted and the yield per 1% F calculated to compare all the results with one

another. The standard deviation of the results is given before and after the range correction was carried out. Clearly shown is the increase in precision which results from a consideration of the range.

Table 9 Effect of range correction on precision of analysis using the 197-keV gamma-ray

Sample No.	Known fluorine content %	Yield per 1% F = A	A per unit range
63/70	46.89	96.20	16.66
9/69	40.19	96.03	17.12
42/70	32.04	91.10	16.71
27/72	18.08	104.56	17.21
36/72	3.35	85.07	15.54
	Mean	94.369	16.689
	Error	± 6.176	± 0.766
	Error %	6.54%	4.59%

Having established the use of alpha-induced prompt gamma-ray spectrometry for the analysis of fluorine, it was decided to apply the method to the analysis of fluorine in the complex matrix of cement.

DETERMINATION OF FLUORINE IN CEMENT

Introduction

Cement is a common industrial material produced all over the world. Its manufacture involves the processing of geological materials from different sources, the composition of the ores having a profound effect on the performance

of the cement as manufactured. It therefore follows that rapid analysis of the raw materials as well as the final product is vital for process control.

When fluorine occurs as a relatively minor component in geological material or industrial raw materials, analysis of the fluorine content is usually preceded by a digestion process in which the fluorine is solubilized, or by distillation of hydrogen fluoride under controlled conditions [St 74]. Such analyses are usually tedious and time-consuming. Activation analysis of fluorine, though rapid, is subject to interference from oxygen, a component which is in high concentrations in the materials discussed here.

Accordingly fluorine is seldom determined in cements unless the expected average fluorine concentration in the raw materials is so high that steps need be taken to decrease it. This is because the analytical procedures cannot yield results sufficiently rapidly to be of value for process control. Prompt gamma-ray spectrometry enabled largely interference-free analyses to be completed within 20 minutes. The gamma-rays of 197 keV were selected as a measure of the fluorine content of the cements.

Results and Discussion

Cement samples were obtained from sources in the Cape and Transvaal in the Republic of South Africa, together with an analysed sample of high fluorine content from England. In addition, analyses were carried out by means of the fluoride ion-selective electrode on one each of the Cape

and Transvaal samples [St 76]. Major component analyses were available for three of the cements from the Transvaal and England. The latter data enabled calculation of the range of 5-MeV $^4He^+$ ions in those cements. The analyses together with the computed ranges for the Transvaal and English samples, are listed in Table 10. It is clear that the range did not vary significantly between samples and therefore no range correction was applied to the gamma-ray data.

Table 10. Calculated range of 5-MeV alpha particles in typical cements

Cement	% composition w/w									Range mg/cm^2
	SiO_2	Al_2O_3	Fe_2O_3	CaO	MgO	SO_3	Na_2O	K_2O	F	
Eng	20.8	6.2	2.3	67.2	0.9	1.3	0.2	0.7	0.1(3)	5.691
Tvl 1	24.0	4.0	2.4	66.4	2.2					5.679
Tvl 2	24.1	3.7	2.4	67.0	1.7					5.684

Figure 19 is the gamma-ray spectrum of a typical cement. The fluorine gamma-rays of 110 and 197 keV give clearly defined peaks.

Examination of the homogeneity of samples was made by replicate fluorine analysis. The standard deviation and the number of analyses for each cement is given in Table 11. It can be seen that the homogeneity of the Transvaal and English samples is better than that of the Cape samples. In order to assess the effect of beam-spot size on the

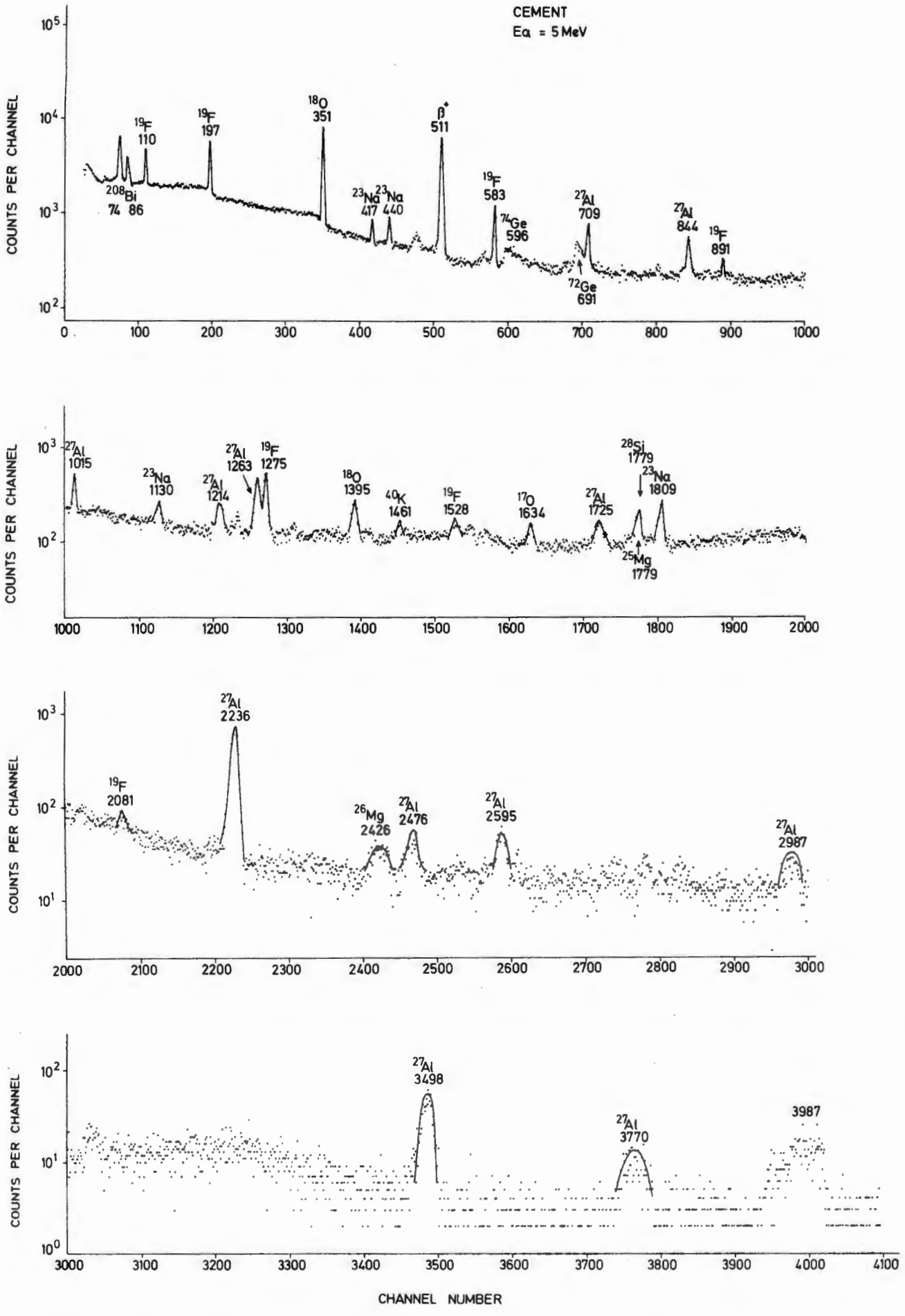

Figure 19 Typical alpha-induced prompt gamma-ray spectrum obtained from a cement.

Table 11. Precision of cement analyses using the 197-keV gamma-rays

Sample	No. of Analyses	Relative Standard Deviation %	Error due to counting statistics
English	12	3.6	0.7%
Transvaal 1	6	2.6	0.9%
Transvaal 2	6	3.0	0.9%
Cape 1	5	4.3	0.7%
Cape 2	4	6.0	0.7%
Cape 3	4	9.8	0.7%
Cape 4	4	4.9	0.7%

relative standard deviation and thus guage the scale on which the samples could be said to be homogeneous, replicate analyses were carried out on the English cement using different beam diameters. The area of the bombarded spot on the target was determined by the diameter of a variable collimator, situated 49 cm from the target. Repeat analyses were carried out by bombarding a fresh portion of the same target. For beam diameters too large to permit replicate analyses on the same target, new pills were used. The relative standard deviations obtained for each set of analyses are shown plotted as a function of collimator diameter in Figure 20. The figure indicates an improvement in precision as the area, and thus the volume of material analysed, increases. Since the range of the alpha particles is small (~20 μm) the volume of material analysed is largely dependant on the area of the

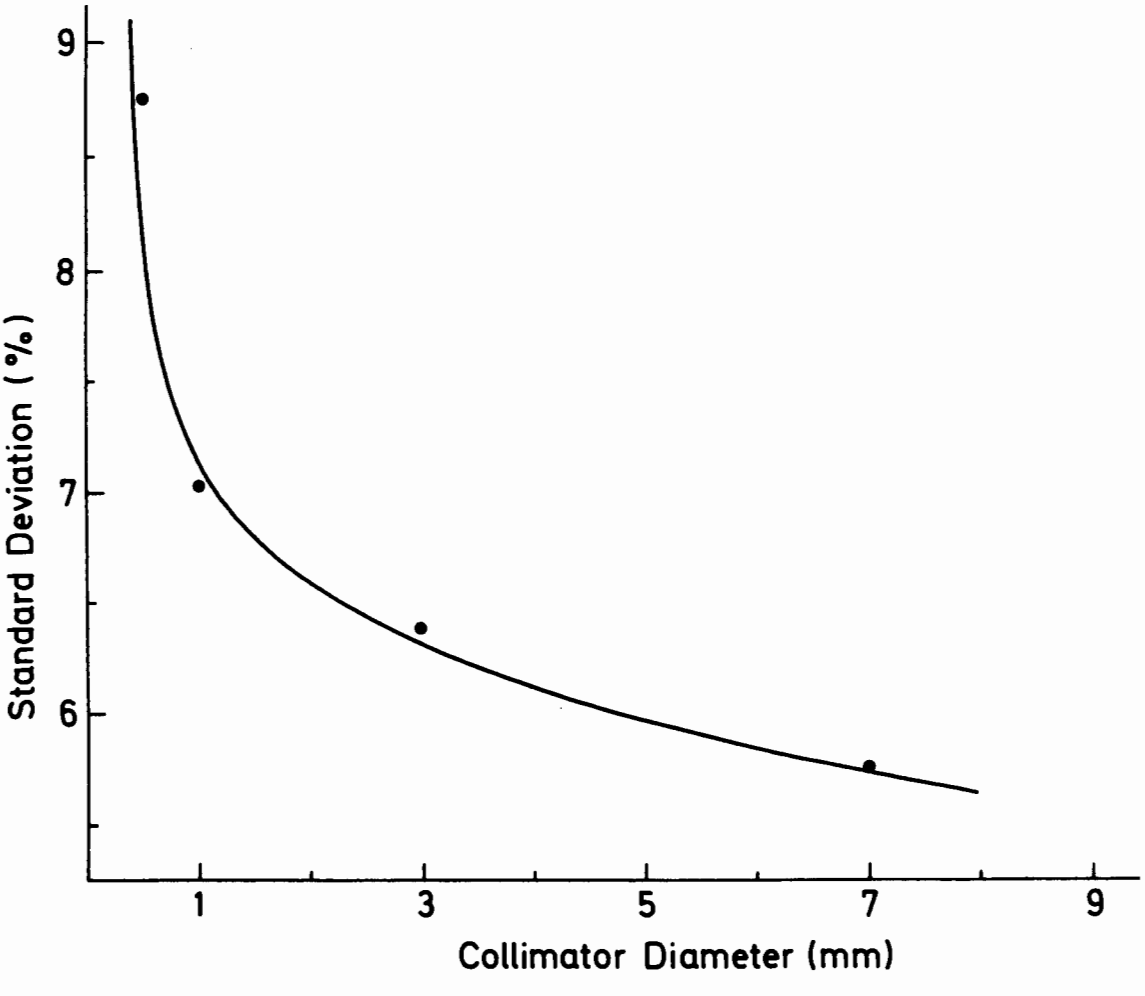

Figure 20 Variation of precision with beam diameter.

beam-spot on the target. Because the granularity of the sample is of the same order as, or greater than, the range of the alpha particles, it is obvious that the larger the number of granules irradiated the greater the precision of the analyses. The same trend of increased precision with increased bombarding-beam diameter, illustrated in the figure for the results obtained using the 197-keV gamma-ray was also observed in data obtained using the 110- and 1275-keV gamma-rays. From Figure 20 it can thus be deduced that the cement samples were homogeneous to within about 8.7% (implying a relative standard deviation of 8.7% in the analysis) at the 1.1 mg sample size. This sample size corresponds to the irradiated volume using a 0.5 mm diameter collimator. Similarly the cements are homogeneous to within 5.7% at the 2.2 mg level (7 mm collimator).

The determination of the fluorine content of the seven cements was calibrated by the use of the cements of known fluorine content. As explained earlier, no range corrections to the gamma-ray yields were necessary. The observed data points are shown in Figure 21, fitted to a line through the origin by the method of least squares. The determined values of the fluorine concentrations of the unknown cements are given in Table 12. The Transvaal cements show a very similar fluorine concentration, whilst the Cape cements show a spread with the fluorine content of Cape 2 approaching that of the English cement. Since the latter comes from a site where the fluorine content of the raw materials is high enough to warrant monitoring,

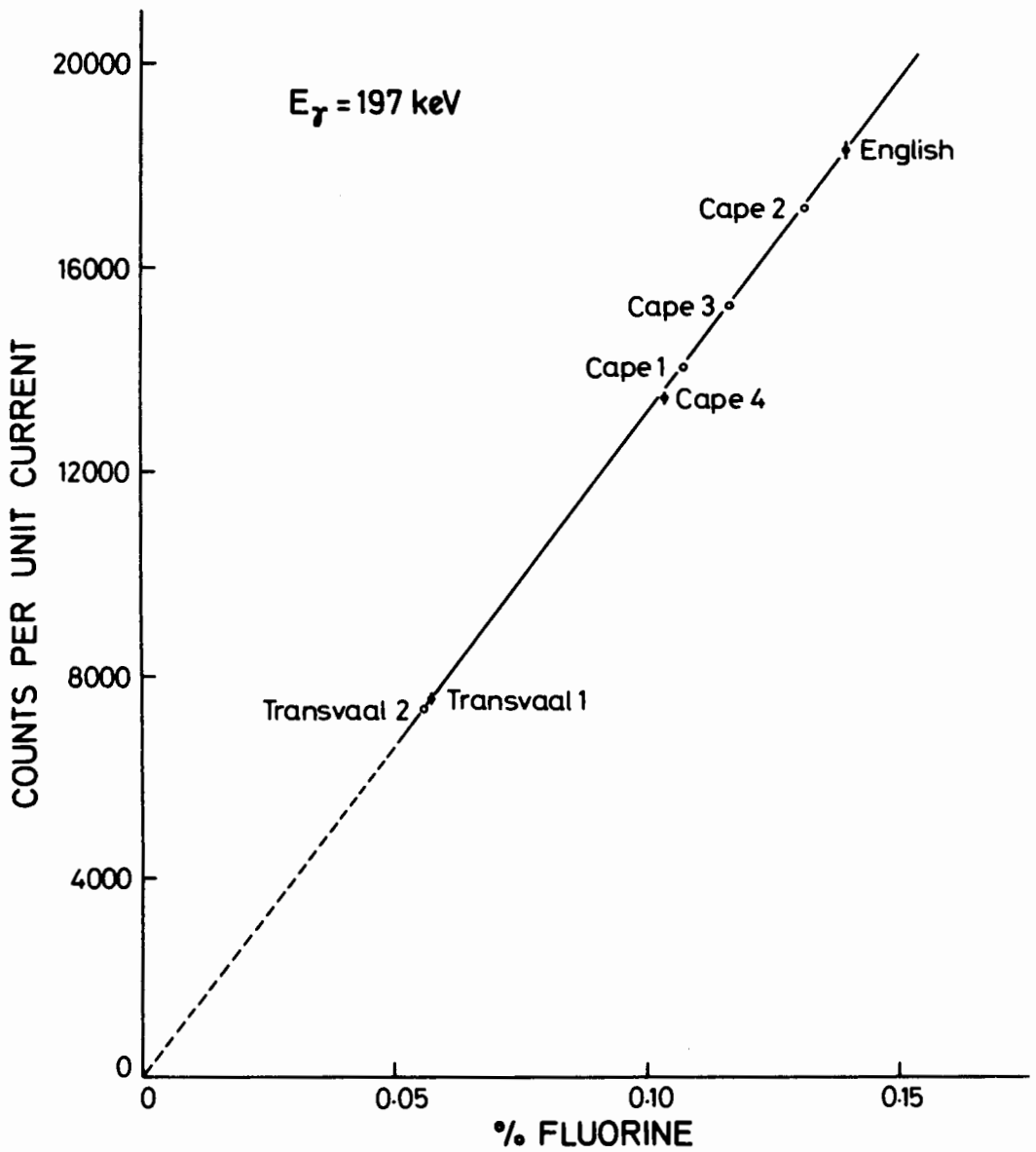

Figure 21 Variation of the count rate for the 197-keV gamma-rays with fluorine content of cements.

the routine analysis of Cape 2 is suggested.

Table 12. Measured fluorine content of cements

Cement	Fluorine content %
Transvaal 2	0.056
Cape 1	0.108
Cape 2	0.131
Cape 3	0.117

CONCLUSION

The use of alpha-induced prompt gamma-rays for the analysis of fluorine has been established. The method yields rapid results for fluorine contents over a wide concentration range. These results should be corrected for range differences in order to attain improved accuracy and precision. The method offers a sensitive and rapid procedure for the determination of fluorine in cements and also serves as a check on the homogeneity of the product, provided the diameter of the bombarding beam is selected appropriately.

Chapter V

Analysis of Steels

INTRODUCTION

Steel is a very extensively used industrial material, the properties of which depend upon its composition and heat treatment. Thus the concentration of carbon in steel varies from about 0.1% to 1.5% by weight and largely determines the tensile strength of the product, while nitrogen, introduced in trace amounts from the atmosphere during manufacture, may have a detrimental effect. Special steels, for example, stainless steel and high-speed tool steel, are produced by the addition of other metals, those most commonly used being titanium, vanadium, chromium, manganese, nickel, molybdenum and tungsten. Many steels therefore contain a range of elements in addition to the basic iron/carbon matrix.

Standard steels were obtained from the U.S. Bureau of Standards and from the Atomic Energy Research Establishment Harwell (AERE Harwell). Bombardment of these samples with 5-MeV $^{4}He^{+}$ ions permitted multi-element analysis. The particular element under consideration was nitrogen thus irradiation currents and durations were selected to suit the analysis of this element. However, it was possible simultaneously to determine the concentrations of other elements from the experimental data. Vanadium and manganese were chosen as examples of such additional analyses. Carbon and oxygen were not determined in the steels since the incident alpha energy was too low

and analysis of oxygen using the 351-keV ^{18}O n(1,0) gamma-ray was subject to interference from iron.

Typical results were selected from those obtained to illustrate the multi-element capability of prompt gamma-ray spectrometry for analysis of a matrix in which suitable elements occur together.

NITROGEN

Introduction

The standard analytical techniques for the analysis of nitrogen at low concentrations are tedious and time-consuming. A nuclear method [O1 75] has been described which uses deuteron-induced prompt particle spectrometry and is capable of providing analytical information on nitrogen in steels, but the concentration range of applicability is not much below about one percent. A different approach also using the same technique [O1 76], extends the determination of nitrogen to the µg/g level but, at the same time, places severe restrictions on the irradiation conditions.

The use of the 871-keV gamma-rays from the reaction $^{14}N(\alpha,p\gamma)^{17}O$ offers a sensitivity comparable with that attained by the latter method whilst the experimental procedure is much simplified.

Results and Discussion

In order to determine the excitation function of the $(\alpha,p\gamma)$ reaction, foils of KAPTON were used as targets. This

material $(C_{22}H_{10}N_2O_4)_n$, contains 7.65% w/w nitrogen and the foils used were 1.052 mg/cm^2 thick. The energy loss in these foils for bombarding $^4He^+$ beams of between 3 and 5 MeV is about 1 MeV. A typical spectrum is shown in Figure 22. The excitation function obtained up to 5 MeV is shown in Figure 23. The resonances that are known to exist for this reaction [Aj 72] were not observed because of the thickness of the target foil. The curve is smoothly varying, and is thus well-suited for the determination of average nitrogen contents.

The reproducibility or precision of the method was examined also with a KAPTON foil target, using an incident beam of 5-MeV $^4He^+$ ions. The results of fourteen repeat determinations are shown in Table 13. From these values the relative standard deviation was better than 1.6% which compares well with the precisions attained for the determination of fluorine as shown in Table 7, Chapter IV.

Table 13. Precision of nitrogen determinations in KAPTON

mean count/μC	533.0
standard deviation	±7.98
relative standard deviation	±1.50%
number of analyses	14

This method was applied to the analysis of nitrogen in steels, by measuring the yield of the 871-keV gamma-rays. The steel samples were Standard Reference Materials from the U.S. Bureau of Standards, Washington and analysed specimens from AERE Harwell. The SRM 1090 series of standard

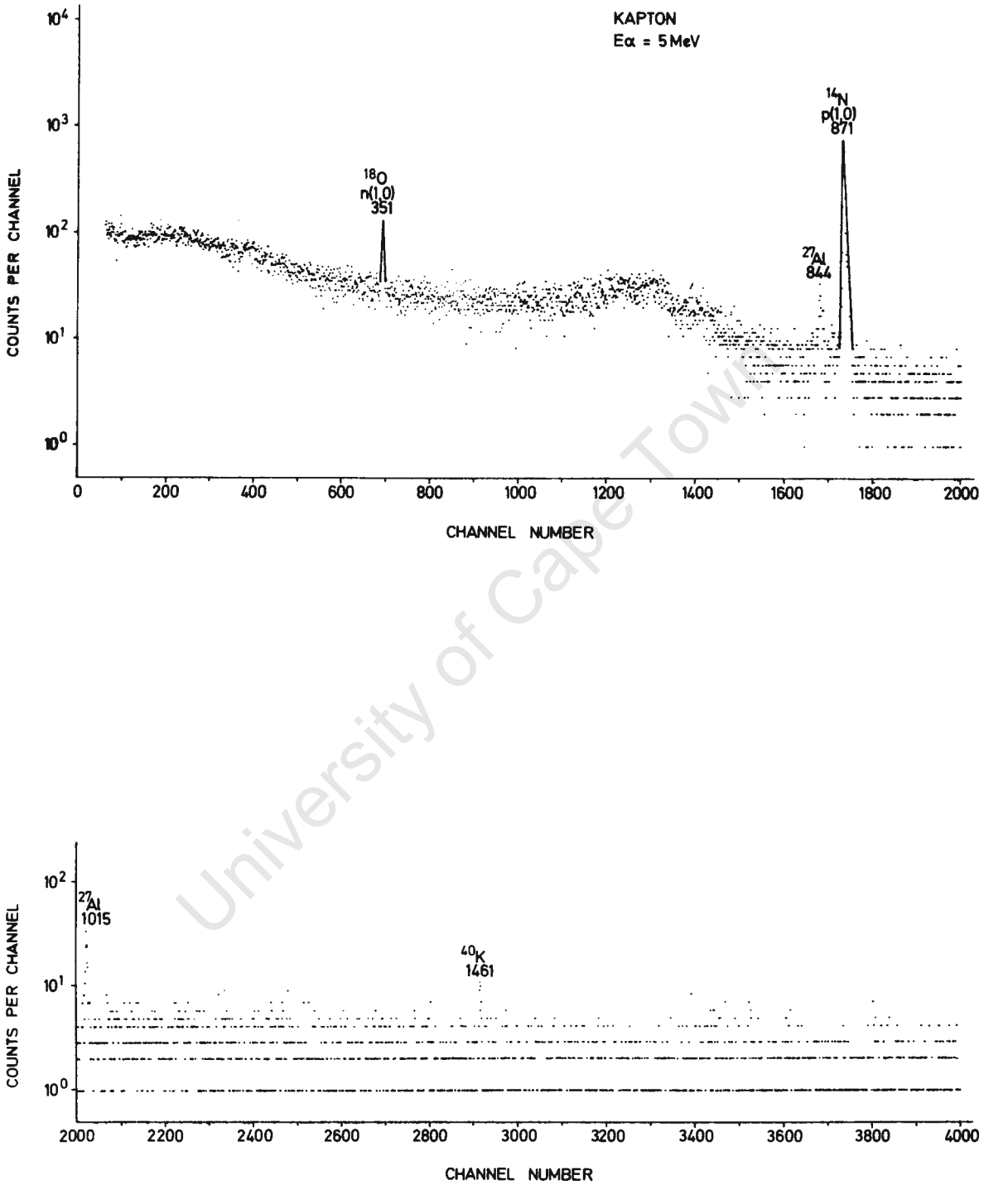

Figure 22 Typical gamma-ray spectrum of alpha bombarded KAPTON foil.

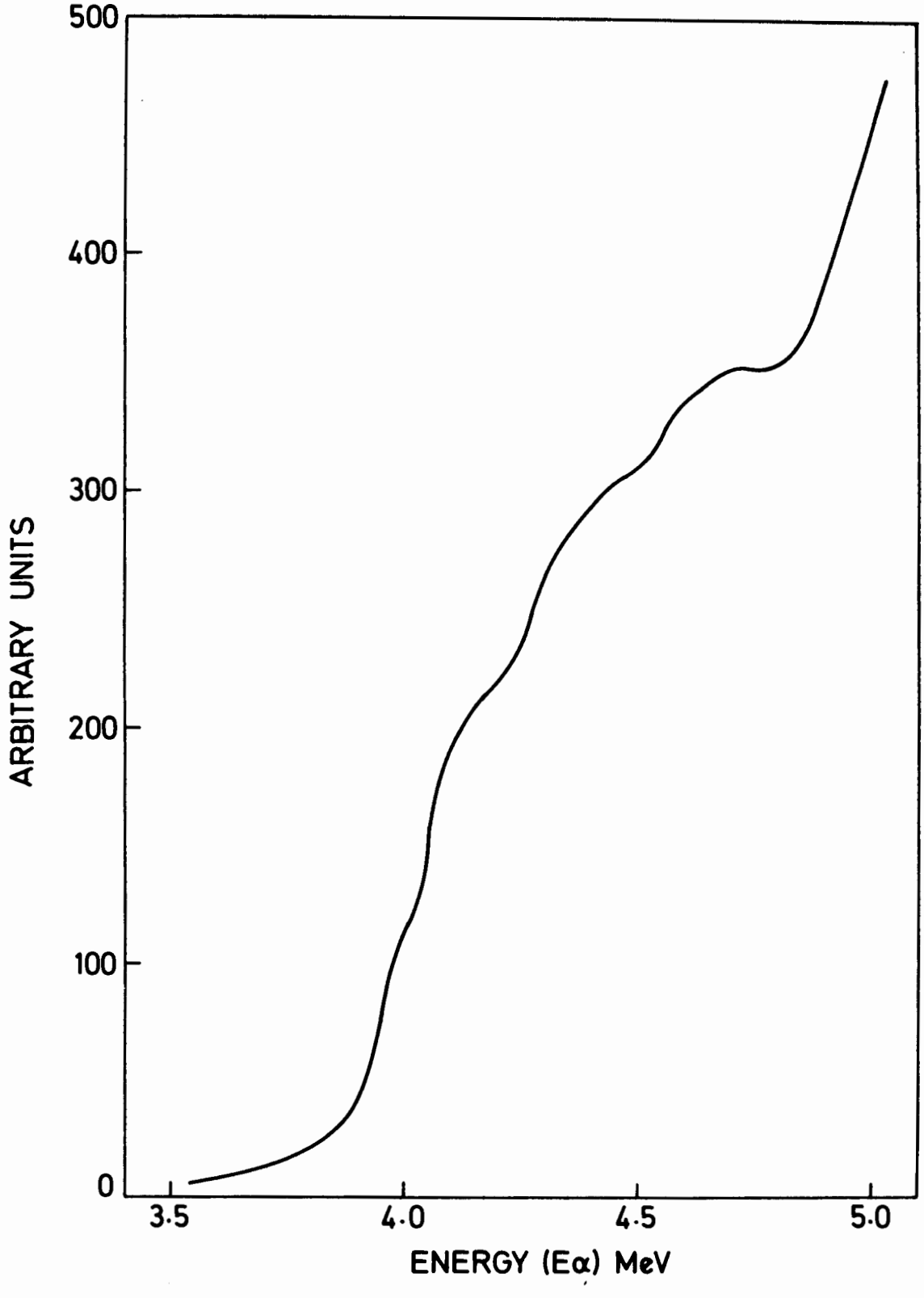

Figure 23 Excitation function for the production of 871-keV gamma-rays from nitrogen by the reaction $^{14}N(\alpha,p\gamma)^{17}O$ measured to 5 MeV.

steels from the U.S. Bureau of Standards were in the form of rods 6.4 mm in diameter, which were cut into discs 1.5 mm thick. Specimens R 50 and B 19 (see Table 14) from Harwell measured 7 mm across and 0.25 mm in thickness, the remaining samples being 20 mm in diameter and 1 mm thick. Prior to analysis all specimens were polished to a mirror-like finish with fine diamond dust powder at the Department of Gemology, University of Stellenbosch, and carefully washed to remove traces of the abrasive.

The small physical size of most of the samples compared with the diameter of the beam (3 mm) caused difficulties during irradiation since there was a possibility that a small change in the field of the steering magnets could have resulted in a portion of the bombarding beam falling off the target during part of the irradiation. For this reason samples were mounted on a silvered metal frame. Any beam current falling on the silver would thus be detected by the appearance of silver gamma-rays. Bombarding currents up to 250 nA were used. Typically, analyses were completed within 10 to 20 minutes, depending on the nitrogen concentration and the precision required. A typical spectrum, that of steel R 50, is shown in Figure 24.

The Harwell samples B 19 and R 50 were reported to contain 0.6 and 0.49% N by weight respectively. For the purposes of the present investigation these values were assumed to be 6000 and 4900 ppm respectively. Samples AP and BO had been analysed by the Micro-Kjeldahl method. The nitrogen contents of all the remaining samples were not

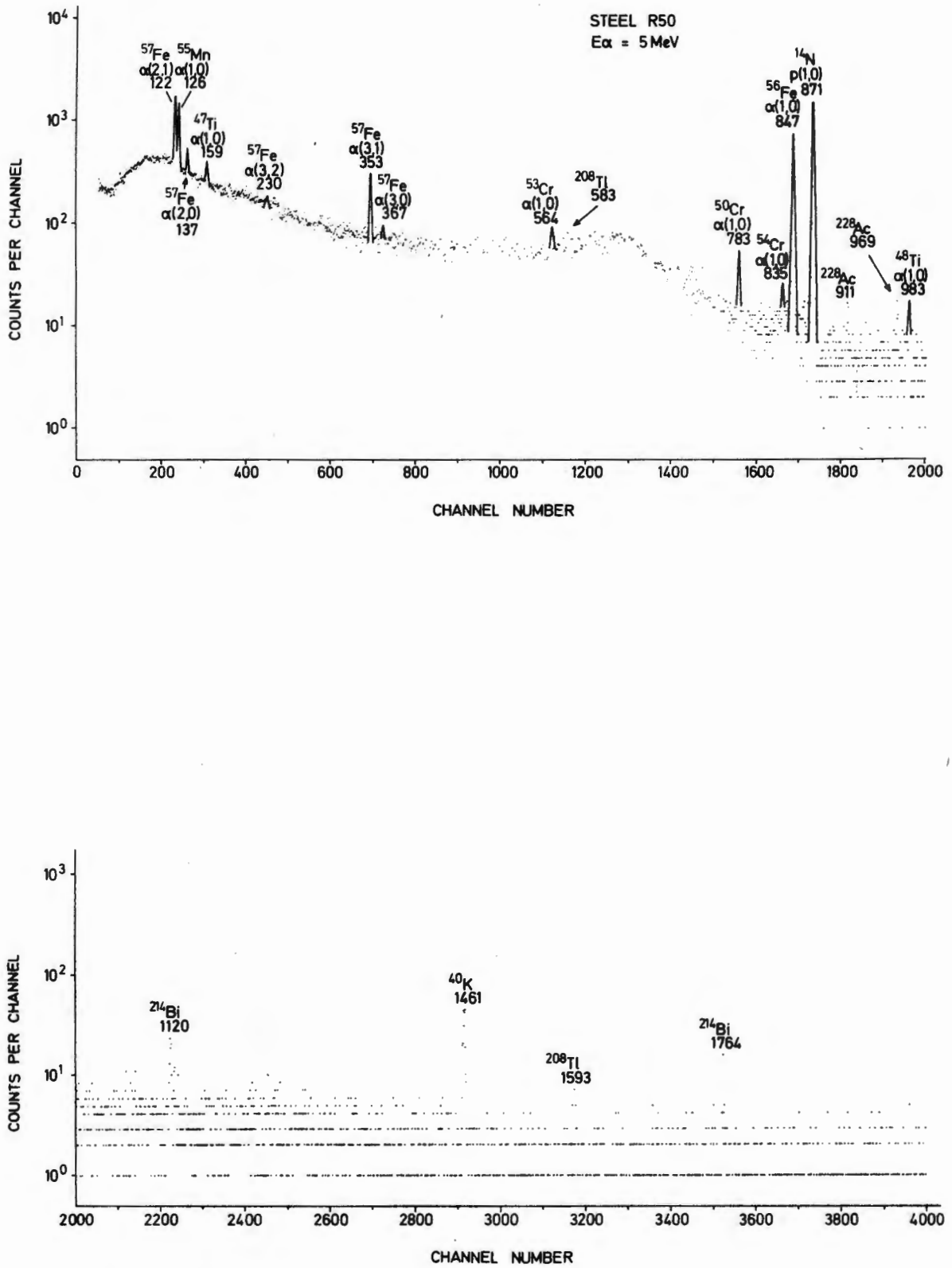

Figure 24 Typical gamma-ray spectrum of alpha-bombarded steel specimen.

certified values but were given as supplementary information determined by relatively few analytical procedures. It is therefore noted that the nitrogen content of these materials is not known absolutely.

Since the analysed standards had nitrogen contents between 4 and 6000 µg/g it was not a simple matter to obtain the calibration curve over such a wide range of concentrations. Minor fluctuations in the high-nitrogen region will cause relatively little difference in the slope of the line and hence will have a small influence on values obtained for high nitrogen content steels. The same variations will however, materially alter the intercept of the calibration line and markedly change the apparent content of steels containing trace concentrations of nitrogen. A plot (Figure 25) of all the results and the best straight line drawn through them is shown on a log-log scale in order to accommodate all four orders of magnitude of the nitrogen content. In Table 14 the "known" values of the nitrogen contents are compared with "found", the latter being calculated form the equation of the straight line determined by the method of least squares. Whereas high-nitrogen steel samples show a small relative error, low-nitrogen steel samples have a low absolute error. For determining very low concentrations, the root mean square error, for standards within that concentration range, is often more significant than the relative standard deviation calculated for all the standards. From the data obtained for the low-nitrogen steel samples the root mean square error was found to be ± 9 µg/g, which is acceptable and

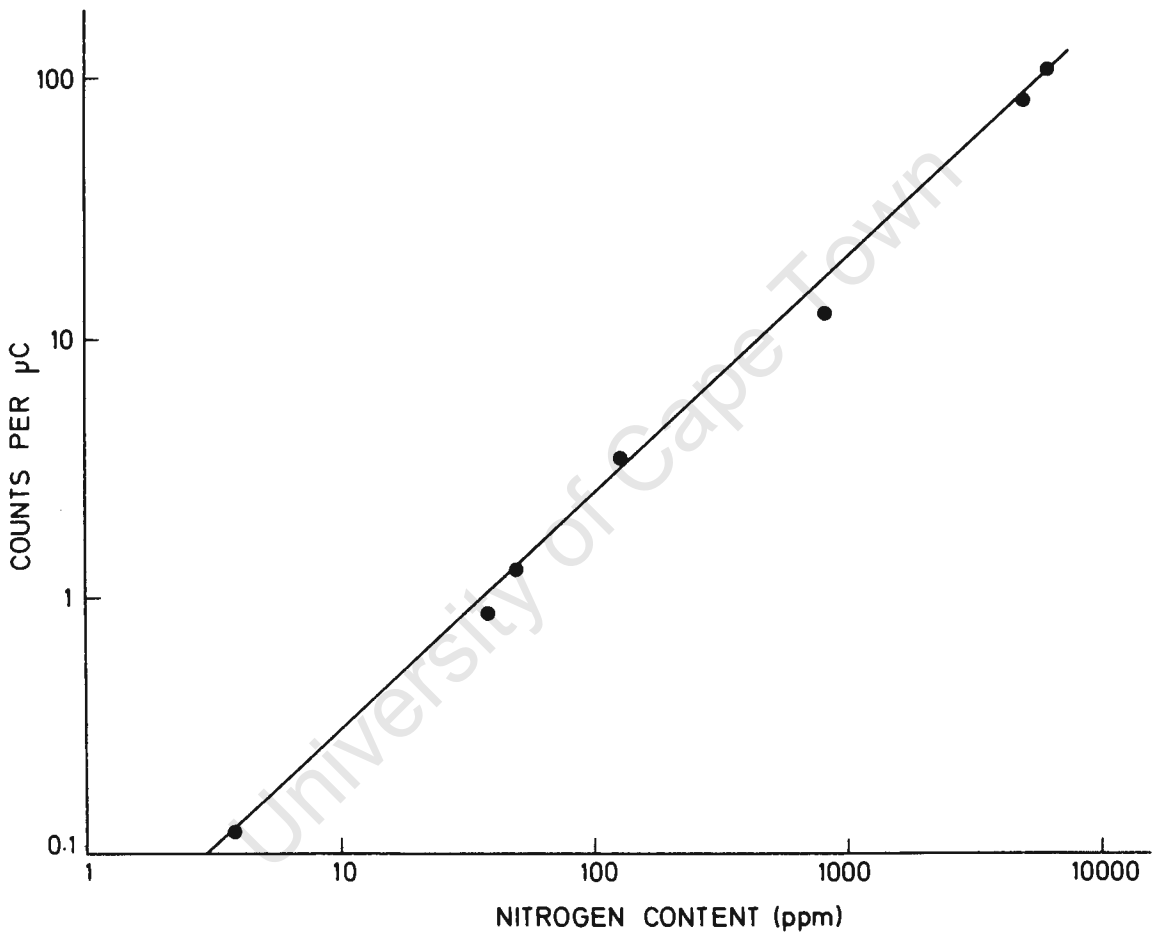

Figure 25 Variation of count rate of the alpha-induced 871-keV gamma-rays with nitrogen content.

compares favourably with the error of the previously reported method [O1 76]. The relative standard error in the higher nitrogen concentration region was about 4%.

Table 14. Determination of nitrogen in standard steels

Target	Known nitrogen content, µg/g	Count/µC	Found nitrogen content, µg/g
B 19	6000	107.240	6373.2
R 50	4900	82.752	4915.4
1091	837	12.539	735.6
1090	60	3.539	119.5
AP	49.5	1.276	65.1
BO	39.5	0.845	39.4
1092	3.8	0.196	0.76
		Root mean square error : 9	

It should be noted that, in common with the deuteron irradiation method, Ref. O1 76, an anomalously high value was obtained for SRM 1090. Since no adequate explanation has yet been put forward to explain this result, this steel was not included as a standard in this investigation.

A calibration using the steels in the low-nitrogen region only, thereby eliminating errors caused by extrapolation of data from the high-nitrogen region, yielded the results shown in Table 15 from which a root mean square error of ± 4 µg/g was obtained.

From these preliminary results the spanning of four decades

of nitrogen concentration, though an ambitious undertaking, is not impractical, provided calibration is performed with sufficient care. More replicate and repeat analyses would provide smaller standard deviations for the individual data points, whilst longer irradiations would improve the error due to counting statistics, which is appreciable for the low-nitrogen samples. Only a marginal improvement in the results would be expected as a result of range corrections since all the materials have essentially similar stopping power. The method is obviously very sensitive to any nitrogen on the surface of the steel and thus adsorbed nitrogen could play a large rôle in the scatter of the results, and possibly yield spuriously high values.

Table 15. Analyses of low-nitrogen steels

Target	Known nitrogen content, µg/g	Count/µC	Found nitrogen content, µg/g
AP	49.5	1.276	53.6
BO	39.5	0.845	34.2
1092	3.8	0.196	4.9
		Root mean square error	: 3.9

The practicability of the detection and analysis of nitrogen in very low concentrations by this technique has been demonstrated. Potentially the method is as good as, or better than, other nuclear methods available.

OTHER ELEMENTS

In addition to the determination of nitrogen, simultaneous analyses were possible on some minor constituents of the steels; vanadium and manganese were selected as examples of such analyses.

Vanadium

Introduction

The addition of vanadium to steel produces a product with enhanced toughness, elasticity and tensile strength. Typically the vanadium contents of the resulting alloys are in the range of about 1 to 3%. Analysis of vanadium in this concentration range is possible using the 320-keV, ^{51}V $\alpha(1,0)$ gamma-ray, which is free of interference from other elements normally found in steel. In this respect alpha-induced prompt gamma-rays are preferred over proton-induced X-rays since no interference from other transition metals is possible.

Results and Discussion

Steels with vanadium contents in the concentration range of interest were chosen as standards. Irradiation with 5-MeV $^{4}He^{+}$ ions and beam currents of the order of 250 nA was followed by integration of the peak corresponding to the 320-keV gamma-ray. The results obtained for the analyses, performed in triplicate, are given in Table 16. which lists the U.S. Bureau of Standards' concentration as well as the "found" value for each standard. These latter values were calculated from the equation of the

straight line determined by the method of least squares. The root mean square error of the analyses was ± 0.08% V whilst the overall relative standard deviation of each result was 1.7%. The calibration line obtained is given in Figure 26.

Table 16. Determination of vanadium in standard steels

Standard	Known V content, mg/g	Found V content, mg/g	Difference	Difference %	Count/μC per 1% V
D 841	11.3	10.6	0.7	6.49	5.693
D 838	11.7	12.6	0.9	7.14	6.611
D 839	15.0	15.2	0.2	1.33	6.289
D 840	21.1	20.4	0.7	3.32	6.036
D 837	30.4	30.7	0.3	0.99	6.374
	Root mean square error :		0.8		
		Mean			6.201
		Relative standard deviation :			± 1.71%

The results demonstrate the possibility of determining vanadium concentrations in the minor component range, rapidly and simultaneously with analyses of other elements in the same sample.

Manganese

Introduction

The use of the 126-keV, ^{55}Mn $\alpha(1,0)$ gamma-ray for the determination of manganese had a good interference-free potential sensitivity. However in the presence of iron, the spectral peak due to manganese was subject to a measure

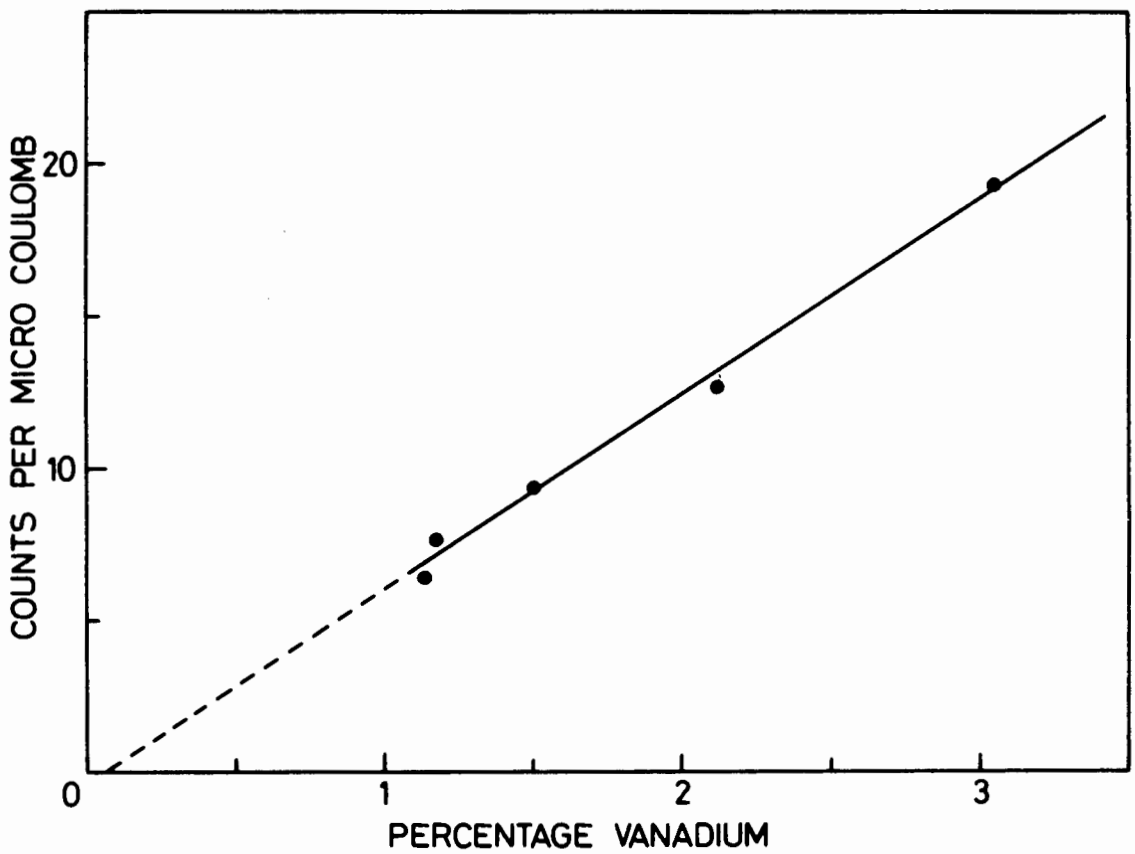

Figure 26 Variation of count rate of the alpha-induced 320-keV gamma-rays with vanadium content.

of interference because the 122-keV ^{57}Fe $\alpha(2,1)$ gamma-rays, although resolved from the 126-keV manganese gamma-rays, were not clearly separated from them, as may be seen from Figure 24. It was necessary therefore to use stripping procedures in the analysis of manganese.

Results and Discussion

The steels selected as standards for the analyses had manganese contents from 0.3% to 1.8%, representative of the range of concentrations commonly used for alloys. On completion of each irradiation, the peak in the spectrum corresponding to the 126-keV gamma-ray of manganese was stripped from that due to iron, by hand. The region of the spectrum from 110 to 135 keV was plotted on semi-log graph paper, thus ensuring that the peaks retained their shapes. These shapes were then superimposed on each of the peaks and the resulting stripped manganese peak was integrated. Clearly, for routine determinations, computer stripping would have to be used.

Results of the analyses are given in Table 17 which shows the comparison of the U.S. Bureau of Standards' value for the manganese content of each steel and its "found" value. The latter was calculated from the equation of the straight line determined by the method of least squares. The calibration line obtained is given in Figure 27.

The root mean square error was found to be ± 0.06% Mn whilst the relative standard deviation was 2.65%, which was an acceptable result. An improvement in precision could

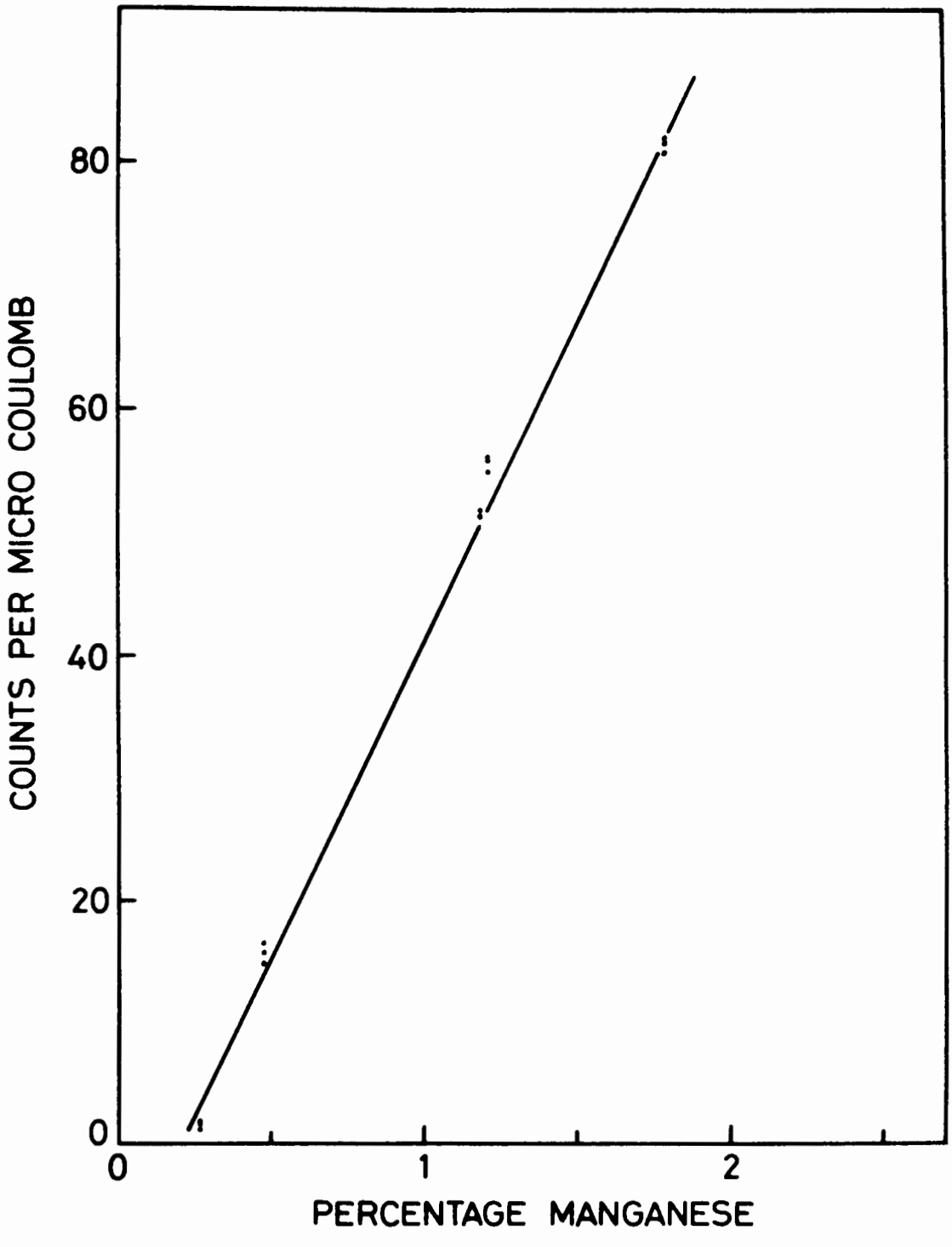

Figure 27 Variation of count rate of the alpha-induced 126-keV gamma-rays with manganese content.

be expected as the result of increased irradiation times, thus improving the errors due to counting statistics. In addition, a change in the energy calibration of the spectrometer to give more channels per keV, would facilitate the estimation of the shape of the spectral peaks, thus improving the accuracy with which they are stripped, either manually or using computer programmes. The peak stripping was the most critical factor affecting the precision of the analyses.

Table 17. Determination of manganese in standard steels

Standard	Known Mn content, mg/g	Found Mn content, mg/g	Difference	Difference %	Count/μC per 1% Mn
SRM D841	2.7	2.2	0.5	18.52	40.53
SRM D837	4.8	5.0	0.2	4.17	52.19
SRM 1152	11.9	12.2	0.3	2.52	51.15
SRM 1185	12.2	13.1	0.9	7.38	53.26
SRM 1171	18.0	18.2	0.2	1.11	50.46
	Root mean square error :		0.6		
		Mean			49.52
		Relative standard deviation :			2.65%

Conclusion

Simultaneous analysis of vanadium and manganese has been demonstrated. The precision attained for the determination of any particular element in such multi-element analysis may be improved by the careful selection of irradiation conditions to suit that element. However, the usefulness of additional information on components of the matrix, other

than that under direct consideration, when it is obtained without expenditure of additional irradiation time, cannot be over stressed. The sample analyses of vanadium and manganese were sufficiently precise for concentrations in the minor component range, to provide a useful illustration.

Other elements that may be analysed in this way would be titanium and molybdenum for concentrations in the minor component range. With the use of higher energy alpha particles carbon and oxygen could also be determined.

APPENDIX

ENERGIES AND ASSIGNMENTS OF ALL OBSERVED GAMMA-RAYS ARRANGED IN ORDER OF INCREASING ENERGY

E_γ (keV)	Assignment	E_γ (keV)	Assignment
54.3	^{51}V n(1,0)	113.0	^{177}Hf α(1,0)
61		122.1	^{57}Fe α(2,1)
72.8	^{208}Bi	122.3	^{186}W α(1,0)
73.0	^{193}Ir α(1,0)	122.7	^{179}Hf α(1,0)
74.0	^{19}F n(2,1)	125.4	^{185}Re α(1,0)
74.8	^{212}Pb	125.9	^{55}Mn α(1,0)
75.0	^{208}Bi	127.2	^{101}Ru α(1,0)
77.1	^{212}Pb	129.1	^{228}Ac
77.4	^{197}Au α(1,0)	129.4	^{191}Ir α(2,0)
78.1	^{29}Si p(1,0)	129.7	^{195}Pt α(2,0)
84.8	^{208}Bi	134.3	^{187}Re α(1,0)
87.2	^{212}Pb	136.3	^{181}Ta α(1,0)
89.4	^{99}Ru α(1,0)	136.5	^{57}Fe α(2,0)
91		138.9	^{193}Ir α(2,0)
93	^{67}Zn α(1,0)	140.4	^{195}Pt α(5,1)
93.2	^{178}Hf α(1,0)	151.3	^{85}Rb α(1,0)
93.3	^{180}Hf α(1,0)	156.9	^{51}V n(2,0)
98.3	^{107}Ag α(2,1)	158.4	^{199}Hg α(1,0)
98.9	^{195}Pt α(1,0)	158.8	^{47}Ti α(1,0)
99.1	^{183}W α(2,0)	159.4	^{185}Re α(2,1)
100.1	^{182}W α(1,0)	165.2	^{181}Ta α(2,1)
103.3	^{109}Ag α(3,2)	166.8	^{187}Re α(3,1)
107	^{193}Ir α(3,1)	169.9	^{10}B p(3,2)
109.9	^{19}F α(1,0)	177.6	^{167}Er α(2,0)
111.2	^{184}W α(1,0)	178.9	^{191}Ir α(4,0)

E_γ (keV)	Assignment	E_γ (keV)	Assignment
180.0	^{193}Ir α(3,0)	280.5	^{105}Pd α(1,0)
181.5	^{170}Er α(2,1)	284.8	^{185}Re α(2,0)
184.3	^{168}Er α(2,1)	285.0	^{214}Bi
184.4	^{166}Er α(2,1)	293	
184.6	^{67}Zn α(2,0)	295.0	^{103}Rh α(3,0)
186.0	^{226}Ra	295.2	^{214}Pb
191.5	^{197}Au α(2,1)	296.0	^{210}Tl
197.1	^{19}F α(2,0)	298.6	^{113}Cd α(2,0)
203.9	^{95}Mo α(1,0)	301	^{187}Re α(3,0)
207.1	^{51}V n(3,2)	301.4	^{181}Ta α(2,0)
208.2	^{199}Hg α(2,0)	306.4	^{79}Br α(4,0)
211.3	^{195}Pt α(4,0)	311.8	^{109}Ag α(2,0)
213.8	^{191}Ir α(5,2)	313.1	^{39}K p(2,1)
217.0	^{79}Br α(2,0)	316.5	^{192}Pt α(1,0)
219.1	^{193}Ir α(4,2)	319.8	^{51}V α(1,0)
230.4	^{57}Fe α(3,2)	322	
238.6	^{212}Pb	324.8	^{107}Ag α(1,0)
239.3	^{195}Pt α(5,0)	328.3	^{228}Ac
241.9	^{214}Pb	328.5	^{194}Pt α(1,0)
261.3	^{79}Br α(3,0)	338.7	^{228}Ac
268.8	^{197}Au α(2,0)	341.9	^{111}Cd α(2,0)
270.5	^{228}Ac	343.2	^{191}Ir α(5,0)
276.0	^{81}Br α(1,0)	350.5	^{18}O n(1,0)
277.4	^{208}Tl	352.0	^{214}Pb
278.9	^{197}Au α(3,0)	352.5	^{57}Fe α(3,1)

E_γ (keV)	Assignment	E_γ (keV)	Assignment
355.7	^{196}Pt α(1,0)	493	
357.5	^{103}Rh α(4,0)	510.7	^{208}Tl
358.0	^{104}Ru α(1,0)	511.0	β^+
358.0	^{193}Ir α(4,0)	523.0	^{79}Br α(6,0)
361.8	^{193}Ir α(5,0)	535.6	^{100}Mo α(1,0)
363.6	^{45}Sc α(2,1)	538.2	^{81}Br α(3,0)
366.9	^{57}Fe α(3,0)	539.6	^{100}Ru α(1,0)
368.0	^{200}Hg α(1,0)	540	
373.8	^{110}Pd α(1,0)	547.5	^{197}Au α(6,0)
397.4	^{79}Br α(5,0)	555.8	^{104}Pd α(1,0)
407.2	^{198}Pt α(1,0)	556.6	^{102}Pd α(1,0)
411.8	^{198}Hg α(1,0)	558.3	^{114}Cd α(1,0)
415.1	^{109}Ag α(3,0)	563	^{76}Ge n,n'(1,0)
416.9	^{23}Na n(2,0)	564.1	^{53}Cr α(1,0)
423.1	^{107}Ag α(2,0)	573	
433.9	^{108}Pd α(1,0)	583.0	^{19}F n(1,0)
439.4	^{202}Hg α(1,0)	583.1	^{208}Tl
439.9	^{23}Na α(1,0)	583.7	^{113}Cd α(6,0)
440.0	^{110}Pd α(2,1)	585.1	^{25}Mg α(1,0)
463.3	^{228}Ac	595.9	^{74}Ge n,n'(1,0)
475.1	^{102}Ru α(1,0)	598.2	^{10}B p(2,1)
477.6	^{7}Li α(1,0)	604	
477.6	^{7}Be	606.0	^{79}Br α(7,0)
480.9	^{97}Mo α(1,0)	608.4	^{74}Ge n,n'(2,1)
481		608.9	^{51}V α(2,1)

E_γ (keV)	Assignment	E_γ (keV)	Assignment
609.3	^{214}Bi	806	
617.4	^{112}Cd $\alpha(1,0)$	810.6	^{58}Fe $\alpha(1,0)$
637.0	^{19}F n(4,3)	829.6	^{23}Na n(3,1)
657.7	^{110}Cd $\alpha(1,0)$	834.0	^{72}Ge n,n'(2,0)
666		834.8	^{54}Mn
666.0	^{214}Bi	835.3	^{54}Cr $\alpha(1,0)$
669.6	^{63}Cu $\alpha(1,0)$	843.8	^{24}Mg p(1,0)
677.2	^{27}Al n(1,0)	843.8	^{27}Mg
691.2	^{72}Ge n,n'(1,0)	843.8	^{27}Al $\alpha(1,0)$
709.0	^{27}Al n(2,0)	846.8	^{56}Fe $\alpha(1,0)$
718		858.4	^{55}Mn $\alpha(2,1)$
718.3	^{10}B $\alpha(1,0)$	860.5	^{208}Tl
727.2	^{212}Bi	870.8	^{14}N p(1,0)
749.2	^{48}Ti n(1,0)	871.0	^{94}Mo $\alpha(1,0)$
754.9	^{26}Mg n(2,1)	884.8	^{73}Ge n,α(1,0)
768	^{10}B p(3,1)	889.2	^{46}Ti $\alpha(1,0)$
768.7	^{214}Bi	890.9	^{19}F n(3,0)
770.8	^{65}Cu $\alpha(1,0)$	894.2	^{72}Ge n,n'(4,2)
778.3	^{96}Mo $\alpha(1,0)$	899.2	^{39}K p(3,1)
783.3	^{50}Cr $\alpha(1,0)$	900	
786.2	^{95}Mo $\alpha(2,0)$	911.2	^{228}Ac
786.7	^{23}Na (1809-2m_e)	929	^{51}V $\alpha(2,0)$
787.4	^{98}Mo $\alpha(2,0)$	934.8	^{214}Bi
795.0	^{210}Tl	962.1	^{63}Cu $\alpha(2,0)$
795.0	^{228}Ac	964.4	^{228}Ac

E_γ (keV)	Assignment	E_γ (keV)	Assignment
968.8	^{228}Ac	1235.8	^{19}F α(3,1)
983.4	^{48}Ti α(1,0)	1238.0	^{214}Bi
984		1262.7	^{27}Al p(2,1)
991.5	^{64}Zn α(1,0)	1266.1	^{28}Si p(1,0)
1002.5	^{23}Na p(4,2)	1266.1	^{31}P α(1,0)
1014.5	^{24}Mg p(2,0)	1273.3	^{26}Mg n(1,0)
1014.5	^{27}Al α(2,0)	1273.3	^{29}Si α(1,0)
1039.4	^{66}Zn α(1,0)	1274.6	^{19}F p(1,0)
1040		1275	
1066		1279.9	^{19}F n(5,2)
1077.4	^{68}Zn α(1,0)	1290.8	^{11}B (2313-2m_e)
1099		1297.7	^{23}Na (1809-m_e)
1105.4	^{31}P (2127-2m_e)	1311.2	^{27}Al p(5,2)
1115.5	^{65}Cu α(2,0)	1332.0	^{27}Al p(6,2)
1120.4	^{214}Bi	1348.6	^{19}F α(4,1)
1129.7	^{23}Na p(2,1)	1357.0	^{19}F α(5,2)
1145.6	^{35}Cl (2168-2m_e)	1368.6	^{24}Na
1155.4	^{214}Bi	1368.9	^{19}F n(6,1)
1176.1	^{31}P p(2,1)	1378.0	^{214}Bi
1193		1395.1	^{18}O n(2,1)
1209.8	^{35}Cl p(2,1)	1400.1	^{19}F n(7,1)
1211.8	^{28}Si (2234-2m_e)	1406	
1213.5	^{27}Al (2236-2m_e)	1408.0	^{214}Bi
1213.5	^{30}Si (2236-2m_e)	1411.7	^{23}Na p(7,2)
1223		1454.0	^{27}Al n(3,0)

E_γ (keV)	Assignment	E_γ (keV)	Assignment
1458.5	^{19}F $\alpha(4,0)$	1732.1	^{24}Na $(2754-2m_e)$
1460.8	^{37}Cl $p(1,0)$	1756	
1460.8	^{40}K	1764.0	^{214}Bi
1463.9	^{72}Ge $n,n'(3,0)$	1778.9	^{25}Mg $n(1,0)$
1509.0	^{214}Bi	1778.9	^{28}Si $\alpha(1,0)$
1524.2	^{39}K $p(1,0)$	1779.6	^{23}Na $p(3,1)$
1527.9	^{19}F $n(4,0)$	1793.8	^{26}Mg $n(4,1)$
1534.1	^{27}Al $p(3,1)$	1801.8	^{11}B $(2313-m_e)$
1552.2	^{27}Al $p(4,1)$	1808.7	^{23}Na $p(1,0)$
1570.4	^{19}F $(2081-m_e)$	1849.5	^{214}Bi
1588.3	^{228}Ac	1896.7	^{23}Na $p(8,2)$
1592.0	^{208}Bi $(2614-2m_e)$	1916.4	^{23}Na $(2938-2m_e)$
1592.5	^{208}Tl $(2615-2m_e)$	2028.2	^{26}Mg $n(2,0)$
1594	^{96}Zr $\alpha(1,0)$	2081.4	^{19}F $p(2,1)$
1616.4	^{31}P $(2127-m_e)$	2103.0	^{208}Bi $(2614-m_e)$
1633.8	^{17}O $n(1,0)$	2103.5	^{208}Tl $(2615-m_e)$
1642.5	^{35}Cl $p(3,1)$	2127.4	^{31}P $p(1,0)$
1656.6	^{35}Cl $(2168-m_e)$	2132.2	^{23}Na $p(4,1)$
1693.0	^{214}Bi $(2204-m_e)$	2160.4	^{19}F $(3182-2m_e)$
1701		2167.6	^{35}Cl $p(1,0)$
1720		2204.0	^{214}Bi
1722.8	^{28}Si $(2234-m_e)$	2212	
1724.5	^{27}Al $(2236-m_e)$	2233.8	^{28}Si $p(2,0)$
1724.5	^{30}Si $(2236-m_e)$	2235.5	^{27}Al $p(1,0)$
1728.0	^{214}Bi	2235.5	^{30}Si $\alpha(1,0)$

E_γ (keV)	Assignment	E_γ (keV)	Assignment
2243.1	^{24}Na (2754-m_e)	3062	
2281.5	^{31}P (3304-2m_e)	3086	^{10}B p(1,0)
2312.8	^{11}B n(1,0)	3092.4	^{23}Na p(9,1)
2327.9	^{25}Mg (2839-m_e)	3173.2	^{10}B (3684-m_e)
2425.6	^{26}Mg n(3,0)	3182.4	^{19}F p(3,1)
2427.4	^{23}Na (2938-m_e)	3258.6	^{27}Al (3770-m_e)
2438.0	^{18}O n(3,1)	3303.5	^{31}P p(2,0)
2476.2	^{27}Al p(2,0)	3343	^{10}B (3854-m_e)
2511.1	^{23}Na p(5,1)	3417.2	^{12}C (4439-2m_e)
2523.6	^{23}Na p(6,1)	3498.2	^{27}Al p(2,0)
2541.4	^{23}Na p(7,1)	3684.2	^{10}B p(2,0)
2573.9	^{27}Al p(5,1)	3769.6	^{27}Al p(3,0)
2594.7	^{27}Al p(6,1)	3854	^{10}B p(3,0)
2613.5	^{17}O n(2,1)	3928.2	^{12}C (4439-m_e)
2614.0	^{208}Bi	3987	
2614.5	^{208}Tl	4439.2	^{12}C α(1,0)
2662.2	^{10}B (3684-2m_e)	5108.7	^{16}O (6131-2m_e)
2671.4	^{19}F (3182-m_e)	5619.7	^{16}O (6131-m_e)
2747.6	^{27}Al (3770-2m_e)	6130.7	^{16}O α(2,0)
2754.1	^{24}Na		
2792.5	^{31}P (3304-m_e)		
2832	^{10}B (3854-2m_e)		
2838.9	^{25}Mg n(2,1)		
2938.4	^{23}Na p(2,0)		
2987.2	^{27}Al (3498-m_e)		

Reference Index

Aj 72 F. Ajzenberg-Selove, *Nucl. Phys.*, A109 (1972) 1.

Al 56 K. Alder, A. Bohr, T. Huus, B. Mottelson and A. Winther, *Revs. Mod. Phys.*, 28, 4 (1956) 432.

An 74 D.S. Andreev, K.I. Erokhina, V.S. Zvonov, I. Kh. Lemberg and A.S. Mishin, *Izv. Akad. Nauk. SSSR, Ser. Fiz.*, 38, No. 8 (1974) 1661 *Nucl. Sci. Abstr.*, 31 (1975) 31436.

Au 75 R.L. Auble, *Nuclear Data Sheets*, 16 (1975) 1.

Be 69 J.M. Bewers and F.C. Flack, *Analyst*, 94 (1969) 1.

Bo 77 R.B. Boulton and G.T. Ewan, *Anal. Chem.*, 49, 9 (1977) 1297.

Br 70 E.J. Bruton, J.A. Cameron, A.W. Gibb, D.B. Kenyon and L. Keszthelyi, *Nucl. Phys.*, A152 (1970) 495.

Ch 65 C. Chasman, K.W. Jones and R.A. Ristinen, *Nucl. Instr. Methods*, 37 (1965) 1.

Ch 72 J.F. Chemin, J. Roturier, B. Saboya and G.Y. Petit, *J. Radioanal. Chem.*, 12 (1972) 221.

Co 59 D.F. Covell, *Anal. Chem.*, 31, 11 (1959) 1785.

Co 72 G.E. Coote, N.E. Whitehead and G.J. McCallum, *J. Radioanal. Chem.*, 12 (1972) 491.

De 72a G. Deconninck, *J. Radioanal. Chem.*, 12 (1972) 157.

De 72b G. Deconninck and G. Demortier, *J. Radioanal. Chem.*, 12 (1972) 189.

De 72c G. Demortier and F. Bodart, *J. Radioanal. Chem.*, 12 (1972) 209.

De 73 G. Deconninck and G. Demortier, *Nuclear Techniques in the Basic Metal Industries*, IAEA Vienna, (1973) 573.

Du 72 E.K. Duursma, *Oceanogr. Mar. Biol. Ann. Rev.*, 10 (1972) 137.

En 65 C. Engelmann, *Proceedings of the Symposium on Radiochemical Methods of Analysis*, IAEA Vienna, Vol. 1 (1965) 405.

Er 75 G. Erdtmann and W. Soyka, *J. Radioanal. Chem.*, 26 (1975) 375; 27 (1975) 137.

Fr 64 G. Friedlander, J.W. Kennedy and J.M. Miller, *Nuclear and Radiochemistry*, Second Edition, John Wiley and Sons Inc., New York (1964).

Ga 72 S. Gangadharan and S. Yegnasubramanian, *Bhabha Atomic Research Centre Report, B.A.R.C.* 654 (1972).

Gi 75 I.S. Giles and M. Peisach, *Trans. Amer. Nucl. Soc.*, 21, Suppl. 3 (1975) 15.

Gi 76 I.S. Giles and M. Peisach, *J. Radioanal. Chem.*, 32 (1976) 105.

Gi 77 I.S. Giles and M. Peisach, *Radiochem. Radioanal. Lett.*, 28, 2 (1977) 135.

Go 72 I. Golicheff, M. Loeuillet and Ch. Engelmann, *J. Radioanal. Chem.*, 12 (1972) 233.

Ha 69 B.G. Harvey, *Introduction to Nuclear Physics and Chemistry*, Second Edition, Prentice-Hall Inc., Englewood Cliffs, New Jersey (1969).

He 36 G. Hevesy and H. Levi, *Kgl. Danske Videnskab. Selskab, Mat.-Fys. Medd.*, 14 (1936) 5.

He 56 N.P. Heydenburg and G.M. Temmer, *Ann. Rev. Nucl. Sci.*, 6 (1956) 77.

Hu 53 T. Huus and C. Zupancic, *Kgl. Danske Videnskab. Selskab, Mat.-Fys. Medd.*, 28 (1953) 1.

Ku 69 H.W. Kugel, R.R. Borchers and R. Kalish, *Nucl. Phys.*, A137 (1969) 500.

La 62 D. Lal, *Proceedings of the Symposium on Radioactive Dating*, IAEA Vienna, (1962) 19.

Le 72 M.B. Lewis, *Nuclear Data*, B7 (1972) 129.

Lu 74 H.O. Lutz, *Private Communication* (1974).

Ma 73 J.W. Mandler, R.B. Moler, E. Raisen and K.S. Rajan, *Thin Solid Films*, 19 (1973) 165.

Mc 53 C.L. McClelland and C. Goodman, *Phys. Rev.*, 91 (1953) 760.

Mc 58 F.K. McGowan and P.H. Stelson, *Phys. Rev.*, 109 (1958) 901.

Mc 59 F.K. McGowan and P.H. Stelson, *Phys. Rev.*, 116 (1959) 154.

Mi 55 W.R. Mills, H.H. Hilton and C.A. Barnes, *Phys. Rev.*, 100 (1955) 1794.

Mo 67 E. Möller and N. Starfelt, *Nucl. Instr. Methods*, 50, (1967) 225.

No 70 L.C. Northcliffe and R.F. Schilling, *Nuclear Data Tables*, A7 (1970) 233.

Nu 77 *Nuclear Data Sheets*, 20, No. 1 (1977).

Ol 75 C. Olivier, J.W. McMillan and T.B. Pierce, *Nucl. Instr. Methods*, 124 (1975) 289.

Ol 76 C. Olivier, M. Peisach and T.B. Pierce, *J. Radioanal. Chem.*, 32 (1976) 71.

Pe 73 M. Peisach, *Thin Solid Films*, 19 (1973) 279.

Pe 74 M. Peisach, *J. Radioanal. Chem.*, 12 (1974) 251.

Ra 71 S. Raman and H.J. Kim, *Nuclear Data Sheets*, B5 (1971) 181.

Ri 65 E. Ricci and R.L. Hahn, *Anal. Chem.*, 37, 6 (1965) 742.

Ri 67 E. Ricci and R.L. Hahn, *Anal. Chem.*, 39, 7 (1967) 794.

Ri 72 E. Ricci, *Advances in Activation Analysis*, Vol. 2, Academic Press, New York (1972) p. 221.

Ro 57 L. Rosen and L. Stewart, *Phys. Rev.*, 107 (1957) 824.

Ru 74 H. Rudolph, J.J. Kraushaar, R.A. Ristinen and R.R. Meglen, *Proceedings from a Symposium on Trace Substances in Environmental Health*, VII (1974) 387.

Sa 64 A. Savitzky and M.J.E. Golay, *Anal. Chem.*, 36, 8 (1964) 1627.

Sh 54 R. Sherr, C.W. Li and R.F. Christy, *Phys. Rev.*, 96 (1954) 1258.

Si 60 R.F. Sippel and E.D. Glover, *Nucl. Instr. Methods*, 9 (1960) 37.

Sl 21 F.P. Slater, *Phil. Mag.*, XLII (1921) 904.

St 63 P.H. Stelson and F.K. McGowan, *Ann. Rev. Nucl. Sci.*, 13 (1963) 163.

St 74 H. Stoch, *National Institute for Metallurgy Report* 1649 (1974).

St 76 T.W. Steele, *National Institute for Metallurgy Report of Analysis*, Project No. 50921 (1976).

Te 58 J. Terrell and D.M. Holm, *Phys. Rev.*, 109, 6 (1958) 2031.

Va 61 J.J. van Loef, *Nucl. Phys.*, 24 (1961) 340.

Wi 66 C.F. Williamson, J.-P. Boujot and J. Picard, *Commissariat A L'Énergie Atomique, Report CEA-R* 3042 (1966).

Table 2
Some analyses of cements using the 197 keV gamma-rays

	Fluorine content, %wt			
	Cement 1	Cement 2	Cement 3	Cement 4
	0.269	0.280	0.259	0.256
	0.265	0.284	0.257	0.258
	0.269	0.282	0.258	0.256
	0.272	0.293	0.260	0.264
	0.273	0.273	0.255	0.268
	0.258	0.249	0.264	0.256
Mean	0.267	0.277	0.259	0.260
Rel. stand. dev.	±2 05%	±5.37%	±1.22%	±1.96%

*

Financial assistance from the South African Council for Scientific and Industrial Research and the Atomic Energy Board is gratefully acknowledged. The University of Stellenbosch is thanked for the use of their hydraulic press in the early stages of this investigation and our gratitude is expressed to the National Institute for Metallurgy for supplying samples of their standards free of charge.

References

1. E. MOLLER, N. STARFELT, Nucl. Instr. Methods, 50 (1967) 225.
2. S. GANGADHARAN, S. YEGNASUBRAMANIAN, Bhabha Atomic Research Centre, Report B.A.R.C. 654 (1972).
3. N. P. HEYDENBURG, G. M. TEMMER, Ann. Rev. Nucl. Sci., 6 (1956) 77.
4. H. STOCH, National Institute for Metallurgy Report 1649, 1974.
5. C. CHASMAN, K. W. JONES, R. A. RISTEN, Nucl. Instr. Methods, 37 (1965) 1.
6. M. PEISACH, J. Radioanal. Chem., 12 (1974) 251.

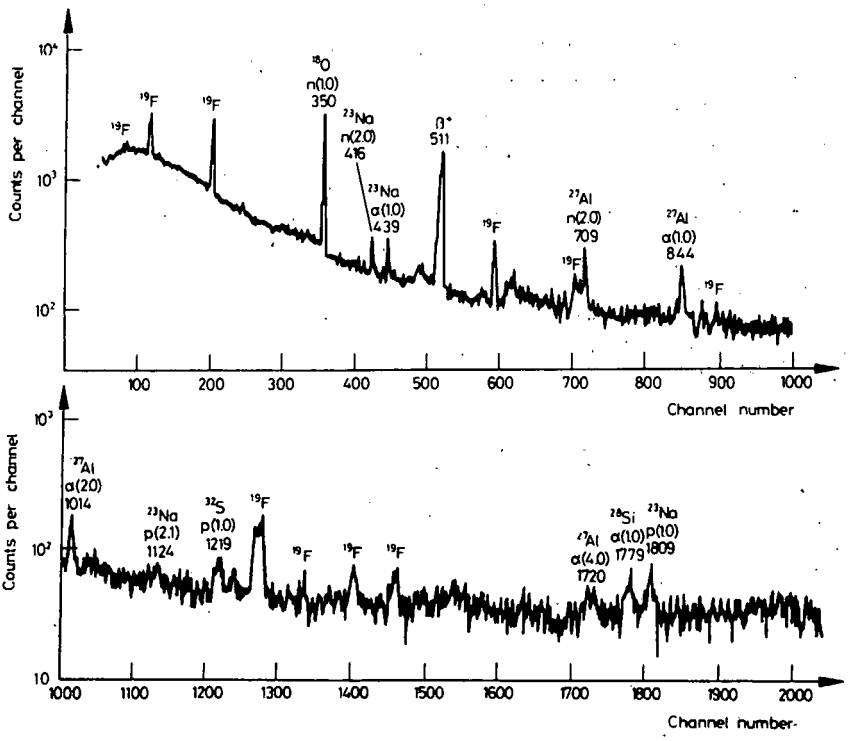

Fig. 7: Typical prompt gamma-ray spectrum obtained from cement bombarded with 5 MeV $^4He^+$ ions. Gamma-ray peaks from fluorine are marked but their energies are omitted. (For gamma-ray energies from fluorine, see Fig. 5)

Some of the results are given in Table 2. The observed standard deviation is of the same order as the measured precision, except for one sample, where the difference is ascribed to inhomogeneity.

The total volume of material analysed is determined by the diameter of the beam used and the effective range of the alpha-particles in the matrix which at these energies is very small. It can be calculated that the total mass sampled is of the order of 0.5 mg. The accuracy of the analysis will then depend on the extent to which this small sampled mass represents the bulk of the material. For control purposes the cited results were considered to be sufficiently accurate.

It may be pointed out that the results of the N. I. M. standards reported in the previous section show a remarkable degree of homogeneity.

Table 1
Precision of the method

Material	Known fluorine content, %wt	Counts per μC per 1% F		
		110 keV	197 keV	1275 keV
CaF_2	46.86	546.6	761.9	103.1
		549.2	768.9	102.2
		551.4	769.1	103.2
		548.2	768.3	103.9
		539.5	767.2	102.1
		537.9	766.9	103.6
		540.7	766.9	102.1
		575.9	786.4	105.0
		562.5	779.2	103.4
		574.1	783.4	102.8
Fluorspar 63/70	46.89	555.9	771.3	102.9
		556.7	778.1	104.6
		562.2	782.5	104.8
		560.7	778.2	103.1
		544.3	767.9	103.4
		538.3	764.5	103.5
Fluorspar 9/69	40.19	551.7	765.1	100.1
		560.4	774.6	100.3
		553.9	770.7	102.7
		547.9	760.9	100.9
		554.4	772.8	102.7
		557.0	772.4	102.2
		555.8	771.1	101.9
	Mean	553.27	771.68	102.80
	Rel. stand. dev.	±1.84%	±0.89%	±1.24%

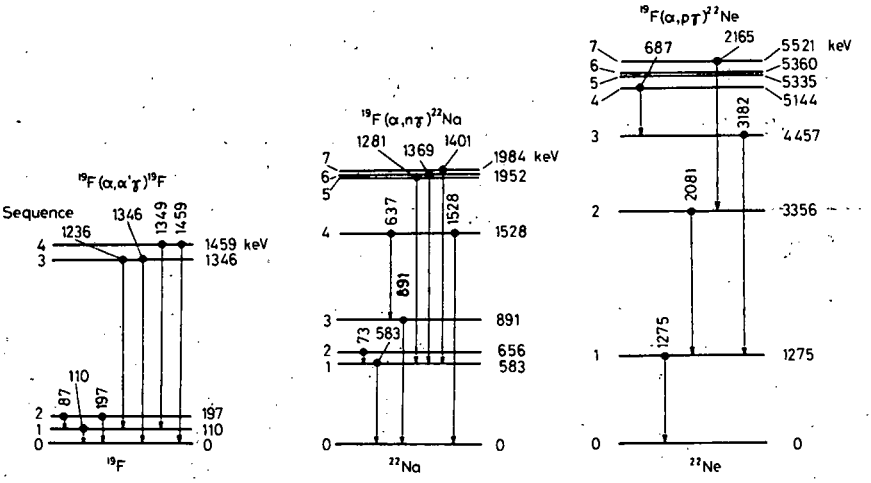

Fig. 6. Decay transitions resulting in observed gamma-rays for the reactions $^{19}F(\alpha, \alpha'\gamma)^{19}F$, $^{19}F(\alpha, n\gamma)^{22}Na$ and $^{19}F(\alpha, p\gamma)^{22}Ne$

results for these are given in Table 1, using each of the gamma-rays 110, 197, 1275 keV as a measure of the fluorine content. The observed relative standard deviations were 1.84, 0.89 and 1.24%, respectively. The improved precision using the 197 keV as compared to that using the 110 keV gamma-rays reflects the decreased efficiency of measuring the lower energy radiation. The good precision using the 1275 keV gamma-rays is ascribed to the comparatively lower background in the vicinity of this energy.

Sensitivity of the method

Attempts to deduce the practical sensitivity limit of the method were made using targets consisting of small known amounts of aqueous solutions of NaF evaporated on backings of carbon. Backings of tantalum could not be used because of the large number of low energy gamma-rays this element generated. Although the precision of the results decreased with decreasing fluorine content, it was found that fluorine contents of the order of 100 ng could still be measured and concentrations of 10 ppm could be detected.

Application to cement analyses

Cement samples from local producers were analysed by the method of prompt gamma-ray spectrometry. A typical spectrum is shown in Fig. 7.

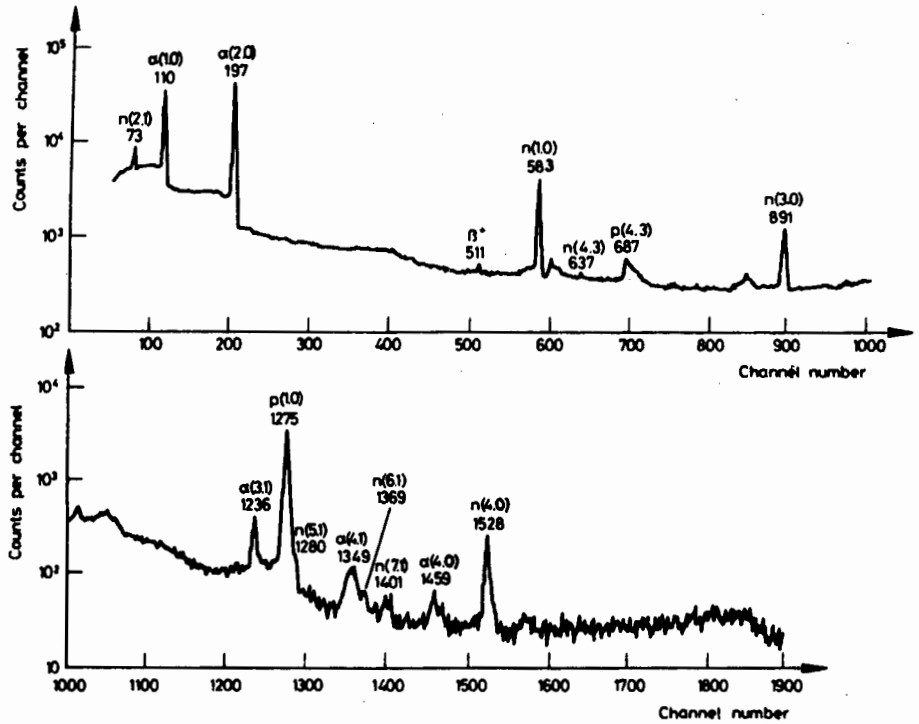

Fig. 5. Prompt gamma-ray spectrum of calcium fluoride bombarded with 5 MeV $^4He^+$ ions. Peak energies are given in keV and the peak assignment is written in the convention described in the text. Gamma-rays from calcium were not observed

Precision of the method

Using the mixtures of calcium hydroxide and calcium fluoride described above, repeat and replicate analyses were carried out using the intensity of the 197 keV γ-rays as a measure of the fluorine content. Samples covered the fluorine range from 0.8 to 32.8% by weight and the relative standard deviation of the results was $\pm$6%. Since the statistical precision based on the count rate was far better than this value it was deduced that this relative standard deviation referred largely to the degree of inhomogeneity of the mixture.

A more detailed test of the precision was carried out using accurately analysed fluorspar standards from the National Institute for Metallurgy. The

the heavy product nucleus from level r to level s. If the target nucleus can be inferred unambiguously it may be omitted. All prompt gamma-ray peaks in spectra reported in this paper are labelled according to this convention.

Fig. 5 shows the intense peaks from gamma-rays of 110, 197 and 1275 keV each of which can be used for analytical purposes. The gamma-rays of 583 keV appear to be intense but the signal to background ratio in this region of the spectrum is detrimental to attaining good precision. Strong peaks were

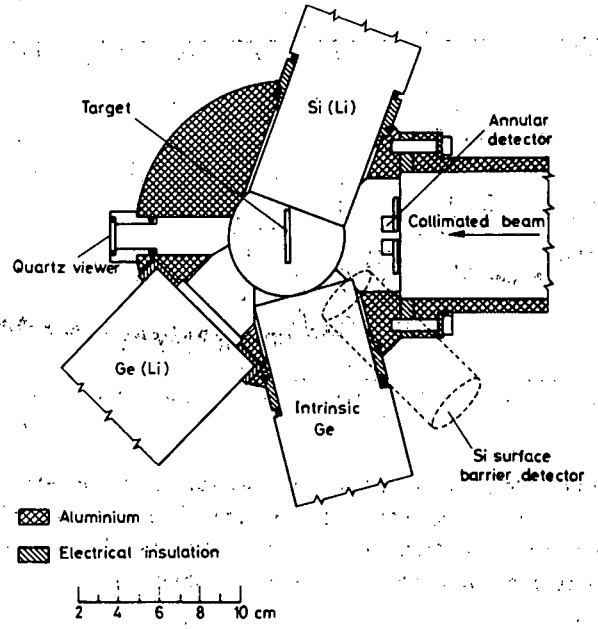

Fig. 4. The construction of the scattering chamber for analysis

observed corresponding to gamma-rays of 87, 110, 197, 1236, 1355 and 1459 keV that could be assigned to the decay of excited levels of ^{19}F produced by $(\alpha, \alpha'\gamma)$ inelastic scattering. In addition gamma-rays from the reaction $^{19}F(\alpha, n\gamma)^{22}Na$ were observed with energies of 73, 583, 637, 891, 1281, 1369 and 1528 keV as well as the 511 keV annihilation gamma-ray. The strong 1275 gamma-ray already mentioned and the gamma-rays of 687, 2081, 2165 and 3182 keV were observed from the reaction $^{19}F(\alpha, p\gamma)^{22}Ne$. The origin of these prompt gamma-rays is shown diagrammatically in Fig. 6.

the chamber. Secondary electron loss from the target could take place at two points, through the beam entrance aperture and through the collimator in front of the surface barrier detector, but their combined solid angle subtended at the target was negligibly small.

Irradiation and measurement

The sample pills were mounted in a target holder placed normal to the direction of incidence of the bombarding beam. The axis of the Ge(Li) detector was at an angle of 45° and the surface barrier 135° to the incidence direction. Both detectors could be shifted away from the target to cope with excessive count rates but could be positioned to cover a large solid angle when warranted by the low count rate.

Beams of 5 MeV $^4He^+$ ions collimated to 3.5 mm in diameter were used to generate the prompt gamma-rays. Beam currents were adjusted so that the deadtime in the multichannel analyser did not exceed 10%. With this restriction the beam currents ranged from 10 to 100 nA. When qualitative data were accumulated, irradiations lasted about 30 minutes each, but during routine analysis on materials with fluoride content 0.1% or more sufficient counts were accumulated within a much shorter time.

Results and discussion

Energy spectrum of prompt gamma-rays

A typical gamma-ray spectrum obtained from the irradiation of calcium fluoride is shown in Fig. 5. Under the conditions of the experiment gamma-rays from calcium were not observed in the spectrum. In the figure the energies corresponding to the peak positions are given in keV.

Prompt gamma-rays are emitted from the product nucleus of a reaction but the analyst is really concerned with that component of the sample on which the nuclear reaction was carried out. Accordingly, for analytical purposes, it is more meaningful to label spectral peaks with the target nucleus. In defining the conditions of the analysis the nature of the bombarding beam is known and need not be stressed; thus the reaction is uniquely identified if the light product particle is given. Accordingly the following convention is used for peak assignment.[6]

In the nuclear reaction

$$A(a, b\gamma)B$$

peak assignment is written A b(r, s) where b is the prompt light particle of the reaction and the gamma-ray quantum is emitted by the de-excitation of

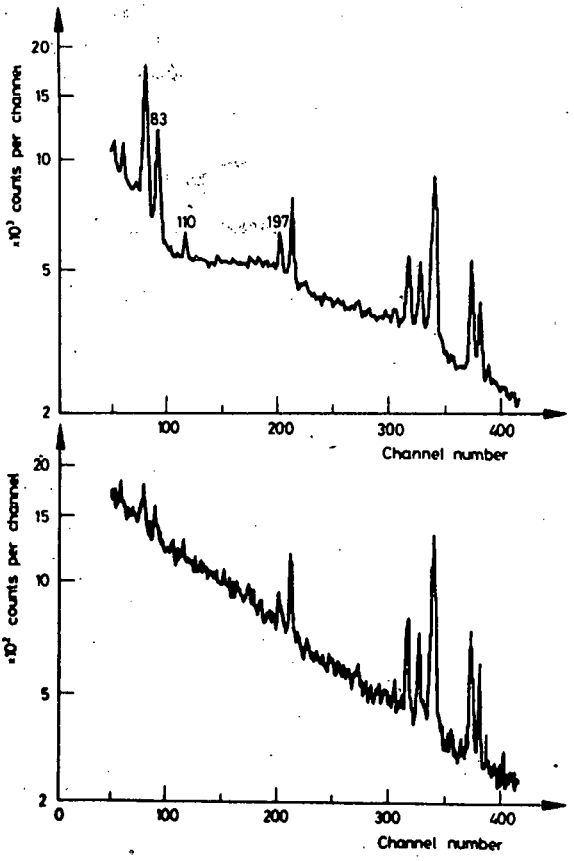

Fig. 3. Comparison of spectra generated by fast neutrons in two different Ge(Li) detectors. The presence of fluorine peaks in the upper curve is clearly evident

annular surface barrier detector for charged particle measurements near 180° scatter. The wall of the scattering chamber in front of the Ge(Li) detector was thinned to reduce absorbtion of gamma-rays.

Because it is essential that the total bombarding current be accurately integrated, the chamber was constructed as a self-contained Faraday cup, electrically insulated from the beam tube and from all the detectors. Collimation of the bombarding beam was achieved in the beam tube outside the chamber. The beam entered the chamber through an aperture about 5 mm in diameter in front of which was placed an anti-scatter copper collimator electrically charged to −300 V to prevent secondary electrons from entering

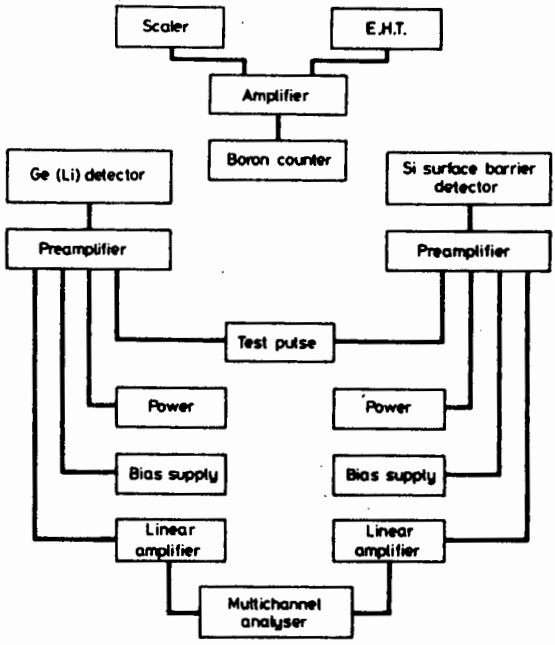

Fig. 2. Block diagram of the electronic apparatus

elements in the sample matrix. Data from the multichannel analyser were stored on magnetic tape and processed by computer.

It was necessary to monitor the neutron yield from the sample under bombardment. Some Ge(Li) detectors contain fluorine in their assembly and these are known[5] to show characteristic fluorine gamma-ray peaks in spectra collected under neutron bombardment. When such a detector was used, background effects were corrected for through the use of the monitored neutron count. At a later stage it was possible to select a Ge(Li) detector which showed a drastically reduced fluorine content. Spectra generated by fast neutrons in each of these detectors are shown in Fig. 3.

The scattering chamber

The irradiations were carried out in a scattering chamber specially designed for analytical purposes. Although constructed for simultaneous use with five detectors (Fig. 4) in this investigation only two of these were used, the surface barrier and the Ge(Li) detectors. The remaining three positions that were available were ports for a Si(Li) X-ray detector, a thin planar intrinsic germanium detector for low energy gamma-rays and an

occur with much reduced probability. The Coulomb barrier for alpha-particles is much higher than for protons or deuterons, hence at energies of a few MeV alpha-particles cause reactions with far fewer nuclei. In practice the cross-section for 5 MeV alpha-particles falls to a negligible level if the atomic number of the target nucleus exceeds 16. When, therefore, inelastic scattering is used for the analytical determination of fluorine, interference from heavier nuclides is much reduced by the utilisation of alpha-particles as the means of excitation.

Experimental

Preparation of standards and samples

Samples for bombardment, whether standard or unknown, were crushed and pressed into pills with a diameter of 13 mm, using a 10-ton press. In a few cases where the material itself did not form a suitable pill, a known weight of binder, usually KBr or borax, was added to a weighed amount of the material and the analytical results were then corrected for the dilution effect.

Chemically pure fluorides of many different metals were bombarded in order to establish the identity of the large number of gamma-ray peaks recorded in the spectrum. The yields of fluorine gamma-rays from these pure fluorides served to establish the linear relationship between yield and concentration, and were used to construct a coarse calibration.

Standards of known fluoride content were prepared by mixing known weights of calcium fluoride and calcium hydroxide in the solid state in a mill. Since it is known that such mixing may result in a product that is not always homogeneous an attempt was made to improve homogeneity, by combining suspensions of known amounts of each of these materials in hexane under agitation with ultrasonic sound waves, and subsequently removing the hexane by distillation. Analyses of the different mixtures later showed that there was no discernible difference in homogeneity of the products.

For the final calibration homogeneous powdered samples of the standard[4] fluorspar materials, 9/69, 42/70, 63/70, 27/72 and 36/72 were obtained from the National Institute for Metallurgy, Johannesburg, South Africa.

The electronic measuring system

A block diagram of the electronic system is shown in Fig. 2. Essentially there are three separate measuring systems counting gamma-rays, charged particles and neutrons. The gamma-ray spectra are required for the analysis, while the charged particle data are used to obtain information on the major

gamma-rays resulting from inelastic scattering of alpha-particles on a calcium fluoride target are shown in Fig. 1.

The inelastic scattering reaction

$$^{19}F(\alpha, \alpha')^{19}F$$

causes excitation of the fluorine nucleus which on prompt decay emits gamma-rays characteristic of the excited levels of ^{19}F. This Coulomb excitation occurs by purely electromagnetic interaction between passing charged particles and nuclear protons.[3] As long as the energy of the bombarding particle is below the Coulomb barrier, other types of reaction

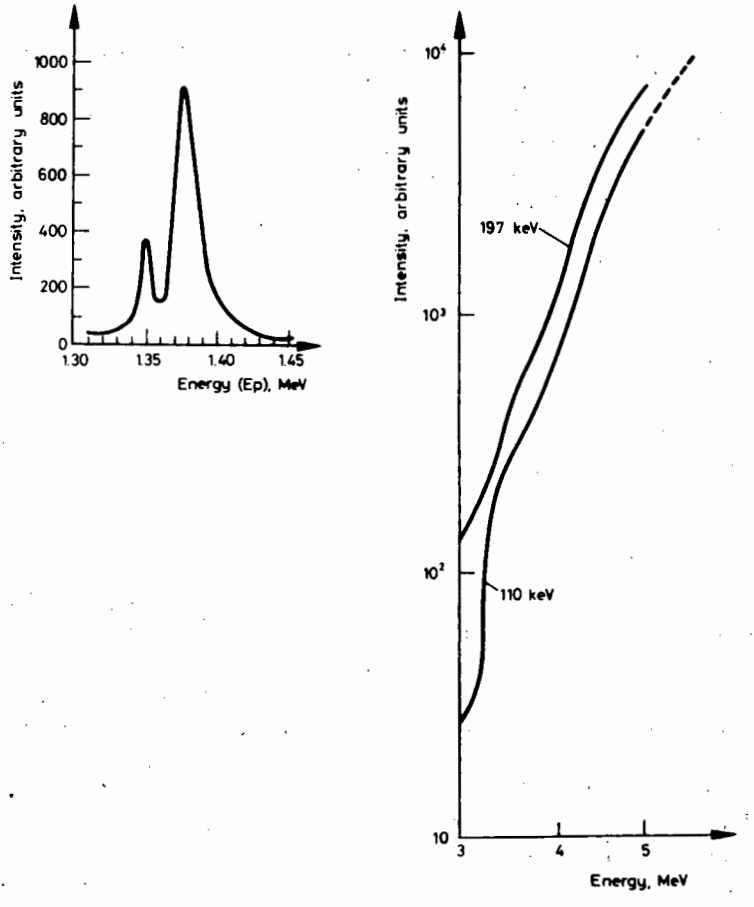

Fig. 1. Excitation function for the gamma-rays of 110 and 197 keV generated by bombardment with $^4He^+$ ions from 3 to 5 MeV. The inset shows the yield from the proton-induced resonance[2]

Journal of Radioanalytical Chemistry, Vol. 32 (1976) 105–116

DETERMINATION OF FLUORINE BY THE SPECTROMETRY OF PROMPT GAMMA-RAYS

I. S. GILES, M. PEISACH

Southern Universities Nuclear Institute, P. O. Box 17, Faure, 7131 (South Africa)

The use, for analysis, of prompt gamma-rays excited by 5 MeV alpha-particles from the reactions $^{19}F(\alpha,\alpha'\gamma)^{19}F$, $^{19}F(\alpha, n\gamma)^{22}Na$ and $^{19}F(\alpha, p\gamma)^{22}Ne$, was studied. The precision of the analyses depended on the gamma-ray energy used for the measurement. Relative standard deviations were ±1.8, ±0.9 and ±1.3% using the 110-, 197- or 1275 keV gamma-rays. The method was tested with N. I. M. standard materials of calcium fluoride and fluorspar, and was used as a rapid method for the determination of fluorine in cements.

Introduction

Nuclear methods for the determination of fluorine frequently make use of resonances in the reaction

$$^{19}F(p, \alpha\gamma)^{16}O$$

and the one most often used[1] occurs for a proton energy of 1375 keV: a smaller resonance is also observed at 1348 keV. The gamma-rays emitted are from excited levels of ^{16}O and those used for analytical purposes have energies of 6.058 MeV, 6.138 MeV and 7.122 MeV. The use of these gamma-rays enables very sensitive depth determination to be made because the cross-section of the reaction is very high over the short proton energy range of the resonance. On either side of the resonances the cross-section falls to a very low value.[2] The yield is thus highly sensitive to fluorine concentration changes in the proximity of that part of the particle range where the energy passes through the resonance.

By contrast the gamma-rays produced as a result of inelastic scattering are much less subject to drastic yield changes. The use of such gamma-ray yields for analyses is much more suitable for the determination of average fluorine concentrations. The excitation functions for two of the different

Summary

Prompt gamma-rays are generated by bombardment with relatively low-energy alpha particles through Coulomb excitation and, in the case of some elements, by nuclear reactions. In general, excitation functions for such gamma-rays are smoothly varying. When thick targets are bombarded the yields increase smoothly with energy and hence such yields can readily be used for analytical purposes. Previously protons have been used for analysis but alpha particles have the following advantages :

(1) The number of different gamma-ray energies from nuclear reactions is low, resulting in a simplified spectrum for analysis.

(2) Interference from heavier elements can be reduced by varying the bombarding energy because the Coulomb barrier increases with the Z of the target more rapidly than with protons.

(3) Gamma-ray producing nuclear reactions suitable for analysis occur with light elements giving characteristic peaks in relatively underpopulated regions of the spectrum.

(4) Heavy metal X-rays that may be generated are little absorbed within the target thickness corresponding to the range of the alpha particle.

In this work 57 elements were studied in a survey to select those that can be analysed by this method at alpha-particle bombarding energies of 5, 11 and 16 MeV.

Amongst the light elements, useful applications of this technique can be expected for the determination of lithium, boron, carbon, nitrogen, oxygen, fluorine, sodium, aluminium, silicon and phosphorus. Carbon and oxygen would require higher energy alpha particles to excite the 4439-keV level in ^{12}C and the 6131-keV level in ^{16}O. Yields of gamma-rays from decay of these states were measured with 11- and 16-MeV alpha particles.

Some medium weight elements also yield suitable low-energy gamma-rays that could be used for qualitative and quantitative analysis, the most promising cases being vanadium, manganese, rhodium, palladium and silver. Those heavy elements for which this approach offers analytical potential are tantalum, rhenium, platinum and gold.

As a result of the initial survey the elements selected for more detailed study were nitrogen, fluorine, manganese and vanadium.

Analyses based on the very intense gamma-rays of 110, 197 and 1275 keV from fluorine proved to be sufficiently sensitive to determine this element in concentrations of the order of parts per million. This method was applied to the determination of fluorine in cement samples containing that element in concentrations between 0.05 and 0.15% by weight. The precision of the method was better than 1% after a twenty-minute bombardment. This method of fluorine analysis is sufficiently precise to be used for detecting inhomogeneities in solid samples. Quantitation was effected through the

use of National Institute for Metallurgy standards and pure materials, the data from which necessitated the use of range corrections owing to their widely differing compositions.

The use of the 871-keV gamma-rays from ^{14}N offers a sensitivity comparable with that attained by the method using the reaction $^{14}N(d,p)^{15}N$ which has previously been used for the analysis of steels, but the present method has the advantage that the irradiation conditions are not critical. Gamma-ray spectroscopy of steel samples proved useful for the determination of nitrogen even for concentrations in the parts per million range. Also analysed in steels were manganese and vanadium which are both common constituents of specialised alloys.

7. Determination of Fluorine by Spectrometry of Prompt Gamma Rays, *I. S. Giles, M. Peisach (So. Univ Nucl Inst-S. Africa)*

Nuclear methods for determination of fluorine frequently make use of resonances in the $^{19}F(p,\alpha\gamma)^{16}O$ reaction which result in the emission of characteristic gamma rays[1] between 6 and 7 MeV. Use of these gamma rays has the disadvantage that the yield is sensitive to fluorine concentration changes in the proximity of that part of the particle range where the energy passes through the resonance energy. By contrast, gamma rays produced by inelastic scattering are less subject to drastic yield changes, and analyses using the yields of such gamma rays are more suitable for determining average fluorine concentrations. To decrease the number of possible sources of interference, α-particle beams were chosen as the means of excitation.

Pure fluorides were bombarded with 5-MeV $^4He^+$ ions and the prompt gamma rays were measured in a 50-cm^3 Ge(Li) detector approximately at right angles to the beam. Intense peaks were observed corresponding to gamma rays of 87, 110, 197, 1236, 1355, and 1459 keV that could be assigned to the decay of excited levels of ^{19}F produced by (α,α') inelastic scattering. In addition, gamma rays from the $^{19}F(\alpha,n\gamma)^{22}Na$ reaction were observed with energies of 73, 583, 637, 891, 1281, 1369, and 1528 keV as well as the 511-keV annihilation gamma ray from the positron decay of ^{22}Na. Some gamma rays were also noted from the $^{19}F(\alpha,p)^{22}Ne$ reaction, but these were not sufficiently intense for analytical purposes.

Despite the apparent complexity of the gamma-ray spectrum, the low-energy gamma rays of 110 and 197 keV were so intense that relatively short irradiations could be used for the analyses and the rest of the spectrum could be ignored. The estimated sensitivity for fluorine analysis is on the order of parts per million.

The method was applied for rapid determination of fluorine in cement samples in which the fluorine concentration commonly varies between 0.1 and 4%. For fluorine concentrations in this range, bombardments with 100-nA currents required about 20 min to obtain an integrated count with better than 0.2% statistical precision. Under these conditions, precision of the analysis is determined by other experimental parameters, the most important of which is the sampling error. Since the charged-particle method analyzes a relatively small portion of the specimen, reliability of the result will depend on the extent to which the small analyzed portion represents the bulk of the material.

Absolute calibration of the method was attempted by preparing mixtures of finely powdered CaF_2 and $Ca(OH)_2$ to yield powders with average fluorine concentrations ranging from 1 to 40%. Approximately 1-g specimens of these powders were pressed into pellets which were analyzed by prompt-gamma-ray spectrometry. The relative standard deviation of replicate analyses over the whole range of fluorine concentrations was 6%. It is inferred that the largest component in this error is inhomogeneous mixing.

1. E. MÖLLER and N. STARFELT, *Nucl. Instrm. Methods*, 50, 225 (1967).

Reprinted from Transactions of the American Nuclear Society, 21 Suppl. 3 (1975) 15.

Journal of Radioanalytical Chemistry, Vol. 37 (1977) 141–154

Fundamental Contributions, Technical Development

RECENT DEVELOPMENTS IN THE ANALYTICAL APPLICATION OF PROMPT SPECTROMETRY

I. S. GILES,* C. OLIVIER,** M. PEISACH*

**Southern Universities Nuclear Institute, P. O. Box 17, FAURE 7131, (South Africa)*
***Chemistry Department, University of Stellenbosch, STELLENBOSCH 7600, (South Africa)*

(Received November 15, 1976)

A survey of the possibilities of analysis by alpha-induced prompt gamma-ray spectrometry is reported for 57 elements at a bombarding energy of 5 MeV. Additional data obtained at 11 and 16 MeV are given. Interference-free sensitivities are presented. The use of the position sensitive detector is introduced to overcome problems such as occur in prompt alpha spectrometry from (p, α) reactions. The technique is illustrated by studies on the reaction $^{19}F(p, \alpha)\ ^{16}O$ and severely tested for boron analysis using the reaction $^{11}B(p, \alpha)\ ^{8}Be$ and measuring the α_0 and α_1 groups.

Introduction

The emission of particles or radiation resulting from a nuclear reaction can occur either during the reaction or from the radioactive products that are formed. Both these processes can find application for elemental analysis. The oldest and most widely used techniques rely on emission of the latter type where advantage is taken of the *delayed* decay of the product enabling it to be measured after the reaction has occurred or at a site remote from the irradiation position. It is implicit in this technique that the product be radioactive, and reactions which lead to the formation of stable products are thus eliminated from possible analytical application. No such restriction applies to analytical methods based on the former type of emission where prompt products are measured during the irradiation. In principle the distinction between these two procedures is obvious, but in practice the boundary between them is determined by experimental conditions and the live-times of the products. It can thus happen that short-lived radio-nuclides are measured by prompt techniques while long lived metastable states use delayed methods. Currently the boundary is accepted to be half-lives of the order of 0.1 μs.

In this work results are presented of recent studies on

(a) the analytical use of prompt gamma-rays induced by alpha-bombardment, in which a survey is made of the most intense gamma-rays observed from some 50-odd elements; and

(b) the application of position-sensitive detectors for analysis by prompt particle spectrometry.

Analysis by alpha-induced prompt gamma-ray spectrometry

Prompt gamma-rays are generated by bombardment with relatively low energy alpha particles through Coulomb excitation and, in the case of some light elements by nuclear reaction. Since in general the excitation functions for such gamma-rays are smoothly varying, the yield from thick targets increases smoothly with energy and hence can readily be used for analytical purposes. Previously protons have been used[1,2] but alpha particles have the advantages that

(1) the number of different gamma-ray energies from nuclear reactions is relatively small, resulting in a simplified spectrum,

(2) interference from heavier elements can be reduced by decreasing the bombarding energy, because the Coulomb barrier increases with the atomic number of the target nucleus more rapidly than with protons,

(3) gamma-rays from nuclear reactions with light elements give characteristic peaks in relatively underpopulated regions of the spectrum,

(4) prompt x-rays which may be generated from heavy metals are sufficiently energetic to escape from the irradiated region of the target with little absorption.

Fig. 1 shows diagrammatic outlines of the periodic table in which the elements that are listed are those studied in this investigation with 5, 11 and 16 MeV alpha particles, respectively.

Experimental

Where appropriate, elements were bombarded in the metallic state in the form of discs or sheets about 1 mm thick which were "infinitely" thick to the bombarding beam. Powdered compounds were compressed to pellets 13 mm in diameter, but when the material did not form pellets easily or where insufficient powder was available the target material was housed in a small target cell with a beam entrance window of Kapton 8 μm thick. In all cases the Ge(Li) detector which measured the gamma-ray spectra was mounted outside the aluminium irradiation chamber opposite a portion of the wall that had been thinned to reduce absorption. Bombarding cur-

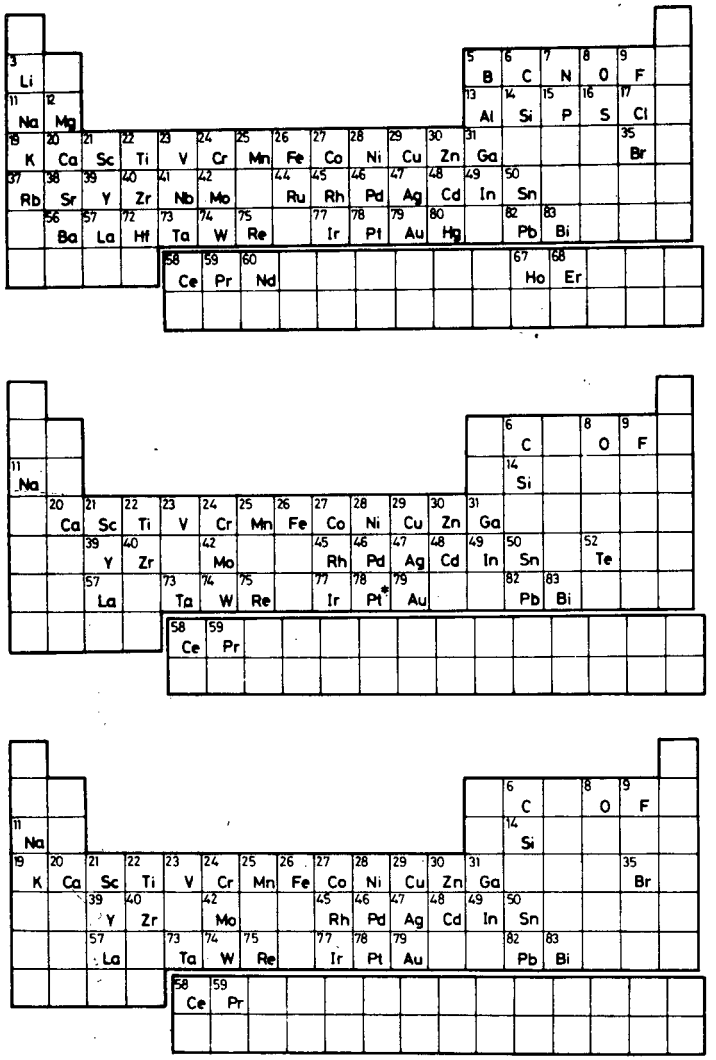

Fig. 1. The elements entered in the outline of the periodic tables show the elements that have been studied with 5 MeV alpha particles (top), 11 MeV (middle) and 16 MeV (bottom)

rents were adjusted to ensure that the dead time of the counting equipment did not exceed 10%.

Recorded spectra were stored on magnetic tape and analysed off-line by computer stripping programmes.

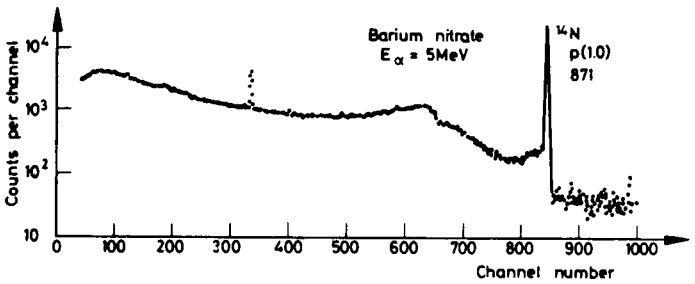

Fig. 2. Prompt gamma-ray spectrum of nitrogen as obtained from the bombardment of barium nitrate

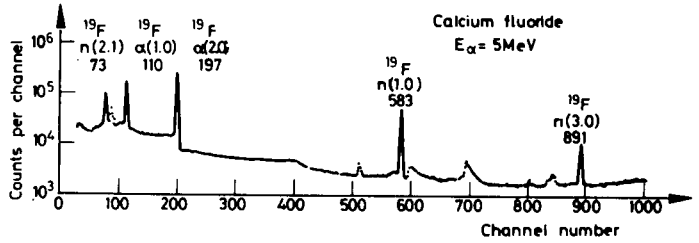

Fig. 3. Prompt gamma-ray spectrum of fluorine as obtained from the alpha bombardment of calcium fluoride

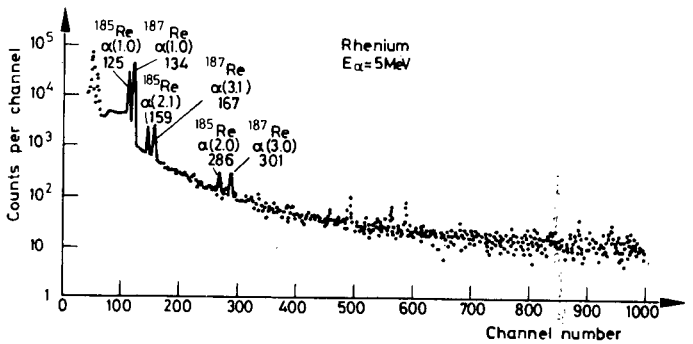

Fig. 4. Prompt gamma-ray spectrum from the alpha bombardment of metallic rhenium

Results and discussion

Typical spectra for the elements nitrogen, as measured from barium nitrate, fluorine, from calcium fluoride, and metallic rhenium are shown in Figs 2, 3 and 4, respectively. Only those gamma-rays that may have potential use for analysis are annotated. In each case the energy of the gamma-ray is given together with its origin according to the con-

vention A b(r, s), where A refers to the target nucleus and b the light prompt product emitted from the reaction A(a,b)B, and r and s are the initial and final states of B defining the emitted gamma-ray.[3] This nomenclature has the advantage that it stresses the target element, which is of interest to the analyst. It is clear from these spectra that the number of gamma-rays excited is small so that the occurrence of double peaks in a spectrum is rare and accordingly simple stripping programmes can be used to obtain peak intensities with the concurrent advantage that the computation time per spectrum is reduced to a minimum.

Sensitivities

From measured spectra interference-free sensitivities were computed with the criterion that the sensitivity cited represents the concentration of the element for which the nett integrated counts under the peak was three times the standard deviation of the background over which the peak was measured. Table 1 lists the results obtained for some of the elements studied and includes results obtained from irradiations with alpha particle beams of 5, 11 and 16 MeV. From the table it is evident that the method is sufficiently sensitive to determine elemental concentrations in the parts per mil range. In a few cases the sensitivity extends well below this.

Light elements

Useful application of this technique can be expected for the determination of carbon, nitrogen, oxygen, fluorine, sodium, silicon and aluminium. In all these cases tge Coulomb barrier is sufficiently low to allow detectable yields of gamma-rays from nuclear reaction even with 5 MeV particles. The exceptions are ^{12}C and ^{16}O, not because of Coulomb barrier effects, but because their first excited levels decaying by gamma emission are respectively 4439 and 6131 keV above the ground state.

The use of the 871 keV gamma-rays from ^{14}N offers a sensitivity comparable with that attained by the method using the reaction $^{14}N(d, p)\ ^{15}N$ which has been used for the analysis of steels,[4] but has the advantage that the irradiation conditions are not critical. This method can therefore also be used for the routine determination of nitrogen in steels.

Oxygen analyses can be carried out either through the use of the 350 keV gamma-ray from ^{18}O or by measuring the 6131 keV gamma-ray from ^{16}O. The former suffers from the disadvantage that this heavy isotope has a low abundance in nature (0.205%) and the latter from the fact that high energy alpha-particles have to be used, and that therefore the measurement would have to be made in the presence of appreciable neutron fluxes generated by (α, n) reactions.

Table 1

Some results on interference-free sensitivities for alpha-induced prompt gamma-ray spectrometry

Element	E_γ	Sensitivities $^0/_{00}$		
		5 MeV	11 MeV	16 MeV
N	871	0.1	–	–
O	350	2.9	1.6	–
	5 109	–	0.2	0.1
	5 620	–	0.4	0.2
	6 131	–	0.2	0.2
F	110	0.6	0.1	0.1
	197	0.2	0.1	0.1
	583	0.4	0.1	0.2
	1 275	0.2	0.2	0.2
Na	417	1.5	0.1	0.1
	439	0.8	0.1	–
	1 809	0.3	0.1	0.2
Si	1 784	55.6	0.2	0.3
	2 244	5.2	0.5	0.5
Ti	159	2.3	26.3	–
	983	4.4	3.2	1.5
V	320	0.9	–	–
	930	42.8	–	–
Cr	564	41.8	–	–
Mn	126	0.6	–	–
Cu	669	15.2	–	–
Zn	995	15.9	1.9	3.0
	1 043	50.0	1.9	3.4
Y	1 530	15.6	7.5	–
Mo	204	9.0	–	–
	785	50.4	5.5	–
Ru	127	30.6	–	–
	470	32.7	–	–
Rh	357	0.8	0.5	1.0
Pd	374	3.6	0.4	3.7
	434	4.5	0.3	13.8
Ag	309	2.1	2.7	3.5
	325	2.0	2.5	3.8
Ta	137	1.1	0.8	1.7
W	122	2.4	8.3	–
Re	125	3.0	1.6	3.0
	134	1.2	4.6	8.5
	167	12.0	3.8	4.1
Pt	329	4.3	1.9	1.3
	356	9.5	2.5	1.9
Au	279	5.2	3.1	–

Nevertheless, both these reactions can be used for analysing high oxygen content materials such as geological ores. In addition the ^{18}O reaction can be used as a rapid means of determining this isotope in studies involving enriched material.

Fluorine has already been analysed by this method[5] in materials such as cement which contains fluorine from below 0.1 to about 4%. Sodium and aluminium are usually present in many matrices as major or minor but not trace constituents; they can therefore be determined by this method analogously to the technique used previously[2] with protons.

Medium weight elements

Few medium weight elements are determinable with sufficient sensitivity by Coulomb excited prompt gamma-ray spectrometry. The most promising elements in this region are vanadium, chromium, manganese, yttrium, rhodium, palladium and silver. Vanadium and manganese which often are important constituents in steels can be determined by the present method. Silver and palladium can be analysed by alpha-induced Coulomb excitation similar to the method described earlier[1] where proton-induced excitation was used.

Heavy elements

Tantalum, platinum and gold yield relatively high intensity low energy gamma-rays which show promise for determining these elements.

The use of position sensitive detectors for analysis by prompt particle spectrometry

The position sensitive detector (PSD) is a surface barrier detector constructed from n-type silicon, with the p–n junction formed by boron, implanted to form a resistance chain across the face of the detector surface and the implantation process controlled so that this resistance is optimised to obtain information on the position of impact of a charged particle. The amplitude of the signal obtained from one end of the resistance chain is proportional to Ex/l where x is a measure of the position of impact of a particle energy E and l is the length of the detector surface. This amplitude pulse is in coincidence with a pulse proportional to energy from the surface barrier mode of the detector. By suitably recording both these pulses energy spectra may be recorded as a function of detector position.

Principle of the analytical method

Analytical methods that make use of prompt charged particle spectrometry have to cope with a high flux of back-scattered bombarding particles. When the target is thin these particles do not seriously hinder the analysis, but thick targets cause such a high flux of back-scattered particles to reach the detector that the dead-time of the measurement becomes large and may introduce serious errors in the analysis. To overcome this problem several approaches may be used, such as particle identification devices, commonly a dE/dx detector placed in front of the surface barrier detector with suitable electronic circuitry, or the bombarding beam may be drastically reduced to prevent pile-up. However, the energy spectrum of the back-scattered particles will cover a large portion of the energy region thereby introducing a synthetically high background for low energy particles. For this reason analyses based on reaction with low or negative Q-values are not often used. When the reaction is highly exoergic the measured particles will usually have an energy far exceeding that of the back-scattered particles and it then is possible to use an absorber of suitable thickness placed immediately in front of the detector to absorb back-scattered particles, while transmitting the prompt reaction products of interest. Even this approach is limited to the case where the required particle has a higher penetration than the back-scattered ones.

Many reactions in which alpha particles are produced have potential application for analysis, especially those that are highly exoergic such as $^{19}F(p, \alpha)\ ^{16}O$ and $^{11}B(p, \alpha)\ ^{8}Be$. Unfortunately the penetration of alpha particles is much less than that of protons. In Fig. 5 the range of the main alpha particle groups from these two reactions are compared with that of scattered protons from the substrate as a function of the bombarding energy. If the absorber technique is used, Fig. 5 shows that bombarding energies are limited to about 1.9 MeV in the former reaction and about 1.5 and 1.0 MeV in the latter when the α_0 and α_1-groups are measured respectively. This technique was, however, used[6] to determine boron in steels by carefully balancing the bombarding proton energy and the absorber thickness, thereby sacrificing optimum sensitivity.

The increased cross section that can be attained with high energies could therefore not be used with advantage then. In the present work a new approach is described which overcomes this problem.

When a magnetic field is interposed between the target and the detector, the paths of the required prompt alpha groups and the scattered protons will then be altered so that they no longer arrive at the same point on the plane of the detector. By using a PSD the position pulses will enable the different particles to be distinguished. Since the energy of the scattered protons will be far less than that of the alpha particles they

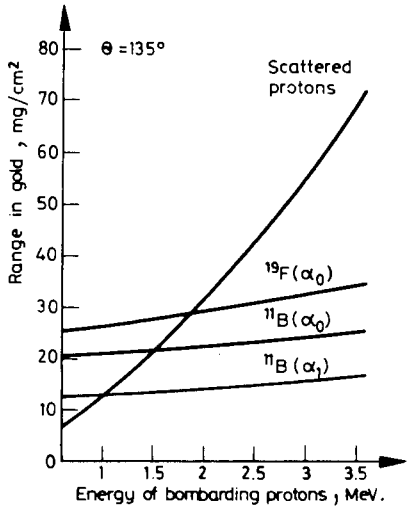

Fig. 5. The range in gold of backscattered protons and alpha-groups from fluorine and boron-11 as a function of the bombarding energy

will be deviated further. It then becomes possible to shift the detector so that most of the scattered particles fall off the detector while the required alpha particles may be measured without loss. Accordingly, alpha particle spectrometry can be used without the concurrently large increase in the dead-time of the measuring system, while yet enabling comparatively high intensities of bombarding beam to be retained. This work describes in principle the application of this method to the use of (p, α)-reactions for the determination of fluorine and boron without dealing with the details of the analysis.

Experimental

High temperature distillation in vacuum was used to prepare fluoride targets as deposits of known thicknesses of CaF_2 on tantalum. Boron targets of elemental boron, boron nitride and boron-containing materials such as glass powders and tourmaline ores were prepared by centrifugation from alcohol suspensions onto aluminium and tantalum.[7]

Targets were bombarded with 3 MeV proton beams of 3.5 mm diameter and measurements were made in a direction 135 ° to the bombarding beam defined by a collimator of 0.5 mm. The PSD was mounted on a rotatable arm in the scattering chamber at a convenient distance from the target. An electromagnet capable of generating a field of up to about 3 kilogauss was mounted between the target and the detector with the

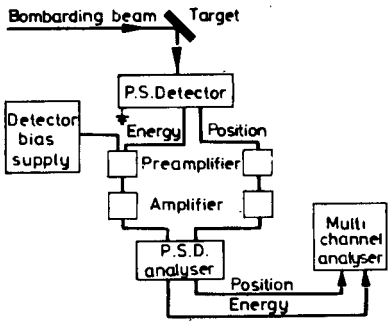

Fig. 6. Block diagram of the electronic equipment

deflection plane parallel to the measuring length of the PSD. Without any magnetic field the position pulses from the PSD were calibrated by rotating the detector arm through different angles within the range ± 5°, thus altering the point of incidence on the PSD. The energy pulses of the PSD were calibrated by the use of scatterers with different atomic numbers and from the known energies of the alpha groups from fluorine and boron.

A block diagram of the electronic apparatus is shown in Fig. 6. In this investigation the energy and position pulses were each spread over 64 channels of the multi-channel analyser resulting in a 64 X 64 channel matrix. Spectra were viewed on the CRT display of the multi-channel analyser as a three-dimensional figure in isometric display where the z-axis referred to counts per channel. Data were recorded on magnetic tape and processed off-line.

Results and discussion

Spectra from backscattering

After the detector and measuring systems had been calibrated both with regard to energy and position axes, the plateau spectrum obtained from a thick target of iron was recorded and the measuring equipment was then again tested with magnetic fields first in one direction and then in the other. The combined spectra are shown in Fig. 7 where the central reef represents the spectrum obtained with the magnetic field switched off. The reefs on either side are spectra obtained under identical conditions but with magnetic field switched on in different directions.

The broadening of the reef toward lower energy (the upper portion of the figure) is due to poorer resolution. Although the current flowing through the magnet was the same in both directions the difference between the distances by which the outer reefs were deflected from the original position is ascribed to hysteresis in the magnet. The

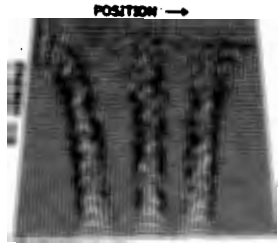

Fig. 7. Backscattered spectra from thick iron with magnetic field off (central reef) and on in either direction (other two reefs)

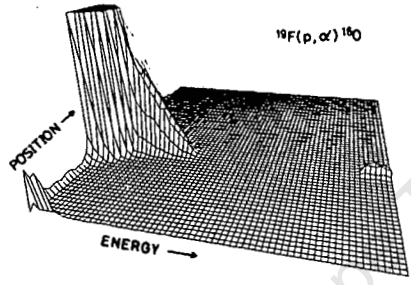

Fig. 8. Spectrum from calcium fluoride without magnetic field

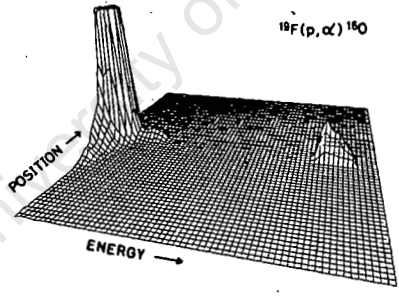

Fig. 9. Spectrum from calcium fluoride with magnetic field on

blank regions along the top were caused by electronic cutoff. From Fig. 7 the amount of deviation caused by the magnetic field can readily be discerned and shows that the detector can easily be shifted to eliminate unwanted low energy particles.

Application to fluorine determination

Spectra shown in Figs 8 and 9 were obtained from a target of calcium fluoride with the magnetic field off for the spectrum in Fig. 8 and on for that in Fig. 9. Not only

is the α_0-peak position slightly changed, but the backscattered protons can be seen materially diminished in intensity by the effect of the magnetic field. In addition, pile-up effects which cause encroachment of apparent backscattered protons in the region between the true backscatter plateau and the α_0-peak is entirely eliminated. The result was that the bombarding current could be increased from 110 to 250 nA while at the same time the dead-time of the measuring equipment fell dramatically from 20% to 2%.

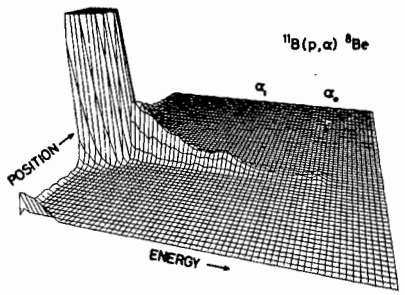

Fig. 10. Spectrum from boron without magnetic field. Note how the α_1-peak rides on the pile-up slope

A further test showed that the average current could be increased to 700 nA while yet retaining the dead-time to an acceptable level of about 10%. The implication of this effect is that analyses can be carried out in about 1–7th of the time with the same precision, or, that the sensitivity can be improved by almost an order of magnitude, without increase in bombarding time.

This case is, however, not a true test of the possibilities of this new technique, because of the very large energy gap between the α_0-group and the scattered protons.

Application to boron determination

The determination of boron using the reaction $^{11}B(p, \alpha)\ ^{8}Be$ has the advantage that the more abundant 80.2% boron-11 is used for the measurement, in contrast with previous methods[7] which used the (d, p)-reaction on the 19.8% abundant boron-10. There is therefore the inherent advantage of using analytical methods based on more abundant isotopes. The (p, α)-reaction produces two groups of α-particles both of which can provide a useful measure of the boron content. However, the cross section of the reaction leading to the emission of the $^{11}B(\alpha_1)$-group is markedly greater than that for the formation of the $^{11}B(\alpha_0)$-group. It is therefore advantageous both from the point of view of sensitivity and of precision to make use of the α_1-group.

Typical spectra obtained from boron-containing samples without and with the magnetic field are shown respectively in Figs 10 and 11. In Fig. 10 the α_1-group is

shown riding on the slope of the backscatter pile-up while in Fig. 11 the same group is clearly free from such interference. This reaction therefore provides a more stringent test of the usefulness of the present technique.

The same effect of current increase was observed here as was the case with fluoride described above. Typical analyses of samples containing boron in the 1%-range could be completed with a bombarding time of less than one minute using currents

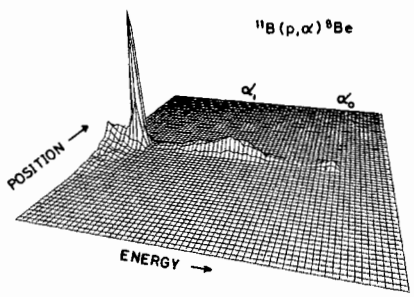

Fig. 11. Spectrum from boron with magnetic field on

between 200 and 500 nA, while the dead-time increased respectively only from 5 to 9%. However, with such high currents there was the danger of damage to the target, so that for routine analyses it was preferred to increase the measuring time to about 10 min while using currents of about 100 nA.

Conclusion

This survey of the potential use of alpha-particle induced prompt gamma-ray spectrometry shows that the method has potential for the determination of several elements, particularly in those cases where the elements are present as minor components with concentrations in the parts per mil range. The method has the advantage that the experimental procedure is simple and the target preparation is not critical.

It has also been shown that prompt alpha-particle spectrometry from (p, α)-reactions can be used for analysis with little or no interference from backscattered protons, by measuring with position sensitive detectors when magnetic deflection is employed. The spectra obtained are simple to interpret and point to improved resolution, with a potential improvement in sensitivity and precision. Quantitative data are currently being accumulated and will be reported elsewhere. Analyses can be carried out under these conditions much faster than was the case previously especially under routine conditions.

*

The helpful co-operation from the staff of S.U.N.I. and of the Nuclear Physics Research Unit, University of the Witwatersrand, is gratefully acknowledged. We thank the South African Atomic Energy Board and the South African Council for Scientific and Industrial Research for financial assistance.

References

1. G. DECONNINCK, G. DEMORTIER, J. Radioanal. Chem., 24 (1975) 437.
2. G. E. COOTE, N. E. WHITEHEAD, G. J. McCALLUM, J. Radioanal. Chem., 12 (1972) 491.
3. M. PEISACH, J. Radioanal. Chem., 12 (1974) 251.
4. C. OLIVIER, M. PEISACH, T. B. PIERCE, J. Radioanal. Chem., 32 (1976) 71.
5. I. S. GILES, M. PEISACH, J. Radioanal. Chem., 32 (1976) 105.
6. C. OLIVIER, T. B. PIERCE, Radiochem. Radioanal. Letters, 17 (1974) 335.
7. C. OLIVIER, M. PEISACH, J. Radioanal. Chem., 11 (1972) 105.

ABSTRACT NO 18

RAPID DETERMINATION OF FLUORINE IN CEMENTS

by

I.S. GILES and M. PEISACH
Southern Universities Nuclear Institute, P.O. Box 17, Faure 7131

Reprinted from
Proc. Intern. IUPAC Symp. "Analytical Chemistry in the Exploration, Mining and Processing of Materials", (Johannesburg) 1976.

INTRODUCTION

When fluorine occurs as a relatively minor component in geological material or industrial raw materials of geological origin, analysis of the fluorine content is usually preceded by a digestion process in which the fluoride is solubilised or in distillation of hydrogen fluoride under controlled conditions[1]. Such analyses are usually tedious and time - consuming. Accordingly fluorine is seldom determined in cements, because the procedures cannot yield results sufficiently rapidly to be of value for process control.

Consideration of the nuclear methods available for determining fluorine shows a division of the techniques into activation analysis and prompt spectrometry. When the former is carried out with neutrons, thermal neutrons result in the formation of 11.1-sec ^{20}F while fast neutrons form 109.8-min ^{18}F, both of which are produced in relatively low yields and hence analyses are not sensitive. Charged particle activation is usually subject to interference from oxygen, a component that is present in high concentrations in the materials discussed here. By contrast, prompt methods make use of specific properties of the ^{19}F-nucleus so that analyses are less subject to interference, yield results relatively quickly and, where high precision is needed, it may be achieved by extending the duration of the bombardment.

The prompt nuclear method previously used depended on the measurement of prompt gamma-rays that are emitted from the high resonances that occur in the reaction $^{19}F(p,\alpha\gamma)^{16}O$ at proton energies of 1 348 and 1 375 keV. This technique is sensitive and well-suited for measuring spatial distribution of fluorine concentration, because the resonance is sharp thus limiting the region of analysis. In order to determine *average* fluoride concentrations, the value most often required, the method reported here is preferred[2]. This method uses the inelastic scattering of alpha particles from the reaction $^{19}F(\alpha,\alpha'\gamma)^{19}F$, the excitation function of which is more smoothly varying with bombarding energy.

EXPERIMENTAL

The cement samples were pressed into 13 mm diameter pills, about 2 mm thick, by means of an hydraulic press. These were bombarded with beams of $^{4}He^{+}$ of 5 MeV. At this energy the range of particles is about 20 μm, so that the pills were effectively infinitely thick. The beam diameter was collimated to 3.5 mm diameter and the bombarding current varied from 50 to 100 nA depending on the dead time of the gamma-ray spectrometer.

Spectra were measured with a Ge(Li) detector placed about 10 cm from the point of irradiation, and the data were stored on magnetic tape for off-line processing. Analyses could be completed within 20 minutes.

RESULTS AND DISCUSSION

The lower energy levels of ^{19}F that may be excited by 5 MeV alpha particles in the reaction $^{19}F(\alpha,\alpha'\gamma)^{19}F$ and their de-excitation gamma-ray energies are shown in Figure 1. Figure 2 shows a spectrum observed from a cement sample containing fluorine. Only the lower energy gamma-rays are sufficiently intense to be used for analytical purposes. The gamma-ray of 583 keV resulted from the reaction $^{19}F(\alpha,n\gamma)^{22}Na$ and that of 1 275 keV from $^{19}F(\alpha,p\gamma)^{22}Ne$. The gamma rays of 110, 197 and 1 275 keV were selected in this study as a measure of the fluorine content of the sample.

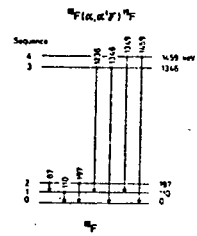

Figure 1: Some energy levels of ^{19}F.

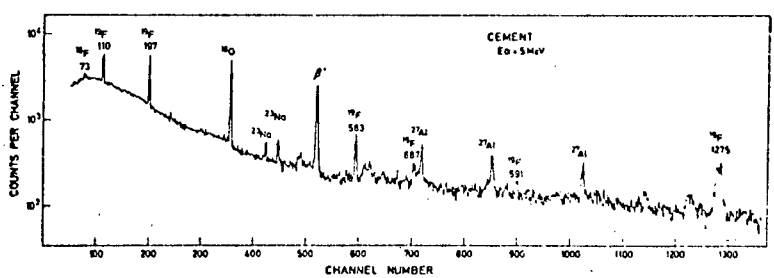

Figure 2: Prompt gamma-ray spectrum from alpha-bombarded cement.

TABLE I

PRECISION OF THE METHOD

Values given in counts per μC for 1% F w/w

CaF_2 46.86% F			Fluospar 63/70 46.89% F			Fluospar 9/69 40.19% F		
110-keV	197-keV	1275-keV	110-keV	197-keV	1275-keV	110-keV	197-keV	1275-keV
546.6	761.9	103.1	555.9	771.3	102.9	551.7	765.1	100.1
549.2	768.9	102.2	556.7	778.1	104.6	560.4	774.6	100.3
551.4	769.1	103.2	562.2	782.5	104.8	553.9	770.7	102.7
548.2	768.3	103.9	560.7	778.2	103.1	547.9	760.9	100.9
539.5	767.2	102.1	544.3	767.9	103.4	554.4	772.8	102.7
537.9	766.9	103.6	538.3	764.5	103.5	557.0	772.4	102.2
540.7	766.9	102.1				555.8	771.1	101.9
575.9	786.4	105.0						
562.5	779.2	103.4						
574.1	783.4	102.8						

Mean values 553.27 ±1.84% (110-keV)
771.68 ±0.89% (197-keV)
102.80 ±1.24% (1275-keV)

The precision of the analytical procedure was tested using Fluorspar standards obtained from the National Institute of Metallurgy. The results of repeat and replicate analyses are given in Table I for each of the selected gamma-ray energies. In all cases the relative precision was better than ±2%. Differences in the precision obtained from the use of the respective gamma-rays reflect the statistical errors in counting of both peak and corresponding background. This precision is acceptable for this investigation. From the intensities of the gamma-rays and from similar analyses of specimens containing fluorine at a much lower concentration level (0.1%) it was deduced that the method would be sensitive to fluorine concentrations of the order of some tens of parts per million.

Cement samples from South African and overseas sources were analysed for their fluorine content. Some typical results are listed in Table 2 together with the measured relative precisions for each sample.

TABLE 8

TYPICAL RESULTS OF CEMENT ANALYSIS

Sample	Fluorine Concentration (% w/w)	Relative Standard Deviation (%)	Number of Analyses
English	0.130†	3.6	12
Transvaal 1	0.051	2.6	6
Transvaal 2	0.049	3.0	6
Cape 1	0.093	4.3	5
Cape 2	0.116	6.0	4
Cape 3	0.103	9.8	4
Cape 4	0.091	4.9	4

† Used as standard.

All the specimens contained fluorine below 0.2% by weight. It is interesting to note that the relative precision for the various analyses exceeded that obtained with the standard fluorspars. The increased scatter of the results is ascribed to the inhomogeneous nature of the material. The effective mass of cement sampled by the bombarding beam is of the order of 0.25 mg. Any deviation from homogeneity at this sample-size level may be expected to be shown by the final result. This conclusion was borne out on check analysis carried out on mixtures of calcium fluoride and calcium hydroxide prepared by mixing the solids mechanically. In all cases these mixtures gave results with a higher variation than that obtained for the standards, but which approximated to those obtained with cements.

CONCLUSION

The method of alpha particle induced prompt gamma-ray spectrometry offers a sensitive and rapid procedure for determining fluorine in cements. The technique also serves as a check on the homogeneity of the product, if the diameter of the bombarding beam is suitably selected to decrease the size of the sampled material.

REFERENCES

1. H. STOCH. Summary of methods for CaF_2 analysis. In: Report 1649, National Institute for Metallurgy, Johannesburg, 1974.
2. GILES, I.S. and PEISACH, M., J. Radioanal. Chem. (in press) 1976.

RADIOCHEM. RADIOANAL. LETTERS 28(2) 135-144 (1977)

CORRECTING FOR RANGE EFFECTS IN THE CHARGED PARTICLE ANALYSIS OF COMPLEX MATERIALS

I. S. Giles, M. Peisach

Southern Universities Nuclear Institute
P.O. Box 17, Faure 7131, South Africa

Received 1 November 1976
Accepted 8 November 1976

A simple method based on backscattering data is proposed as a rapid procedure for correcting for range effects in charged particle analysis of infinitely thick targets. Improvements in accuracy and precision are thereby attained.

INTRODUCTION

When charged particles are used to analyse thick, homogeneous samples, the yield of the measured nuclear product depends on the number of nuclei of the required element encountered along the path of the bombarding beam. This number is itself determined by the concentration of the element and the range of the bombarding particles in the target material. Since analysts are usually interested in the concentration, a knowledge of the range is required but this parameter is difficult to determine. One usually resorts to one of the following three approaches:

a) the experimental procedure of the "equivalent thickness" method[1];

b) the semi-empirical calculation of the "average cross-section" method[2]; or

c) comparison with standards[3], where it is assumed that the stopping power of the standard is approximately equal to that of the unknown sample.

None of these procedures can be used when the composition of samples in a batch is unknown and varies markedly, but the number of samples of any one type is too small to warrant the manufacture of a suitable comparison standard.

If the elemental composition of a material can be determined, the range R of the particle in the matrix can be obtained from tables calculated for elements[4, 5] and the approximate summation rule[6]

$$\frac{1}{R} = \sum_i \frac{W_i}{R_i}$$

where W_i and R_i are respectively the weight fraction and the corresponding range for each of the component elements. In this report an easy method is proposed for determining the empirical composition of a complex matrix thereby enabling the calculation of the range. It is assumed that only the major components will contribute appreciably to the stopping power of the sample and that the error introduced by ignoring minor and trace components is negligible compared to the accuracy of the analysis being undertaken.

An empirical composition which can be used to carry out range corrections for charged particle analysis may be deduced from a Rutherford backscattering spectrum of the thick target. A single spectrum sufficient for characterization can be recorded at the same time as the analysis whether prompt or delayed. The composition is deduced from backscatter events in the surface and near-surface layers of the target where penetration is minimal and energy losses within the sample can be neglected. A disadvantage of using Rutherford backscattering is the fact that the backscatter cross-sections for light elements are relatively very small. However, the ease with which the heavier elements can be determined and an

empirical composition deduced are such important advantages that they outweigh the above disadvantage.

The nature of the sample analysed is seldom entirely unknown. In many metal samples, for example, the analyst knows that he can safely ignore the presence of light elements in range calculations because their concentrations are too low to affect the accuracy of his result. On the other hand geological material is likely to contain oxides, the presence of which can safely be taken into account from a knowledge of the metal composition, even though the observed spectrum gives only slight indication of the presence of oxygen, because of its low backscatter cross-section.

PRINCIPLE OF THE METHOD

Rutherford backscatter spectra from infinitely thick targets ideally consist of a series of steps[7], the energy of which can be used to determine the mass number of the component and the height of which is proportional to the atomic concentration in the material. It is assumed that the material is homogeneous. When such a spectrum is differentiated[8] the differential will consist of a series of peaks, the maxima of which correspond to the energies of the inflection points at the steps in the original spectrum whilst the areas under the peaks correspond to the step heights. Such spectra can easily be handled by available computer programes and areas under peaks in the differentiated spectrum can readily be integrated.

Since all the elements in a particular target are thus determined from a single bombardment the number of counts recorded for each element will be proportional to the product of its atomic concentration and backscatter cross-section. The latter can be calculated from a knowledge of the peak position even though the element may be identified with an error of a few units of atomic number. (The assumption is made here that the

stopping powers of elements of approximately equal atomic number would be sufficiently alike and acceptable within the error of determination). Accordingly, the relative atomic concentrations, N_i/N_j, of any two elements i and j in the sample can be calculated from

$$\frac{N_i}{N_j} = \frac{h_i}{h_j} \cdot \frac{\sigma_j}{\sigma_i} \tag{1}$$

where h represents the integral step height.

The Rutherford backscatter cross-section, σ, is calculated from:

$$\sigma = \left(\frac{Z_1 Z_2 e^2}{4E}\right)^2 \cdot \operatorname{cosec}^4(\phi/2) \left[\frac{M_1 + M_2}{M_2}\right]^2 \cdot f(M, \theta) \tag{2}$$

where

$$f(M,\theta) = \frac{(M_1 \cos\theta + M_2 \cos\alpha)^2}{M_2^2 \cos\alpha} \tag{3}$$

$$\sin = \frac{M_1}{M_2} \sin\theta$$

$$\phi = \alpha + \theta$$

The subscripts 1 and 2 refer respectively to bombarding and target nuclei of mass M and charge Z. e. The incident beam has an energy E and the backscattering is measured at a laboratory angle θ.

From concentration ratios involving all the elements under consideration an approximate empirical composition can be calculated. If light elements are known to be present their expected backscatter yields can be compared with the observed spectrum for confirmation. Finally the appropriate range can be calculated from tables.

APPLICATION TO GEOLOGICAL MATERIAL

The following example arose from an investigation of a charged particle method for determining fluorine[9] by measuring the yield of prompt gamma-rays. Geological standards used for calibration were fluospars with different fluorine contents, obtained from the National Institute for Metallurgy, Johannesburg. It was found that a plot of the measured gamma-ray yield against the fluorine content of the material was not linear, but two linear calibration lines could be fitted to the data corresponding to the two different geological ore types (see Fig. 1). The line which fitted the high fluorine content standards corresponded essentially to calcium fluoride-rich ores. The other line represented ores with a high iron oxide content. It was interesting to note that the lines passed acceptably close to the origin, but had negative and positive intercepts respectively.

Since the stopping power of these ores would be materially different, the above method was applied to all the data used for the calibration. A

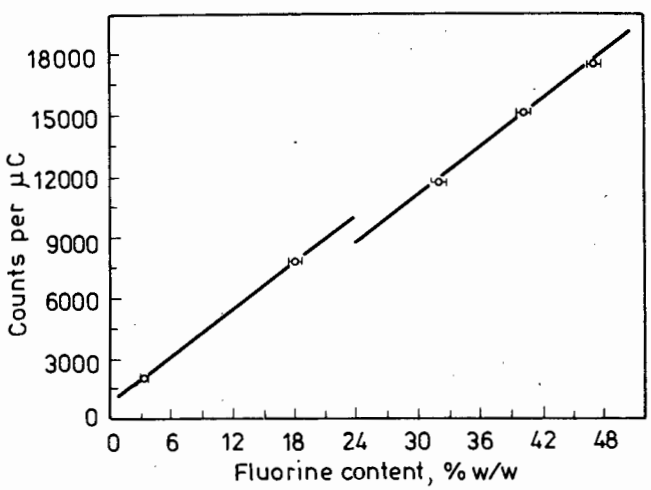

Fig. 1. The variation of alpha-induced prompt gamma-ray yield with fluorine content uncorrected for range effects showing two lines corresponding to two essentially different ore types. Error bars correspond to 95% confidence limits of NIM standards[10]

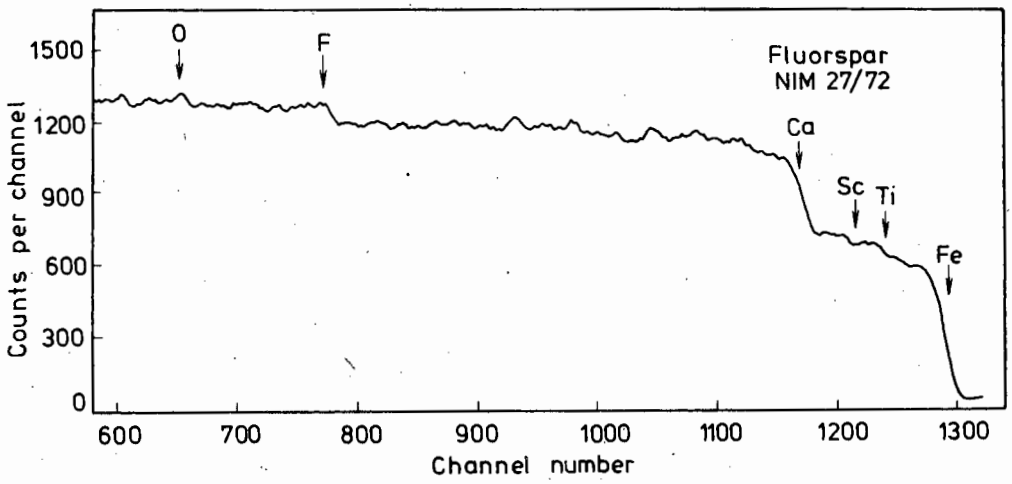

Fig. 2. Alpha particle backscatter spectrum from a thick target of NIM standard material Fluospar 27/72. Unmarked peaks and steps are due to prompt reaction products. E α = 5 MeV, $\theta = 135^{o}$

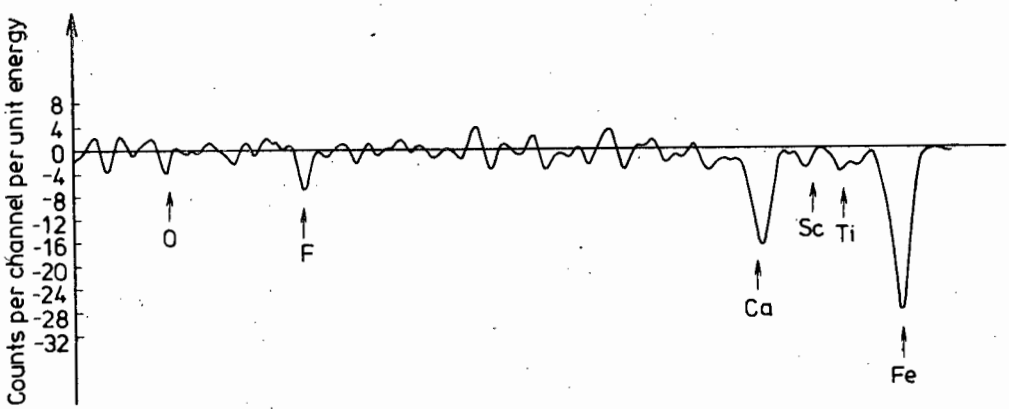

Fig. 3. Differentiated spectrum of the same data as shown in Fig. 2. Abscissae have been plotted on the same scale as in the previous figure

typidal backscatter spectrum of a sample is shown in Fig. 2, and its differential in Fig. 3. Unmarked steps and peaks in the figures other than statistical fluctuations may be ascribed to nuclear reactions occuring within the specimen. From the original and differentiated spectra the empirical composition of the sample was derived.

As an example the data obtained from Figs. 1 and 2 are given in Table 1.

It should be noted that it is irrelevant for the present purpose whether these elements were correctly identified or not. It is only important that the bombarding beam of alpha particles behaved as if these elements were present in the observed proportions at the bombarded spot on the target. From these data the ranges were calculated and the measured gamma-ray yield of the analysis was expressed per unit range in order to normalize the results from all the standards. The corrected data is shown plotted in Fig. 4. As expected, the points now lie on a single straight line. The

TABLE 1

Example of empirical composition derived from back-scatter data

Element	Fe	Ti	Sc	Ca	F	O
Atomic fraction	0.308	0.036	0.023	0.238	0.226	0.169

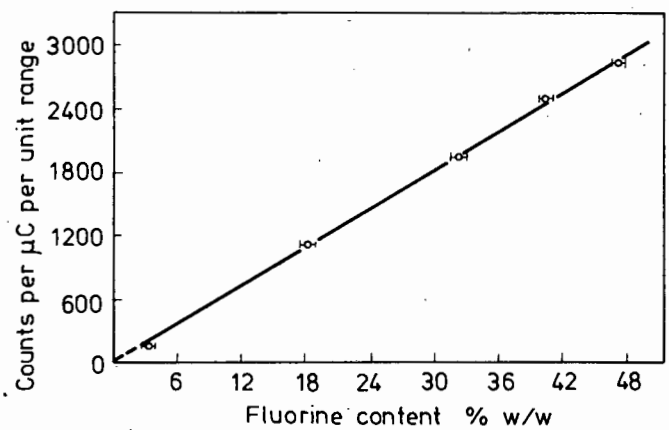

Fig. 4. Data from Fig. 1 corrected for range effects

line shown in Fig. 4 was drawn through the origin and fitted to the points by the method of least squares.

The example shows not only that range corrections were necessary, but that the method used was sufficiently accurate for the purpose.

APPLICATION TO FLUORIDE-HYDROXIDE MIXTURES

During the same investigation standards were prepared by mixing together known weights of calcium fluoride and hydrated calcium oxide. It may have been expected a priori that the ranges in mixtures of such compounds would not vary significantly with the mixture composition.

Replicate analyses showed that the mixtures were homogeneous within 6-8% at the milligram level sampled by the beam. It was therefore expected that experimental values of yield per unit concentration (A) of the

TABLE 2
Effect of range correction on precision

F, %	Yield per 1% F = A	A per unit range
0.808	203.0	29.20
1.120	185.1	28.61
1.617	185.0	30.89
2.279	168.6	29.16
3.216	158.5	28.20
4.931	148.7	27.10
6.395	147.2	27.09
9.164	160.3	29.80
12.31	146.8	27.23
18.01	158.7	29.25
24.32	148.3	26.97
32.81	160.8	28.67
Mean	164.25	28.51
Error	±18.5	±1.66
Error %	11.25%	5.82%

Number of analyses = 36.

analysed element (fluorine) would show a standard deviation of about the same amount. Experimental values for the series of mixtures gave a standard deviation of the parameter A about double that expected even though a plot of yield as a function of elemental composition did not visibly deviate from linearity.

When range corrections were applied as before, but using the known composition of the mixtures, the relative standard deviations of all the results fell to the expected value. An example of the results obtained using the intensity of the 197 keV gamma-ray is summarised in Table 2, where the values given are the mean values for each composition. This case indicates the improvement in precision obtained for samples where the need to apply range corrections is not immediately obvious.

CONCLUSION

Empirical elemental compositions of infinitely thick targets can be obtained from backscatter data. Such compositions may be used to calculate approximate ranges of the bombarding particles in the target material. Corrections for different ranges may be made to enhance the accuracy and precision of the analyses.

Financial assistance from the South African Council for Scientific and Industrial Research and the Atomic Energy Board is gratefully aknowledged. Our gratitude is expressed to the National Institute for Metallurgy for supplying samples of their standards free of charge.

We would like to thank the staff of the Southern Universities Nuclear Institute for technical help during the experiments.

This work will form part of a doctoral thesis to be submitted to the University of Cape Town (by I.S.G.) and is published with permission.

REFERENCES

1. C. Engelmann, Proc. Symposium Radiochemical Methods of Analysis, Vol. I, p. 405, I.A.E.A., Vienna 1965.

2. E. Ricci, R. L. Hahn, Anal. Chem., 37 (1965) 742; 39 (1967) 794.

3. R.F. Sippel, E. D. Glover, Nucl. Instr. Methods, 9 (1960) 37.

4. C. F. Williamson, J.-P. Boujot, J. Picard, Report CEA-R 3042, 1966.

5. L. C. Northcliffe, R. F. Schilling, Nucl. Data Tables, A7 (1970) 233.

6. G. Friedlander, J. W. Kennedy, J. M. Miller, Nuclear and Radiochemistry, (2nd Ed.) p. 98, Wiley, New York, 1964.

7. M. Peisach, D. O. Poole, Proc. 1965 Intern. Conf. Modern Trends Activation Analysis, Texas A and M University (College Station) 1965, p. 206; Anal. Chem., 38 (1966) 1345.

8. M. Peisach, Thin Solid Films, 19 (1973) 279.

9. I. S. Giles, M. Peisach, J. Radioanal. Chem., 32 (1976) 105.

10. H. Stoch, National Institute for Metallurgy Report 1649, 1974.